Order Number 8822816

Origin of sedimentary facies in the Upper San Rafael Group (Middle Jurassic), east-central Utah

Caputo, Mario Vincent, Ph.D.

University of Cincinnati, 1988

U·M·I
300 N. Zeeb Rd.
Ann Arbor, MI 48106

ORIGIN OF SEDIMENTARY FACIES IN THE UPPER SAN RAFAEL GROUP (MIDDLE JURASSIC) EAST-CENTRAL UTAH

A dissertation submitted to the

Division of Graduate Studies and Research
of the University of Cincinnati

in partial fulfillment of the
requirements for the degree of

DOCTOR OF PHILOSOPHY

in the Department of Geological Sciences
of the College of Arts and Sciences

1988

by

Mario Vincent Caputo

B. Sc., San Diego State University, 1976

M. Sc., Northern Arizona University, 1980

UNIVERSITY OF CINCINNATI

December 4 19 87

I hereby recommend that the thesis prepared under my supervision by Mario V. Caputo

entitled Origin of Sedimentary Facies in the Upper San Rafael Group (Middle Jurassic) East Central Utah

be accepted as fulfilling this part of the requirements for the degree of Doctor of Philosophy

Approved by:

Wayne A. Pryor

David L. Rhyer

David B Nash

ABSTRACT

In east-central Utah, tide-, wind-, and wave-currents deposited the Middle Jurassic (Callovian) Curtis and Summerville Formations and the Moab Member of the Entrada Sandstone along the southern and eastern coastal plain of an interior seaway. The three units comprise a transgressive-regressive cycle. Four facies in the Curtis were deposited during maximum transgression and incipient regression. Interbedded heterogeneous litharenite and sublitharenite microsequences in the sandstone-mudstone facies record the initial transgression and development of sedimentation on a nearshore shelf. Sand and mud were intermittently transported by tidal- and wave-currents at near wavebase depths. The composite sandstone facies contains amalgamated, crossbedded and parallel-bedded subarkosic microsequences which were deposited during late transgression, stillstand and incipient regression in a tidal channel, sand-shoal, berm system. Sand, silt and mud were transported in the form of large ripples, sand waves and dunes in tidal channels which were controlled by spring and neap tide cycles and time-velocity asymmetry. At shallower intertidal depths, interchannel sand shoals and berms were constructed by plane- and cross-laminated strata. Contemporary crosslaminated and locally crossbedded sublitharenites in the rippled silty facies and the redbed facies were deposited by spring-tide and wind- or storm-enhanced tidal currents in higher intertidal and supratidal zones respectively.

Three quartzarenitic facies in the Moab Tongue, a crossbedded sandstone facies, a wrinkled sandstone facies, and a wavy sandstone facies record a brief episode of wind sedimentation on a sandy coastal

plain. Complexly bedded dune-draa deposits of the erg interior are interstratified with wet-dry interdune and marginal windflat deposits locally reworked by marine currents. Subarkosic and sublitharenitic microsequences within the reddish-brown silty facies and gypsiferous facies of the Summerville Formation indicate regression of the Callovian seaway under restricted, evaporative conditions. Chaotic microsequences of the gypsiferous facies record periods of sand-mud sedimentation interrupted by early diagenetic crystallization of gypsum in a supratidal coastal sabkha. Primary gypsum accumulated in local small ponds or salinas. Contemporary upward-fining microsequencs of the reddish-brown silty facies originated in upper intertidal-supratidal sand flat, tidal channel, and channel bank subenvironments influenced by storm- and wind-enhanced tidal flooding. The Curtis-Moab-Summerville interval is the last Jurassic marine-eolian sequence in the Western Colorado Plateau.

The general northeastward paleoshoreline and isopach trends suggest structural control on sedimentation by gentle deformation along the San Rafael and Monument Uplifts. Petrologic data suggest a western source area consisting of uncertain older Jurassic and Paleozoic strata uplifted during middle Jurassic time in the Sevier orogenic belt.

ACKNOWLEDGMENTS

It is nearly impossible to express in this short space, the total gratitude and respect I hold for the members of the research committee, Dr. Wayne Pryor, Dr. David Meyer, and Dr. David Nash, who so kindly and willingly agreed to supervise this study. Dr. Wayne Pryor, chairman of the committee, devoted much personal time imparting the wisdom of his experiences. He not only enlightened me with keen perspectives on university teaching, sedimentary geology, and general geology but offered me ideas that have changed my personal life. Without reluctance, he calmly guided my study of Jurassic geology of southern Utah. I thank him for patiently enduring those four relentlessly hot, dry July days when he visited southern Utah to offer me assistance. Wayne was an extremely patient coach and counselor during the preparation of my doctoral examinations and always made time to talk to me and foster the successful completion not only of the exams but of the dissertation. Thank you very much, Wayne.

Dr. David Meyer and Dr. David Nash have been most proficient and knowledgeable research advisors by introducing me to fresh, useful ideas in their respective fields of paleontology and geomorphology. They have been wise, comforting friends who always set aside time to advise me on technical or personal problems. I am most grateful for their sincere, regardful coaching offered during the preparation of my doctoral examinations and their tremendous efforts and patience in guiding the dissertation through to completion.

I greatly appreciate the kind assistance and encouragment offered me by Dr. Richard Moiola of the Mobil Oil Corporation Research Division. Through his recommendations, Mobil Oil Corporation supported

the field study of Jurassic rocks in southern Utah with a generous research grant.

This study was also generously supported with the cooperation and contributions from the Union Oil Company, Sohio Petroleum Company, Walter H. Bucher Fund, Utah State Park System, and the Research Council and the Department of Geology at the University of Cincinnati.

A wholehearted thank you is given to Mike Westerfield and William Harrar for enduring weeks with me in the hot, wind-blown tablelands of Utah and for unparalleled ribaldry and conversation.

Pete Peterson (USGS, Denver) has been and always will be an invaluable resource and inspiration in my study of Jurassic geology of southern Utah.

I gained valuable perspectives from Ron Blakey (Northern Arizona Univ.), Ralph Hunter (USGS), Gary Kocurek (Univ. Texas, Austin), and Mike Porter (Exxon Prod. Res.) on Colorado Plateau geology, bedforms and stratification, eolian sedimentation, sealevel changes, and sequence stratigraphy. I am very indebted to Mark Pawlewicz (USGS, Denver) for his expert coal petrography and identification of carbonaceous material in the Curtis Formation, and to Richard Pollastro (USGS, Denver) for supplementing this study with a superb analysis of clay minerals in the Curtis and Summerville.

TABLE OF CONTENTS

LIST OF TABLES

LIST OF FIGURES

CHAPTER 1

INTRODUCTION

Sedimentologic Overview

Toward the end of early Jurassic time, a vast eolian erg (dune field or sand sea) extended across an area of what is now the state of Utah and parts of adjacent states and produced crossbedded strata of the Navajo Sandstone and equivalent Aztec and Nugget Formations. Following subaerial erosion and deflation of the sand sea, a shallow epicontinental seaway advanced into southern Utah from the north.

Throughout middle Jurassic time in southern Utah, recurring eolian, shoreline, and nearshore shelf associations were related to fluctuations in sea level, a persistence of similar sedimentary processes, and the repetition, through time, of laterally adjacent sedimentary environments. The history of middle Jurassic sedimentation in southern Utah is preserved in the San Rafael Group which overlies the Navajo Sandstone. In east-central Utah, the San Rafael Group consists of the Carmel, Page, Entrada, Curtis, and Summerville Formations, in ascending order (fig. 2.1).

Gypsiferous siltstones and sandstones, and oolitic and fossiliferous limestones of marginal and nearshore marine origin in the Carmel Formation mark the first marine transgression. Crossbedded strata of eolian origin in the Page Sandstone are characteristic of other regressive eolian deposits in the San Rafael Group and represent

an eolian dune field accumulating at the shoreline on a nearly featureless coastal plain. During late Middle Jurassic time (middle Callovian), the seaway partially withdrew from southern Utah as silty, sandy marginal marine and sandy, crossbedded eolian deposits prograded northwestward forming the Entrada Sandstone, a regressive unit more widespread than the Page.

The nature and origin of sedimentary strata deposited during a second major transgression is the topic of this report. The time is late Middle Jurassic (Callovian) and the sedimentary events are recorded in the Curtis and Summerville Formations, and Moab Tongue of the Entrada. Gray and red, complexly bedded fine-grained sandstones in the Curtis preserve a history of sedimentation by tide-, wind-, and storm-currents in coastal embayments with sand shoals, inter-shoal channels and sand flats. A red sandstone facies of the Curtis accumulated on wind-tidal flats contemporary with complex sandstone facies of eolian origin in the Moab Tongue. Red and dark brown, ripple-laminated sandstone and siltstone in the Summerville were deposited in a slowly regressive sand-flat-sabkha complex as the Jurassic seaway completely withdrew from Utah. These deposits mark the final episode of marine sedimentation in southern Utah during the Middle Jurassic and the onset of continental sedimentation in complex alluvial-lacustrine systems of the Morrison Formation.

Purpose

There are several main purposes in completing this study. One purpose is to recreate the middle Jurassic paleogeographic setting at the time of deposition of the Curtis Formation, Moab Tongue of the Entrada Sandstone, and Summerville Formation in east-central Utah. The paleogeographic reconstructions will attempt to illustrate how shoreline morphology evolved through time. A second purpose is to interpret how water- and wind-currents transported sediment and ultimately deposited facies and other sediment bodies. The third main purpose is to identify the sedimentary facies in the above intervals, show their areal distribution, and interpret their origin. The distribution and origin of facies may show a relationship to the tectonic framework and evolution of the Western Interior during middle Jurassic time.

This dissertation focuses on a limited aspect of Jurassic geology of the Western Interior of the United States. It is part of a grander, continuing study by colleagues at the U. S. Geological Survey, namely Dr. Fred Peterson (Denver, Colorado), and at universities including Dr. Ron Blakey, (Northern Arizona Univ.), Dr. Gary Kocurek (Univ. of Texas), and Dr. John Marzolf (Southern Illinois Univ.) in order to better understand sealevel fluctuations, sedimentary processes and facies, tectonic/structural events, and regional paleogeography for the Western Interior during Jurassic time.

In 1977, I set a long-term goal to describe how the sedimentary history and, perhaps, tectonic history, of a part of the Western Interior had been preserved in middle Jurassic rocks. Work was begun in 1977 on intervals in the Carmel and Page Formations of the lower San

Rafael Group of southwestern Utah. Field studies were resumed in 1984 on the Curtis and Summerville Formations in relation to the Moab Tongue of the Entrada Sandstone. These stratigraphic intervals comprise a genetic package of rocks bounded by the regional unconformities, J-3 and J-5 (Chapter 2, Stratigraphy), and are the subject of this report. Thus, with a study of nearly the entire San Rafael Group, the evolution of the shoreline, sedimentary environments, and the processes operating within those environments throughout middle Jurassic time in southern Utah may be interpreted more clearly.

The specific objectives of this study are to present the following:

1. A correlation of stratigraphic horizons and intervals based on physical, lithologic features.

2. An identification and origin of sedimentary facies as suggested by composition, texture, geometry, distribution, and physical and biogenic features.

3. A description of detrital minerals in relation to facies and sedimentary environments.

4. An analysis of ancient wind- and water-currents to help clarify ideas on basin circulation, provenance (combined with petrologic studies, no. 3 above), and local and regional paleogeography.

5. Paleohydraulic conditions as suggested by grain size, thickness of foreset beds, preserved bedforms, and paleocurrents.

6. Thickness and distribution of sedimentary units which may be related to local or regional structural features and the tectonic events which produced those structural features.

Location and Methods of Study

The San Rafael Group is well exposed in the dissected table lands of southern and eastern Utah particularly along monoclinal folds associated with dome-like uplifts (fig. 1.1). Exposures of the upper San Rafael Group, Curtis-Summerville-Moab interval, were examined in Wayne, Emery, and western Grand Counties, east-central Utah, in an area of approximately 7000 square miles (11,670 sq. km) (fig.1.2). Seven thousand cumulative feet (2121 m) of strata were measured and described in twenty-five stratigraphic sections exposed along the gently dipping (15 degrees or less) flanks of the San Rafael Swell, northern Henry Mountains, and northern Monument Uplift (Green River Desert) in August, 1985 and July, August, and September, 1986. Sections are designated as Z-2, Z-3, etc., in the order in which they were examined. Names and locations of stratigraphic sections corresponding to those locations in Figure 1.1 are listed in Table 1.1. Other data from published stratigraphic sections were used to construct isopach and facies maps (Chapter 3, Sedimentary Facies) and are included as Table 1.2. Original stratigraphic sections from the study are duplicated in diagrammatic form as fold-out illustrations in Appendix C.

Section Z-24 at Mussentuchit Wash is only a sampling locality and is not described in this report. Section Z-1 is located in western Colorado in the Colorado National Monument near Grand Junction, Colorado (not shown in fig. 1.1). The section includes the Middle Jurassic Wanakah Formation, a stratigraphic equivalent of the Summerville, and was part of an earlier proposal to study the Curtis-Summerville-Moab interval and equivalent strata in eastern Utah and

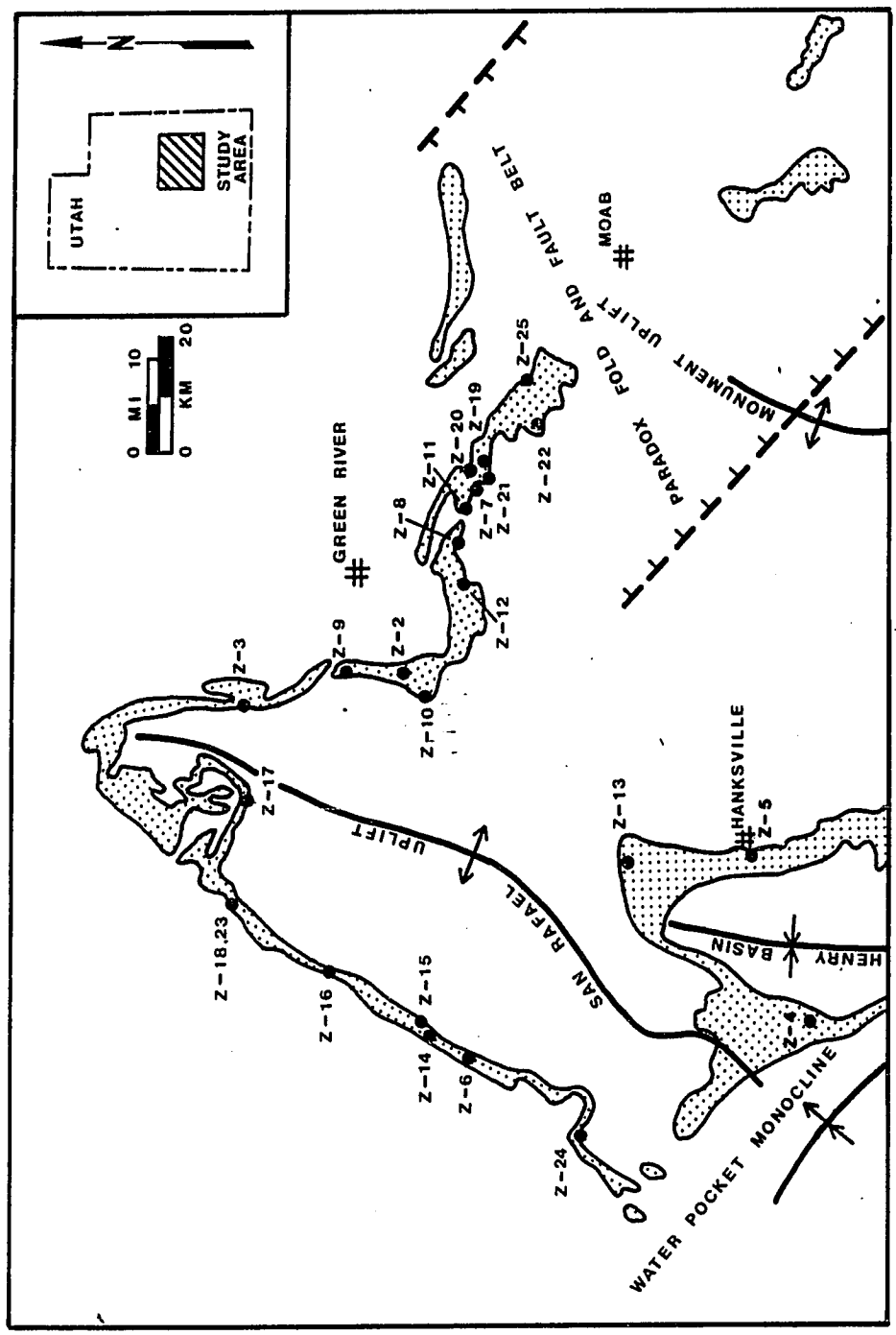

Figure 1.1. Map of the outcrop distribution of the Curtis-Moab-Summerville interval and location of structural elements in east-central Utah (after Hintze, 1975; Peterson, 1987; Blakey, in press). Solid circles (Z-2 through Z-25) are original stratigraphic sections

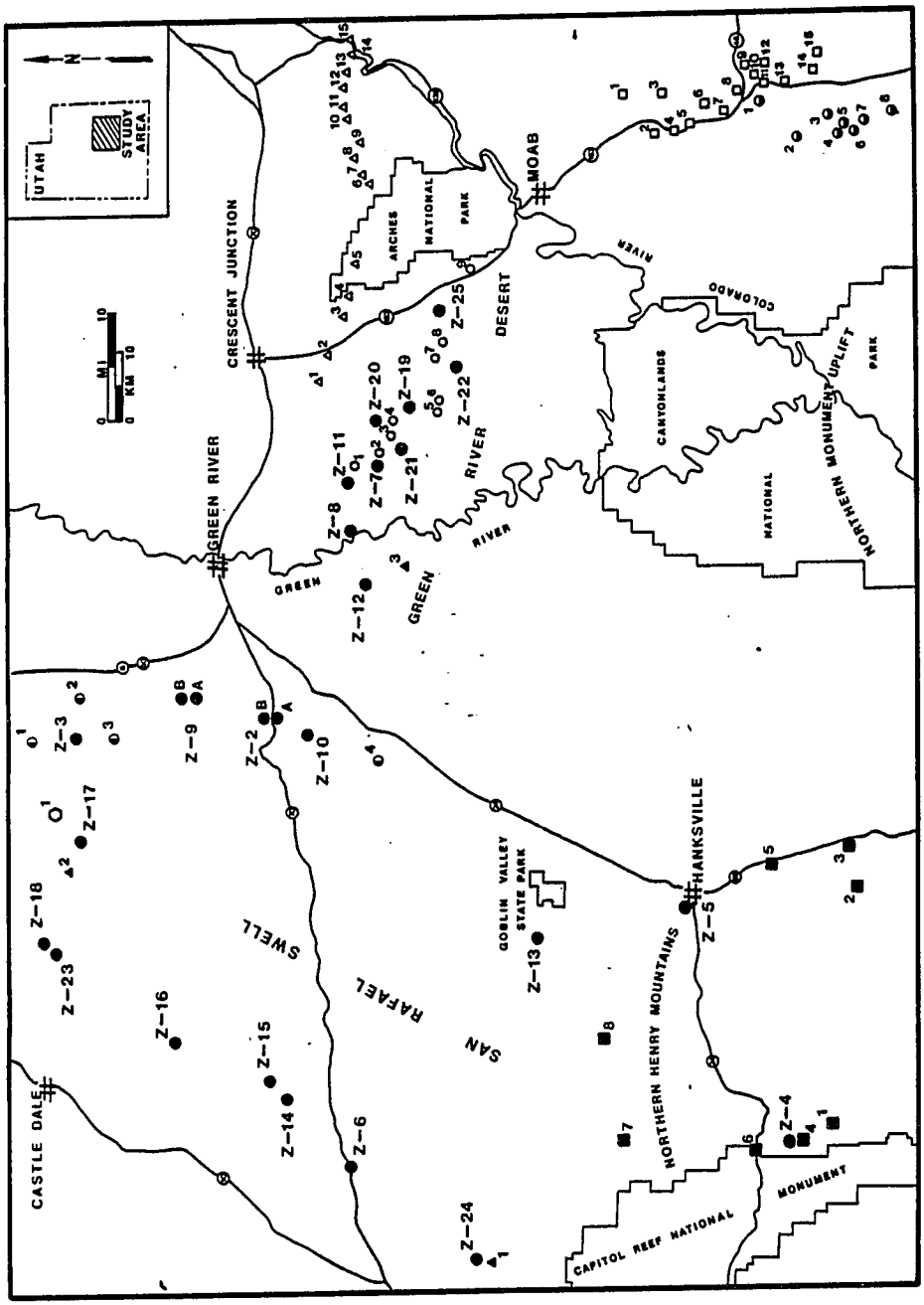

Figure 1.2. Map of the study area in east-central Utah. Solid circles (Z-2 through Z-25) are original stratigraphic sections measured and described in this report. Other symbols mark locations of published stratigraphic sections from which data have been used in this report (tables 1.1, 1.2. 1.3)

Table 1.1. Names and Locations of Stratigraphic Sections Described In This Report (Fig. 1.1).

Name	Location T	R	Sec
Northern Henry Mountains			
Z-4: Pleasant Creek	29s	7e	w 1/2 sec 36
Z-5: Hanksville	28s	11e	s 1/2 sec 9
San Rafael Swell			
Z-6: Wild Horse Creek	26s	10e	se 1/4 sec 1
Z-24: Mussentuchit Wash	25s	5e	ne 1/4 sec 1
Z-6: San Rafael Swell West	23s	7e	nw 1/4 sec 16
			n 1/2 sec 17
			se 1/4 sec 7
Z-14: Lookout Point	22s	8e	sw 1/4 sec 16
			se 1/4 sec 18
Z-15: South Sand Bench	22s	8e	nw 1/4 sec 10
Z-16: North Salt Wash	20s	9e	n 1/2 sec 31
Z-23: Buckhorn Wash South	19s	10e	ne 1/4 sec 4
Z-18: Buckhorn Wash North	18s	10e	w 1/2 sec 35
			n 1/2 sec 34
Z-17: Cedar Mountain	19s	12e	sw 1/4 sec 18
Z-3: San Rafael Swell Northeast	19s	13e	s 1/2 sec 10
			n 1/2 sec 15
Z-9B: Tidwell Draw North	20s	14e	w 1/2 sec 32
Z-9A: Tidwell Draw South	21s	14e	sw 1/4 sec 4
Z-2B: San Rafael Swell East	22s	14e	w 1/2 sec 5
Z-2A: San Rafael Swell East	22s	14e	nw 1/4 sec 8
Z-10: Hatt Ranch West	22s	13e	n 1/2 sec 25
Green River Desert			
Z-12: Horse Bench	23s	16e	s 1/2 sec 18
Z-8: Dellenbaugh Butte	23s	16e	s 1/2 sec 12
Z-11: White Wash	23s	17e	sw 1/4 sec 11
Z-7: Duma Point	23s	18e	s 1/2 sec 30
Z-21: Tenmile Canyon South	24s	18e	nw 1/4 sec 5
Z-20: Tenmile Canyon North	23s	18e	n 1/2 sec 27
Z-19: Dubinky Well North	24s	18e	nw 1/4 sec 12
Z-22: Bartlett Flat	24s	19e	w 1/2 sec 32
Z-25: Mill Canyon	24s	20e	sw 1/4 sec 20

Table 1.2. Names and Locations of Published Stratigraphic Sections From Which Thickness Data Have Been Used In Contour Maps In This Report

Number	Name	Location T	R	Sec
	Gilluly and Reeside (1928)			
1.	Summerville Point	18s	13e	sw 1/4 sec 22
2.	Woodside Anticline	19s	14e	sec 17 and 18
3.	Curtis Point	19s	13e	sec 34
4.	Straight Wash	23s	13e	nw 1/4 sec 27
	Wright and Dickey (1978b)			
1.	Last Chance Creek	25s	5e	sec 13
2.	Cedar Mountain	19s	11e	sec 10
3.	Chaffin Ranch	24s	16e	sec 4
	Wright, Dickey, and Snyder (1979)			
1.	Notom Bench	30s	8e	sec 9
2.	Granite Ranch	30s	11e	ne 1/4 sec 34 nw 1/4 sec 35
3.	Goatwater Point	30s	12e	se 1/4 sec 30
4.	Notom	30s	7e	nw 1/4 sec 1
5.	Penitentiary Point	29s	11e	sw 1/4 sec 24
6.	Fremont River	29s	7e	sec 14
7.	Black Mountain	27s	7e	sw 1/4 sec 13
8.	Factory Butte	27s	9e	sec 4
	O'Sullivan and Pierce (1983)			
1.	San Rafael Swell	19s	12e	w 1/2 sec 3 se 1/4 sec 4
	O'Sullivan (1980a)			
1.	White Wash C	23s	17e	nw 1/4 sec 13 ne 1/4 sec 14
2.	Duma Point	23s	18e	sw 1/4 sec 30 nw 1/4 sec 30
3.	Tenmile Canyon, west	23s	18e	nw 1/4 sec 33
4.	Tenmile Canyon, east	23s	18e	nw 1/4 sec 34
5.	Tenmile Butte	24s	18e	sw 1/4 sec 23
6.	Dubinky, west	24s	18e	sw 1/4 sec 24
7.	Bartlett Wash, west	24s	19e	sw 1/4 sec 21 se 1/4 sec 21 ne 1/4 sec 21 sw 1/4 sec 22

Table 1.2. Continued

Number	Name	Location T	R	Sec	
8.	Bartlett Wash, east	24s	19e	se 1/4	sec 23
				nw 1/4	sec 23
				ne 1/4	sec 23
9.	Sevenmile Canyon	25s	20e	se 1/4	sec 2
	O'Sullivan (1981b)				
1.	Salt Valley	22s	20e	se 1/4	sec 30
				nw 1/4	sec 32
2.	Long Valley	22s	20e	se 1/4	sec 34
		23s	20e	nw 1/4	sec 3
3.	Yellow Cat Flat A	23s	21e	se 1/4	sec 6
				ne 1/4	sec 7
4.	Mine Draw	23s	21e	ne 1/4	sec 13
				nw 1/4	sec 13
5.	Lost Spring A	23s	22e	nw 1/4	sec 20
6.	Lost Spring B	23s	22e	sw 1/4	sec 17
				nw 1/4	sec 17
7.	Fish Seep Draw A	23s	22e	se 1/4	sec 10
				nw 1/4	sec 15
8.	Fish Seep Draw B	23s	22e	ne 1/4	sec 14
9.	Auger Spring A.	23s	23e	ne 1/4	sec 7
	O'Sullivan (1981a)				
1.	Spanish Valley, south	27s	23e	se 1/4	sec 9
				nw 1/4	sec 16
2.	Behind the Rocks 3	27s	22e	nw 1/4	sec 36
3.	Pole Canyon	27s	23e	ne 1/4	sec 33
				sw 1/4	sec 34
4.	Kane Springs 2	28s	22e	nw 1/4	sec 1
5.	Kane Springs 4	28s	22e	se 1/4	sec 12
		28s	23e	sw 1/4	sec 7
6.	Muleshoe Canyon 2	28s	23e	se 1/4	sec 20
7.	La Sal Junction, northwest	28s	23e	se 1/4	sec 30
8.	La Sal Junction	29s	23e	nw 1/4	sec 3
				ne 1/4	sec 4
9.	West Coyote	29s	23e	nw 1/4	sec 12
10.	Wilson Arch, east	29s	23e	nw 1/4	sec 14
				ne 1/4	sec 15
11.	Wilson Arch	29s	23e	se 1/4	sec 15
				sw 1/4	sec 15
12.	Hook and Ladder	29s	23e	ne 1/4	sec 25
13.	Wilson Arch, south	29s	23e	se 1/4	sec 27
14.	Lopez Gulch 1	30s	23e	nw 1/4	sec 1
15.	Lopez Gulch 2	30s	24e	sw 1/4	sec 6

Table 1.2. Continued

Number	Name	Location T	R	Sec
	O'Sullivan (1980b)			
1.	Looking Glass Rock	29s	23e	sw 1/4 sec 16
2.	Hatch Rock	29s	22e	se 1/4 sec 35
				sw 1/4 sec 36
		29.5s	22e	nw 1/4 sec 36
				ne 1/4 sec 36
3.	Rone Bailey 1	30s	23e	sw 1/4 sec 8
4.	Wind Whistle Draw	30s	22e	nw 1/4 sec 13
5.	Rone Bailey 2	30s	23e	c sec 19
6.	Rone Bailey 3	30s	22e	se 1/4 sec 24
				ne 1/4 sec 25
7.	Rone Bailey, southeast 1	30s	23e	ne 1/4 sec 31
8.	Lightening Draw, north	31s	23e	ne 1/4 sec 8

Table 1.3. List of symbols used on maps and figures in the text and in stratigraphic sections in appendix

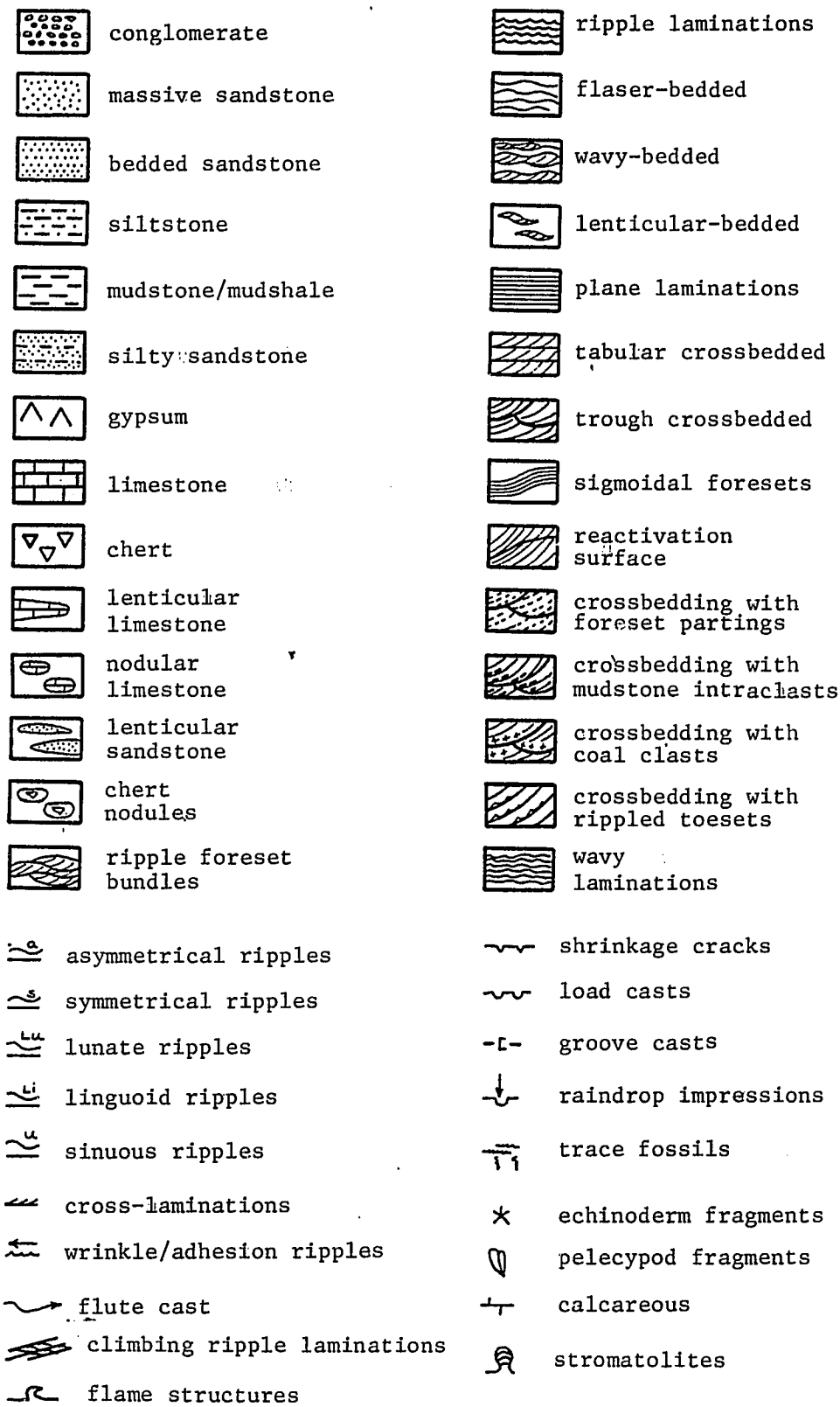

Table 1.3. Continued. Symbols for locations of original and published stratigraphic sections

●	This Study
◐	Gilluly and Reeside (1928)
▲	Wright and Dickey (1978b)
■	Wright et al. (1979)
◒	O'Sullivan (1980b)
□	O'Sullivan (1981a)
△	O'Sullivan (1981b)
⬡	O'Sullivan and Pierce (1983)
○	O'Sullivan (1980a)

western Colorado. Stratigraphic relationships are uncertain in the Monument Uplift area in southeastern Utah (fig. 1.1) because of eroded strata there. Thus, the area in western Colorado and eastern Utah has been abandoned and the study has been restricted to that area in east-central Utah where the significant stratigraphic relationships and facies changes can be observed in a northwest-southeast traverse, approximately perpendicular to the trend of the middle Jurassic shoreline. Hence, the location pattern of stratigraphic sections. The J-3 unconformity is a reference horizon marking the base of each stratigraphic section; it is also the contact between the Curtis and Entrada and equivalent strata. Because of lateral facies changes in both Curtis and Entrada, different units are present above and below this horizon at different locations. These stratigraphic relationships are explained in Chapter 2. The top of each stratigraphic section is the J-5 unconformity which separates a uniform sequence of gypsum and reddish- and orangish-brown sandstones and siltstones in the Summerville from a sequence of thick (5 feet or more) gypsum and gray, pink and lavender siltstones and limestones in the Tidwell Member at the base of the Morrison.

Paleogeographic and sedimentologic-tectonic settings are interpreted from physical and biogenic sedimentary features, vertical and lateral bedding sequences, textural, isopachous, and paleocurrent patterns, and facies geometry and distribution. Rock texture and mineralogic composition were estimated in the field. Rocks are simply referred to as conglomerate, sandstone, siltstone, mudstone, claystone, and limestone in field descriptions and were later assigned specific names based on thin sections of 95 samples. Grain sizes were described

according to the grade-scale and class of Wentworth (1922). Rocks are specifically classified according to Folk et al. (1970) for sandstones, Folk (1959) for limestones and Potter et al. (1980) for shales. In describing sedimentary sequences, cross-stratified units are described according to McKee and Weir (1953). Furthermore, the term, crossbed (Rubin and Hunter, 1983), is used to denote either a cross-stratified bed (set of crossbeds) or the individual foreset beds themselves. The thickness of beds and laminae is described according to Ingram (1954) and Campbell (1967). The ancient sedimentary environments and facies described herein are reconstructed without recourse to one well established model, but are demonstrated as resembling parts of several environments and facies, both modern and ancient.

Previous Work

Since the late 1800's more than two hundred field studies have been devoted to the recognition and correlation of Jurassic strata of southern Utah. The history thereof is discussed specifically in Chapter 2 and a partial summary of this previous work is provided in Table 2.1. The few investigations that have dealt with origins of Jurassic strata, mainly in the San Rafael Group, are summarized in the following paragraphs.

Among the studies listed in Table 2.1, those of Gilluly and Reeside (1928), Gregory and Moore (1931), Baker (1933, 1946), Dane (1935), Baker et al. (1936), McKnight (1940), Craig et al. (1955), Imlay (1957, 1980), Young (1978), Stokes (1980), O'Sullivan (1981c), and Blakey (in press) have mentioned the general marine or non-marine nature of units in the San Rafael Group and other intervals.

Transgressive and regressive episodes preserved in the Carmel-Page interval of southwestern Utah have been described by Blakey et al. (1983). Voorhees (1978), Geesaman (1979), and Caputo (1980) have provided the most detailed stratigraphic analysis, to date, of the Carmel-Page interval. They have interpreted a lateral association of coastal environments extending northwestward from eolian dune and wind-flat to tidal flat-sabkha and nearshore marine shelf along the eastern shoreline of the middle Jurassic (Bajocian-Bathonian) seaway. Rigby (1986) confirmed these interpretations for the southwestern-most exposures of Carmel in southwestern Utah.

Johnston (1975) showed how Jurassic tectonic events in the west-central Colorado Plateau region affected sedimentation in the Carmel and Entrada Formations, the only components of the San Rafael Group near Black Mesa, Arizona and the Kaiparowits Plateau, Utah.

From one exposure in the western San Rafael Swell, Smith (1976) has described the general marine nature of facies in the Curtis and their relationship to transgression and regression. Stanton (1976) has interpreted a generalized tidal flat origin from one exposure of Summerville in the eastern San Rafael Swell. Studies of the Curtis-Entrada relationships in northeastern Utah by Eschner and Kocurek (1982a, b; 1986) have described tidal sand bar sequences in the Curtis and the effects of marine reworking of eolian deposits in the underlying Entrada Sandstone during Curtis time. The Entrada Sandstone has recently been the focus of comprehensive studies on eolian stratification and bedform and erg reconstruction by Kocurek (1981a, b) and Kocurek and Dott (1981).

CHAPTER 2

STRATIGRAPHY

Jurassic System

Jurassic strata of the western Colorado Plateau region have been recognized and described since the early geological expeditions of Howell (1875), Powell (1876), Dutton 1880) and Gilbert (1880) (fig. 2.2). Since then, these strata have been involved in numerous miscorrelations, revisions and age reassignments. Hence, it is the intent of this chapter to summarize the evolution and development of the stratigraphic framework for the Jurassic System of southern Utah, particularly for the Curtis-Summerville-Moab interval.

In the Jurassic System of southern Utah, there are two main subdivisions (fig. 2.1). The oldest subdivision is the Glen Canyon Group and consists of, in ascending order, the Moenave, Wingate, Kayenta, and Navajo Formations. The youngest subdivision is the San Rafael Group composed of the Temple Cap, Carmel, Page, Entrada, Curtis, Wanakah, Summerville, and Romana Formations, in ascending order. The Morrison Formation is not assigned to a group and is the youngest Jurassic rock interval in southern Utah (fig. 2.1)

A partial summary of previous stratigraphic studies involving mostly Jurassic and related Triassic or Cretaceous strata of southern Utah comprises Table 2.1. Studies are grouped according to geographic area in Utah.

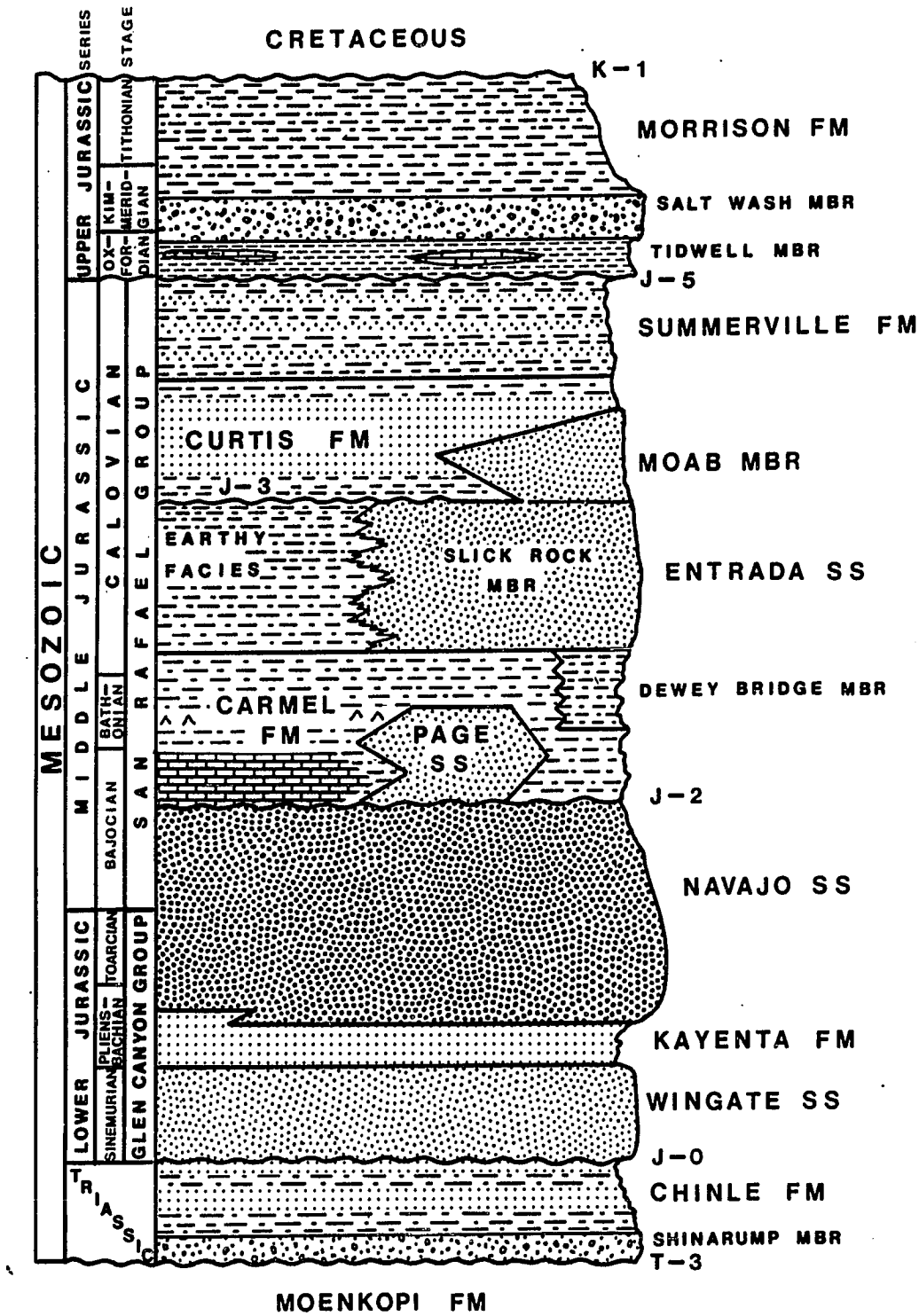

Figure 2.1. Succession of Jurassic and related strata recognized in east-central Utah

Table 2.1. Partial Summary of Previous Stratigraphic Studies of Jurassic and Related Triassic and Cretaceous Strata in Utah

General
Dutton(1880), Dake(1919), Butler et al. (1920), Stokes(1944,1949,1963b), Imlay(1952a, 1957), Craig et al. (1955), Hintze(1973), Pipiringos and O'Sullivan(1978), Rigby(1978), Young(1978)
Western
Gilbert(1875a)
Southwestern
Marvine(1875), Lee(1908), Reeside and Bassler(1922), Gregory et al. (1926), Gregory and Moore(1931), Grater(1948), Gregory(1948, 1950a, b, 1951), Williams(1952), Bissel(1954), Mackin(1954), Averitt(1962), Wright and Dickey(1963a), Stokes(1963a), Peterson and Waldrop(1965), Wilson(1965), Cashion(1967), Blakey(1970), Thompson and Stokes(1970), Doelling(1975), Peterson et al.(1977), Voorhees(1978), Peterson and Pipiringos(1979), Wright et al. (1979), Wright et al.(1979b, 1980), Caputo(1980,1981), Taylor(1981), Blakey et al. (1983), Chapman(1986), Rigby(1986)
Central
Craig and Freeman(1959), Imlay(1967), Wright and Dickey(1978a), Wright et al. (1979), Sprinkle and Waanders(1984)
Southern
Gilbert(1875b), Howell(1875), Dutton(1885), Gregory(1916,1917), Moore(1922), Gregory and Noble(1932), Longwell et al. (1923), Baker et al. (1947), Harshbarger et al. (1951), Harshbarger et al. (1957), Stokes and Holmes(1954), Averritt et al.(1955), Phoenix(1963), Wright and Dickey(1957, 1963b, 1978c), Lessentine(1965), O'Sullivan and Craig(1973), Peterson(1974, in press), Johnston(1975), Freeman(1976), O'Sullivan(1978), Wright(1978), Blakey(in press), Caputo (1987)

Table 2.1. Continued

Southeastern
Woodruff(1912), Forrester(1918), Miser(1924, Lee et al. (1927), Prommel(1927), Baker(1933), Gregory(1938), Baker et al. (1936,1947), Fischer(1942), Stokes(1954), Craig and Dickey(1956), Craig and Cadigan(1958), Wright and Dickey(1958b, 1959), Pipiringos and O'Sullivan(1975), O'Sullivan(1980b), Molenaar(1981), O'Sullivan and Pierce(1983)
East-Central
Gilbert(1880), Lupton(1914), Emery(1918), Baker et al. (1927), Gould(1927), Gilluly and Reeside(1928), Gilluly(1929), Dane(1935), McKnight(1940), Baker(1946), Hunt et al. (1953), Wright and Dickey(1958a, Dickey and Wright(1959), Wright et al. (1962), Smith et al. (1963), Dover(1969), Baars and Molenaar(1971), Molenaar(1971),Stokes(1952, 1972,,1980), Derr(1974), Craig and Shawe(1975), Gard(1976), Smith(1976), Stanton(1976), Bagshaw(1977), Geesaman(1979), Peterson(1978), Wright et al.(1979a), O'Sullivan(1980a, 1981a,b,c, 1984a,b) O'Sullivan and Pipringos(1983), Kocurek and Oakes(1985), Caputo and Peterson(1986), Peterson and Caputo(1986)
Eastern
Whitman(1907), Reeside(1923), Richards(1958), Wright and Dickey(1978b, 1979)
Northeastern
Powell(1876), Hague and Emmons(1877), King(1878), Weeks(1907), Thomas et al.(1945), Stokes(1957), Rigby(1964), Otto and Picard(1975), Lowrey(1976), Fritz(1977), Kocurek(1981a,b), Kocurek and Dott(1981, 1983), Eschner and Kocurek(1982a,b 1986)
Northern
Imlay(1952), Hinman(1957), Bullock(1965), Lord and Picard(1984)

History of Stratigraphic Nomenclature

The discussion on the evolution and development of stratigraphic nomenclature for the Jurassic System of mostly southeastern Utah is summarized in Figure 2.2. Evolution of nomenclature at the member level is shown for the Entrada, Curtis, Summerville and Morrison Formations.

Glen Canyon Group (fig.2.2)

Throughout southern Utah and northern Arizona, the upper part of the Glen Canyon Group consists of the Navajo and Kayenta Formations. The lower part includes the Moenave Formation in southwestern Utah and the equivalent Wingate Sandstone in north-central Arizona and south-central and southeastern Utah. These strata were briefly described by Howell (1875) and later called the Vermillion Cliff Group and White Cliff Group by Powell (1876). From exposures in southwestern Colorado, Cross (1899) assigned the name La Plata Group to those strata lying between the Triassic Chinle Formation of Gregory (1917) and the Jurassic calcareous and gypsiferous shales directly overlying the Navajo. Dutton (1880) referred to the lowermost red, cross-bedded sandstone in the La Plata Group as the Wingate Sandstone. Gregory (1917) later designated the massive cross-bedded sandstone of the White Cliff Group (Powell, 1876) or Gray Cliff Group (Gilbert, 1880) as the Navajo Sandstone and the strata between the Navajo and Wingate as the Todilto Formation. Finally, Baker et al. (1936) corrected the miscorrelation between Todilto-like strata in southern Utah and northern Arizona with the type-Todilto of northwest New Mexico. They assigned the name Kayenta Formation to the middle formation of the La

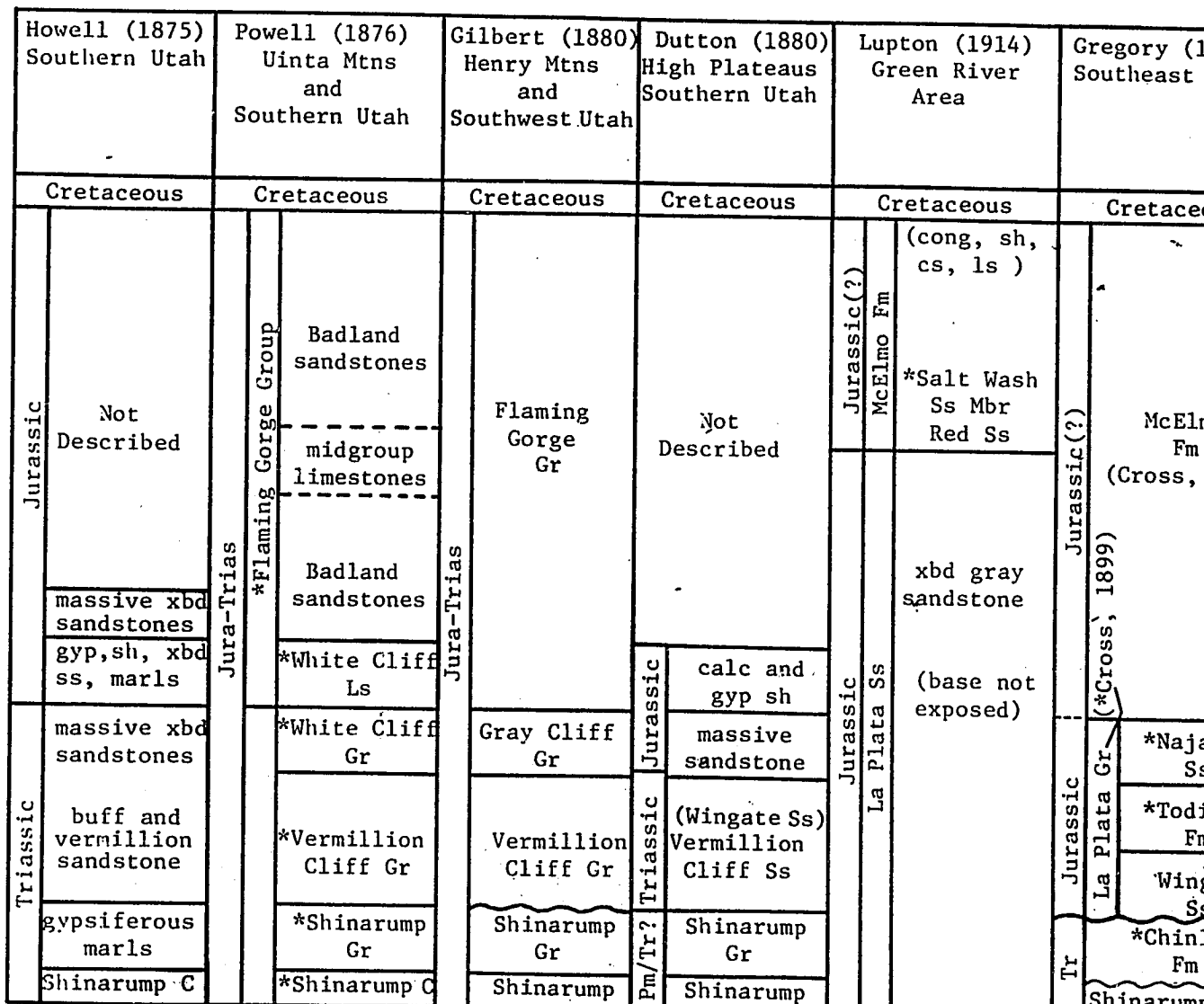

Figure 2.2. Chronological review of stratigraphic nomenclature of the Jurassic system as a
Intervals are not to scale. *Interval formally named in that report. *Jem: Moab Tongue nam

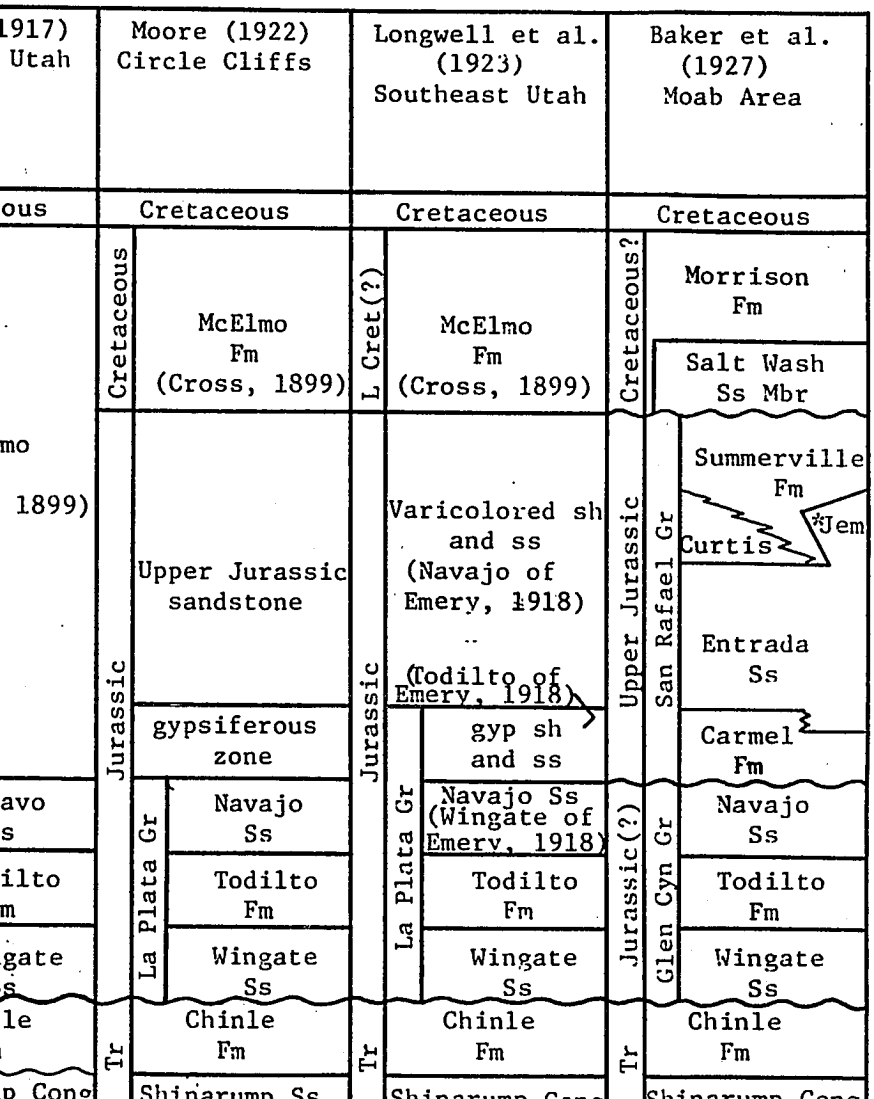

applied by various workers in southern Utah.
med by Lee (unpub. report) +Peterson (1987)

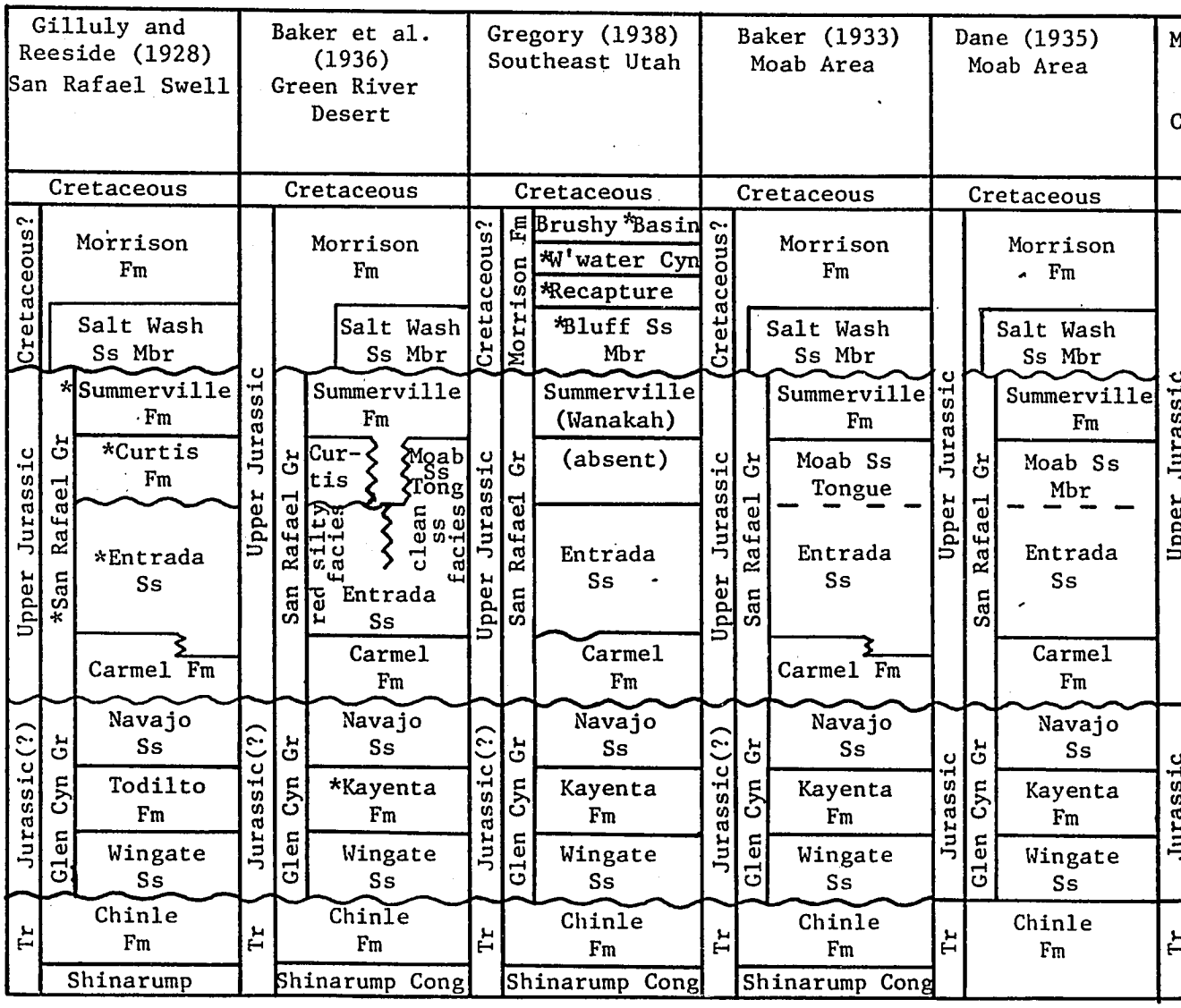

Figure 2.2. Continued

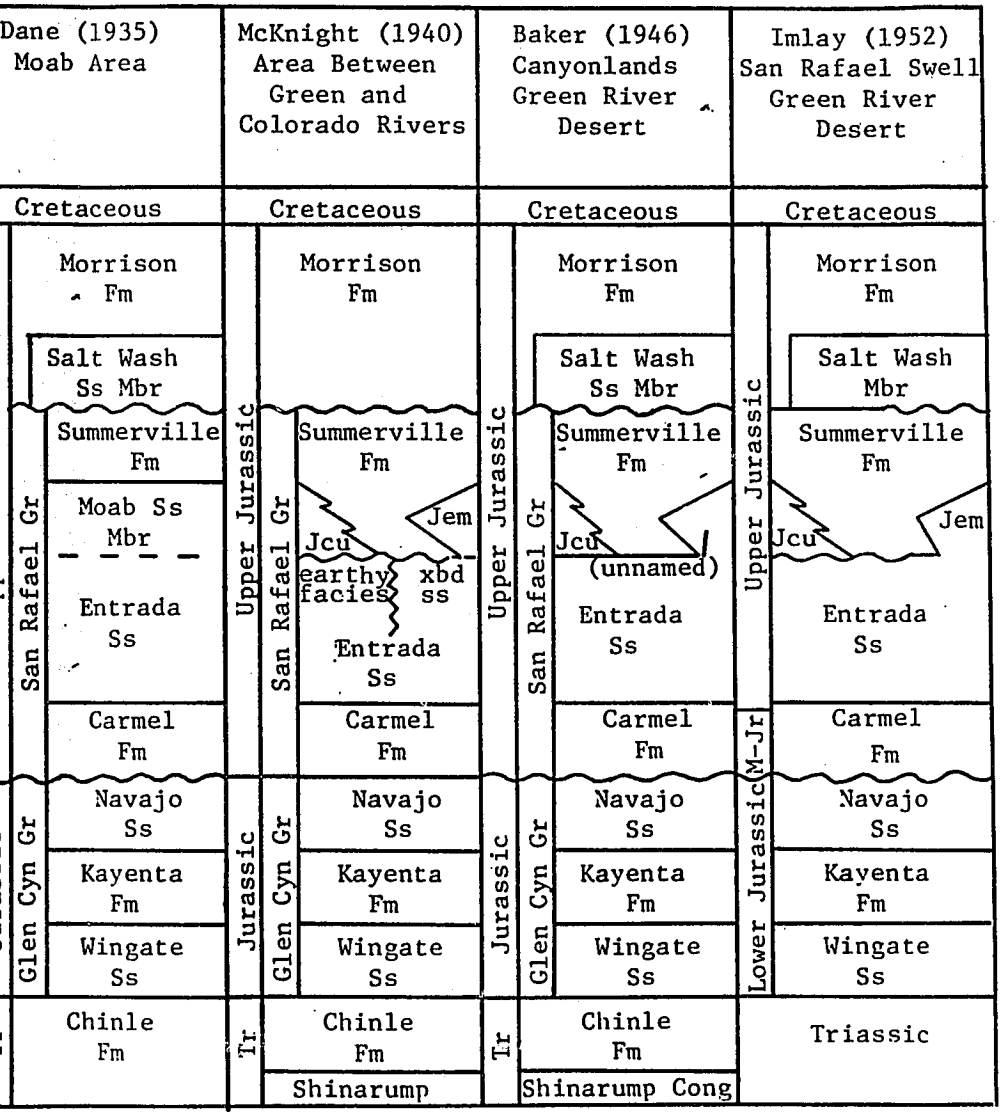

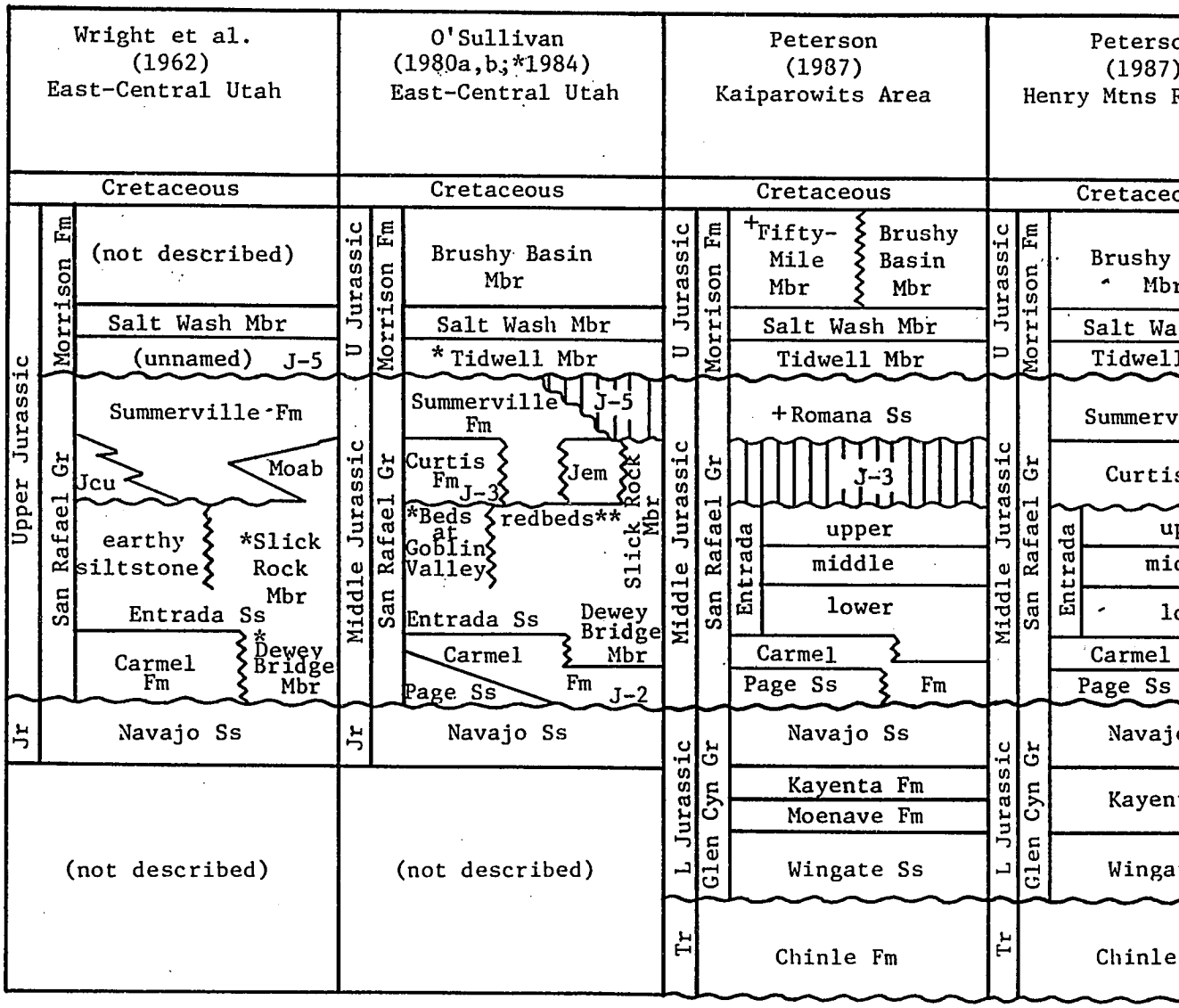

Figure 2.2. Continued

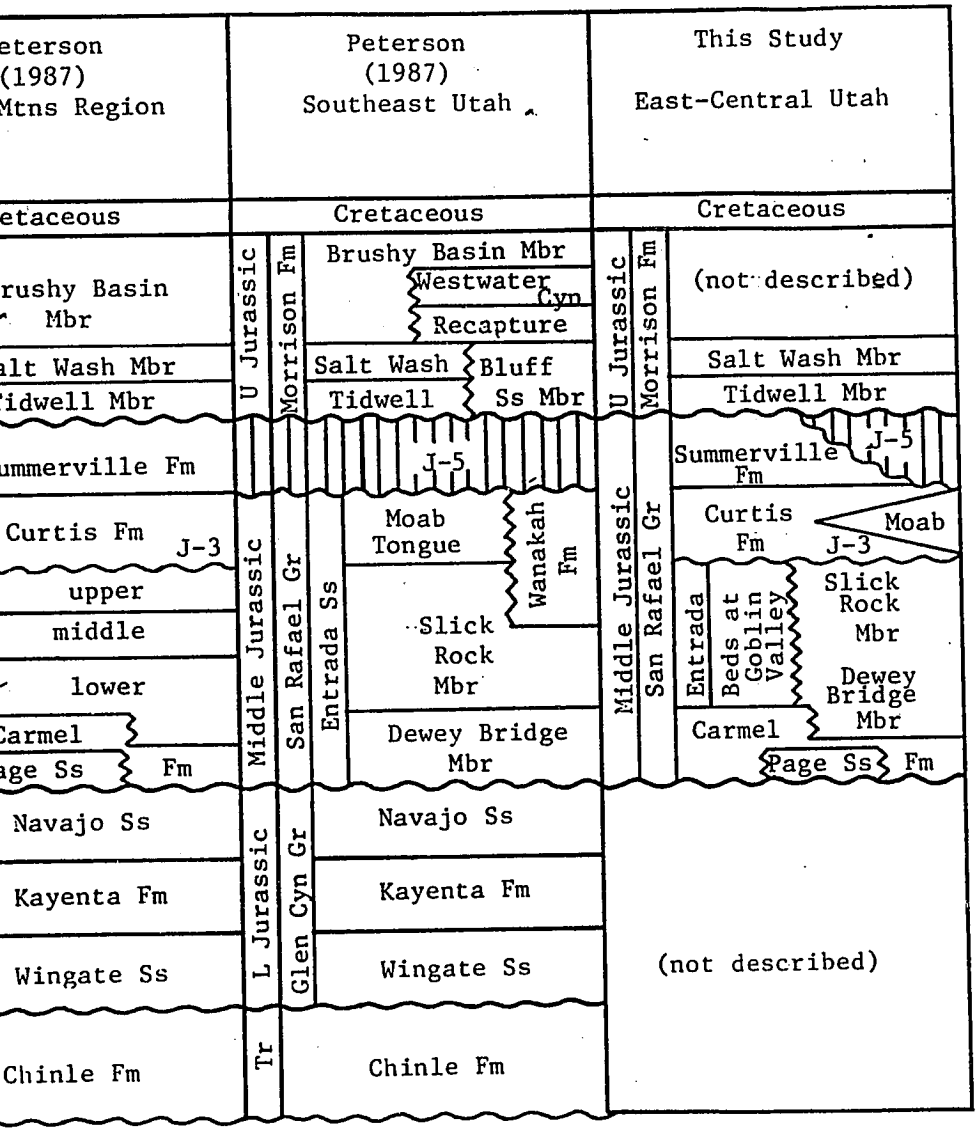

Plata Group and referred to strata in the basal Morrison of New Mexico as Todilto. Thus, the Wingate, Kayenta, and Navajo Formations comprise the present Glen Canyon Group named as such in 1931 by Gregory and Moore. Baker et al. (1927) and Gilluly and Reeside (1928), aware that the formal name awaited publication, referred to the Glen Canyon Group in their earlier reports.

San Rafael Group (figs. 2.2, 2.3)

The San Rafael Group has had a more complex history of miscorrelations and stratigraphic reassignments than the Glen Canyon Group. Because of facies changes and truncation by unconformities, stratigraphic components in the San Rafael Group are variable. In southwestern Utah, in the Zion Canyon area, the group consists of the Temple Cap, Carmel, Page and Entrada Formations; in south-central Utah, Henry Mountains area, the Page, Carmel, Entrada, and Romana Formations are present; in east-central Utah, in the San Rafael Swell area, the Page, Carmel, Entrada, Curtis, and Summerville are present; in southeastern Utah, east of the Monument Uplift, only the Entrada and Wanakah Formations are present (figs. 1.1; figs. 2.1-2.4). Present components of the San Rafael Group in southern Utah were distinguished as recessed cliffs and slopes between the White Cliff Group and Cretaceous strata. They were included within the Triassic-Jurassic System and were named the Flaming Gorge Group by Powell (1876) in the Uinta Mountains, northeastern Utah.

In 1899, Cross named the McElmo Formation for a similar interval of Jurassic rocks in southwestern Colorado and northwestern New Mexico. Gregory (1917) tenuously extended the McElmo interval into northeastern Arizona and southwestern Utah where Moore (1922) and

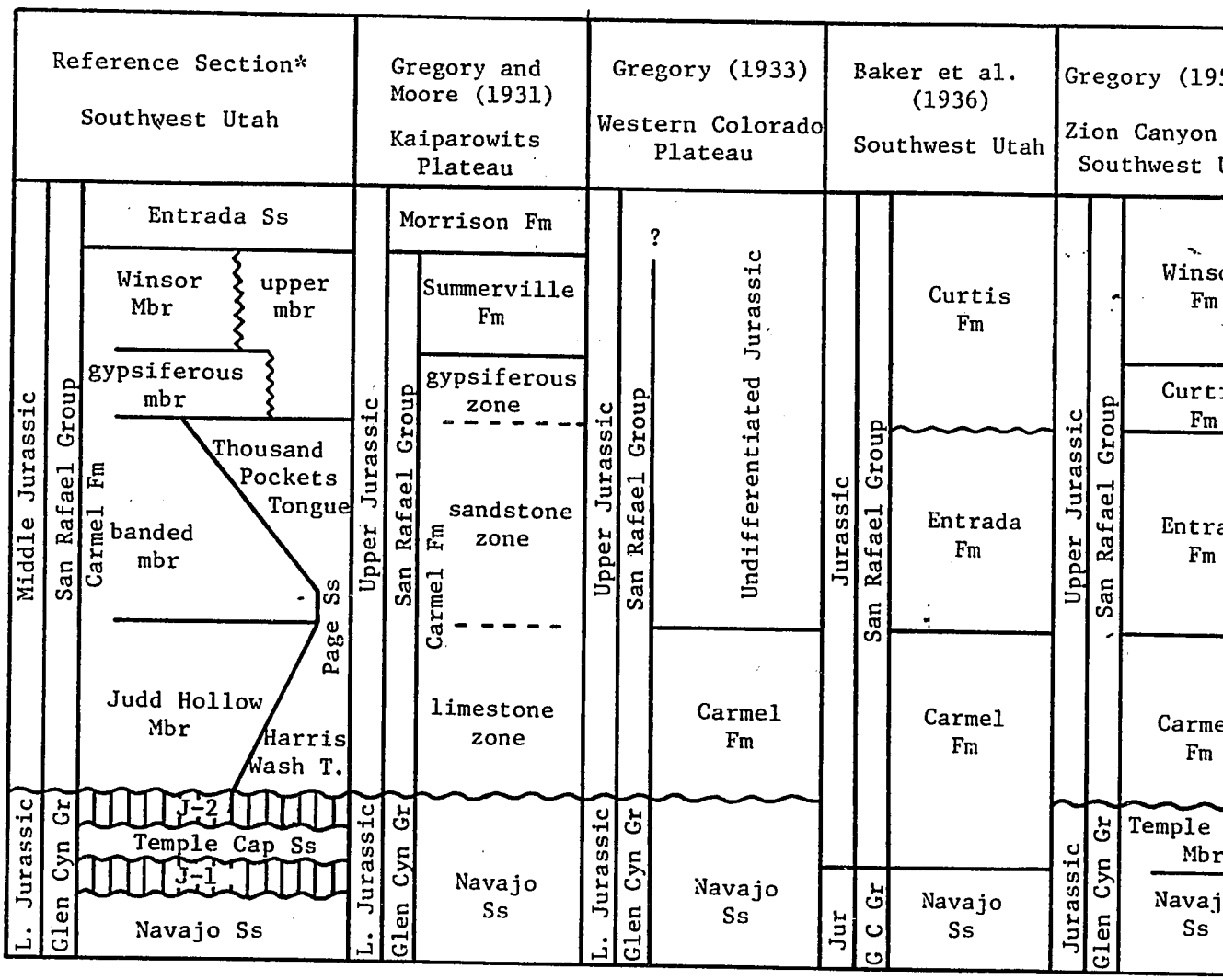

Figure 2.3. Chronological review of stratigraphic nomenclature of the Jurassic system as
Intervals are not to scale. *Modified from Peterson and Pipiringos (1979) and Blakey et

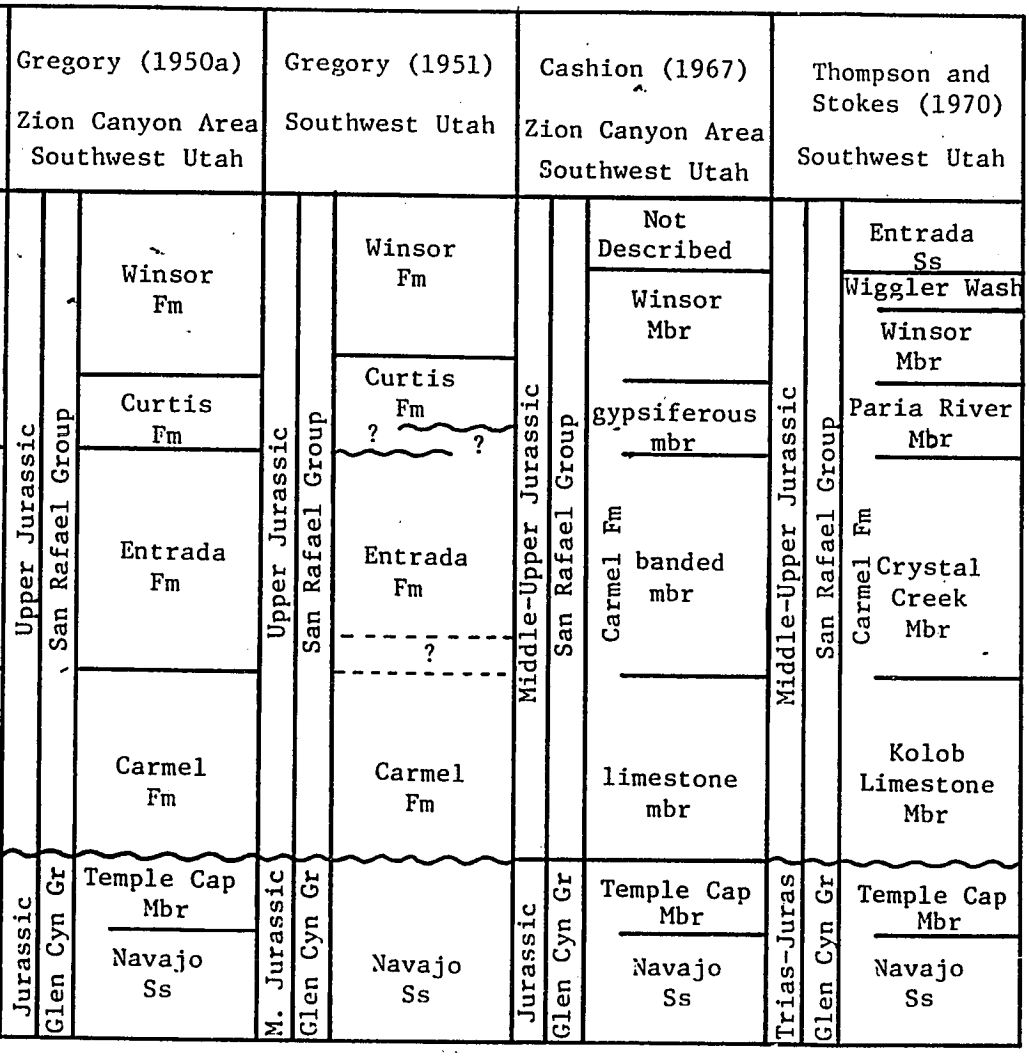

sic system as applied by various workers in southwestern Utah.
ad Blakey et al. (1983)

Longwell et al. (1923) later restricted the McElmo to the upper part of the interval of Gregory (1917).

The original San Rafael Group was named by Gilluly and Reeside (1928) for exposures in the northern and eastern portions of the San Rafael Swell in east-central Utah. At localities named Entrada Point, Curtis Point, and Summerville Point, they respectively designated the Entrada Sandstone, Curtis Formation and Summerville Formation with the Carmel Formation as the components of the San Rafael Group.

Carmel Formation. The history of nomenclature for the Carmel was reviewed by Caputo (1980); it is summarized in Figure 2.3 herein because there were miscorrelations involving the Entrada, Curtis, and Summerville Formations. Gregory et al. (1926) proposed the name Carmel for a sequence of calcareous and gypsiferous shales above the Navajo and designated an exposure observed by Gregory and Noble (1923), just east of Zion Canyon at Mt. Carmel, as the type section. This section was not described until 1931 by Gregory and Moore.

Temple Cap and Page Sandstones. The Temple Cap and Page Sandstones, as newly recognized units of the San Rafael Group, are related to the confirmation of regional Jurassic unconformities present throughout the western Colorado Plateau region. Cross-bedded sandstones and gypsiferous sandstone and mudstone present above the Navajo in Zion National Park were considered basal units of the Carmel by Baker et al. (1936) (fig. 2.3) but later designated as the Temple Cap Member of the Navajo by Grater (1948). Peterson and Pipiringos (1979) recognized the Temple Cap as a distinct, mappable unit separated from the underlying Navajo by the J-1 unconformity and from the overlying Carmel

by the J-2 unconformity. After raising it to formation status, they assigned the name Temple Cap Sandstone and included it as the oldest unit of the San Rafael Group (fig. 2.1).

The pink and gray cross-bedded sandstone interval now known as Page Sandstone was originally considered as the uppermost part of the Navajo in southwestern Utah (Phoenix, 1963; Wright and Dickey, 1963a). Since the J-2 unconformity also separates this interval from the Navajo it was also raised to formation status and included with the San Rafael Group as the Page Sandstone (Peterson and Pipiringos, 1979). Interfingering of the Judd Hollow and banded Members of the Carmel with the Thousand Pockets and Harris Wash Tongues of the Page suggest an origin for the Page contemporaneous with the lower Carmel.

Entrada Sandstone. The type-Entrada in the San Rafael Swell was miscorrelated in southwestern Utah and mistaken for the present banded member of the Carmel by Baker et al. (1936), and Gregory (1950a, b; 1951). In southeastern Utah, distinct upper, middle, and lower units were recognized in the Entrada. Lee, in an unpublished report (cited in Baker et al., 1927) referred to sandstones in the uppermost part as the Moab Sandstone Tongue. Since then, this unit has been called the Moab Tongue or Moab Member in later reports. In the middle part, red, earthy siltstones grade eastward into clean cross-bedded sandstones (Baker et al., 1936; McKnight, 1940). The informal names, earthy siltstone or red earthy facies, have been retained; an upper unit of this siltstone has been termed the Beds at Goblin Valley in the San Rafael Swell and Green River Desert areas (Baker, 1946; O'Sullivan,1980a). In the Green River Desert, where the earthy siltstone grades into the cross-bedded sandstone, the middle unit of

the Entrada has been named the Slick Rock Member (Wright et al. 1962). Beds believed to be the easternmost extension of the upper Carmel Formation are known as Dewey Bridge Member (Wright et al., 1962), the lowermost member of the Entrada which overlies the Navajo Sandstone.

Wanakah Formation. The Wanakah Formation, as a component of the San Rafael Group, is restricted to exposures of middle Jurassic rocks east of the Monument Uplift in southeastern Utah and western Colorado. Strata now recognized as the Wanakah were miscorrelated by Baker et al. (1947) in southeastern Utah and western Colorado as the Summerville Formation. The name, Wanakah, was first applied by Burbank (1930). Later, Goldman and Spencer (1941), Fischer (1942), and Baker et al. (1947) defined a sequence of limestone, gypsum, sandstone and shale between the Entrada Sandstone and Morrison Formation as the Wanakah throughout northeastern Arizona, northern New Mexico, and southwestern and southeastern Colorado (Imlay, 1952a). A type locality was designated in the Ouray mining district of southwestern Colorado for exposures in the Wanakah mine (Northrop, 1973). More recent stratigraphic studies by O'Sullivan (1980a) indicated that the Summerville of the San Rafael Swell area becomes bevelled-out progressively eastward by the J-5 unconformity at the base of the Morrison. The name, Summerville, has therefore been restricted to strata between the Curtis and Morrison west of the Monument Uplift and the name, Wanakah, has been extended from southwestern Colorado for those strata previously correlated as Summerville between the Entrada and Morrison east of the Monument Uplift, in San Juan County, southeastern Utah (O'Sullivan, 1980a). The Wanakah of southeastern Utah is thought to be older than the Summerville and equivalent only to the

Curtis-Moab interval and to upper parts of the Entrada Sandstone (Peterson, 1987) (figs. 2.1, 2.2, 2.4).

Curtis Formation. The Curtis, like the Entrada, was miscorrelated from the San Rafael Swell into the Zion Canyon area where a zone of gypsiferous beds, the present gypsiferous member of the Carmel (Cashion, 1967), was mistaken for the Curtis by Gregory (1950a, 1951) (fig. 2.3). However, in east-central Utah, the Curtis Formation has been mapped as originally designated by Gilluly and Reeside (1928).

Summerville Formation and Romana Sandstone. Beds now known as the Winsor and upper Members of the Carmel (Peterson and Pipiringos, 1979) in southwestern Utah were thought to be the Summerville of the San Rafael Swell by Gregory and Moore (1931) (fig. 2.3). In the area between the Green and Colorado Rivers in east-central Utah, McKnight (1940) described how greenish-gray sandstone beds in the Curtis grade into red sandstone and siltstone beds considered to be in the lower Summerville. These redbeds extend eastward and grade into the Moab Tongue. O'Sullivan (1980a) recognized this relationship and referred to these redbeds as the lower Summerville of McKnight (1940) in reports. Where this lower Summerville is divided in two by the Moab Tongue, O'Sullivan (1980a) has informally named the subdivisions as upper and lower redbeds. O'Sullivan (in prep.) futher distinguished the lower Summerville of McKnight (1940) as the Dubinky unit (Peterson, U.S.G.S, Denver, Colorado, pers. comm., 1985).

In the Kaiparowits Plateau region of south-central Utah, the Romana Sandstone has been recognized as a new formation between the Entrada and Morrison Formations (Peterson, 1987). It is lithologically distinct from and is laterally equivalent to the Summmerville and is

included in the San Rafael Group (figs. 2.1, 2.2).

Morrison Formation

The upper part of the Flaming Gorge Group of Powell (1876) and the McElmo Formation of Cross (1899) eventually became known as the Morrison Formation. Cross (1894) first used the name, Morrison, in published reports. However, Eldridge (1896) defined the interval and designated the type section near the townsite of Morrison, Colorado. As early as 1914, Lupton recognized a lower member of the so-called McElmo and named it the Salt Wash Sandstone Member. This unit included the interval from the crossbedded gravelly sandstone beds down to the interbedded mudstone, limestone, gypsum overlying the Summerville and has been known as the Salt Wash Member of the Morrison in later reports. The name, Tidwell Member (O'Sullivan, 1984), has been assigned to this lower interbedded sequence because it is lithologically distinct from the Salt Wash Member (Peterson, in press) (figs. 2.1, 2.2).

Gregory (1938) recognized successively younger units within the Morrison and designated the Recapture, Westwater Canyon and Brushy Basin as members. In southeastern Utah, the Bluff Sandstone Member (Gregory, 1938) is stratigraphically equivalent to the Salt Wash-Tidwell interval. Lastly, Peterson (in press) named the Fiftymile Member of the Morrison in the Kaiparowits area where it is distinguished from the Brushy Basin and Salt Wash Members (fig. 2.2).

Age

From stratigraphic relationships and the occurrence of nondiagnostic fossils, a general Jurassic age had been established for the Flaming Gorge and La Plata Groups and the McElmo Formation (fig. 2.2). In 1961, Lewis et al. reassigned most of the Glen Canyon Group to the Triassic Period based on reptilian fossils of Triassic age found in the Kayenta Formation. They considered the lower part of the Navajo as Triassic age because of interfingering with the Kayenta; the Triassic-Jurassic boundary had been tentatively placed in about the middle of the Navajo. A lower Jurassic age was assigned to the upper part of the Navajo which was thought to interfinger with the lower Carmel of known Middle Jurassic age. It is now accepted that the Carmel and Navajo do not intertongue but are separated by the J-2 unconformity of Pipiringos and O'Sullivan (1978). The dating of palynomorphs as Jurassic in the Moenave Formation (Peterson et al., 1977; Peterson and Pipiringos, 1979) placed the Glen Canyon Group entirely within the Lower Jurassic.

The Judd Hollow Member at the base of the Carmel is considered early Middle Jurassic (Bajocian) based on molluscan fossils (Imlay, 1964, 1965; Sohl, 1965) and refinement of Jurassic ammonite assemblages (Imlay, 1980).

Prior to the regional stratigraphic work of Pipiringos and O'Sullivan (1978), the Late Jurassic age of the Curtis had been based on collections of echinoderm and molluscan fossils, including ammonites, from the San Rafael Swell and Uinta Mountains (Reeside, 1923; Gilluly and Reeside, 1928). Diagnostic fossils including ammonites of the Cardioceras cordiforme faunal zone of lower Oxfordian

age (Pipiringos and O'Sullivan, 1978; Imlay, 19870) and other molluscs were collected from a unit thought to be the Curtis in the Uinta Mountains. Pipiringos and O'Sullivan (1978) have correlated this unit with the Redwater Shale Member of the Sundance Formation in Wyoming and northeastern Colorado (see Correlation, this chapter) because of its fossil contents and its position above the Jurassic J-4 unconformity (see Unconformities, this chapter). Moreover, they stated how these diagnostic fossils have been used erroneously to date the Curtis and Summerville in the San Rafael Swell. Other than locally occurring trace fossils and echinoderm and molluscan fragments described in this report, diagnostic fossils have not been found in the Curtis-Summerville interval to date. Those fossils occurring in the Curtis of the San Rafael Swell are nondiagnostic and cannot be used confidently to date the Curtis-Summerville. The Curtis in the Uinta Mountains unconformably overlies the Entrada of early to middle Callovian age and is unconformably (J-4 unconformity) overlain by the Redwater Shale of early to middle Oxfordian age; these relationships indicate a late middle or early late Callovian age for the Curtis and overlying Summerville, and preclude an Oxfordian age (Pipiringos and O'Sullivan, 1978). Because the Moab Tongue is thought to be equivalent to the middle and upper Curtis (Local Stratigraphic Setting, this chapter), it is herein considered late middle or early late Callovian in age.

The Middle Jurassic Epoch is subdivided into Aalenian, Bajocian, Bathonian, and Callovian ages (Kent and Gradstein, 1985) and lasted approximately 24 million years. Absolute time boundaries for the Callovian age are determined with uncertainty. Van Hinte (1976) has suggested that the Callovian age began 156 million years ago and ended 149 million years ago. Kent and Gradstein (1985) have suggested that

the Callovian began 169 million years ago and ended 163 million years ago. In southern Utah, the San Rafael Group comprises the entire middle Jurassic series of rocks and ranges in age from lower Bajocian to early late Callovian (Imlay, 1980) (fig. 2.1).

Unconformities

Unconformable stratigraphic relationships between certain Mesozoic strata in southern Utah have been noted since the study by Gilbert (1880) who recognized the truncation at the top of the Shinarump Group, now known as the Chinle Formation. Baker et al. (1927) described the erosional relief at the top of the Navajo Sandstone and truncated strata at the top of the Summerville (fig. 2.2).

The study by Pipiringos and O'Sullivan (1978) combined 20 years of detailed stratigraphic mapping to define the nature and regional extent of erosional horizons which punctuate Triassic and Jurassic sedimentary rocks in the Western Interior. The Jurassic unconformities are: J-0, J-1, J-2, J-3, J-4, and J-5, in order of decreasing age. In east-central Utah only the Jurassic J-0, J-2, J-3, and J-5 unconformities are present (figs. 2.1, 2.2). The J-1 unconformity is restricted to southwest Utah, in the Zion Canyon region (not shown on figure 1.1), where it separates the Temple Cap Sandstone from the Navajo Sandstone (Pipiringos and O'Sullivan, 1978; Peterson and Pipiringos, 1979) (figs. 2.1, 2.2, 2.3). The J-4 unconformity does not extend into east-central Utah because it is truncated essentially southward by the J-5 unconformity, particularly in northeastern Utah, in the Uinta Mountains area (Pipiringos and O'Sullivan, 1978).

Lower and upper contacts of the Glen Canyon Group are delimited by the J-0 and J-2 unconformities respectively and locally by the J-1 surface (figs. 2.1, 2.2, 2.4). Pipiringos and O'Sullivan (1978) estimated that the amount of time represented is 7-10 m.y. along the J-2 surface. These estimates depend on the exact ages of enclosing rock units and represent time elapsed during crustal deformation and erosion.

There were pauses in sedimentation and possibly episodes of uplift and erosion before, during, and after deposition of the San Rafael Group as evidenced by the J-2 and J-3 unconformities. The Temple Cap Sandstone in the lower San Rafael Group is completely enclosed by unconformity surfaces. It overlies the Navajo Sandstone along the J-1 surface; both J-1 surface and Temple Cap Sandstone are bevelled by the J-2 unconformity, the most widespread erosional surface at the base of the San Rafael Group. About 2-3 m.y. elapsed during uplift and erosion along the J-1 surface and deposition of the Temple Cap (Pipiringos and O'Sullivan, 1978).

Previous observations on the unconformity between the Curtis and the Entrada were questioned by Baker (1946) who suggested that local bevelling at the top of the Entrada was related to hydroplastic folding contemporary with the Curtis and unrelated to pre-Curtis tectonic tilting and erosion. Wright et al. (1962) indicated unconformable relationships between the Curtis and Entrada in cross-sections but did not offer stratigraphic evidence. They have described an erosional surface between the Moab and the Slick Rock Members of the Entrada that bevels low-amplitude undulations in beds of the Slick Rock. However, the unconformity is not shown in their cross sections. Pipiringos and O'Sullivan (1978) positively defined the J-3 unconformity between the

Curtis and Summerville based on the regional presence of chert clasts; they estimated a period of less than 1 m.y. between uplift and erosion of the Entrada and deposition of the Curtis.

The J-4 unconformity, as recognized by Pipiringos and O'Sullivan (1978) in Montana, South Dakota, Wyoming, northeastern Utah, and northwestern Colorado, is truncated by the J-5 unconformity at the base of the Morrison just south of the Uinta Mountains and therefore is not recognized in eastcentral Utah. In the Uinta Mountains, the J-4 unconformity divides the formerly-known Curtis interval into two parts (Pipiringos and O'Sullivan, 1978). The upper part is equivalent to the Redwater Shale Member of the Sundance Formation and Redwater Member of the Stump Formation based on fossil content, lithologic aspects, and position above the J-4 unconformity; the lower part beneath the J-4 is correlated with the type-Curtis in the San Rafael Swell (fig. 2.4) (also see Age, this chapter). The amount of time represented along the J-4 surface is estimated at less than 1 m.y. (Pipiringos and O'Sullivan, 1978).

Pipiringos and O'Sullivan (1978) recognized the J-5 unconformity at the base of the Morrison Formation or Sundance Formation throughout most of the Western Interior. In east-central Utah, the J-5 is recognized by erosional relief and truncation of low-amplitude undulations at the top of the Summerville. In southwestern Utah, the J-5 is truncated by the K-1 Cretaceous unconformity at the base of the Dakota Sandstone. The depositional hiatus represented by the J-5 is estimated at less than 2 m.y. (Pipiringos and O'Sullivan, 1978).

Correlation

Correlation of Callovian-age and related Jurassic rocks of the Western Interior region is illustrated in Figure 2.4. The Curtis-Summerville-Moab interval is correlative with middle and upper parts of the Sundance Formation and Stump Sandstone in northeastern Utah, western Colorado, southeastern Idaho, and southwestern South Dakota, and the upper part of the Entrada and Wanakah Formations of western Colorado and northwestern New Mexico. In the Henry Mountains region (fig. 1.1), the newly named Romana Sandstone is considered equivalent to the Summerville Formation. Stratigraphic intervals of southern and western Nevada only include the Aztec Sandstone (Navajo Sandstone equivalent), Sunrise Formation, Dunlap Formation, and Boyer Ranch Formation of Lower Jurassic (Hettangian to Toarcian) age and the Westgate Formation of Middle Jurassic (Bajocian) age; younger Jurassic strata have not been recognized.

Local Stratigraphic Setting

In east-central Utah, strata in the Curtis-Summerville-Moab interval are distinguished from strata in the underlying Entrada and overlying Morrison (fig. 2.1) by color, weathering pattern and profile, stratification style, and local angular unconformable relationships. The following discussion is made with reference to Figure 2.5 which illustrates the stratigraphic relationships within the Curtis-Summerville-Moab interval and the facies contained therein (see Chapter 3, Sedimentary Facies).

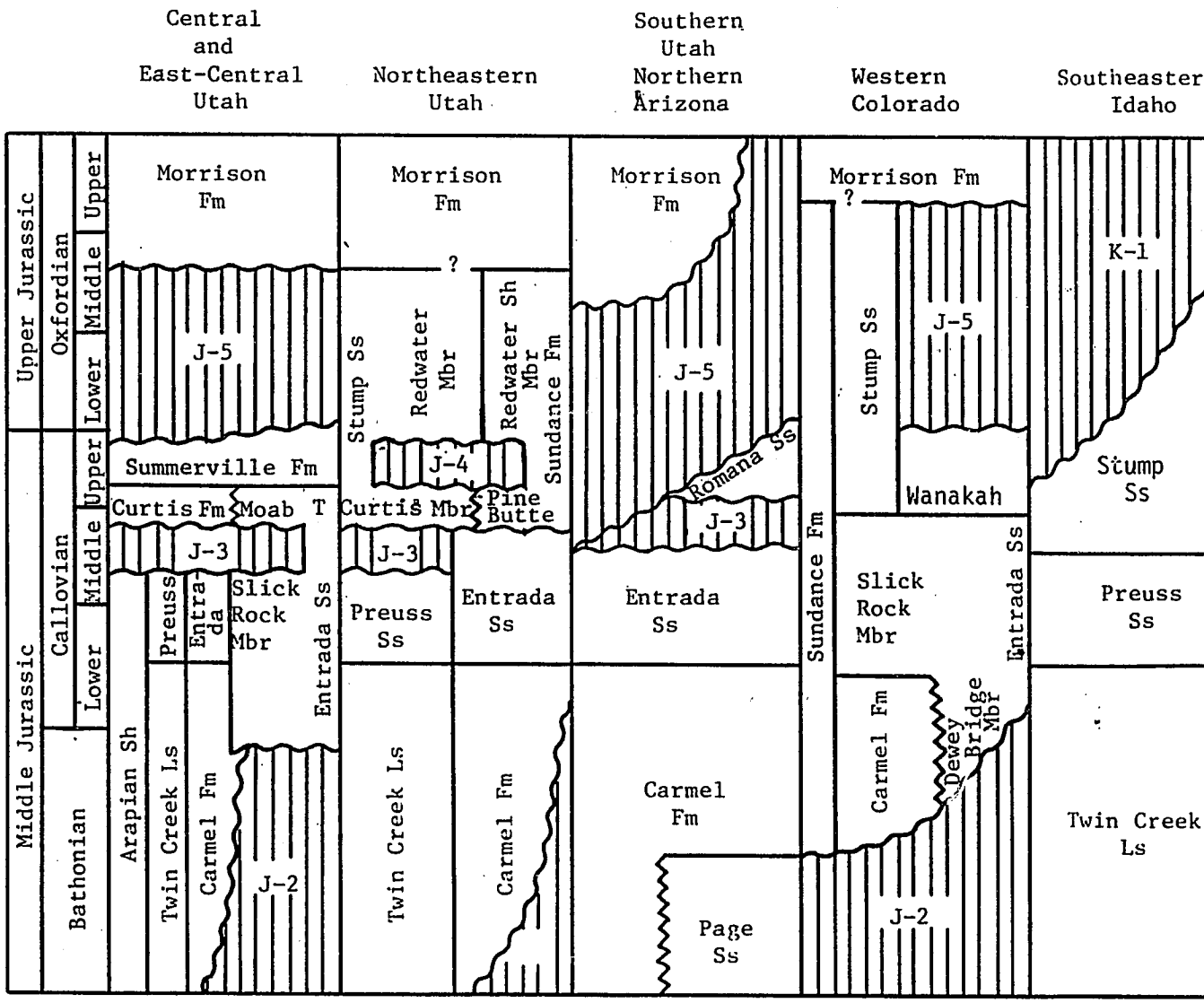

Figure 2.4. Correlation diagram of middle and upper Jurassic strata for parts of the Wes
Modified from Imlay (1952a, 1980), Pipiringos and O'Sullivan (1978), Peterson (1987), an

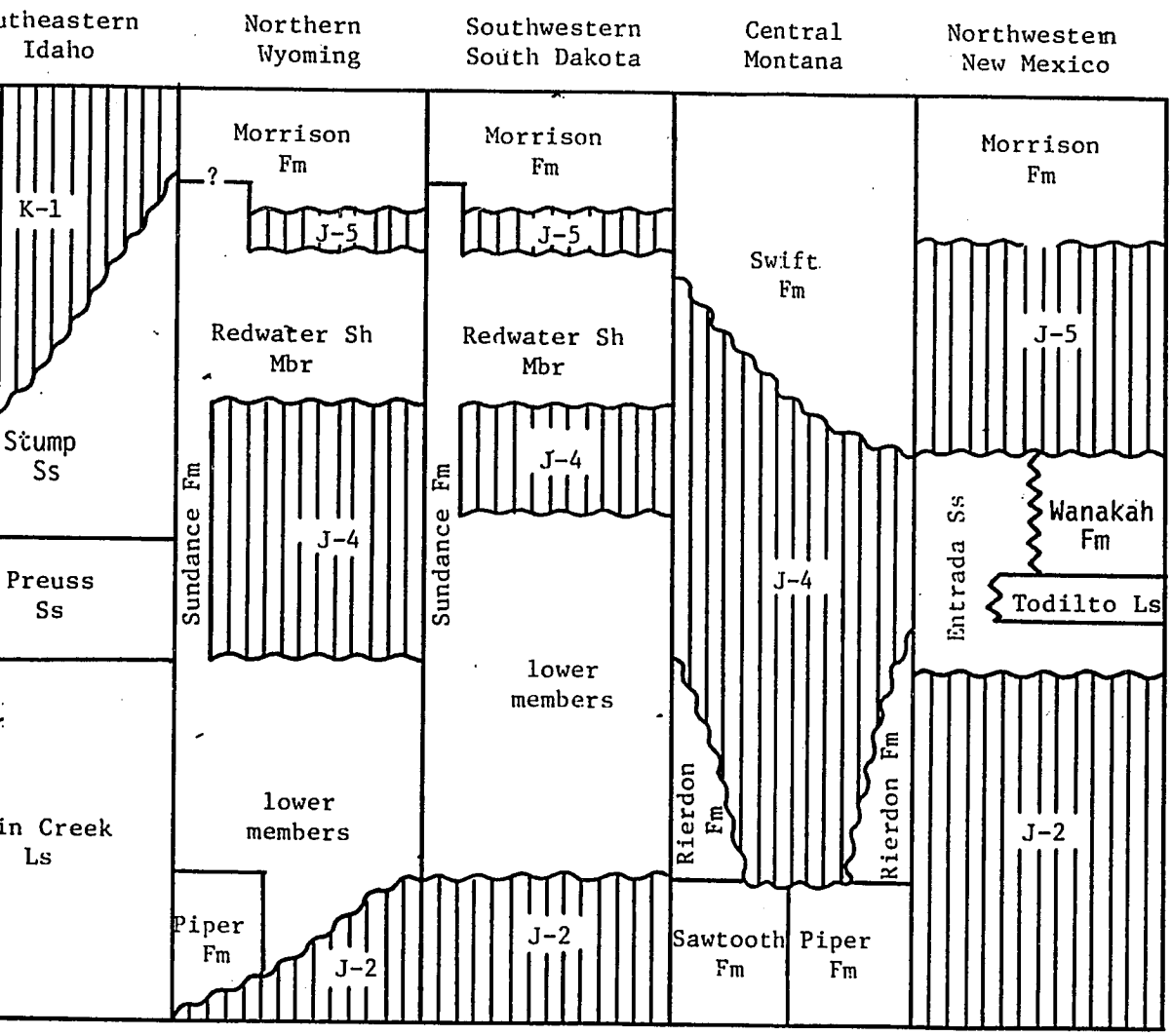

the Western Interior.
987), and Blakey (in press)

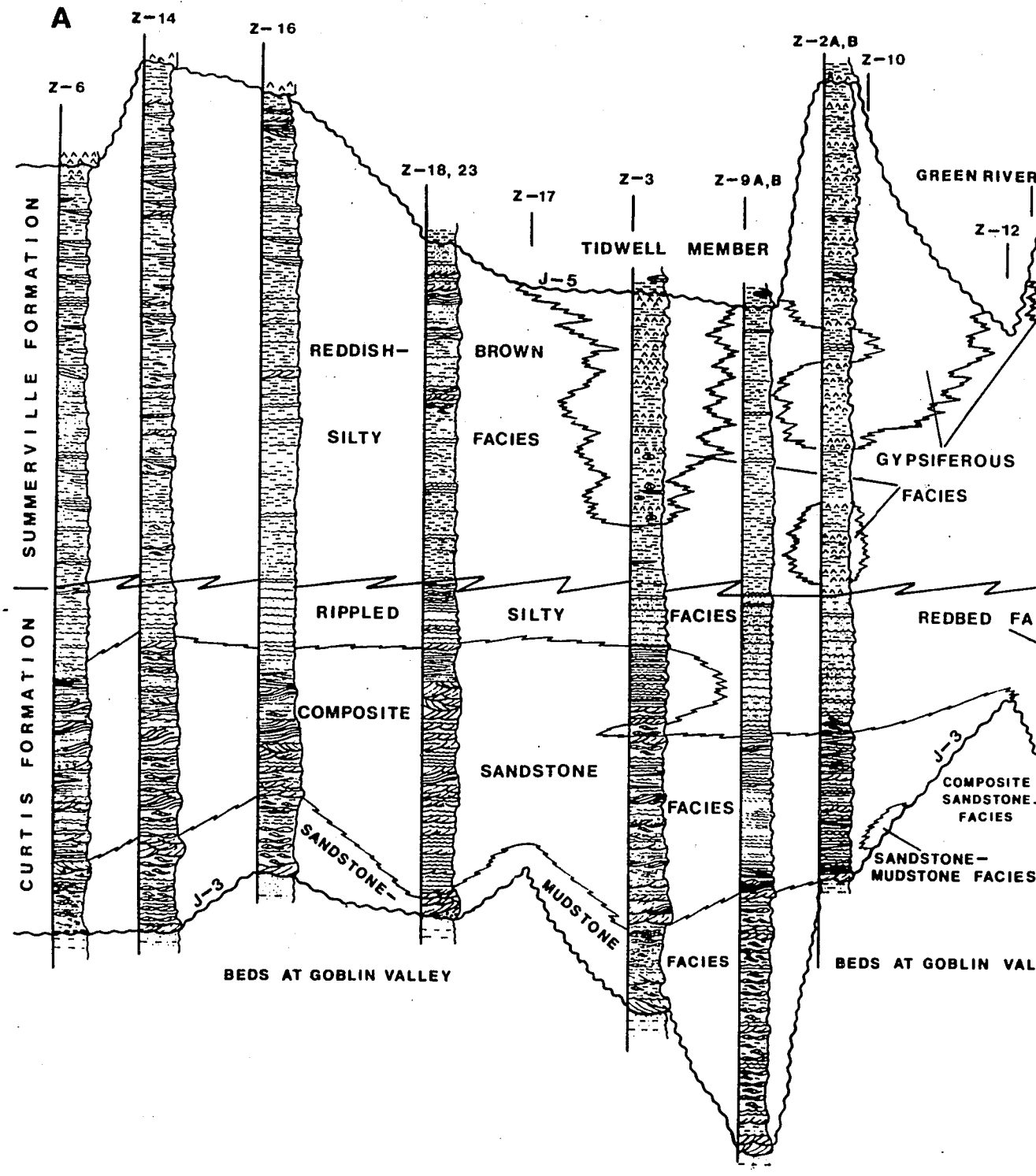

Figure 2.5. Facies and stratigraphic relationships of the Upper San Rafael Group and r

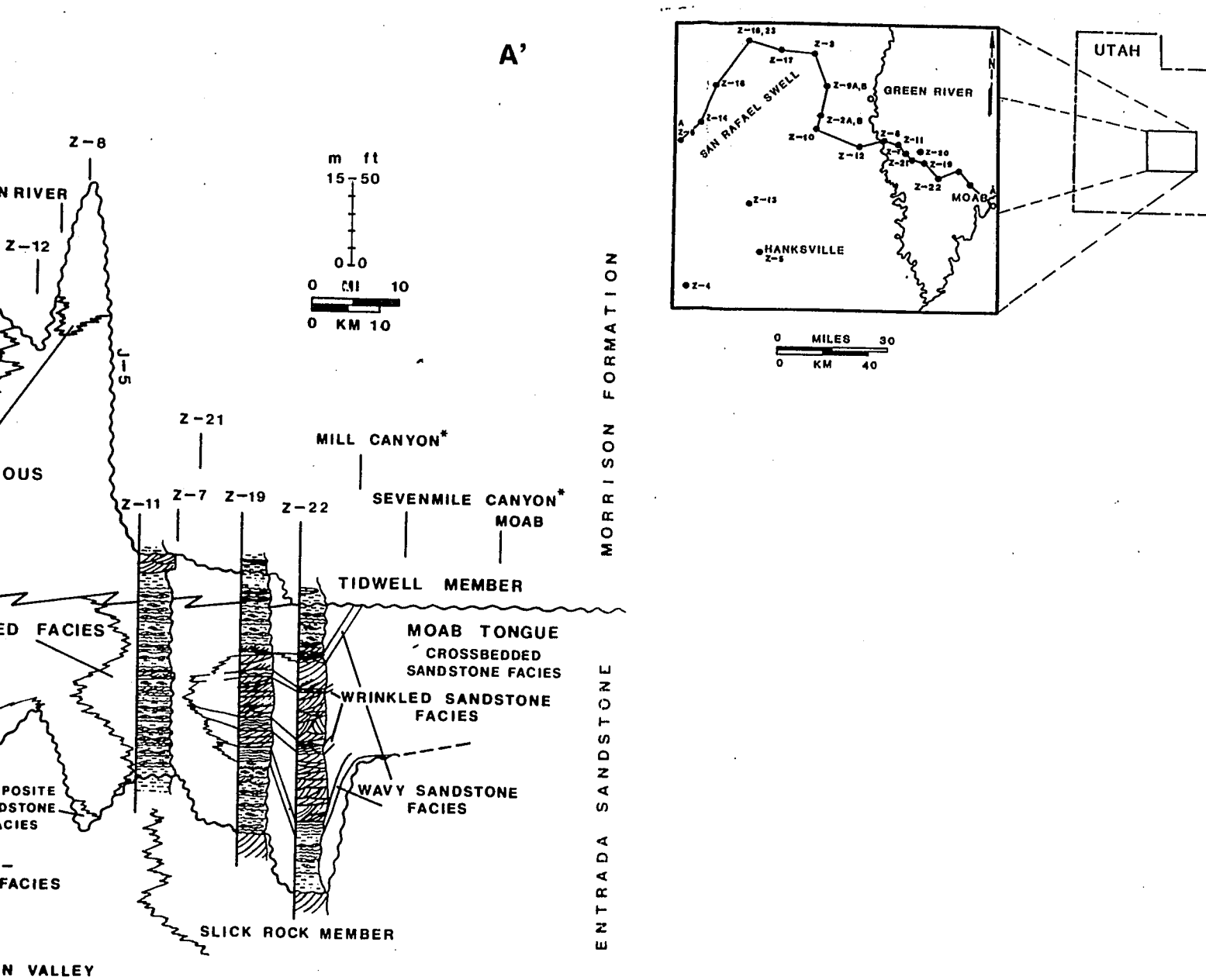

and related Jurassic strata in east-central Utah

Entrada Sandstone. The stratigraphic base of each vertical sequence studied herein coincides with the Curtis-Entrada contact which is also the J-3 unconformity surface. The units of the Entrada beneath this unconformity are the Slick Rock Member and the red, earthy siltstone facies or the Beds at Goblin Valley, so named because of the peculiar weathering forms called hoodoos, goblins or stone babies (fig. 2.6) best developed at Goblin Valley State Park (fig. 1.1). The dark red, cliff-forming Beds at Goblin Valley are present throughout the San Rafael Swell and northern Henry Mountains and grade eastward into the tan and pink, cliff-forming Slick Rock Member between White Wash and Duma Point (Z-11 and Z-7; fig. 1.1). Southeastward from this location toward the Moab area, the Slick Rock Member underlies the J-3 surface (fig. 2.5).

J-3 unconformity. The J-3 unconformity of Pipiringgs and O'Sullivan (1978) is clearly recognizable at most locations studied in east-central Utah. Exposures along the northern flank of the Henry Mountains at Hanksville (Z-5) and south of Pleasant Creek (Z-4) along the Waterpocket Fold show unequivocally the angular discordance between the Curtis and Entrada (fig. 2.7). Baker (1946) suggested that this angular relationship was a consequence of bevelling of broad bedding undulations produced by hydroplastic loading and folding of Entrada beds during Curtis sedimentation; hence a conformable relationship between the Entrada and Curtis was concluded. In most stratigraphic sections, the contact is planar and abrupt with a discrete color and textural change across the boundary. It is also characterized by reworked Entrada clasts and conglomerate beds in the base of the Curtis and local erosional relief of 1 to 3 feet (0.3 to 0.9m) at the top of

Figure 2.6. Weathering phenomenon called stone-babies along cliffs of Beds at Goblin Valley in the Entrada Sandstone (Jeb) below the Curtis Formation (Jcu). (San Rafael Swell Northeast, Z-3)

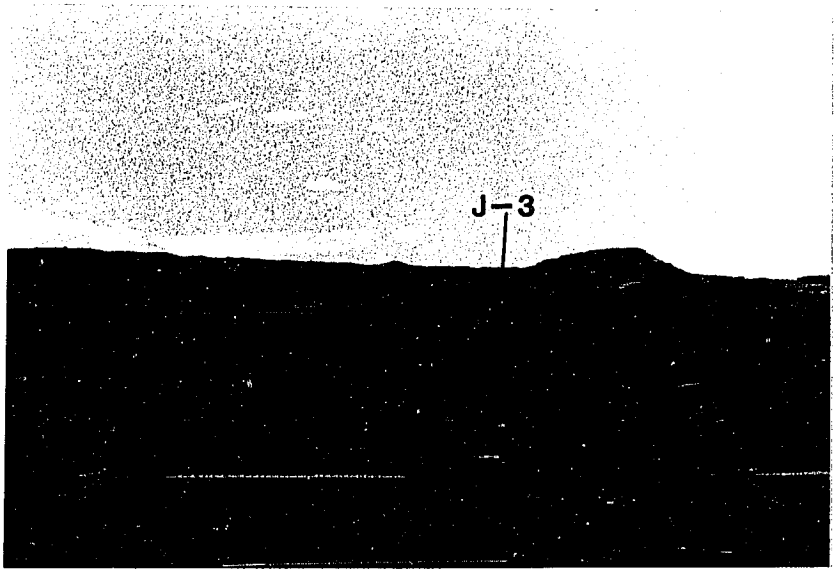

Figure 2.7. Angular discordance along the J-3 unconformity between Beds at Goblin Valley (Jeb) and Curtis Formation (Jcu) (Hanksville, Z-5)

the Entrada.

At North Salt Wash (Z-16), there are vertical and J-and U-shaped trace fossils in a bleached interval in the upper 1-foot (3 dm) of the Beds at Goblin Valley. These traces terminate at the contact and are filled with sandstone characteristic of the basal Curtis Formation (figs. 2.8a, b).

Some of the vertical traces had been unmistakeably produced by pelecypods as suggested by the trigonal outline, a feature of some burrowing clams. Some of the tube- and cone-shaped dwelling traces closely resemble those produced by boring organisms, particularly those with siphon tubes extending downward to bulbous dwelling chambers. Although, J-shaped borings can be excavated by polychaete annelids (Warme and McHuron, 1978), U-shaped borings have not been reported in studies on borings as trace fossils (Boekschoten, 1966; Bromley, 1978, 1975; Warme 1970; Warme and McHuron, 1978). Locally, the burrows resemble the preomission suite of trace fossils described by Bromley (1975) such that some traces have been truncated by a sedimentary event. Other burrows are locally continuous across the erosion surface and partially developed in the lower-most few centimeters of the Curtis. The sedimentary relationships between the traces and Curtis and Entrada beds suggest that infaunal organisms lived very early in the depositional history of the Curtis, probably during the initial transgression, and colonized a firm but unlithified substrate along the J-3 surface. Sedimentary events during Curtis time partially removed burrows and deposited the basal few centimeters of Curtis. This resulted in the omission surfaces of some burrows and the renewed burrow activity which extended up into the freshly deposited Curtis

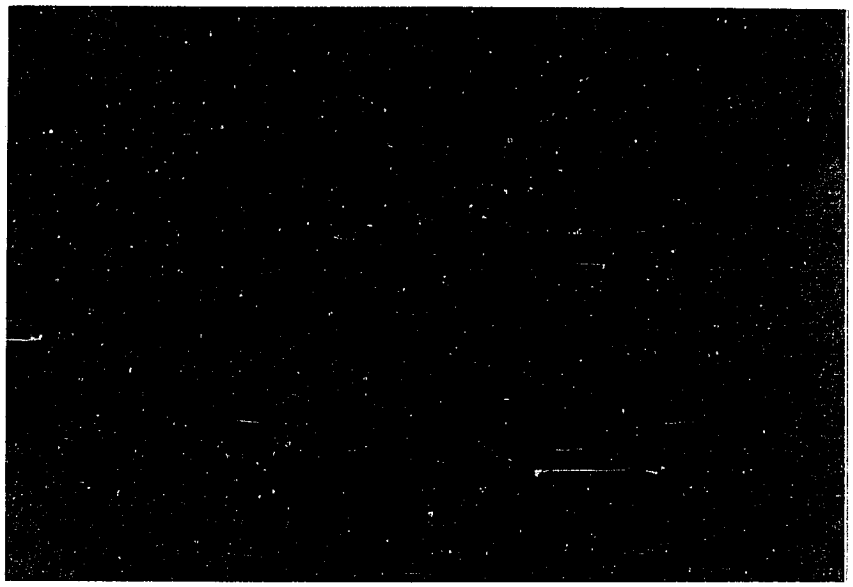

a.

b.

Figure 2.8. Vertical and J- and U-shaped trace fossils in the upper 1-foot (3 dm) of the Beds at Goblin Valley (Jeb) below contact (arrow) with the Curtis Formation (Jcu) (North Salt Wash, Z-16)

sediments as suggested by other burrows.

In the Green River Desert east of Dellenbaugh Butte (Z-8) where the redbed facies of the Curtis overlies Beds at Goblin Valley, the J-3 surface is difficult to recognize and interpret because bedding units form weathered slopes. Southeast of Duma Point (Z-7) the top of the Slick Rock Member has been bevelled and reworked; the horizon is marked by an abrupt color and textural change from tan and pink fine-grained cross-bedded sandstones in the Slick Rock to reddish-brown upward-fining bedding packages in the Curtis redbeds.

Stratigraphic relations between the Moab and Slick Rock Members of the Entrada as described by O'Sullivan (1980a, 1981c) are inconsistent with the transgresssive-regressive history of the Curtis-Summerville-Moab basin. The J-3 unconformity is not shown to be present southeast of the White Wash (Z-11) area. Field observations in this report suggest that the reworked and truncated surface at the top of the Slick Rock extends southeastward into the Mill Canyon area (Z-25) and even farther eastward into the Arches National Park region (Oakes, 1983; Kocurek and Oakes, 1985) The lower tongue of the Curtis redbeds thins down to 4.5 feet (1.35m) at Mill Canyon. Although not observed in this study, it is suspected that farther eastward in the Moab and Arches areas, the redbed interval is diminished to a thin band that may be traceable to where the Moab and Slick Rock Members are in direct contact with each other. This horizon is herein considered to be an extension of the J-3 unconformity. Conformity between Curtis and Entrada beds may exist farther west, near the center of the Jurassic basin, as a result of uninterrupted sedimentation related to partial regression during Entrada time. In contrast, it is likely that strata deposited to the east during the same regression, may have been

interrupted by non-deposition, reworking or erosion during the regression and onset of transgression. Kocurek and Oakes (written comm., 1986) have demonstrated the truncation of first-order (E-1) bounding surfaces of cross-bed sets at the top of the Slick Rock Member by the basal surface of the Moab Member. Such a diastem is either a regional bounding surface (Talbot, 1985; Kocurek and Oakes, 1985) or regional deflation surface (Loope, 1984b, 1985). Recognition of such surfaces adds an order above first-order to the hierarchy of bounding surfaces explained by Brookfield (1977) for eolian sandstones.

Curtis-Moab interval. The Curtis Formation directly overlies the J-3 surface throughout the San Rafael Swell and northern Henry Mountains and forms a distinctive gray cliff- and slope-forming interval between redbeds of the underlying Beds at Goblin Valley and redbeds of the overlying Summerville Formation (fig. 2.9). Although the Curtis interval becomes thin to the south and east, there is a significant facies transition between Dellenbaugh Butte and White Wash (Z-8 and Z-11, fig. 1.1). Here, greenish-gray ripple-laminated siltstones sandstones of the Curtis grade into a reddish-brown sequence of cyclically-occurring beds consisting of fine- and medium-grained sandstones fining-upward into siltstone and mudstone. These redbeds have been referred to as the lower Summerville (McKnight, 1940; Baker, 1946; Wright et al., 1962; O'Sullivan, 1980a) based on the reddish-brown color and the uniform, even-bedded character which are features very similar to those of the Summerville. Gard (1976), however, has assigned these beds to the Curtis. Field relations between the sequence of redbeds and the Curtis and Summerville are yet unclear. Observations in this study suggest that these redbeds lie stratigraphically below

Figure 2.9. Sequence of strata exposed at Molly's Castle (formerly called Molly's Nipple). Beds at Goblin Valley (Jeb), Curtis Formation (Jcu), Summerville Formation (Jsu). (Goblin Valley State Park near Z-13)

the Summerville, are equivalent to the middle and upper parts of the Curtis Formation and the entire Moab Tongue (fig. 2.5). However, they contain bedding units which are stratigraphically related to facies in the Curtis and Moab Tongue but display sedimentologic characteristics genetically related to the Summerville (Chapter 3, Sedimentary Facies). These redbeds seem to mark a zone of transition between processes and events related to the origin of the above intervals and can be thought of as facies of either the Curtis, Summerville, or Moab Tongue. Tentatively, these redbeds are included as a facies (redbed facies) of the Curtis Formation (figs. 2.2, 2.4).

At Duma Point (Z-7), the Curtis redbeds are present as an uninterupted reddish-brown, even-bedded succession. A conspicuous 4- to 5-foot (1.2-1.5 m) dark red ledge- and cliff-forming unit is exposed in about the middle of the section at White Wash (Z-11) and Duma Point (Z-7) (fig. 2.10). This unit has served as a useful stratigraphic marker in studies by O'Sullivan (1980a, b; 1981a, b, c), has been informally named the Bed at Black Steer Knoll (O'Sullivan, 1980b) and has been recognized as a bedding interval within the Wanakah Formation south of Moab in San Juan County, southeastern Utah. Southeastward from Duma Point, O'Sullivan (1980a, 1981c) has correlated the Bed at Black Steer Knoll in the Tenmile Canyon, Dubinky Well, and Bartlett Flat areas (Z-19, 20, 21, 22) with beds which are recognized in this study as beds of the upper part of the Moab Tongue. The correlation is justifiable because the Black Steer Knoll bed in the White Wash (Z-11) and Duma Point (Z-7) area contains stratification microsequences similar to and genetically related to the beds in the upper Moab Tongue southeast of Duma Point.

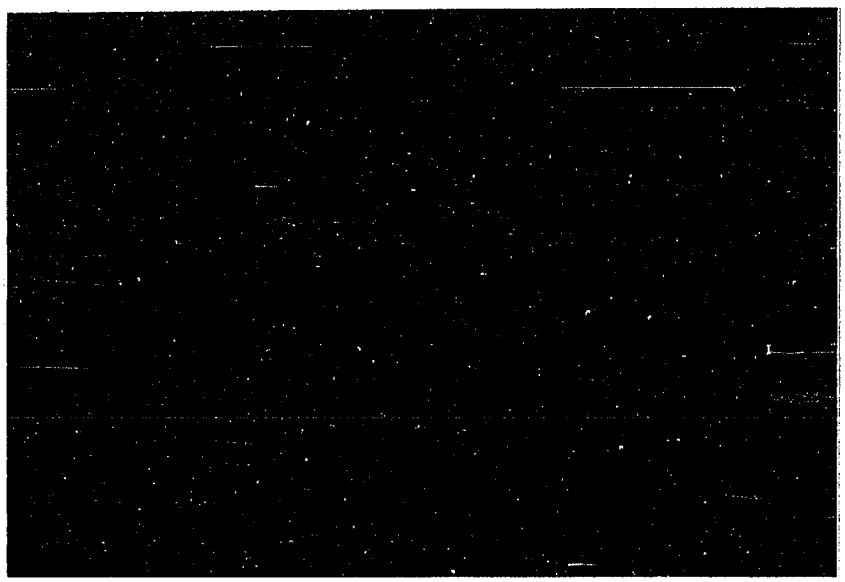

Figure 2.10. Bed at Black Steer Knoll (arrow) at Duma Point (Z-7). Slick Rock Member, Entrada Sandstone Jes), redbed facies, Curtis Formation (Jcu), Summerville Formation (Jsu), Morrison Formation (Jm)

The Moab Tongue of the Entrada is a light tan and light gray wedge-shaped interval that extends generally northwestward from the Moab-Arches area and interfingers with the Curtis redbeds in the Green River Desert area (fig. 2.11) It is distinguishable from the underlying pink and tan Slick Rock Member in color, lesser thickness, vertical fractures or joints, weathering pattern of rounded columns, and exposure as a tabular cliff slightly recessed above a distinctive notch or bench at the top of the Slick Rock Member. As it thins westward, it subdivides the Curtis redbeds into lower and upper tongues until at an inferred position just west of Tenmile Canyon South (Z-21), it is replaced by Curtis redbeds.

Summerville Formation. The Summerville Formation of the San Rafael Swell and adjacent east-central Utah is everywhere conformable over the Curtis Formation. Beds in the upper one-third of the Curtis contain a greater proportion of siltstone beds and show a progressive upward-fining character. Greenish-gray siltstones and mudstones at the top of the Curtis grade very noticeably into pinkish-gray siltstone and mudstone of the basal Summerville and ultimately into reddish-brown siltstones and mudstones (fig. 2.12).

In the Green River Desert area, the Summerville thins markedly between Dellenbaugh Butte (Z-8) and White Wash Z-11). From White Wash southeastward to Dubinky Well (Z-19), the Summerville is present as a thin interval of 20 feet (6m) or less between the overlying J-5 unconformity and the Curtis redbeds. In this area, outcrop expression and bedding style in the Summerville are very similar to those of the Curtis redbeds (fig. 2.13). However, the Summerville is characterized by dark brown and reddish-brown, randomly occurring siltstones and

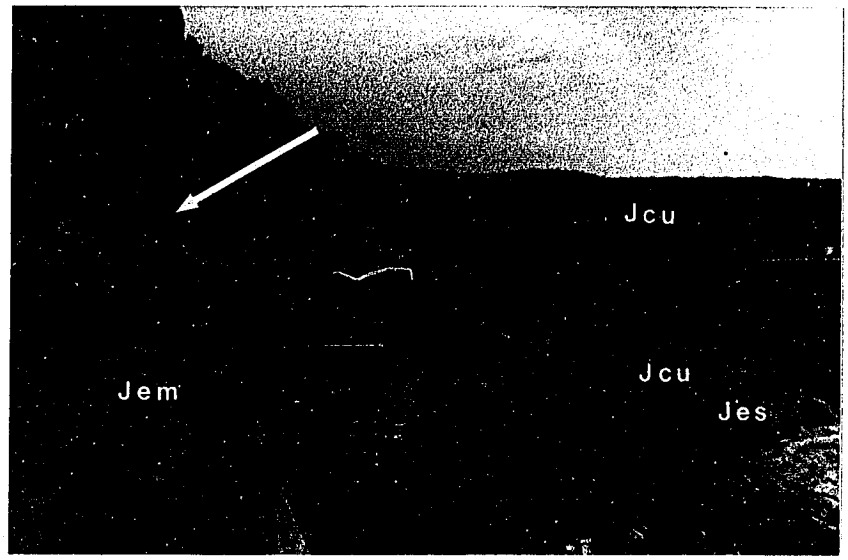

Figure 2.11. Moab Tongue (Jem) of the Entrada Sandstone interbedded with redbed facies of the Curtis Formation (Jcu) near Dubinky Well (Z-19). Person (arrow) in foreground for scale. Slick Rock Member, Entrada Sandstone (Jes)

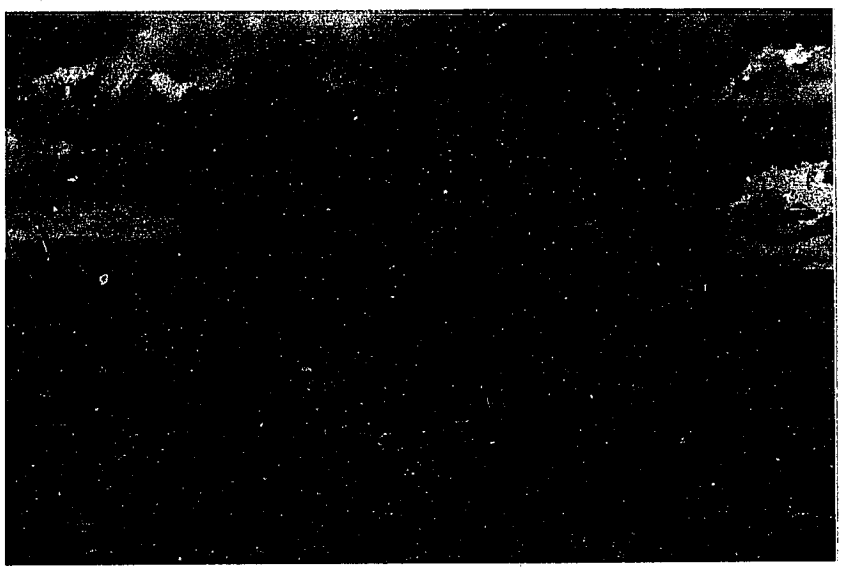

Figure 2.12. Slope-forming rippled silty facies in upper Curtis (Jcu, marked interval) grading into slope-forming, reddish-brown silty facies in the basal Summerville (Jsu) near San Rafael Swell Northeast (Z-3). Morrison Formation (Jm)

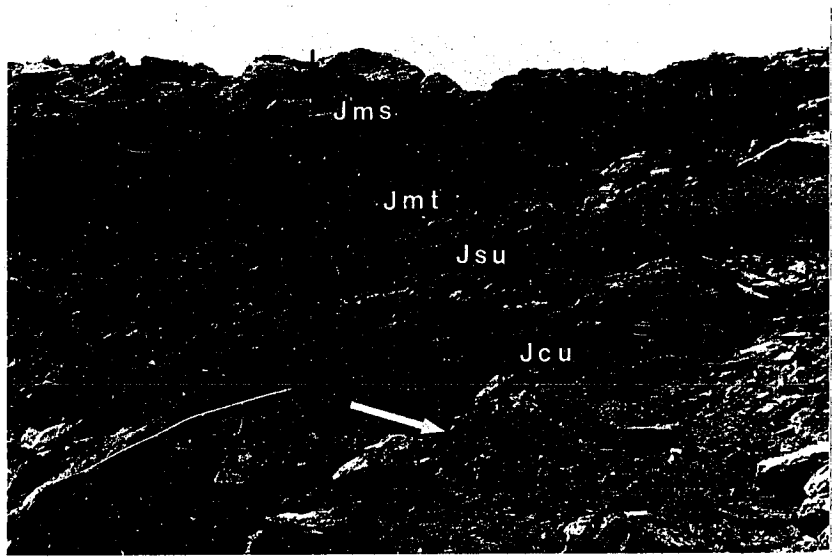

Figure 2.13. Stratigraphic similarity between redbed facies of the Curtis Formation (Jcu) and reddish-brown silty facies of the Summerville Formation (Jsu). Staff is marked in feet and person is in foreground for scale (arrows). Tidwell (Jmt) and Salt Wash (Jms) Members of Morrison Formation (Duma Point, Z-7)

mudstones interbedded with flaser-, lenticular-, and wavy-bedded sandstones and siltstones. In contrast, the Curtis redbeds are distinctly orangish-brown in color and are typified by cyclically occurring upward-fining bedding packages. The Summerville has been truncated by the J-5 unconformity and consequently is not present southeast of the Bartlett Wash area (Z-22) (O'Sullivan, 1980a).

J-5 unconformity and Morrison Formation. Erosional truncation by the J-5 unconformity at the top of the Summerville is evident along the Waterpocket Fold south of Pleasant Creek (Z-4), San Rafael Swell-East (Z-2A,B), and at Hatt Ranch (Z-10). What is typically seen are light-colored parallel beds at the top of Summerville successively terminated against a gently discordant angular unconformity (fig. 2.14).

A cliff-forming, generally inaccessible gypsum bed as thick as 20 feet (6m) is usually present in the basal Tidwell Member of the lower Morrison Formation (fig. 2.15). The bed forms a protective ledge above the Summerville and together with the angular discordance marks the contact with the Summerville. At locations such as Buckhorn Wash (Z-18, 23), San Rafael Swell-Northeast (Z-3), Tidwell Draw (Z-9A,B), Horse Bench (Z-12), and all sections east of the Green River, the unconformity is not clearly recognizable; local erosional truncation or relief is not developed. Gypsum beds in the Tidwell are either absent or not distinguishable from those in the upper Summerville; the angular discordance at the J-5 surface, apparent at other locations, is not visible. However, in these sections, uniformly parallel-bedded reddish-brown and tan beds of the Summerville are clearly distinct from ledge-forming, gray, lenticular micrites (cf. micstone or lithographic limestone) and gray, lavender and pink slope-forming siltstones and

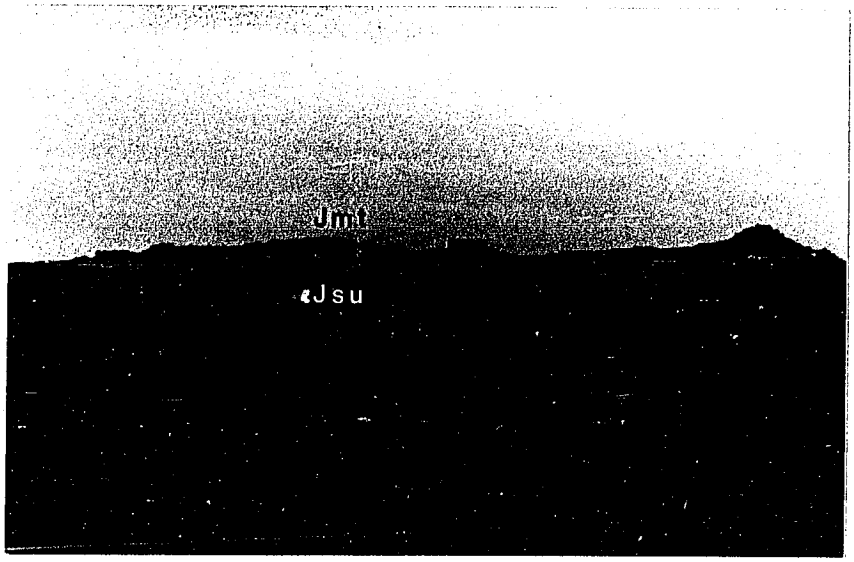

Figure 2.14. Gentle angular discordance between basal gypsum of Tidwell Member of the Morrison Formation (Jmt) and parallel beds in the Summerville Formation (Jsu) along the J-5 unconformity. View is to the south along Interstate 70, one mile west of San Rafael Swell East

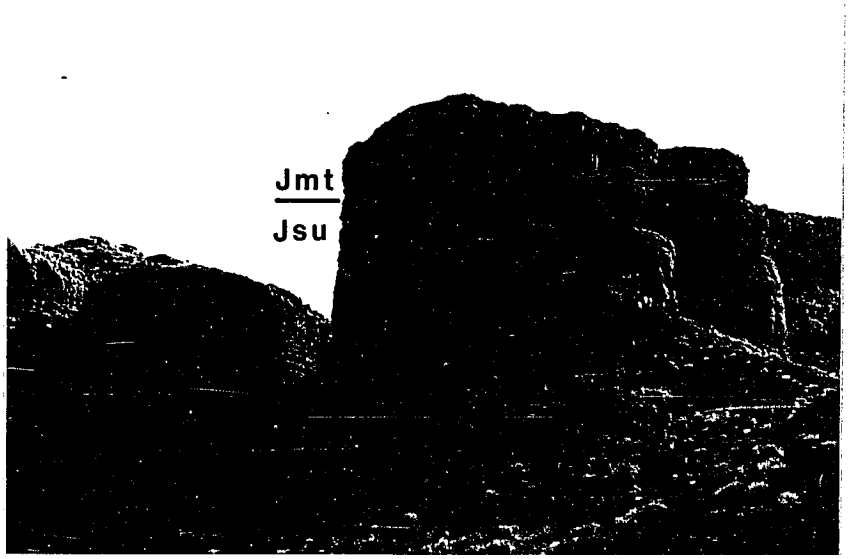

Figure 2.15. Uppermost Summerville Formation (Jsu) overlain by thick gypsum bed of basal Tidwell Member of Morrison Formation (Jmt) near Hatt Ranch Hunting Farm (Z-10B). Person (arrow) in foreground for scale

mudstones of the Tidwell Member. These Tidwell beds are abruptly overlain by gray, lenticular, trough cross-bedded sandy conglomerate beds of the Salt Wash Member.

CHAPTER 3

SEDIMENTARY FACIES

Curtis Formation

At the formation scale, the Curtis Formation generally appears as an evenly bedded, light greenish-gray sandstone. It weathers to a tan color and forms vertical cliffs continuous with the contrasting dark red, cliff-forming sandstones of the underlying Beds at Goblin Valley of the Entrada Sandstone (fig. 3.1). The upper part of the Curtis is mostly a silty sandstone which forms a weathered slope and grades upward into slope-forming red and tan beds of the Summerville Formation (fig. 2.12). Toward the east, especially between Dellenbaugh Butte (Z-8) and White Wash (Z-11), light greenish-gray beds typical of the Curtis are gradually replaced by redbeds at the eastern margin of the Curtis. Farther east, these Curtis redbeds then become interbedded with tan and gray sandstones of the Moab Tongue of the Entrada Sandstone between Tenmile Canyon South (Z-21) and Duma Point (Z-7)(figs. 1.1, 2.5).

Complete stratigraphic sections of the Curtis were examined along the flanks of the San Rafael Swell. Facies were traced as far south as Pleasant Creek (Z-4) along the Waterpocket Fold on the west side of the Henry Mountains, and as far east as Mill Canyon (Z-25) in the Green River Desert (fig. 1.1).

At the macrosequence scale (a term denoting an orderly succession of beds on the order of several tens of meters thick, Terwindt, 1981),

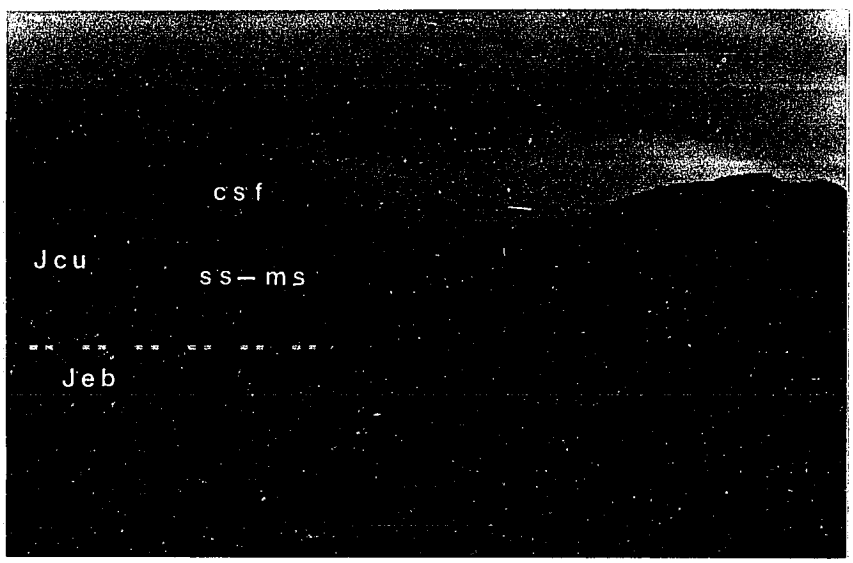

Figure 3.1. Columnar weathering pattern of cliff-forming Beds at Goblin Valley (Jeb) and Curtis Formation (Jcu) at San Rafael Swell East (Z-2). Sandstone-mudstone facies (ss-ms), composite sandstone facies (csf), rippled silty facies (rsf)

the lower half of the Curtis is an upward-coarsening macrosequence and the upper half together with the Summerville Formation is an upward-fining macrosequence. Facies in the Curtis are characterized by lateral-fining to the south and east. Figure 3.2 shows the ratio of cumulative thickness of sandstone beds to that of silty sandstone, sandy siltstone, siltstone, and mudstone beds in the Curtis.

At the facies scale, four facies are contained within the general macrosequences and include the following: a sandstone-mudstone facies, a composite sandstone facies, a rippled silty facies, and a redbed facies. At the microsequence scale (a term denoting an orderly succession of beds at the scale of several decimeters or meters, (de Raaf et al., 1977; Terwindt, 1981), the facies are composed of several heterogeneous or heterolithic microsequences which have distinguishable textural and bedding sequences. Sedimentological aspects of the facies and the microsequences contained therein are described in the following paragraphs beginning with thickness and paleocurrent trends.

Isopach Trends

Isopach maps, showing distribution and thickness trends, were constructed for different intervals in the Curtis from data in this report and other reports (Table 1.2). Although the map in figure 3.3 shows the distribution of both the Curtis Formation and Moab Tongue of the Entrada Sandstone, only the trends exhibited in the Curtis will be discussed in this section. Those in the Moab Tongue will be examined in a later section.

In figure 3.3, there are three main thickness trends within the Curtis. First, the Curtis interval generally becomes thin eastward from the western San Rafael Swell to the Green River Desert. Second, a thick

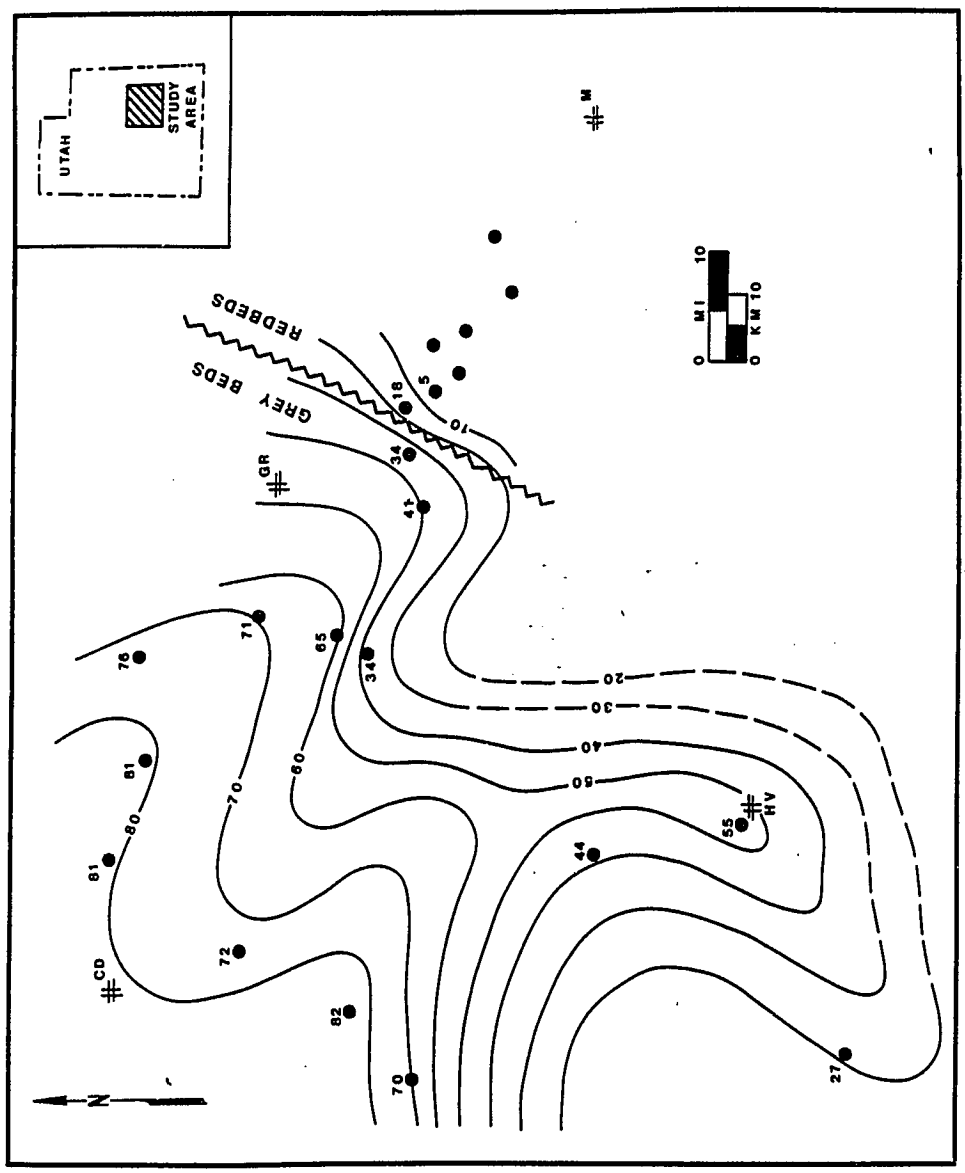

Figure 3.2. Percent net sandstone in the Curtis Formation. Contour interval: 10%.
Map symbols (table 1.3)

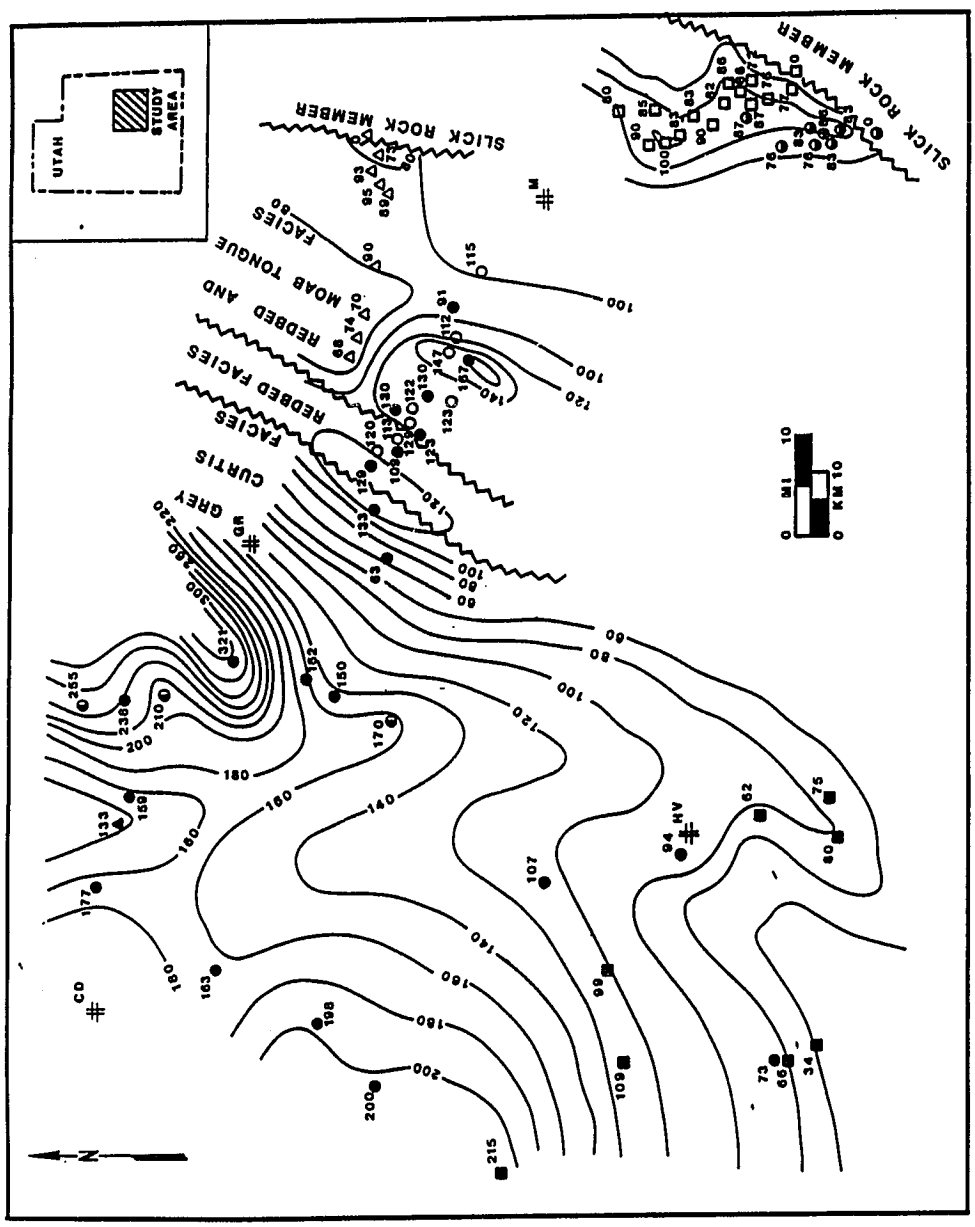

Figure 3.3. Isopach map of the Curtis Formation and Moab Tongue of the Entrada Sandstone. Contour interval: 20 ft (6.1m). Map symbols (table 1.3)

depositional trend or trough extends southward and nearly coincides with the strike of the east flank of the San Rafael Swell in the central part of the distribution. Third, a thick depositional lobe is locally developed near Tidwell Draw (Z-9A, B) in the north-central area of the map. Some of these depositional trends are maintained in maps of separate facies within the Curtis; the similarities and differences between them are examined in the following paragraphs.

The basal gravelly microsequence is restricted to and approximates the areal extent of the San Rafael Swell as do most of the facies intervals in the Curtis. Stratigraphic data suggests that the unit becomes thin and wedges-out mainly to the south and east (fig. 3.4), a pattern similar to other facies intervals in the Curtis. A main depositional trough or fairway is evident in the northwest, near Buckhorn Wash (Z-18,23) where the facies is at a maximum thickness of 12 feet (3.6m) or more. This trough or thickness trend branches to the northeast, southeast, and and as far south as Wild Horse Creek (Z-13).

The distribution of the sandstone-mudstone facies is restricted to the San Rafael Swell area and forms a belt of rocks trending northeast-southwest (fig. 3.5). A secondary thickness trend is developed in the Tidwell Draw area (Z-9), where the facies attains thickness of 146 feet (43.8 m), and roughly extends westward toward the North Salt Wash (Z-16) and Buckhorn Wash (Z-18, 23) areas. The jagged boundary marks the transition with the composite sandstone facies.

The composite sandstone facies is also restricted in areal extent to the San Rafael Swell (fig. 3.6). Thick sedimentary troughs or fairways extend from the western San Rafael Swell area and spread into a more thinly distributed sand system toward the eastern San Rafael

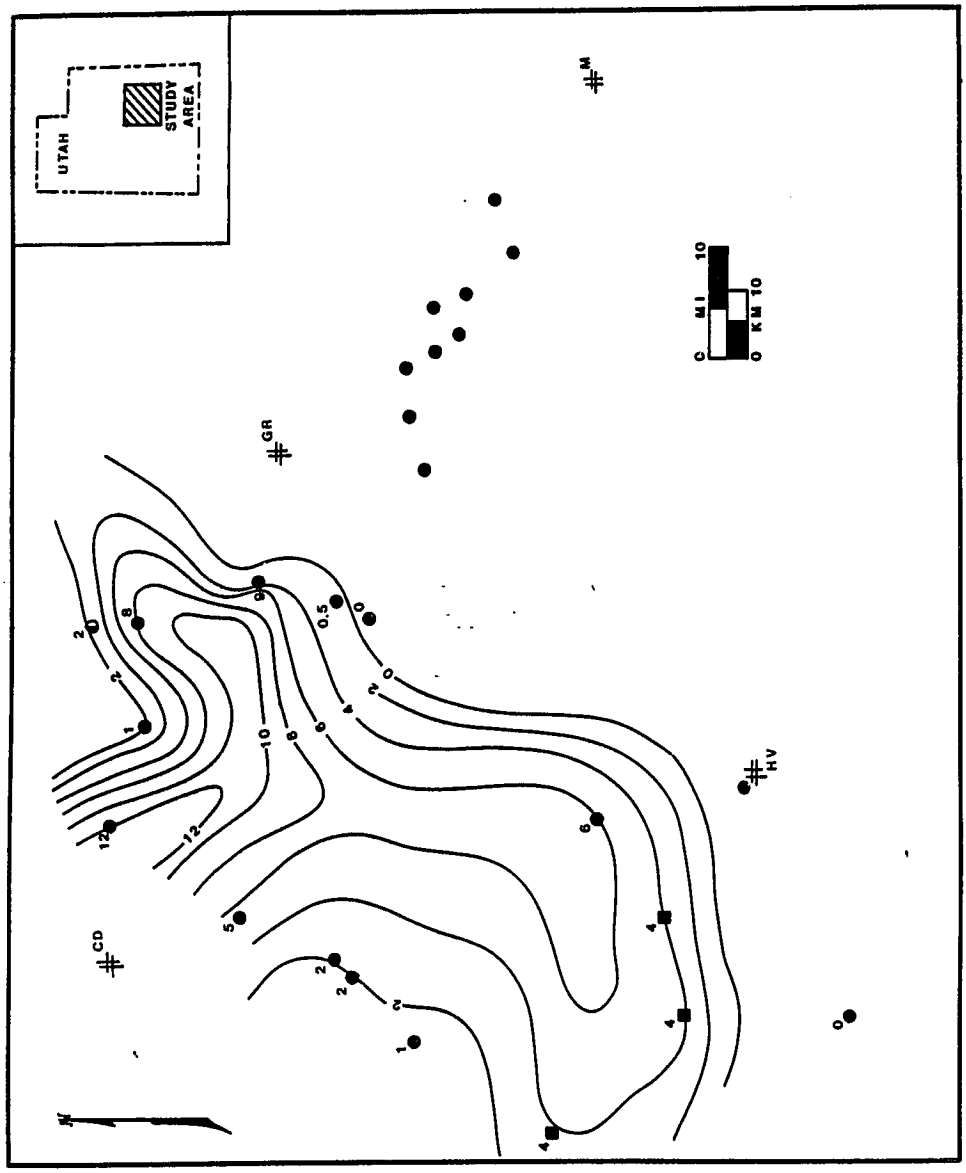

Figure 3.4. Isopach map of the basal gravelly microsequence in the sandstone-mudstone facies of the Curtis Formation. Contour interval: 2 ft (0.61 m). Map symbols (table 1.3)

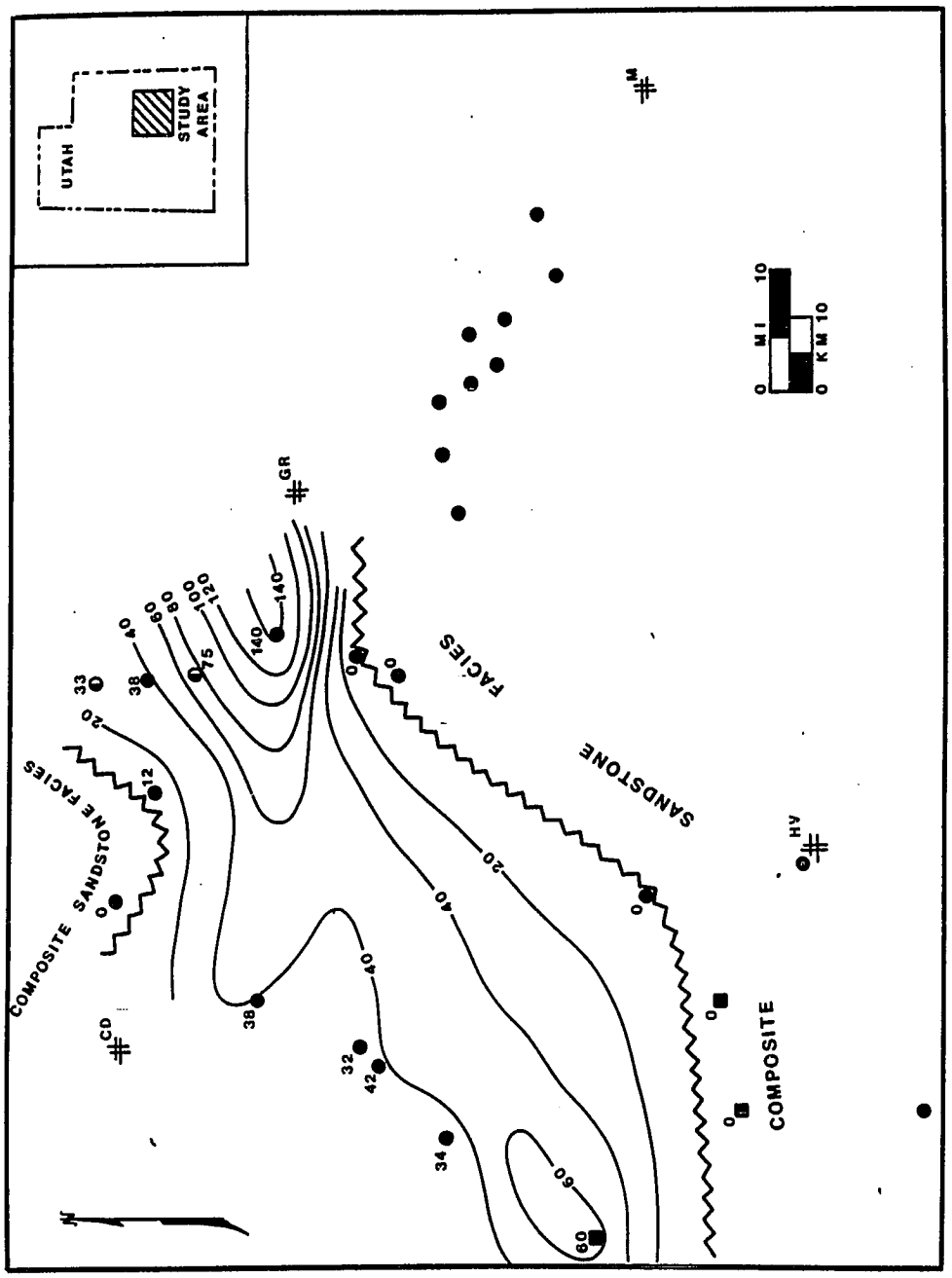

Figure 3.5. Isopach map of the sandstone-mudstone facies in the Curtis Formation. Contour interval: 20 ft (6.1 m). Map symbols (table 1.3)

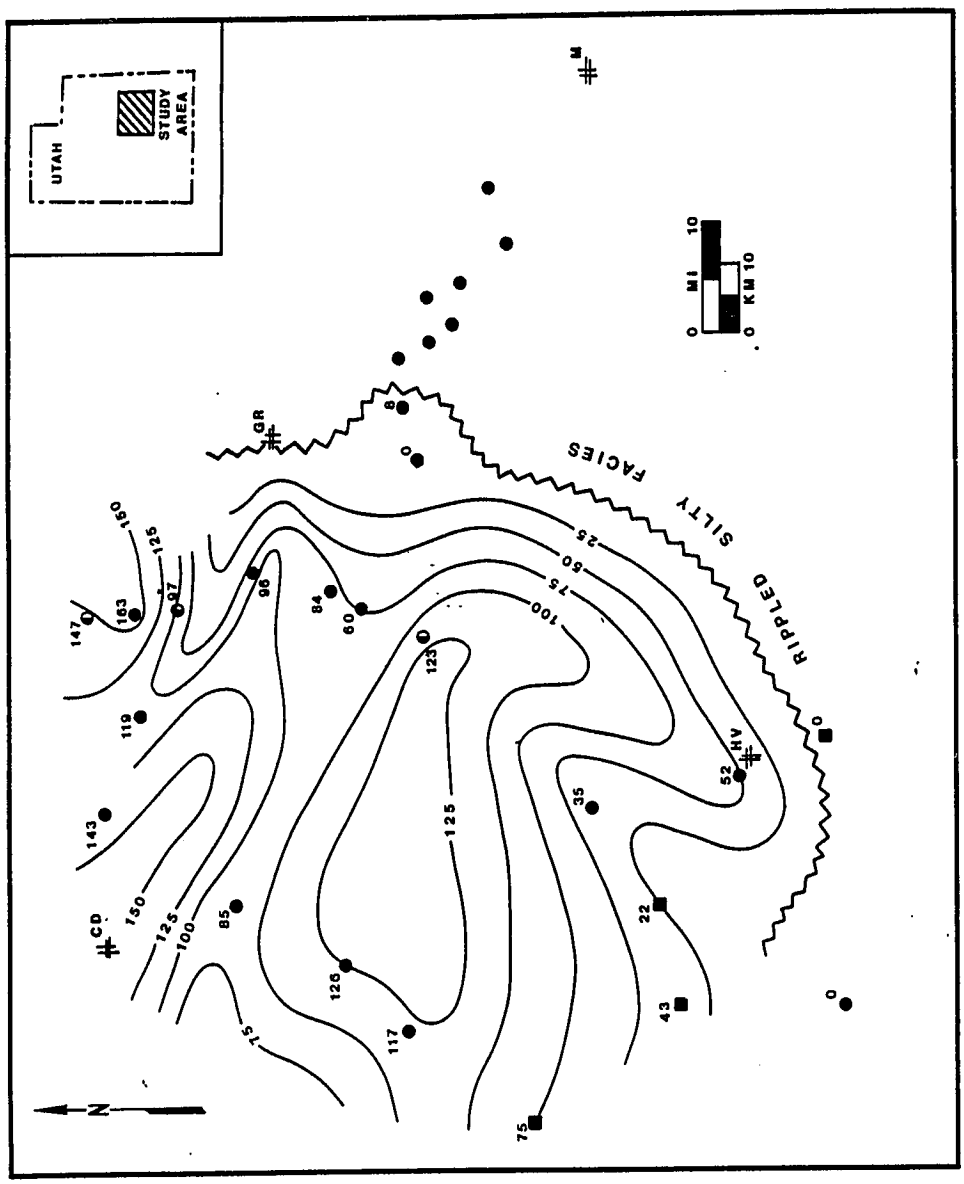

Figure 3.6. Isopach map of the composite sandstone facies in the Curtis Formation. Contour interval: 25 ft (7.6 m). Map symbols (table 1.3)

Swell area. The jagged boundary along the south and east represents the approximate transition between this facies and the ripple-laminated silty facies.

The distribution and thickness patterns of redbed facies are included in the map of the Curtis-Moab interval (fig. 3.3) and the entire Curtis-Moab-Summerville interval (fig. 5.6, Chapter 5, Paleogeography). In the area between Dellenbaugh Butte (Z-8) and White Wash (Z-11) light greenish-gray beds typical of Curtis facies in the San Rafael Swell area grade into a redbed facies as the Curtis continues to become thinner in an easterly direction. The closely-spaced isopach contours in figure 3.3 show a somewhat rapid thinning of Curtis beds southeast of the Green River townsite. From Dellenbaugh Butte (Z-8) southeastward to the east edge of the map there are irregular thickening and thinning patterns affected by the presence of the Moab Tongue. As shown in figure 2.5, the redbed facies gradually decreases in thickness from White Wash (Z-11) to southeast of Duma Point (Z-7) where it is interrupted by the Moab Tongue. Here, the facies is subdivided by the Moab into upper and lower portions. The upper part has been completely bevelled-out at Mill Canyon (Z-25) as the J-5 unconformity completely eroded through the Summerville to the Moab Tongue. Consequently, the Tidwell Member of the Morrison directly overlies the Moab Tongue. The lower part of the redbed facies is as thin as 4.5 feet (1.4 m) at Mill Canyon (Z-25). Although the complete lateral extent of the facies was not mapped, it probably decreases in thickness to a centimeter or less about 3 miles (5 km) southeast of Mill Canyon. It may continue as a diastem or super bounding surface separating the Moab Tongue from the Slick Rock Member of the Entrada.

Thickness patterns in the isopach map (fig. 3.7) of the rippled

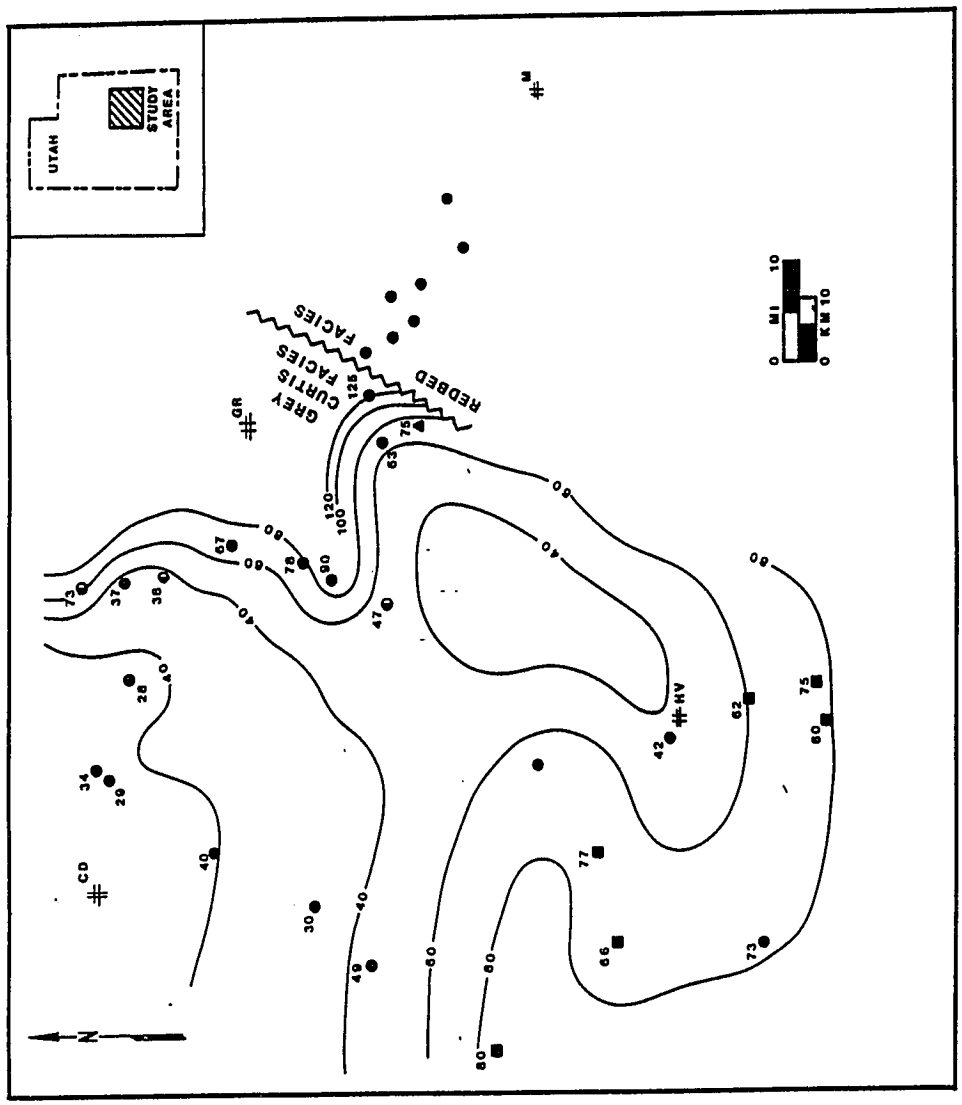

Figure 3.7. Isopach map of the ripple silty facies in the Curtis Formation. Contour interval: 20 ft (6.1 m). Map symbols (table 1.3)

silty facies, the uppermost greenish-gray facies in the Curtis, suggest that the interval becomes thicker to the east and south. This trend is opposite to those of stratigraphically lower facies in the Curtis. In the Green River Desert, between Dellenbaugh Butte (Z-8) and White Wash (Z-11), the facies grades somewhat abruptly eastward into the redbed facies, which becomes thin to the east.

Paleocurrent Trends

A total of 1455 azimuth measurements have been recorded from field exposures of crossbedding, ripple foresets (crosslamination), ripple asymmetry, rib-and-furrow structures, and parting lineation throughout the Curtis-Moab-Summerville interval (table A.1, appendix). The data have been analyzed by a desk-top computer program developed by Mr. Kenneth Cruikshank at the University of Cincinnati. The data are presented as circular histograms (rose diagrams) in figures 3.8-3.12. The width of each wedge represents the azimuth range and is mostly in 20 degree segments; a few diagrams have been plotted at an azimuth range of 10 degrees. The length of each wedge and therefore the tiering in a cluster of wedges is determined by the number of data points which fall within each 20-degree segment. A mean paleocurrent direction is given by means of a "stick" protruding from the rose plot.

A statistical index determines the reliability or consistency of mean azimuth in each rose diagram. The index serves as a measure of dispersion of azimuth. Hence, an index of 100 indicates high reliability or perfect uniformity in the paleocurrent data and an index of 1 indicates low reliability or high dispersion of data. Often, an analysis of less than 10 data points yields a misleading, high reliability index (table A.1, appendix).

In the sandstone-mudstone facies, crossbed azimuths in the basal crossbedded sandstone microsequence are treated separately from other paleocurrent features stratigraphically higher in the facies. Paleocurrent patterns of this microsequence are presented in figure 3.8.

Measurement of azimuth of foreset beds, mainly sandflow (McKee et al. 1971) strata, within the basal gravelly microsequence indicates paleoflow chiefly to the northeast and locally to the west (Buckhorn Wash, Z-18). Similar measuring of imbrication of pebble clasts at San Rafael Swell West (Z-6) also indicates a northeastward paleoflow (fig. 3.8). Relatively high reliability or consistency factors between 70 and 87 (table A.1, appendix) suggest a fairly uniform paleoflow directions. Data collected by Dickey and Wright (1959) indicated a northeastward paleocurrent flow and were supported by high reliability indices.

Azimuth of ripple foresets, ripple asymmetry and local ribs-and-furrows preserve the direction of paleoflow in the sandstone-mudstone facies (fig. 3.9). The plots of ripple data indicate polymodal or multidirectional paleocurrents with mean currents flowing to the northeast, southwest, northwest and southeast. The moderately low reliability indices ranging from 19 to 70 (table A.1, appendix) support a multidirectional pattern.

Beds of the composite sandstone facies display the greatest variety of paleocurrent structures including crossbedding, ripple foresets, ripple asymmetry, ribs-and-furrows, and parting lineation. Sedimentary structures produced by ripples and plane beds are the most abundant; crossbedding is second in abundance. Parting lineation occurs either in the same bedding horizon as, or within a few centimeters of,

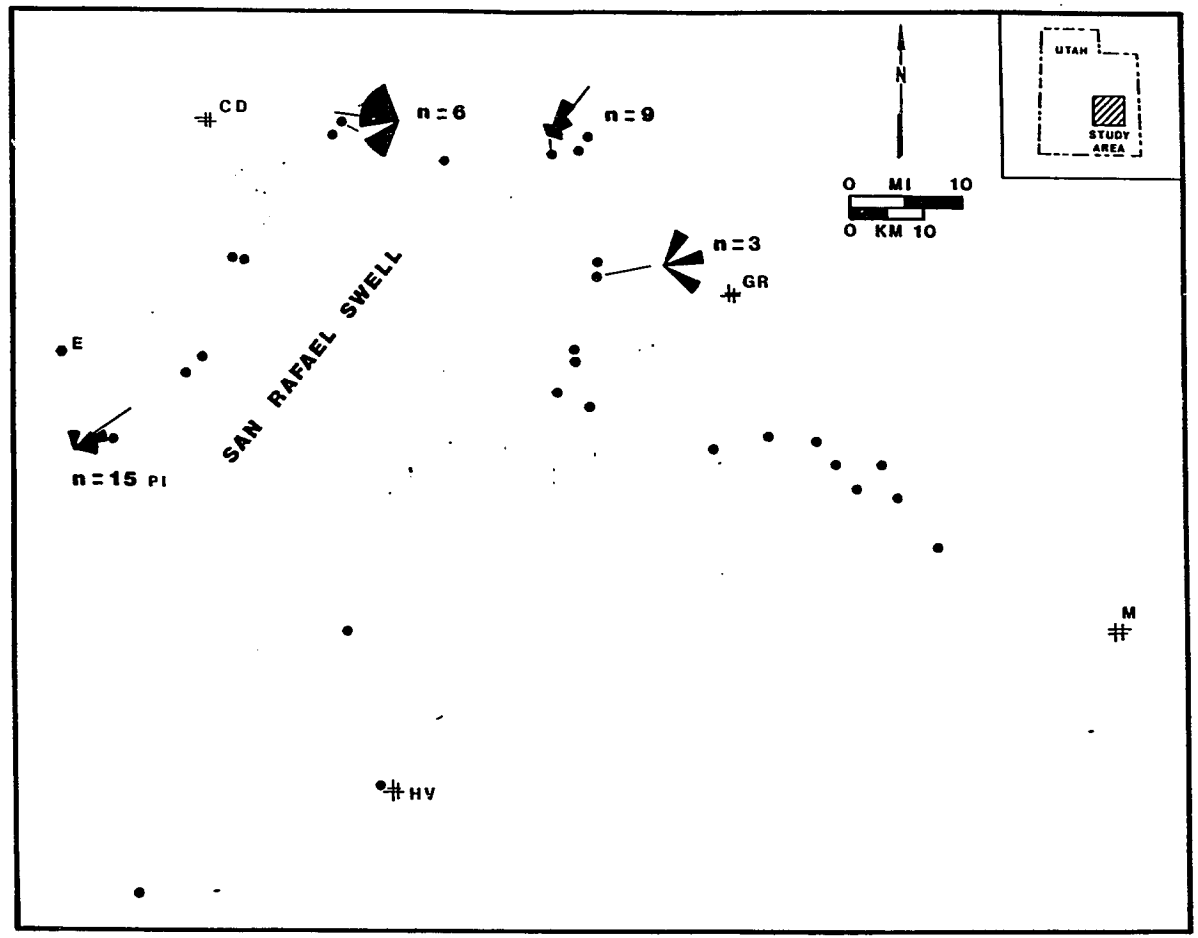

Figure 3.8. Paleocurrent patterns of crossbedding in the basal gravelly microsequence of the sandstone-mudstone facies, Curtis Formation; n = number of measurements; stick = mean paleocurrent azimuth; azimuth of pebble imbrication (PI). Map symbols (table 1.3)

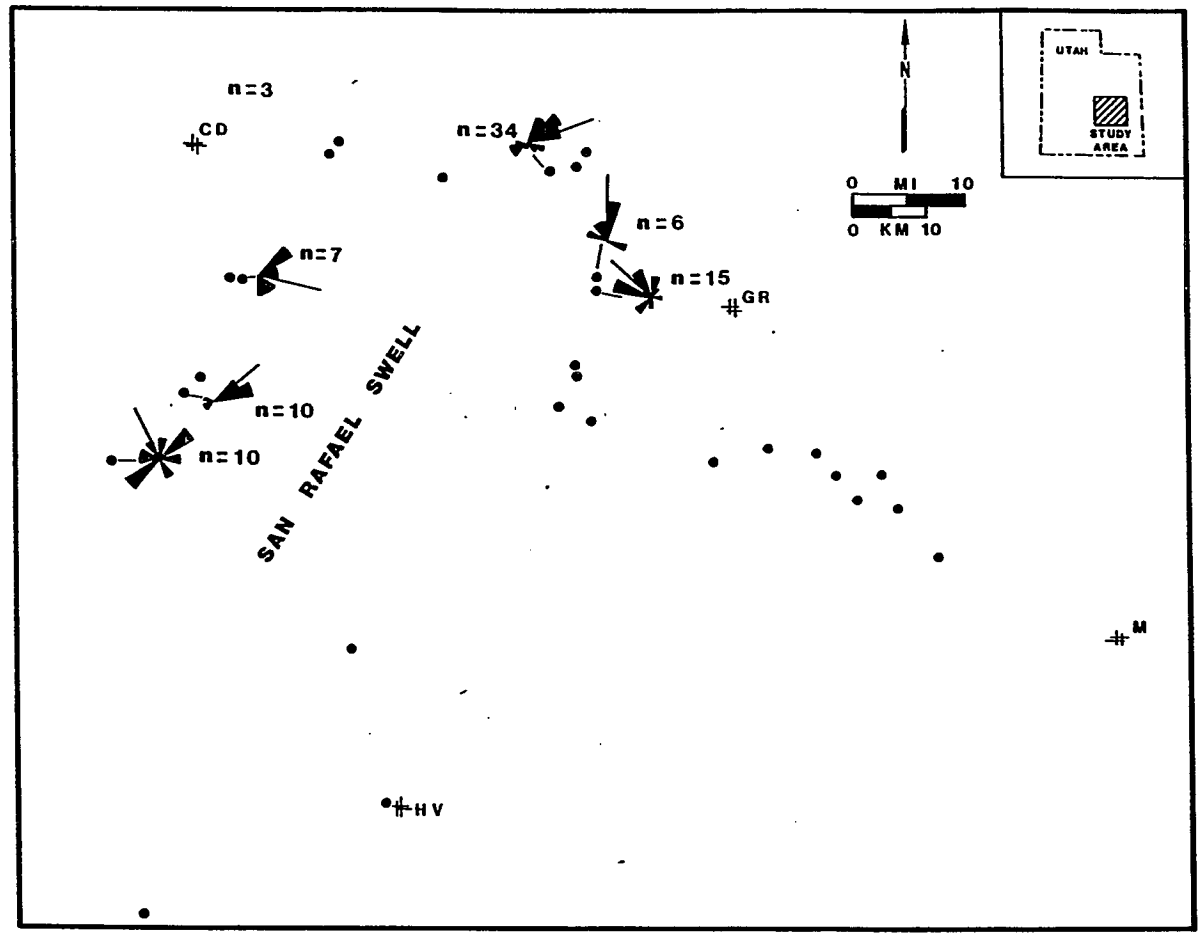

Figure 3.9. Paleocurrent patterns of ripple crosslamination in the sandstone-mudstone facies of the Curtis Formation; n = number of measurements; stick = mean paleocurrent azimuth. Map symbols (table 1.3)

ribs-and-furrows and ripple marks, so data from parting lineation and ripples are combined on one map (fig. 3.10).

Linear features, like parting, produced by air or wind currents, give ambiguous directional or vectoral properties. However, when combined with indicators of unidirectional paleocurrents such as crossbedding or crosslamination, the unidirectional aspect of the parting becomes apparent. There is very good correspondence between mean transport vector for ripples and parting lineation. Both features show an overall polymodal paleocurrent distribution with strong bimodal trends developed at locations except South Sand Bench (Z-15), and Wild Horse Creek (Z-13) which show a stronger tendency toward unimodal paleoflow. Analysis of crossbedding in the composite sandstone facies also indicates a polymodal pattern with subordinate bimodal trends developed especially at San Rafael Swell West (Z-6), Lookout Point (Z-14), South Sand Bench (Z-15), Buckhorn Wash (Z-18), and San Rafael Swell Northeast (Z-3) (fig. 3.11). Reliability indices of less than 60 (table A.1, appendix) also suggest a non-uniform paleocurrent distribution. Misleading indices of greater than 90 are associated with fewer than 10 data measurements, particularly of crossbed azimuths.

Paleocurrent aspects of the ripple-laminated silty facies in the Curtis are poorly preserved and exposed. Only small-scale structures such as ripple crosslaminations and local parting lineations are observed. The sparse data collected around the southern San Rafael Swell near Pleasant Creek (Z-4) and Hanksville (Z-5) and the Green River Desert suggest an approximate polymodal pattern (fig. 3.12). Paleocurrents are chiefly northwesterly and southeasterly. Analysis of these data yield intermediate reliability indices between 34 and 69 (table A.1, appendix). However, the data are too few to be able to use

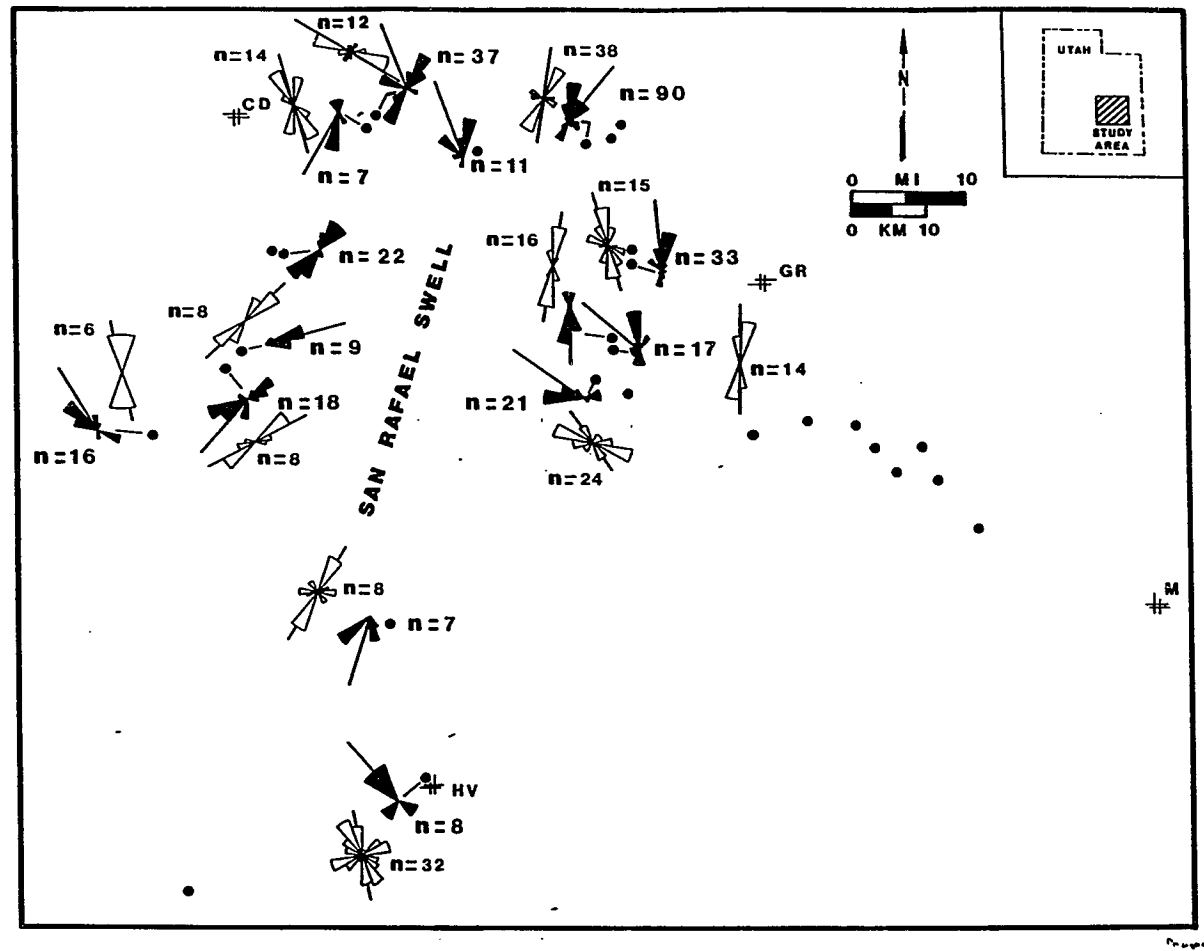

Figure 3.10. Paleocurrent patterns of ripple crosslamination (solid petals) and parting lineation (open petals) in the composite sandstone facies of the Curtis Formation; n = number of measurements; stick = mean paleocurrent azimuth. Map symbols (table 1.3)

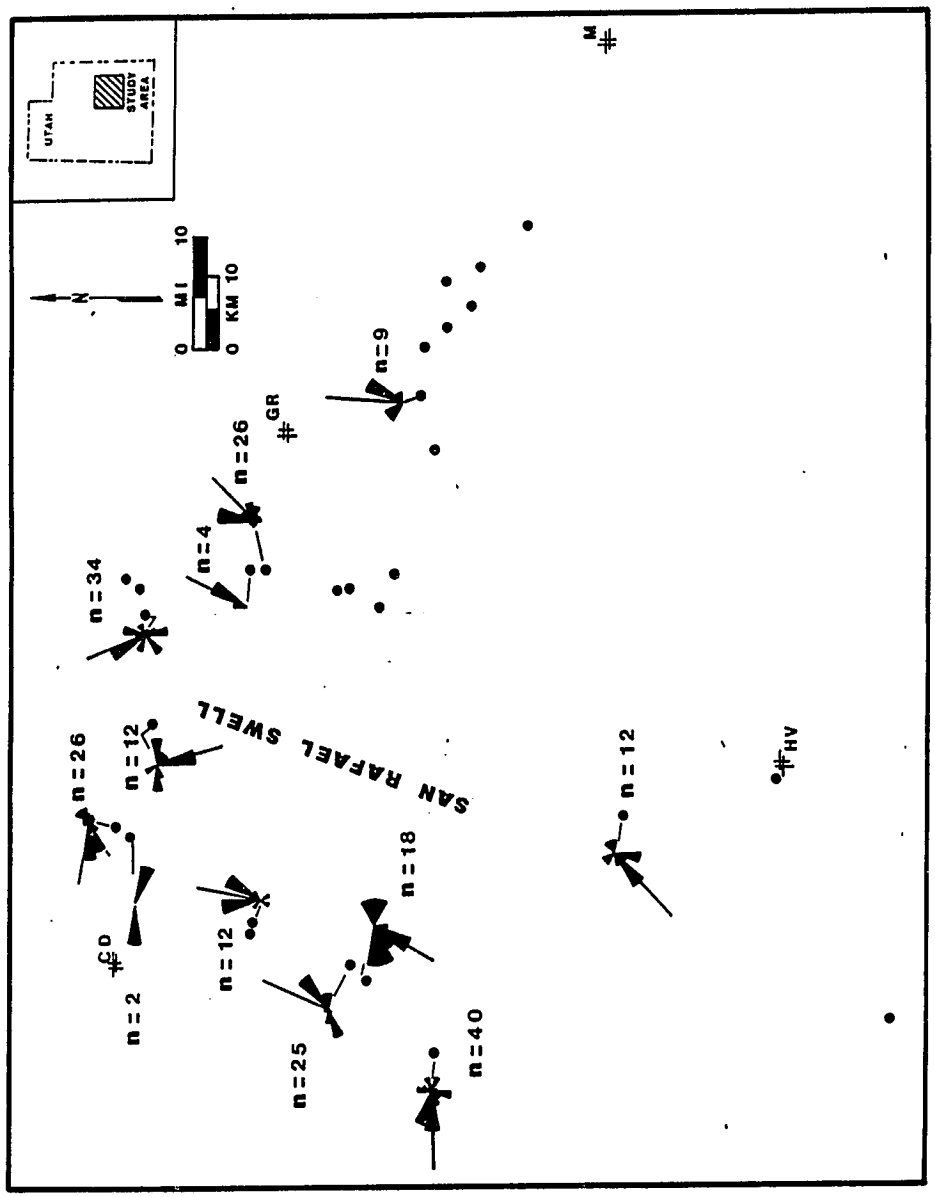

Figure 3.11. Paleocurrent patterns of crossbedding in the composite sandstone facies in the Curtis Formation; n = number of measurements; stick = mean paleocurrent azimuth. Map symbols (table 1.3)

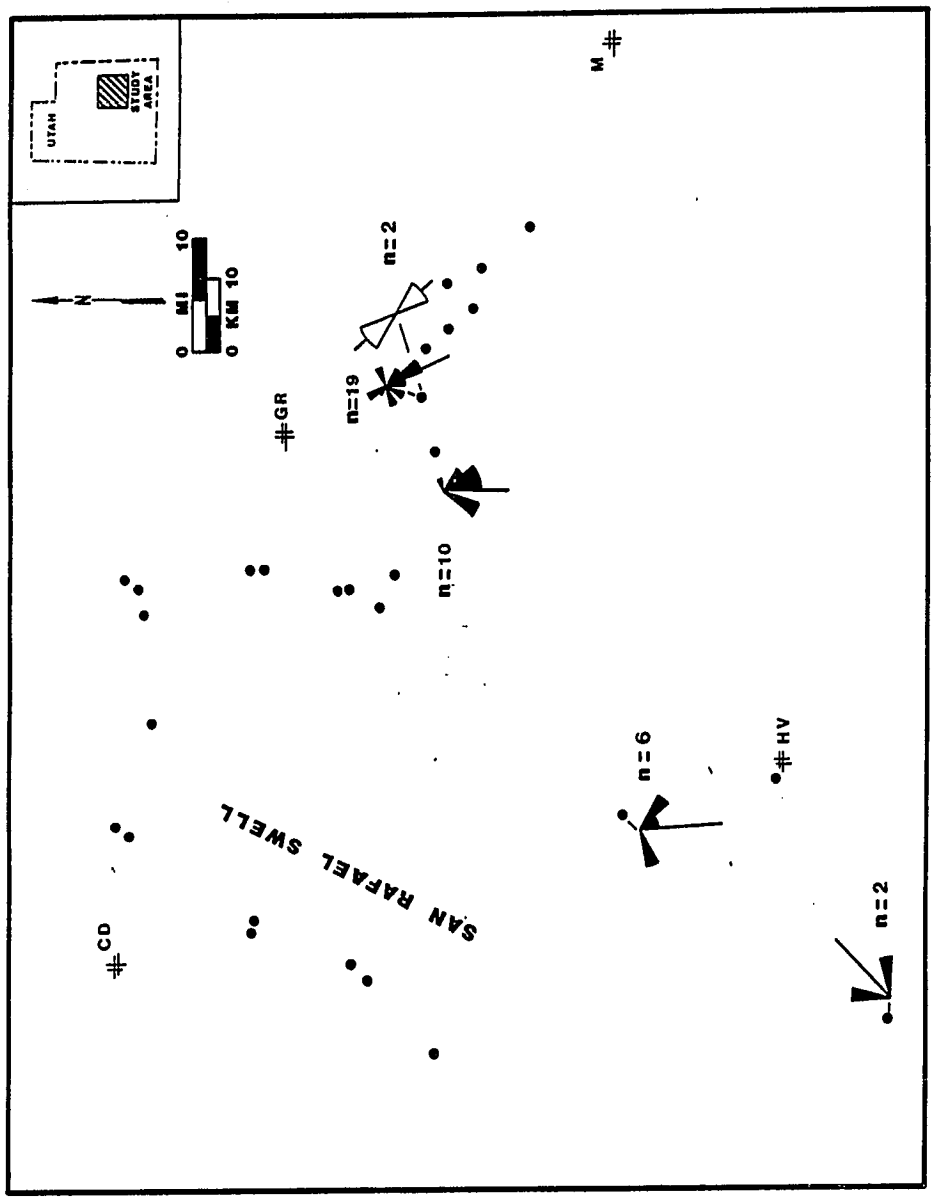

Figure 3.12. Paleocurrent patterns of ripple crosslamination (solid petals) and parting lineation (open petals) in the rippled silty facies of the Curtis Formation; n = number of measurements; stick = mean paleocurrent azimuth. Map symbols (table 1.3)

the reliability indices with confidence.

Based on analysis of paleomagnetic pole positions, Steiner (1986) has reported that the Colorado Plateau rotated as a microplate prior to the Jurassic by about 11(±4) degrees. Because of the timing and the small structural rotation, the paleocurrent data reported herein have not been adjusted for the rotation.

Sandstone-Mudstone Facies

A sandstone-mudstone facies is the stratigraphically lowest facies in the Curtis and is gradational with the overlying composite sandstone facies. Except for a gravelly crossbedded unit at the base, the sandstone-mudstone facies is generally an upward-coarsening macrosequence consisting of heterogeneous or heterolithic lenticular-bedded very fine-grained sandstone, siltstone and mudstone, wavy-bedded very fine-grained sandstone and siltstone and flaser-bedded very fine- to fine-grained sandstone units (fig. 3.13) within which are recognizeable microsequences. Four microsequences are recognized in the facies: 1. basal gravelly, 2. mudshale, 3. upward-fining, upward-thinning, and 4. upward-coarsening, upward-thickening (table 3.1). The mudshale microsequence is observable at San Rafael West (Z-6) and at San Rafael Swell Northeast (Z-3. The other microsequences are best developed at Tidwell Draw (Z-9).

Basal gravelly microsequence. The basal gravelly microsequence is distinguished from the underlying red, flat-bedded siltstone Beds at Goblin Valley by gray color, crossbedding, and gravelly texture. The sedimentary beds are poorly sorted and composed of fine- to very coarse-grained sand- and granule-, pebble-, and cobble-size clasts.

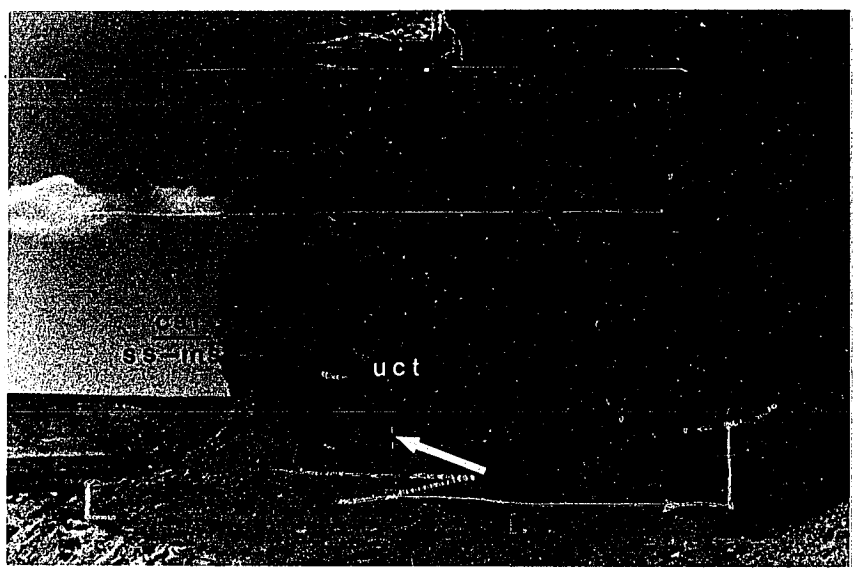

Figure 3.13. Sandstone-mudstone facies (ss-ms) at San Rafael Swell Northeast (Z-3). Basal gravelly microsequence (bg); mudshale microsequence (ms); upward-coarsening, upward-thickening microsequence (uct); composite sandstone facies (csf). Staff (arrow) is in feet

Table 3.1. Sedimentary features of the sandstone-mudstone facies of the Curtis Form

Sedimentary Features	Interpretation	Modern
A. Ripple marks Asymmetrical: straight-to sinuous-crested linguoid lunate interfering	Tidal and some wave currents	
Nearly symmetrical: offshoots; bundle upbuilding; bidirectional lenses; uni- and bidirectional bundled lenses; intricately interwoven x-lams; irregular lower bounding surfaces	Nearshore wave activity	Reineck and Singh de Raaf et al. (19
B. Sole marks on ripple beds: loads flutes gutter casts tool marks (prod, groove, bounce)	Scours and impact marks made by local eddies and transported objects during traction.	
C. Hyporelief trace fossils:	Cruziana ichnofacies; epifaunal, subtidal or slightly below fair weather wave base; washed out and cast by higher energy wave currents	
1. horizontal, cylindrical burrows with crude chevron backfills	Arthropod traces	
2. bilobate cylinders with chevron backfills and median furrow	Arthropod or gastropod trace	
3. Thalassinoides	Arthropod trace	
C. Mudstone-siltstone drapes with crawling/feeding trace fossils	Slack or calm water suspension settling and crawling/feeding activity by benthic organisms	

e-mudstone facies of the Curtis Formation

ion	Modern	Ancient
ome wave		
ave activity	Reineck and Singh (1980), de Raaf et al. (1982)	Moore (1982), de Raaf et al. (1977)
impact marks al eddies and objects during		Aigner (1985)
hnofacies; subtidal or low fair weather washed out and ner energy wave		Aigner (1985)
races		Howard and Frey (1984)
r gastropod		Howard and Frey (1984)
race		Howard and Frey (1984)
lm water settling and eding activity organisms		

Table 3.1. Continued

Sedimentary Features	Interpretation	Modern
E. Microsequences 1. basal gravelly microsequence:	Relict gravels from earlier, pre-Curtis events; reworked by marine currents as transgressive lag	Stride (1982),
-abrupt planar base; erosional relief up to 1 ft(30 cm); overlies J-3 unconformity		
-J-,U-, tear-shaped boring-like trace fossils assoc/w omission surface at Jcu-Je contact	Glossifungites ichnofacies; burrows in firm but unlithified (?) substrate by suspension feeders or carnivores (arthropods, polychaetes)	Pembert
-sandy (m-vc; 250-2000 μ) granule-pebbly cong beds; clasts: limestone, chert, fossil frags; beds 1-7 inches (3-20 cm) thick		
-crossbeds: lenticular sets 3-5 feet (0.9-1.5 m) thick; sandflow beds: 0.4-0.8 in (1-2 cm) thick; granules(2-4 mm), m-c (250-710 μ) ss; reverse grading; normal grading in toe; tangential toesets	Continuous avalanching on slip face of subaqueous megaripple; grainflow mechanics; formation of tangential toesets w/ increasing flow velocity	Bagnold (1965a, Hunter Kocurek
-chiefly northeastward paleocurrents	Shore-parallel tidal currents	Reineck Reineck Johnson and Nie and Bal
-straight to lunate-linguoid fore- and backflow ripples along foresets; draping siltstone lams; trace fossils	Interrupted flow and reactivation	
-clasts: chert, limestone, sandstone, echinoderm frags, oyster frags, Camptonectes(?) frags; discoidal; imbriccated updip along foresets		

etation	Modern	Ancient
gravels from earlier, pre-events; reworked by marine s as transgressive lag	Stride (1963), Stride et al. (1982), Harms et al. (1982)	Clifton (1981)
ungites ichnofacies; burrows but unlithified (?) substrate ension feeders or carnivores pods, polychaetes)	Pemberton and Frey (1985)	Ekdale et at (1984), Frey and Pemberton (1986)
ous avalanching on slip face queous megaripple; grainflow cs; formation of tangential w/ increasing flow velocity	Bagnold (1954a), Jopling (1965a, b), Boothroyd (1978), Hunter (1985b), Hunter and Kocurek (1986)	Buck (1985)
arallel tidal currents	Reineck (1963), Stride (1963), Reineck and Singh (1980), Johnson et al. (1982), Swift and Niedoroda (1985), Johnson and Baldwin (1986)	McCave (1973), Tillman and Martinsen (1984, 1985)
pted flow and reactivation		de Raaf and Boersma (1971)

Table 3.1. Continued

Sedimentary Features	Interpretation	Modern
E. Microsequences (cont.)		
2. Mudshale -bioturbated w/ vf sandy (62-88 μ) starved ripples; local coal clasts	Restricted, low-energy suspension sedimentation in tidal basin	
-trace fossils: bilobed and single-lobed crawling traces; vertical dwelling tubes	Cruziana ichnofacies; lower to upper subtidal (shoreface), medium energy, soft ground at or below fair weather wavebase	Ekdale
3. Upward-coarsening, upward-thickening; 1-8 in (2-21cm) thick c. ripple foreset lmtd ss vf-f (88-177 μ) w/ or w/o ms flasers b. wavy-bdd, crosslmtd; hypore-trace fossils; sole marks a. lenticular-bdd (linsen var.) crosslmtd vf (62-88 μ) ss or slt and ms	Wave- and tidal currents, wind- or storm enhanced, transition to lower shoreface depths; incipient building of shoal-channel complex; accelerating currents; greater availability of sand	Terwir
4. Upward-fining, upward-thinning d. lenticular bdd vf (62-88 μ) ss or cryptic bdd slt or ms; local vertical and horizontal burrows c. wavy-bdd, vf (62-88 μ) crosslmtd ss intbdd w/ slt and ms b. crosslmtd vf (62-88 μ) ss; draping ms lams along toe-sets and foresets; Chondrites (?) traces a. trough x-bdd vf-m (88-350 μ) ss; sets 4-5 in (11-13 cm) thick	Wave- and tidal currents, transition to lower shoreface depths; incipient building of shoal-channel complex; de-celerating currents	Terwin Greer

or units b, c, and d only

tion	Modern	Ancient
, low-energy sedimentation asin		
chnofacies; lower to dal (shoreface), rgy, soft ground at or weather wavebase	Ekdale et al. (1984)	Howard (1972), Bromley (1984) Frey and Pemberton (1984)
tidal currents, wind- nhanced, transition noreface depths; building of shoal- mplex; accelerating greater availability	Terwindt (1971a, 1981)	Sellwood (1972), de Raaf et al. (1977), Cotter (1985)
tidal currents, to lower shoreface cipient building of nel complex; de- currents	Terwindt (1971a, 1981) Greer (1975)	de Raaf and Boersma (1971), de Raaf et al. (1977), Cotter (1985)

Gravel clasts are fragments of chert, silicified and dolomitized limestone, sandstone, molluscs and echinoderms; some of the sandstone pebbles and cobbles texturally and mineralogically resemble the underlying Beds at Goblin Valley (fig. 3.14d). There are unidentified gastropod fragments seen in thin sections. Other mollusc fragments are tentatively identified in hand sample as valves of the pelecypod genera, Ostrea and Camptonectes (fig. 3.14a, b) which have been recognized in the Curtis and in the older Jurassic Carmel Formation (Imlay, 1964, 1980). Trends in percent abundance between eastern samples and western samples are not apparent. Percent gravel in the sandstone ranges from 46% to 72% in the western San Rafael Swell and diminishes to 0% between Wild Horse Creek (Z-13) and Hanksville (Z-5) and east of San Rafael Swell East (Z-2).

Beds rest on the J-3 surface, a scoured and truncated surface at the top of the Beds at Goblin Valley. At North Salt Wash (Z-16) an isolated assemblage of trace fossils was observed within a foot (30 cm) below the Curtis-Entrada contact or J-3 surface (fig. 2.8a,b). The traces consist of vertical, j- and u-shaped burrows which were excavated in the Beds at Goblin Valley. Some of the vertical burrows are tear-drop shaped, that is, having basal, bulbous terminations that in some traces resemble pelecypod molds in geometry (fig. 2.8a). These extend upward to nearly vertical tubes which have been partially truncated along the J-3 unconformity and subsequently filled in with sediment that is similar to that of the overlying Curtis in texture and composition. The Curtis-Entrada contact is also locally sculpted with backflow ripples which have been buried by avalanching, gravelly foreset beds.

Figure 3.14. Outcrop characteristics of the basal gravelly microsequence

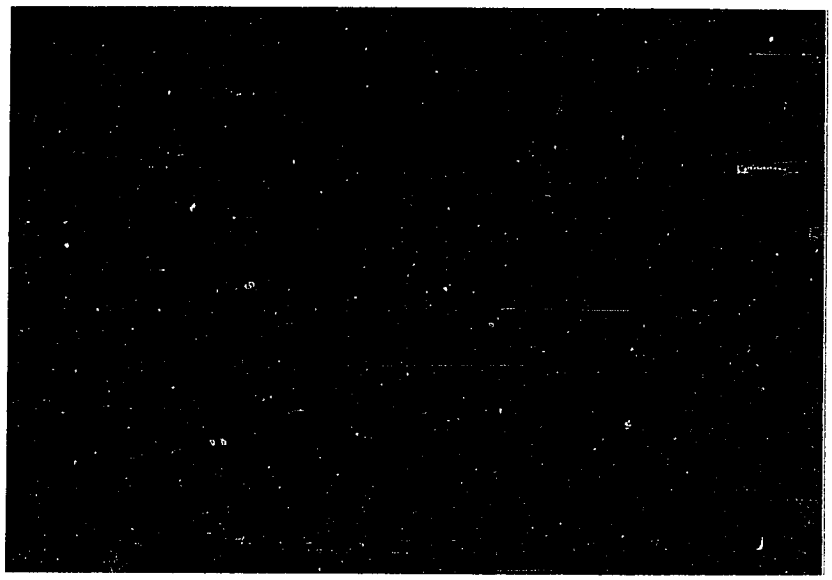

a. Pelecypod valves tentatively identified as Camptonectes

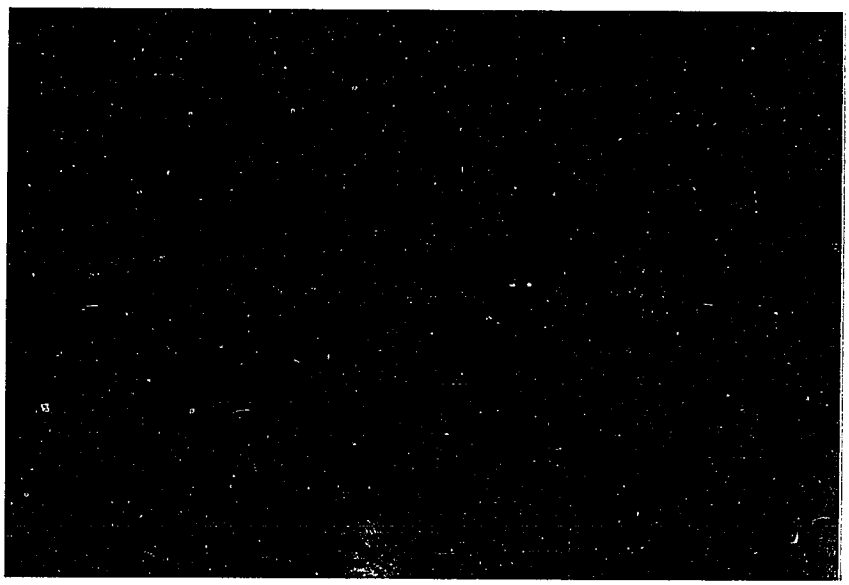

b. Granule-size clasts and echinoderm spine (arrow)

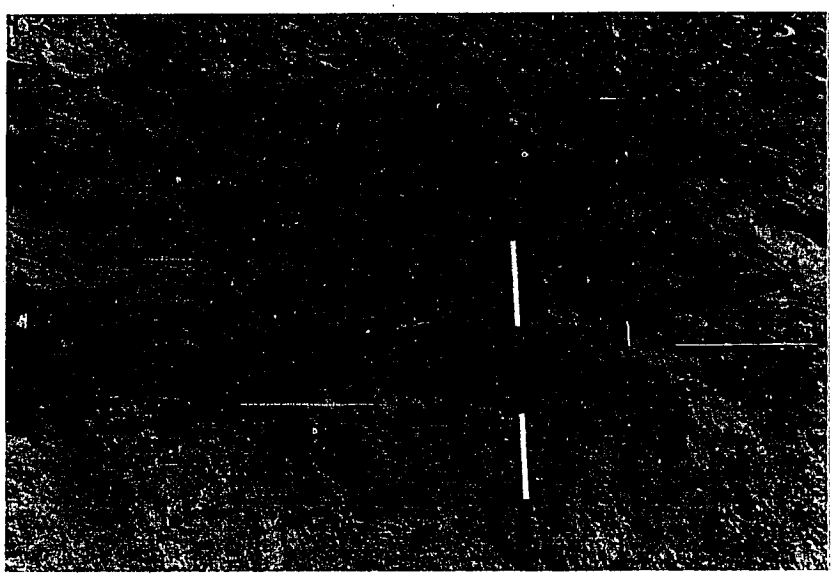

c. Lenticular crossbedded set consisting of sandflow foreset beds (San Rafael Swell Northeast, Z-3). Staff is in inches and feet

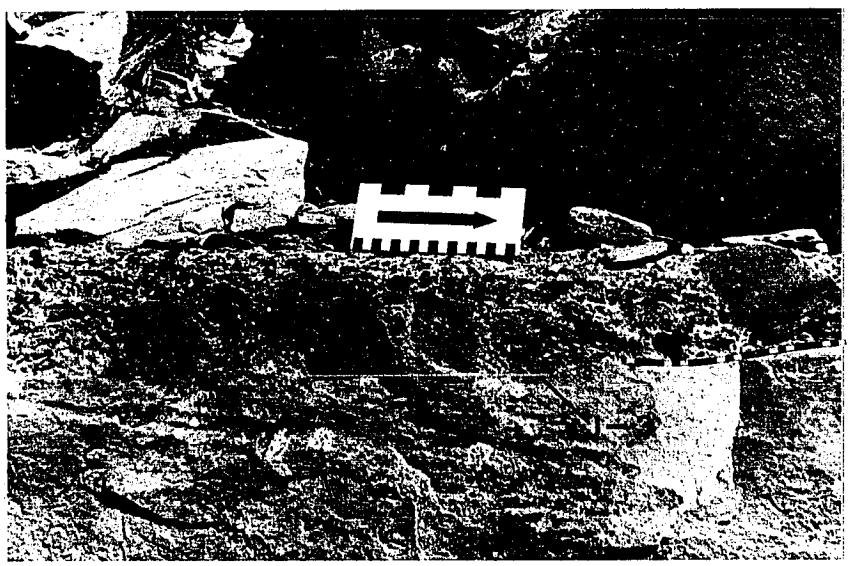

d. Granule-, pebble-, and cobble-size clasts along the J-3 unconformity (North Salt Wash, Z-16). Scale is in inches and centimeters

Stratification is mainly medium- to large-scale tabular- and trough-crossbedding with tangential toesets and concave-upward foresets. Crossbed sets range in thickness from 3 to 5 feet (0.9 to 1.5m) with cosets as thick as 12 feet (3.6m). The foresets consist of sandflow (McKee et al., 1971) strata 1-to-2 cm thick and exhibit reverse grading; normal grading is present in the toesets. There are local transverse and lunate-linguoid fore- and backflow ripples, and draping siltstone laminations along foresets; feeding/crawling trace fossils are locally preserved near the top of the beds. Gravel clasts are locally imbricated up-dip along foresets (fig. 3.14c, d) (Table 3.1). A single set of crossbeds at Buckhorn Wash (Z-18) attains a maximum thickness of 5 feet (1.5 m) and thins to 2 to 3 feet (0.60 to 0.90 m) to the northwest in a distance of a few tens of feet. At San Rafael Swell Northeast (Z-3), two beds of crossbedded gravelly sandstone are interbedded with a mudshale at the base of the wavy-bedded sandstone facies (next section). Crossbedding is locally replaced by massive beds 1-to-7 inches (3 to 20 cm) thick at San Rafael Swell West (Z-6) and Cedar Mountain (Z-17) which are locations near the edge of the unit.

Mudshale microsequence. A localized basal mudshale unit is 12 feet (3.6 m) thick and is composed of a medium gray, slope-forming, thinly bedded mudshale with sparse trace fossils and starved ripples (isolated ripple-form lenses of sandstone enclosed within mudshale) or lenticular bedding with flat isolated lenses (Reineck and Singh, 1980). Trace fossils include single- and bi-lobed, subhorizontal feeding/crawling traces and vertical burrows up 1 inch (2.54 cm) in diameter (table 3.1). Beds of the basal crossbedded sandtone facies are

locally interbedded.

Upward-coarsening, upward-thickening microsequence. An upward-coarsening, upward-thickening microsequence is recognized as a discrete unit. Bedding is similar to that of the upward-fining, upward-thinning microsequence but the order of occurrence is reversed forming a near mirror-image of the microsequence. Beds thicken upward from 1 inch to 8 inches (2 to 21 cm) and coarsen regularly from very fine-grained sandstone, siltstone, or mudstone to crosslaminated very fine- to fine-grained sandstone. Bedding changes vertically upward from lenticular beds with single and connected lenses and incomplete ripple foresets through wavy-beds with similar foresets to completely crosslaminated beds with well developed foreset bundles. Boundaries between crosslaminated beds and mudstones and siltstones are sharp. Foreset bundles display either a). unidirectional, crosslaminated beds that climb or b). complexly interwoven bundles with uni- and some bi-directional foresets, bundle upbuilding, and uneven lower bounding surfaces (fig. 3.15). Mudstone flasers are localy present (table 3.1).

Wavy-bedded intervals are best developed and exposed at San Rafael Swell West (Z-6) and at San Rafael Swell Northeast (Z-3) (fig. 3.16). At the latter location, ledge-forming wavy-bedded sandstones are regularly interbedded with recess-forming mudstones or siltstones less than 0.4 inches (1 cm) thick. Sandstone beds are continuous, are characterized by flat bases, and internal ripple foreset laminations. Ripple forms are asymmetrical to nearly symmetrical; foreset laminations are generally simple and unidirectional but complex bundles with upbuilding and bidirectional foresets are present (table 3.1).

Figure 3.15. Ripple foreset bundles displaying a: near symmetrical forms (s), b: bundle upbuilding (bu), c: irregular lower bounding surface (bs), d: bidirectional foresets (bf) in the sandstone-mudstone facies of the Curtis Formation (San Rafael Swell West, Z-6)

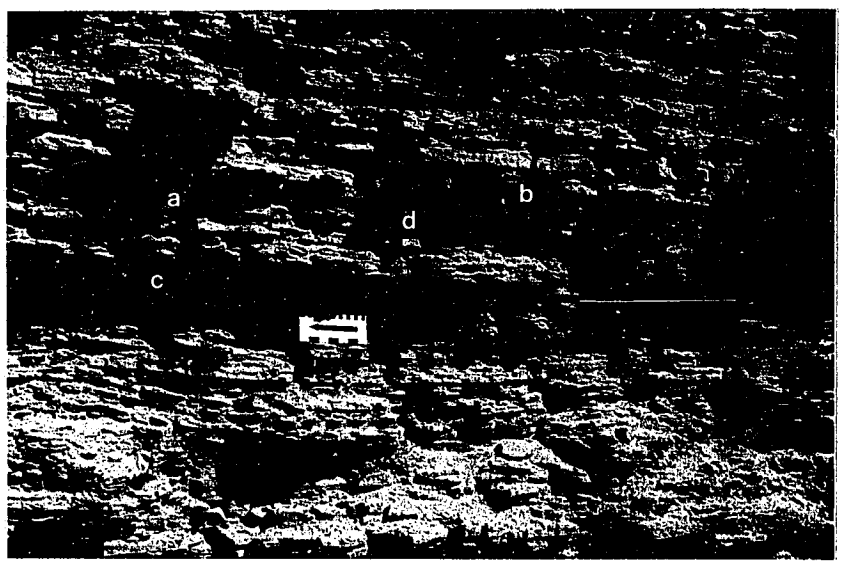

Figure 3.16. Wavy-bedded intervals with a: asymmetrical and near-symmetrical ripple forms, b: continuous, flat-bottomed wavy beds, c: locally superposed lenses, d: pinching and swelling in the sandstone-mudstone facies, Curtis Formation. Scale is marked in inches and centimeters (San Rafael Swell Northeast, Z-3A)

Abundant trace fossils are preserved in the microsequence at San Rafael Swell Northeast (Z-3). The traces are near horizontal, mostly feeding and locomotion traces, which are preserved in the soles of the wavy-bedded sandstones as hyporelief casts and molds. Most of the traces are sinuous and commonly cross one another. They are preserved as cylindrical tubes of different geometries and infill structures. There are simple, near horizontal, sinuous tubes which are less than 1 cm in diameter and lack obvious backfill structures. Another tube-like trace is straight and slightly sinuous and is 0.4 to 1 inch (1 to 2.5 cm) in diameter. It is composed of heavy, irregular backfill structures (fig. 3.17a). A locally identifiable trace consists of branching, compressed cylinders up to 1.2 inches (3 cm) in width and resembles Thalassinoides (fig. 3.17b). There are smaller sinuous traces which are 4 to 5 mm in width and are characterized by bilobate geometry with a median furrow. These are constructed of well-defined chevron backfill structures and are identified as Cruziana traces (fig. 3.17a). Epirelief feeding and crawling traces are locally preserved on silty ripple marked surfaces. They are composed of tubes 0.4 inches (1 cm) long and about 2 mm in diameter. Other sedimentary sole marks include load and flute casts, gutter casts, and various tool marks such as prod, groove, and bounce marks.

Upward-fining, upward-thinning microsequence. An upward-fining, upward-thinning microsequence is named for a succession of beds which grades up from a basal, very fine- to medium-grained sandstone 4 to 5 inches (11 to 13 cm) thick or less. A very locally developed basal sandstone is usually one medium-scale set of concave-upward, tangential crossbedding. More typically, a ripple-laminated very fine-grained

a: Horizontal burrow characterized by heavy, irregular wall structure (a); Cruziana traces consisting of two cylindrical lobes, median furrow, and chevron backfill structures (b)

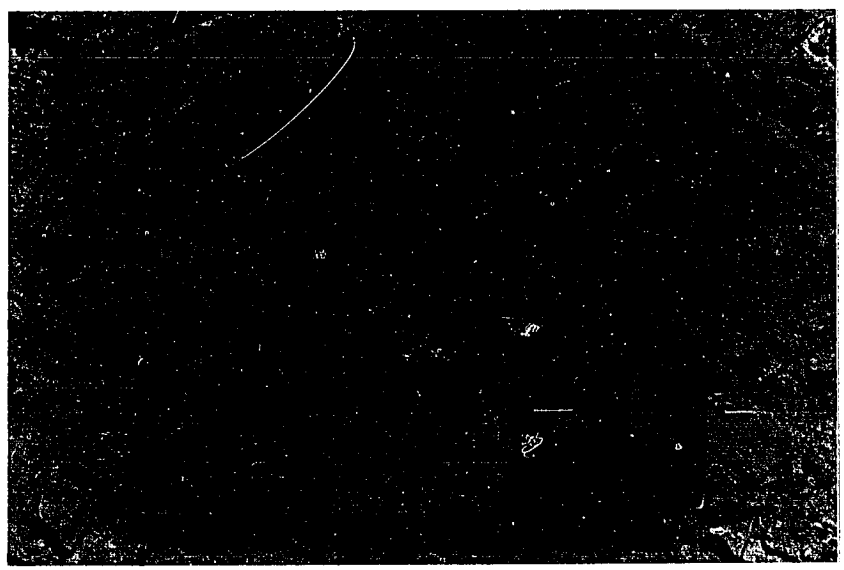

b: Locally preserved smooth-walled, branching horizontal burrows resembling Thalassinoides

Figure 3.17. Hyporelief trace fossils in the soles of crosslaminated wavy beds, upward-coarsening, upward-thickening microsequence in the sandstone-mudstone facies (San Rafael Swell Northeast, Z-3A)

sandstone marks the base of the microsequence. Foreset laminations locally stand out more prominently from between thin mudstone laminations which have been weathered out of the outcrop surface. Ripple-laminated beds have very well developed foreset bundles which display bundle upbuilding, bidirectional lenses, uni- and bidirectional bundled lenses, offshoots and irregular lower bounding surfaces (de Raaf et al., 1977). This bed grades upward into wavy-bedded very fine-grained sandstone, siltstone and mudstone in which the sandstone and siltstone beds are stratified with partial ripple foreset laminations. The top unit consists of lenticular-bedded very fine-grained sandstone with ripple foreset-laminations interbedded with siltstone or mudstone (table 3.1).

At Tidwell Draw (Z-9A, B), the sandstone-mudstone facies is unusually thick, ranging from 91 to 153 feet (27 to 46 m) thick. Here, the facies is characterized by an upward-coarsening, upward-thickening macrosequence in which smaller bedding packages, 1 inch to 2 feet (2 to 60 cm) thick, form partial and complete upward-fining, upward-thinning microsequences. In a complete microsequence, basal beds are typically crosslaminated very fine-grained sandstones which grade upward into local plane laminations or crosslaminated wavy beds interbedded with mudstone or siltstone of similar geometry. Uppermost beds of the microsequence consist of crosslaminated lenticular beds or starved ripple-form lenses in mudstone. Partial microsequences consist of randomly interbedded crosslaminated (simple crosslaminations or complex bundles) sandstone and mudstone beds up to 1 foot (30 cm) thick or wavy- and lenticular-bedded sandstones interbedded with mudstone or siltstone. Locally, complexly knitted or interwoven (de Raaf et al,

1977) ripple foreset bundles are developed. Horizontal burrows are locally developed in mudstones and vertical burrows are locally developed in crosslaminated sandstones.

Ripples are asymmetrical, range in amplitude from 0.5 to 1 inch (1.5 to 3 cm) and include straight- and sinuous-crested linguoid, and lunate types (fig. 3.18).

Composite Sandstone Facies

The thickest facies of the Curtis Formation is the composite sandstone facies so named for the amalgamated parallel beds and tabular and lenticular crossbeds. The apparent parallel bedding is mostly a weathering phenomenon and internally, the beds are more complexly stratified with plane laminations and ripples. This facies comprises the light greenish-gray sandstone interval for which the type-Curtis had been recognized in the San Rafael Swell area. Around most of this area, beds of this facies have a peculiar weathering pattern such that they crop-out as compressed, spheroidally-shaped biscuits (fig. 3.1). This is a distinct feature that was used to identify the Curtis Formation by early stratigraphers. Vertically, these beds are gradually replaced by slope-forming beds in the rippled silty facies at the top of the Curtis and also laterally by the same facies in the northern Henry Mountains and Green River Desert between Horse Bench (Z-12) and Dellenbaugh Butte (Z-8) (fig. 3.19).

At San Rafael Swell West (Z-6) and North Salt Wash (Z-16), the composite sandstone facies crops out as extensive channel-form bodies with fairly flat tops and broadly convex-downward bases. These channel-form lenses are probably hundreds of meters wide and long. Normally, the facies forms a fairly tabular body (fig. 3.20).

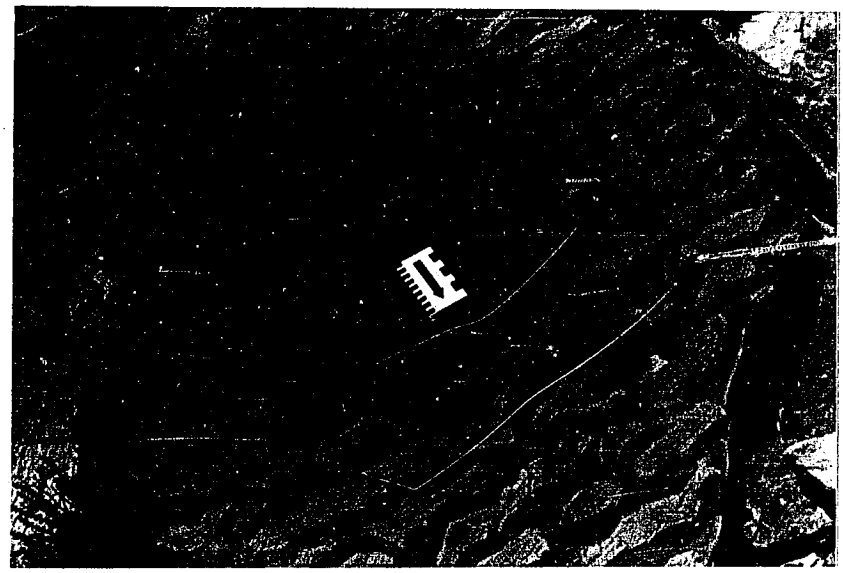

a:

b:

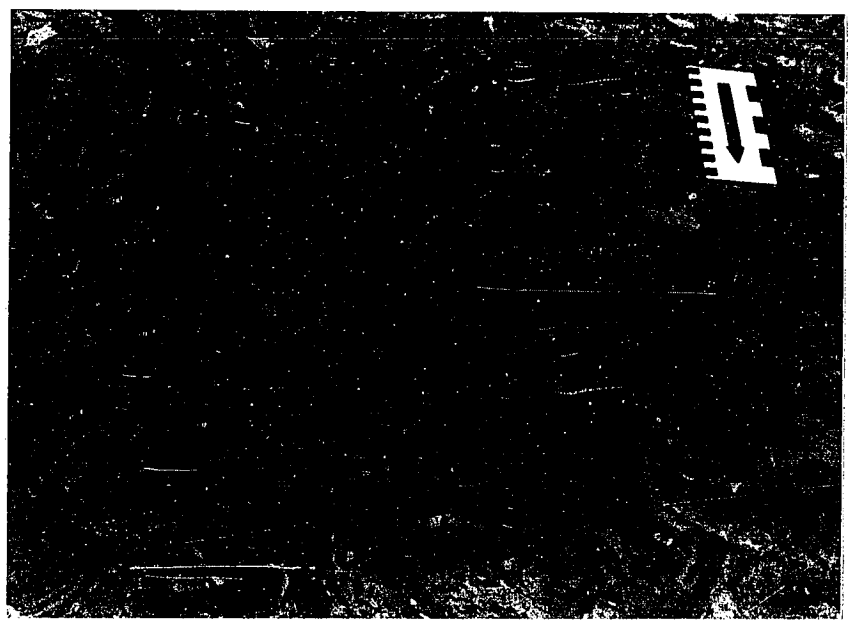

Figure 3.18. Sinuous-crested (sc) and linguoid (li) ripples in the upward-fining, upward-thinning microsequence in the sandstone-mudstone facies. Scale is in inches and centimeters

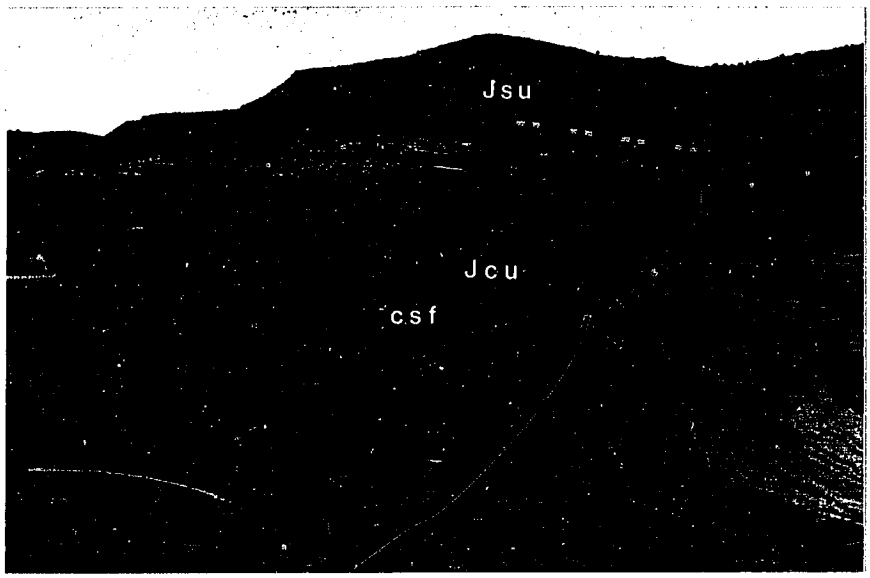

Figure 3.19. Apparent flat beds of the composite sandstone facies (csf) and smooth slope of rippled silty facies (brackets) in the Curtis (Jcu). Dark slope is Summerville Formation (Jsu) (San Rafael Swell Northeast, Z-3A)

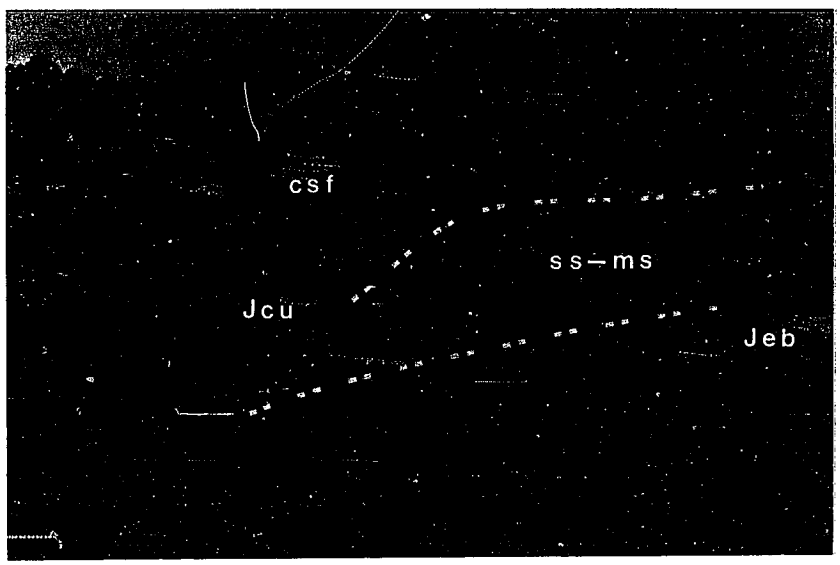

Figure 3.20. Large-scale lensoidal (thickening and thinning) sand-body geometry of the composite sandstone facies (csf) and weathered slope of sandstone-mudstone facies of the Curtis Formation (Jcu). Beds at Goblin Valley (Jeb) (San Rafael Swell West, Z-6)

A complete listing of sedimentary features of the composite sandstone facies (table 3.2), includes both the general features and microsequences and table 3.3 gives details of the crossbedding. The following microsequences are recognized in the facies: 1.upward-fining microsequence, 2. crossbedded microsequence, and 3. parallel-bedded microsequence.

Apart from the microsequences, coalified tree and plant parts (Chapter 4, Petrology) distinguish thissfrom the other facies in the Curtis. Coal fragments are present in all the microsequences and occur as plane beds or laminations, foreset and toeset laminations in crossbeds, and very thin beds and laminations in pause beds. However, coal clasts are rare to absent in facies and microsequences along the eastern, central and southern San Rafael Swell and are completely missing in the Green River Desert. A few coal fragments were found in the mudshale microsequence at San Rafael Swell Northeast (Z-3) and fragments were distributed among crossbed sets at Tidwell Draw (Z-9A). The most abundant occurrence of coal clasts is at San Rafael Swell West (Z-6).

Upward-fining microsequence. Upward-fining microsequences in this facies are locally developed and characterized by incomplete bedding sequences (table 3.2). A complete microsequence (fig. 3.21) begins with a basal crossbedded sandstone (unit a, table 3.2) 3 inches (8 cm) to 1.5 feet (45 cm) thick which is usually trough crossbedded, tabular crossbedded, or indeterminate and composed of fine-to medium-grained sand. Foresets are tangential, sigmoidal, planar, or convex-upward. Complete bedforms have been locally preserved and exposed. They are

Table 3.2. Sedimentary features of the composite sandstone facies in the Curtis Forma

Sedimentary Features	Interpretation	Modern
A. Asymmetric ripples: -straight-crested to in-phase sinuous-crested; local run-off tongues pointing westward; local climbing ripple drift; RI = 5.0-18.4	Wave and non-wave currents; mid- and upper intertidal sand flat; unidirectional currents	Tanner (Thompson
-lunate-linguoid: rib and furrow; polymodal and bimodal paleo-currents; interference ripples	Temporary shoal and higher sand flat emergence and drainage	Ball (196
B. Near symmetrical ripples: irregular lower bounding surfaces; bundle upbuilding; offshoots; bidirectional lenses; complex bundles; local bifurcating crests	Wave orbital currents on shoaling bottom or emerging shoals	
C. Plane lams and beds: parting lineation	Upper flow regime plane bed stage	Harms et
D. Laterally continuous erosion surfaces; 0.5-2 ft (15-60 cm) relief	High-energy sea floor erosion related to storm- or wind enhanced currents	
E. Granule-size ms/slt intraclasts	Rip-up clasts of mud previously deposited during slack or calm water; ripped up during higher energy event	
F. Microsequences 1. Upward-fining d. lenticular-bdd vf (62-88μ) ss and slt; very locally developed c. wavy-bdd cross-lmtd vf ss (88-125 μ) and slt b. plane- and ripple foreset lmtd vf-f ss (88-177); draping ms lams	Base of sand shoal and channel complex; greater availability of sand; little to no mud; higher velocity traction currents; temporary, decelerating currents	Terwindt Greer (19

sandstone facies in the Curtis Formation

ion	Modern	Ancient
n-wave currents; per intertidal sand rectional currents	Tanner (1967), Collinson and Thompson (1982)	Moore (1982)
hoal and higher emergence and drainage	Ball (1967)	Klein (1967, 1970b, 1975a, 1977a), Swett et al. (1971), Moore (1982)
l currents on shoaling emerging shoals		de Raaf et al. (1977)
regime plane bed	Harms et al. (1982)	Harms et al. (1982)
sea floor erosion storm- or wind en- ents		
ts of mud previously during slack or calm ed up during higher t		Harms et al. (1975, 1982)
d shoal and channel reater availability ttle to no mud; higher raction currents; tem- celerating currents	Terwindt (1971a , 1981), Greer (1975)	de Raaf and Boersma (1971), McCave (1973), de Raaf et al. (1977), Cotter (1985)

Table 3.2. Continued

Sedimentary Features	Interpretation	Moder
F. Microsequences (cont.) 1. Upward-fining		
a. med-scale x-bdd set 3 in-1.5 ft (7-45 cm); vf-m ss (88-350 μ); ms partings along foresets; topset and foreset ripples w/ draping ms lams; cylindrical, bilobed trace fossils; shrinkage cracks (?)	Intermittent megaripple bedform migration by shallow marine currents enhanced by wind or storms; slack water and suspension settling and crawling/feeding activity of benthic organisms	Terwi
Generally units bc, bc d, or cd		
2. Parallel-bedded: -locally in cycles 1-1.5 in (2-4 cm) thick w/ low angle discordances/broad erosional scours between cycle sets	Tidal and local wave currents; lower to middle intertidal on topographically higher sand flats or berms; decelerating from plane bed stage or suspension settling from wave currents on submerged shoals; discordances/scours by disharmonic oscillation of shoaling waves; shoal bar build-up and emergence	van S (1958 Reine Ellio
-cycles: 3. draping slt/ms lams 2. ripple foreset lmtd vf ss (62-125 μ); lunate ripples: rib-and-furrow; draping slt/ms lams; angular discordances 1. plane-lmtd vf-f ss (88-177 μ) parting lineation; angular discordances		
-trace fossils: bilobed cylindrical burrows w/ chevron backfills and median furrows; smooth tubes (single lobes) assoc/w ms lams, ripples or plane lams	Cruziana ichnofacies: crawling/deposit feeding tracks of arthropods and gastropods	Howar Ekdal

tation	Modern	Ancient
tent megaripple bedform n by shallow marine currents by wind or storms; slack d suspension settling and /feeding activity of benthic s	Terwindt and Brouwer (1986)	Klein (1970b, 1975a, 1977a), de Raaf and Boersma (1971), Swett et al. (1971)
d local wave currents; middle intertidal on nically higher sand flats ; decelerating from plane e or suspension settling e currents on submerged discordances/scours by nic oscillation of shoaling noal bar build-up and e	van Straaten and Keunen (1958), Terwindt (1971), Reineck and Singh (1980), Elliott and Gardiner (1981)	de Raaf et al. (1977)
ichnofacies: crawling/ feeding tracks of arthro- gastropods	Howard and Dorjes (1972), Ekdale et al. (1984)	Howard (1972), Bromley et al. (1984), Frey and Pemberton (1984)

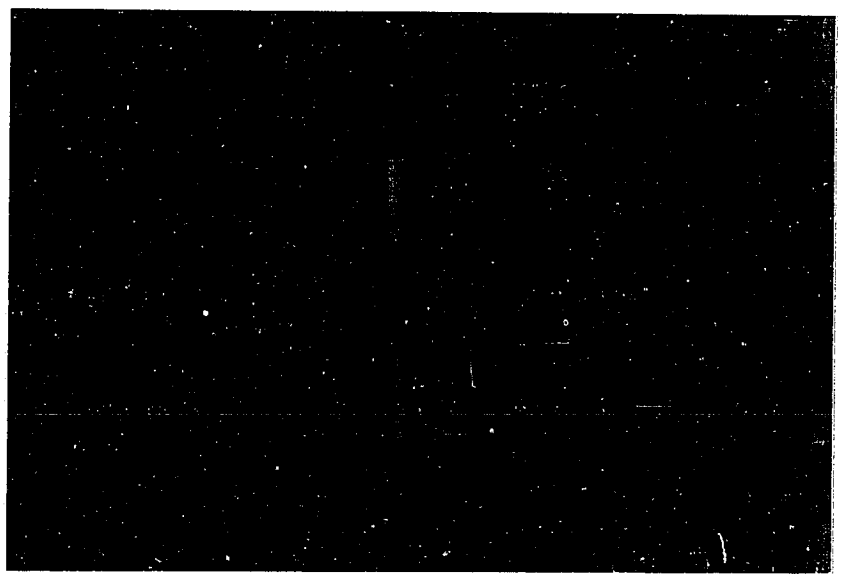

Figure 3.21. Upward-fining microsequence in the composite sandstone facies. Small-scale trough crossbeds (tc), crosslaminations with mudstone flasers (cl), crosslaminated wavy beds (wb). Staff is marked in feet (San Rafael Swell West, Z-6)

characterized by heights of up to 1.5 feet (0.45 m), straight crests and nearly flat stoss sides. They are hereafter referred to as megaripples (Reineck and Singh, 1980) and physically resemble type 1 megaripples of Dalrymple et al. (1978). Topset ripples have been developed on the megaripple stoss side and often extend across the megaripple brinkpoint; ripple crests are usually aligned normal or oblique to megaripple crest (fig. 3.22a). These topset and foreset ripple beds have been thinly buried by darker greenish-gray mudstone laminations with what are identified with uncertainty as shrinkage cracks (fig. 3.22b). In the mudstone laminations, they appear as minute fractures 2 to 3 mm apart and are arranged in polygonal outlines. These questionable shrinkage features are observable along the eastern San Rafael Swell, particularly at San Rafael Swell Northeast (Z-3) and East (Z-2). There are single and bilobed horizontal cylinder-like trace fossils with locally developed chevron back-fill structures that are associated with these mudstone drapes (fig. 3.23). The megaripple beds are successively overlain by irregularly interbedded plane- and crosslaminated fine- to very fine-grained flaser-bedded sandstones (unit b, table 3.2) locally interrupted by mudstone laminations similar to those described above. These beds grade upward into wavy-bedded very fine-grained sandstone and siltstone (unit c, table 3.2) with ripple foresets. Lenticular-bedded very fine-grained sandstone and siltstone (unit d, table 3.2) may be locally developed at the top of the sequence. The microsequence more commonly occurs as partial bedding sequences consisting of combinations of units b and c, units b, c, and d or units c and d.

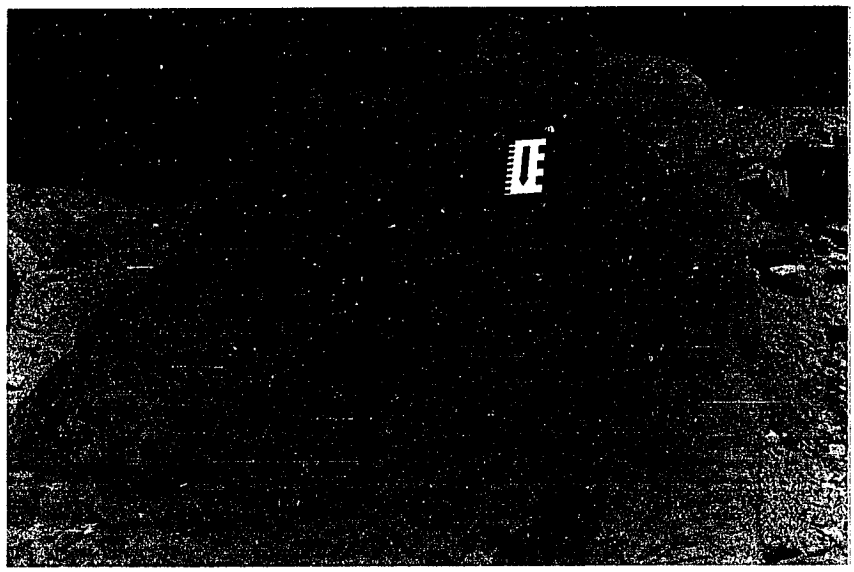

a:

b:

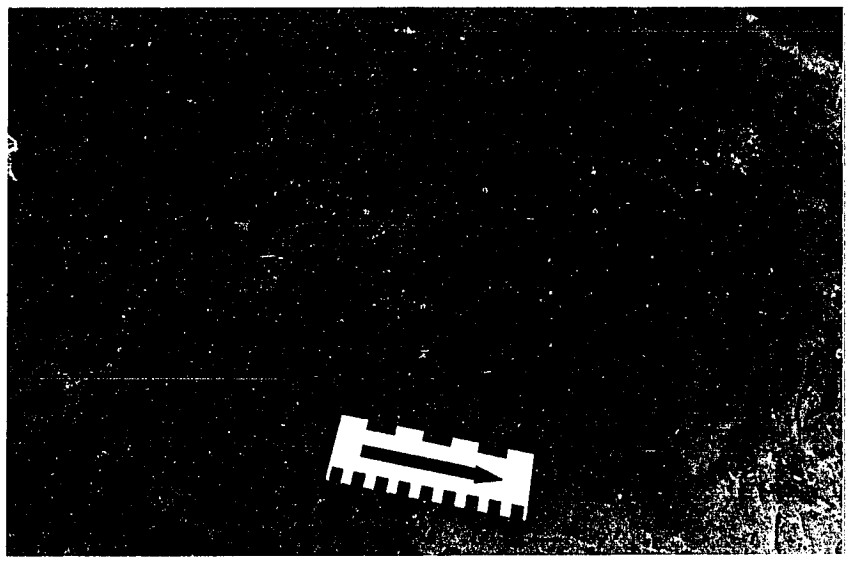

Figure 3.22. Megaripple beds with piggy-back, long-crested ripples on stoss (s) and lee (l) side; crests oriented parallel to migration trend of master bedform (mb) and covered with mudstone laminations with polygonal fractures (f). Scale is in inches and centimeters (San Rafael Swell Northeast, Z-3A)

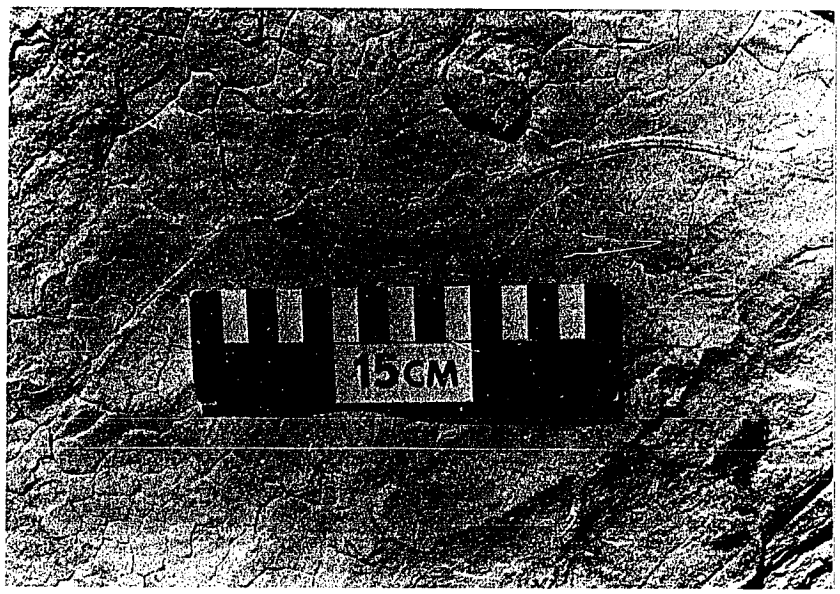

Figure 3.23. Bilobed horizontal trace fossils preserved in draping siltstone/mudstone laminations associated with ripple and megaripple beds; upward-fining microsequence in the composite sandstone facies (San Rafael Swell East, Z-2A)

Crossbedded microsequence. Crossbedded microsequences consist of solitary, simple trough beds 3 inches to 3 feet (7 to 90 cm) thick, cosets or composite trough-beds up to 20 feet (6m) thick, or simple and composite tabular sets with complex internal foreset bundles up to 3 feet (90 cm) thick. Composite trough beds are complexly interbedded with plane- and ripple-laminated sandstone beds of the parallel-bedded microsequence.

Locally, the crossbedded microsequence and parallel-bedded microsequence (next section) form a composite sequence. At least four cycles of the composite sequence are developed and exposed along the Interstate 70 at San Rafael Swell West (Z-6) (fig. 3.24). Here, bedding cycles consist of a basal coset of trough cross-strata. Trough sets are 1 to 2 feet (30 to 45 cm) thick and are composed of fine- to medium-grained sand with local coal clasts. Trough sets become thin upward and are overlain by a succession of rhythmic beds up to 6 feet (1.9 m) thick (fig. 3.25). Each rhythmic bed is a triplet of plane-laminated fine- to very-fine grained sandstone, ripple-laminated very-fine grained sandstone, and laminated siltstone or mudstone.

Crossbeds in the microsequence typically form medium-scale sets or megaripple beds ranging in thickness 3 inches to 3 feet (15 to 90 cm). Generalized features of crossbedding include a. fine- to medium-sand size except for crossbed sets greater than about 2 feet (0.60 m) which are made of medium to slightly coarse sand, b. composite foresets with unidirectional dips; smaller-scale herringbone sets are locally developed, c. coal clasts and granule-size mudstone intraclasts locally compose pause beds, foresets, and toesets, d. foresets are locally interrupted by mudstone laminations, forward- and back-flow ripples, e. sandflow thickness proportional to crossbed set thickness and, f.

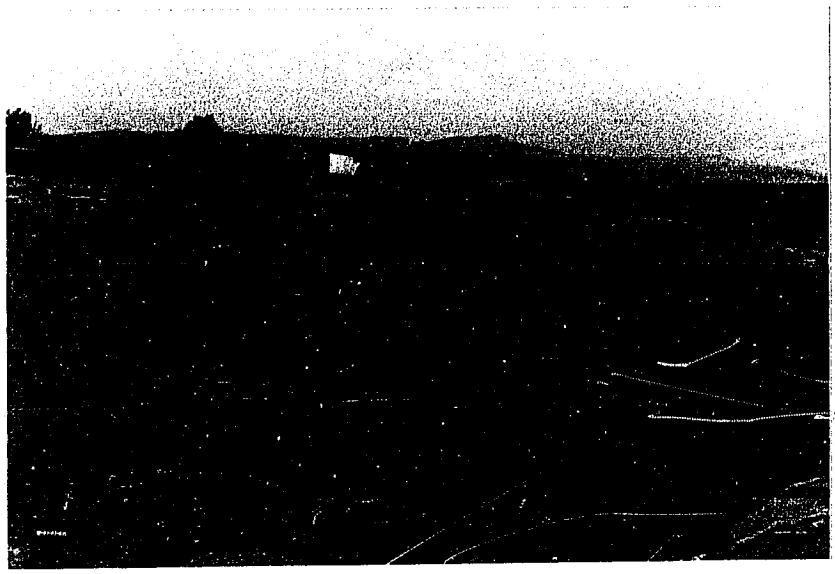

Figure 3.24. Cycles composed of crossbedded microsequences (cb) overlain by parallel-bedded microsequence (pb) (San Rafael Swell West, Z-6)

Figure 3.25. Detail of one upward-fining cycle of trough crossbeds (cb) overlain by parallel beds (pb) in the composite sandstone facies. Staff is in feet (San Rafael Swell West, Z-6)

Table 3.3. Anatomy of crossbedding in the composite sandstone facies in the Curtis Form

Sedimentary Features	Interpretation	Modern
1. Crossbedded microsequence		
a. simple trough sets: 3 in-3 ft (7-90 cm) thick; composite trough sets: up to 20 ft (6 m) thick; simple and composite tabular sets: up to 3 ft (90 cm) thick		
b. f-slightly c ss (250-500 μ); m-c ss in sets greater than 1.5 ft (45 cm); granule-pebble ms intraclasts		
c. unidirectional bedsets with overall bimodal and polymodal paleocurrents; first-order (E-1) erosional surfaces bounding simple sets; second-order (E-2) erosional or discontinuity surfaces	Time-velocity asymmetry; dominant unidirectional currents, either flood- or ebb-tide currents, in separate courses; polymodal crossbed azimuths may reflect sinuous nature of tidal courses	Evans (1965 (1967), Boe Reineck and (1969), de Boersma (19 and Hubbard (1976), All (1976), Kle Allen (1980 Singh (1980
d. foresets: near angle-of-repose sandflow strata dipping 25-32 degrees -planar: straight, or convex upward -tangential: concave-upward and sigmoidal -slt lams along foresets		
e. ripples w/ polymodal paleoflow: -backflow ripples along lower bounding surfaces, buried by sandflows	Waning tidal flow or late-stage emergence run-off	Reineck and Klein (1977 Gardiner (1
-leeside ripples along x-bd foresets	Pause in master bedform migration	Boersma (19 Brouwer (19
-topset ripples w/ draping ms lams and shrinkage cracks	Pause in master bedform migration	
-reverse and forward flow ripples in pits and scoops; loads on ripple bed soles; ripple fans	Falling water stage and emergence	Elliott and
-trough-shaped pits and scoops 2-20 ft (0.6-6 m) wide with trough intersections (ribs)		

e sandstone facies in the Curtis Formation

ion	Modern	Ancient
ty asymmetry; idirectional ther flood- currents, in urses; poly- ed azimuths sinuous nature urses	Evans (1965), Postma (1967), Boersma (1969), Reineck and Wunderlich (1969), de Raaf and Boersma (1971), Boothroyd and Hubbard (1975), Hayes (1976), Allen and Friend (1976), Klein (1977a), Allen (1980), Reineck and Singh (1980), Clifton (1982)	Klein (1970b, 1975a), Swett et al. (1971)
flow or late-stage n-off	Reineck and Singh (1980), Klein (1977a), Elliott and Gardiner (1981)	Klein (1970b, 1975a) Swett et al. (1971)
ter bedform migration	Boersma (1969), Terwindt and Brouwer (1986)	
ter bedform migration		
r stage and emergence		
	Elliott and Gardiner (1981)	

Table 3.3. Continued

Sedimentary Features	Interpretation	Modern
1. Crossbedded microsequence (cont.)		
e. ripples w/ polymodal paleoflow: -coal clasts forming lams and thin beds in toesets, in axial parts of trough x-bds, and as parallel beds -cylindrical burrows w/ bulbous terminations; assoc/w thicker denser coal accumulations	Allochthonous and transported tree/plant frags derived locally near shoreline to southwest; shallow burial and coalification Teredolites trace fossil: dwelling structure of wood-boring marine bivalve in local xylic substrate	

ion	Modern	Ancient
us and transported tree/ derived locally near o southwest; shallow coalification		Bryer and McCabe (1986)
trace fossil: dwelling f wood-boring marine bi- cal xylic substrate		Bromley et al. (1984), Ekdale et al. (1984), Howard and Frey (1984), Kamola (1984)

Table 3.3. Continued

Sedimentary Features	Interpretation
1. Crossbedded microsequence (cont.)	
Bedding Type 1: -up to 6 in (15 cm) thick -poorly sorted; silty vf-f (62-250 μ) ss -local lams formed by coal clasts -boundary with Bedding Type 2 (downcurrent) gradational or unclear -continuous top-, fore- and toeset lams	Depositional pause plane or disco tinuity; may represent low veloci traction and suspension sedimenta and period of immobility of maste bedform during neap tide (?)
Bedding Type 2 -locally developed ripple-lmtd basal beds; foreset lams poorly developed -gently dipping (less than 15 degrees) concordant lams; local complete foreset ripple lams dipping in same direction as master foresets; local coal clasts along ripple foresets and forming part of gently dipping concordant lams -foresets transitional with full-vortex lams; dip: 13-18 degrees -local topset of megaripple crossbeds w/ foresets dipping opposite to that of underlying master foresets (type 3); topset ripples (rib-and-furrow)	Reactivation or acceleration stru resumption of master bedform migr during higher current velocities spring tides Ripple roof: megaripples and rip generated by subordinate, opposi current
Bedding Type 3 -straight-planar, convex-upward and planar to concave-upward and tangential; wedge geometries; thickening downcurrent; -foreset dip: 19-33 degrees -tangential toesets dip: 9-18 degrees -sharp foreset boundaries -normally graded foresets; upward-fining: fine to very fine (177-88 μ) -well-developed sigmoidal foresets -granule-size ms intraclasts along foresets and toesets -up-current truncation and angular relationship with sigmoidal topsets -slumps; ball-and-injection structures	Full-vortex or acceleration fore produced in the dominant tidal c during spring tides when current are greater relative to neap tid Mud previously deposited during and reworked as rip-up clasts Contemporaneous soft-sedimentary deformation caused by liquefacti lateral shearing

Interpretation	References
Depositional pause plane or discontinuity; may represent low velocity traction and suspension sedimentation and period of immobility of master bedform during neap tide (?)	Allen (1980), Boersma and Terwindt (1981a, b), Kohsiek and Terwindt (1981), Terwindt (1981), Terwindt and Brouwer (1986)
Reactivation or acceleration structures; resumption of master bedform migration during higher current velocities of spring tides	Collinson (1970), Boersma and Terwindt (1981a, b), Kohsiek and Terwindt (1981), Terwindt (1981)
Ripple roof: megaripples and ripples generated by subordinate, opposing tidal current	Boersma and Terwindt (1981a)
Full-vortex or acceleration foreset beds produced in the dominant tidal current during spring tides when current velocities are greater relative to neap tides	Boersma and Terwindt (1981a, b), Kohsiek and Terwindt (1981), Terwindt (1981)
Mud previously deposited during slack water and reworked as rip-up clasts	
Contemporaneous soft-sedimentary deformation caused by liquefaction and lateral shearing	Tillman and Martinsen (1984) Casshyap and Kumar (1987)

Table 3.3. Continued

Sedimentary Features	Interpretation
1. Crossbedded microsequence (cont.)	
Bedding Type 4 -sigmoidal beds: continuous topset, foreset and bottomset beds -topset beds dip: 9-13 degrees foreset beds dip: 15-27 degrees toeset beds dip: 9-18 degrees	Decelerating currents in the d tide during spring tide cycle; swept into suspension during f stage settles farther ahead of bedform

Interpretation	References
Decelerating currents in the dominant tide during spring tide cycle; sediment swept into suspension during full-vortex stage settles farther ahead of master bedform	Boersma and Terwindt (1981a, b) Kohsiek and Terwindt (1981) Terwindt (1981)

locally deformed foresets (tables 3.2, 3.3).

Dip-section exposures show that simple trough crossbeds form sets bounded by first-order (E-1) bounding surfaces and are interrupted by second- (E-2) and locally third-order (E-3) surfaces (Allen, 1980; Blakey, 1984); they are characterized by vertically adjacent sets with bimodal paleocurrent azimuths (fig. 3.26). Strike-oriented exposures clearly reveal convex-downward lower bounding surfaces, suggestive of trough crossbedding. Trough cross-sets are composed of approximate angle-of-repose sandflow strata dipping 25 to 32 degrees. Downcurrent extensions of foresets form toesets or bottomsets which approach lower bounding surfaces tangentially. There are discontinuities that interrupt the downcurrent progression of foreset strata and consist of mudstone laminations or intervals 0.5 cm thick or less of foreward- and back-flow ripple crosslaminations. There are crossbed sets with wedge geometries that exhibit concave-upward foresets with tangential toesets and convex-upward foresets that are planar and approach the lower bounding surface at an acute angle (fig. 3.27). Favorable bedding-plane exposures reveal the geometry of intersections between upper bounding surfaces and top of foresets. Foresets have cuspate or arcuate outlines as well as straight outlines. Cuspate foresets are commonly associated with trough-crossbedding with tangential toesets. However, there are foreset intersections exposed along bedding planes that are linear in plan view and are characterized by tangential toesets and somewhat planar (non-trough) lower bounding surfaces.

At certain stratigraphic intervals, crossbed sets are characterized by a distinct suite of foreset geometries and small-scale stratification features. Stratification differs from normal

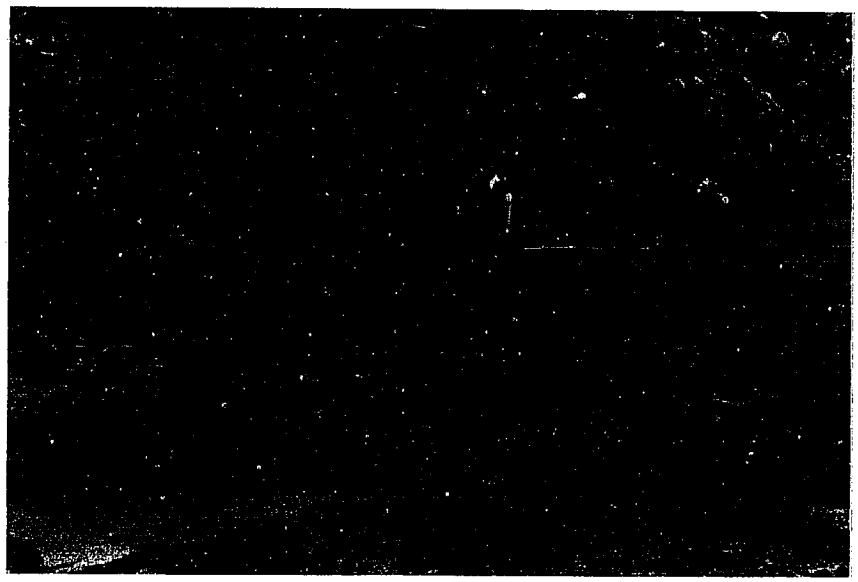

Figure 3.26. Coset of crossbeds with first-order (E-1) and second-order (E-2) bounding surfaces (Buckhorn Wash, Z-18)

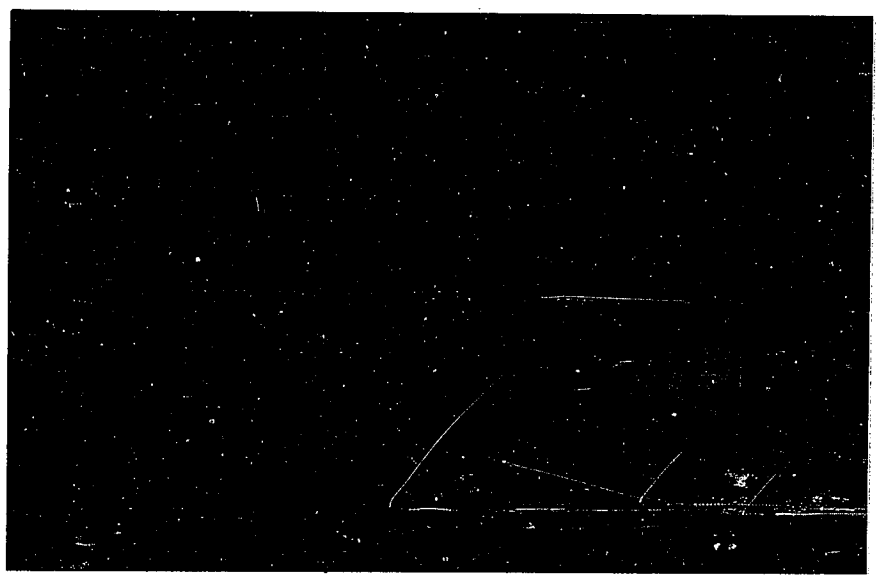

Figure 3.27. Convex-upward planar foresets in crossbedded microsequence, composite sandstone facies. Scale is in inches and centimeters (Lookout Point, Z-14)

sandflow and grainflow strata, and has been described in detail by Boersma and Terwindt (1981a, b), Terwindt (1981), and Kohsiek and Terwindt (1981) in Recent deposits. The different foreset geometries and angles of repose are generated and preserved in a nearly predictable, downcurrent pattern and reflect different, corresponding hydrodynamic conditions. The peculiar foresets form cross-stratified beds at different stratigraphic levels in the facies, particularly in the crossbedded microsequence. Up to four zones or intervals have been described from stratigraphic sections along the San Rafael Swell, especially on the west side. The following discussion is based on observations from various stratigraphic sections but specific examples are illustrated from the roadcut exposure at San Rafael West (Z-6) along Interstate Highway 70 (table 3.3).

a. Bed type 1. Groups or bundles of foresets are separated by sigmoidal or s-shaped beds ranging from 0.75 to 6 inches (2 to 15 cm) thick. The relationship of these sigmoidal beds to contiguous strata is similar to that of sigmoidal E-2a erosional or discontinuity surfaces described by Allen (1980). Pause beds deposited by separate temporal events completely enclose a unit which is rhomboidal in outline and comprises a foreset bundle. Consequently, these beds not only form sigmoidal leeside beds that are concordant with upcurrent and downcurrent foreset bundles but also compose topset and bottomset beds. The beds are poorly sorted silty very fine- to fine-grained laminated and massive sandstones in which are formed dark laminations of coal clasts up to 0.5 inches (1.5 cm) thick and as many as 15 laminations per bed. They form a concordant or conformable relationships between upcurrent and downcurrent foresets (fig. 3.28).

b. Bed type 2. Immediately downcurrent of bed-type 1 may be zone

of indistinct foreset laminations or beds, crinkly bedding (Kohsiek and Terwindt, 1981), interlaminated mudstones, or poorly developed ripple laminations. These features compose bed type 2 and were observed downcurrent of only one type 1 bed. The majority of type 2 beds are typified by tangential foreset laminations which dip 15 degrees or less and are concordant with underlying pause beds. There may be complete ripple foreset laminations locally superimposed on and dipping in the same direction as the master foresets. Coal fragments may occur along ripple or master foresets. Downcurrent, these foresets grade into other foresets which dip more steeply, between 13 and 18 degrees, and mark the transition with stratification type 3 (fig. 3.28).

c. Bed type 3. Downcurrent of the type 2 foreset is a zone of foresets that may by angular or tangential with respect to lower bounding surfaces and may be straight, concave-upward or slightly convex-upward (fig. 3.28). Foresets are composed of distinct wedge-shaped sandflow strata that are characterized by sharp boundaries, down-current thickening, reverse grading from very fine- (88 microns) to fine-grained (140 microns) sand, local ripples and mudstone along grain flow boundaries, and dip angles between 19 and 33 degrees. Low-angle (9 to 13 degrees) topset beds pass downcurrent into foreset beds; the intersection between the two forms a sharp, angular brinkpoint or knickpoint. Slump-, ball- and injection- structures locally deform these foresets. Often and without the development of type 2 beds, type 1 beds pass downcurrent into type 3 beds. In this case, crossbeds are planar to slightly convex-upward, approach lower bounding surfaces at an acute angle and are separated by slightly convex-upward or sigmoidal

second-order (E-2) bounding surfaces. Locally, the lower bounding surface has a thin deposit with crosslaminations diping opposite to that of overlying master crossbeds (fig. 3.28).

d. Bed type 4. The extreme downcurrent structures of bed type 4 are long, draping sigmoidal beds. Topset beds dip between 9 and 13 degrees and are discordant with underlying type 3 foresets. Downcurrent, the wedge thickens as the topset laminations grade into foreset laminations that are now concordant with underlying type 3 foresets. A rounded, brinkpoint is formed at the junction between topset and foreset beds. Foreset beds are nearly straight to slightly concave-upward and dip between 15 and 27 degrees. They extend into long, tangential toesets dipping between 9 and 13 degrees. In some crossbed sets, type 4 toesets are less well developed or absent. Type 4 strata wedge-out into and intertongue with the next downcurrent pause bed (fig. 3.28).

For a given crossbed set or coset, foresets may dip uniformly in one direction. However, when crossbedding is measured at different lateral and vertical stratigraphic positions bimodal and polymodal dip directions are realized (fig. 3.11).

There are other important sedimentary features associated with the above crossbed types. Gravel-sized mudstone intraclasts are concentrated near the tops of foreset beds and along toeset beds or may occur in small pods and lenses associated with erosion surfaces. The intraclasts are equant and prism- or disc-shaped and have usually been weathered from the outcrop to form cavities of similar geometries.

As previously described, coal clasts or coalified tree and plant fragments are associated with toesets or axial parts of trough crossbeds depending on the perspective of the exposure. Coal clasts

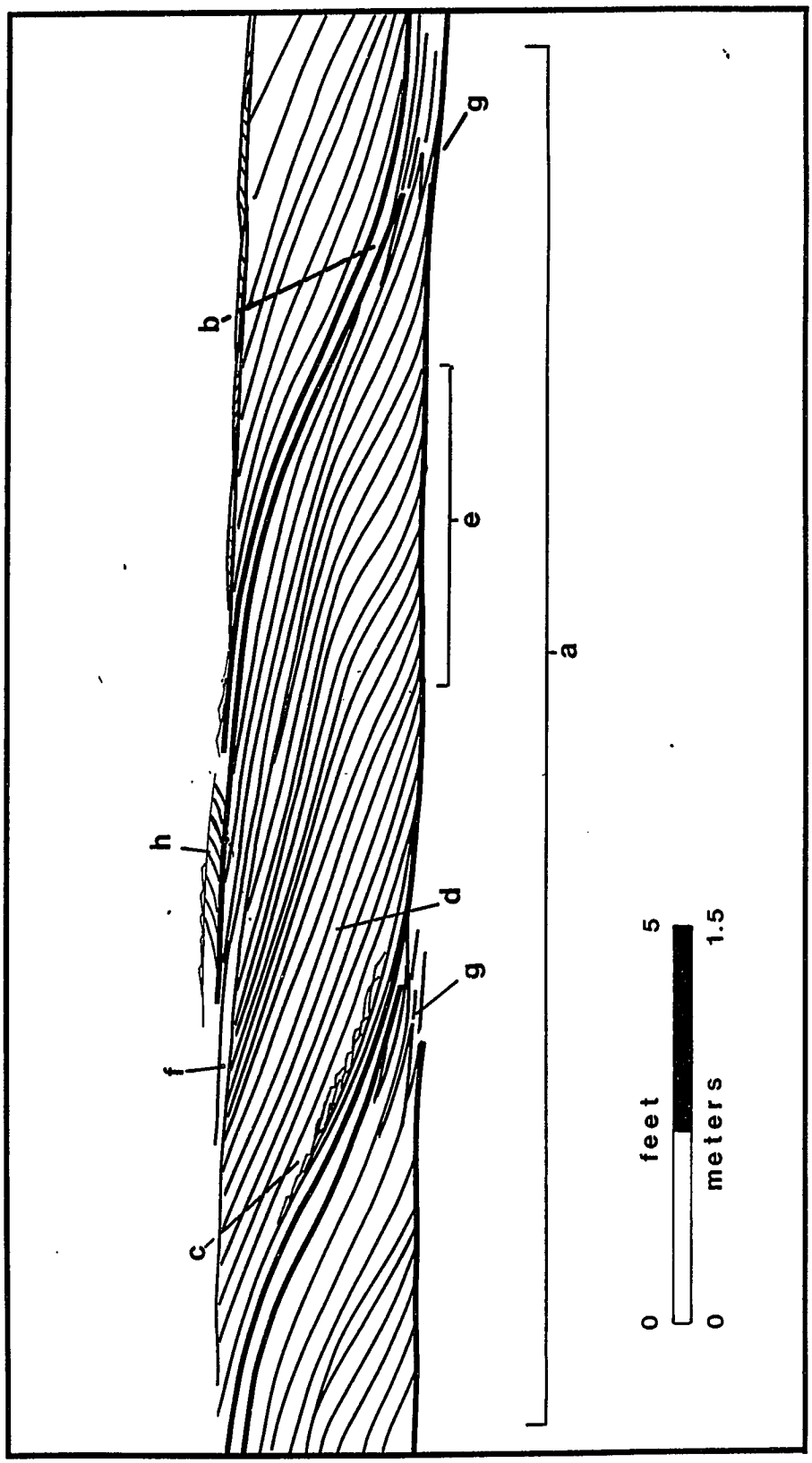

Figure 3.28. Distinctive bedding types in crossbeds of the composite sandstone facies of the Curtis. Letters correspond with plates which follow

Plates for figure 3.28 (San Rafael Swell West, Z-6)

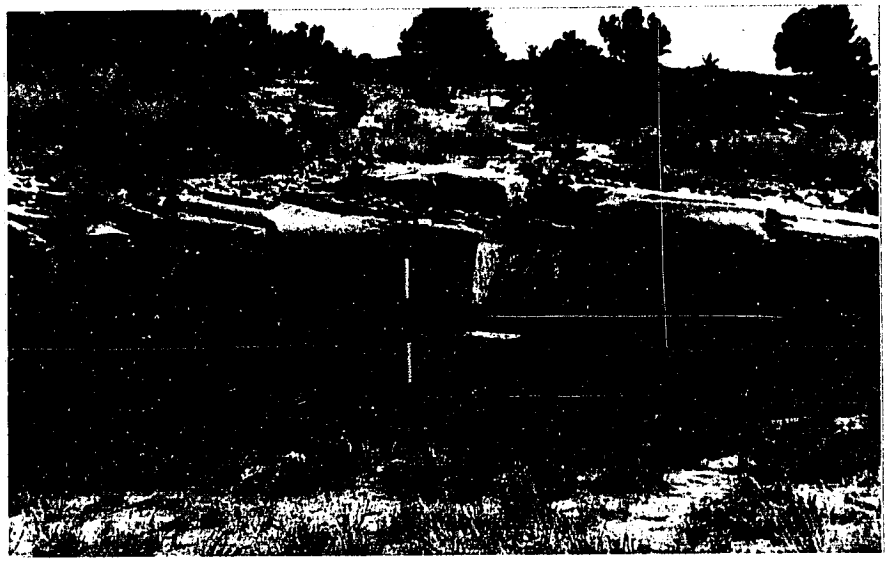

a: Sigmoidal geometry of foreset bundles bounded by recessed bed type 1 (bt1). Staff is in feet

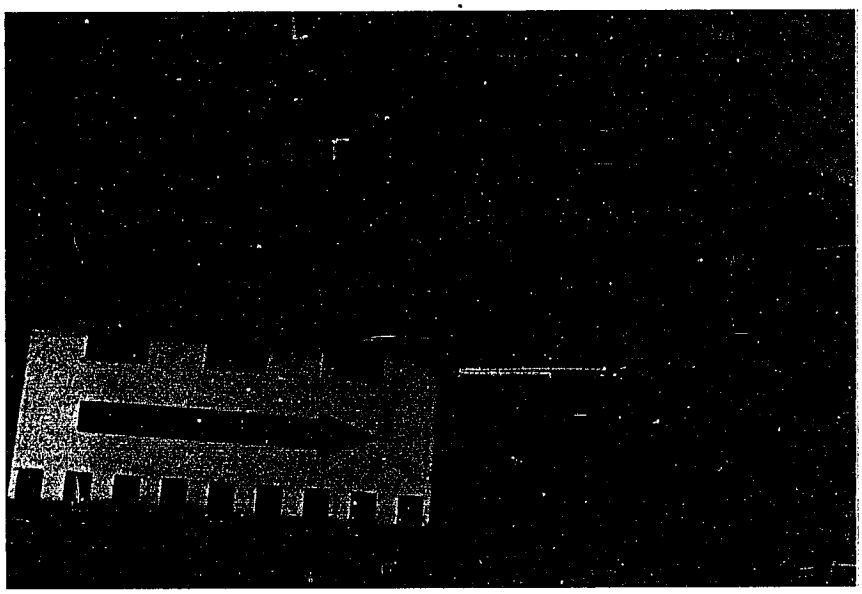

b: Detail of toe of bed type 1 consisting of light-colored silty sandstone and dark laminations composed of coal clasts. Scale is in inches and centimeters

c: Locally developed ripple bundles associated with bed type 2. Scale is 6 inches (15 cm) long

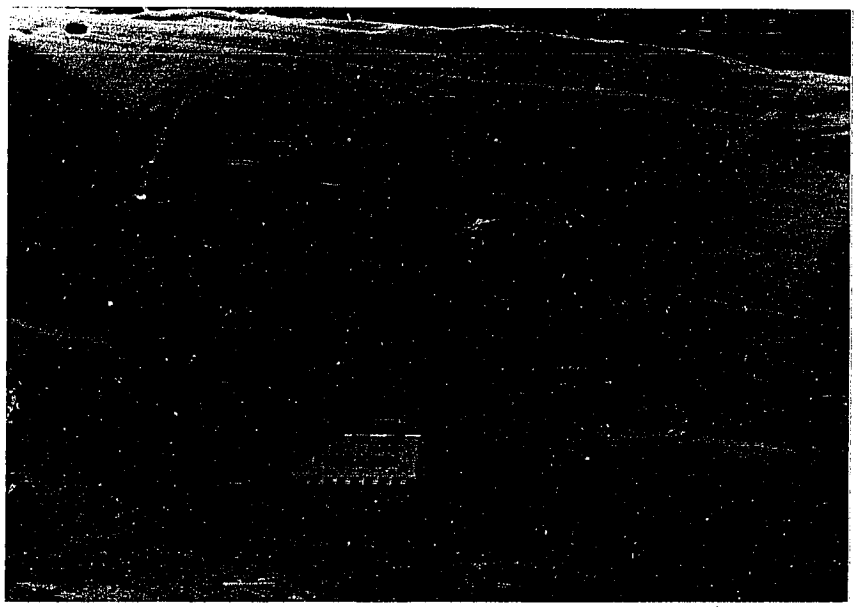

d: Gently-dipping concordant foreset laminations of bed type 2. Scale is in inches and centimeters

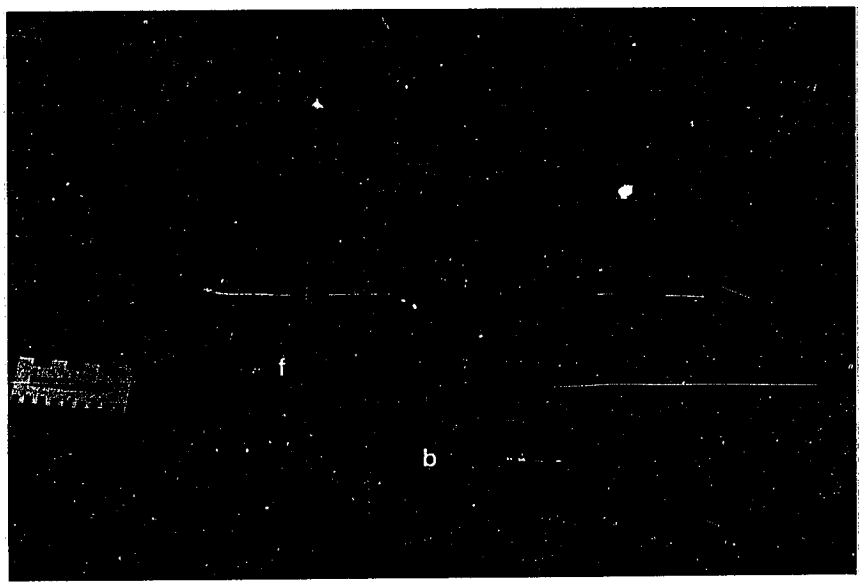

e: Complete megaripple strata consisting of topset (t), brinkpoint (bp), foreset (f), and bottomset (b) of bed type 3. Scale is in inches and centimeters

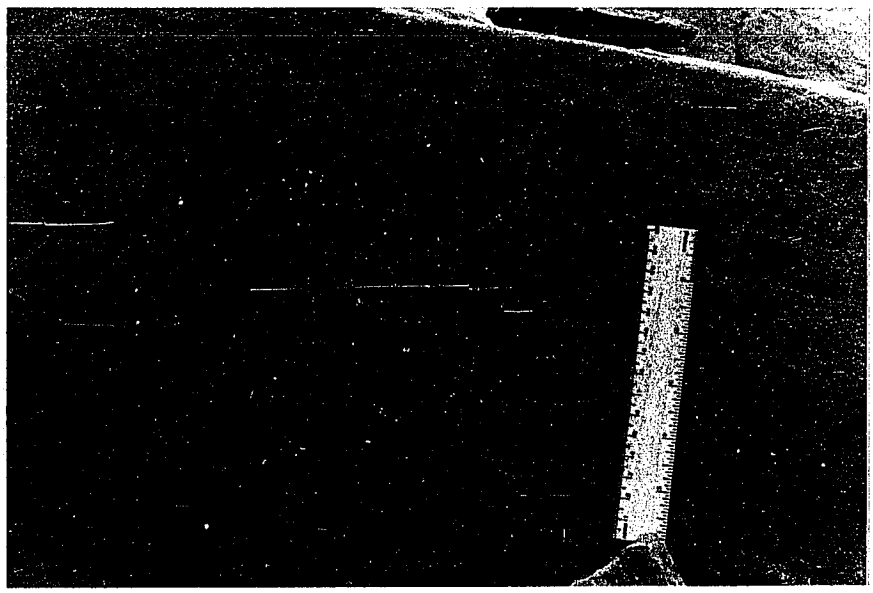

f: Locally developed surface (arrow) which truncates foresets of bed type 3 (bt3). Scale is 6 inches (15 cm) long

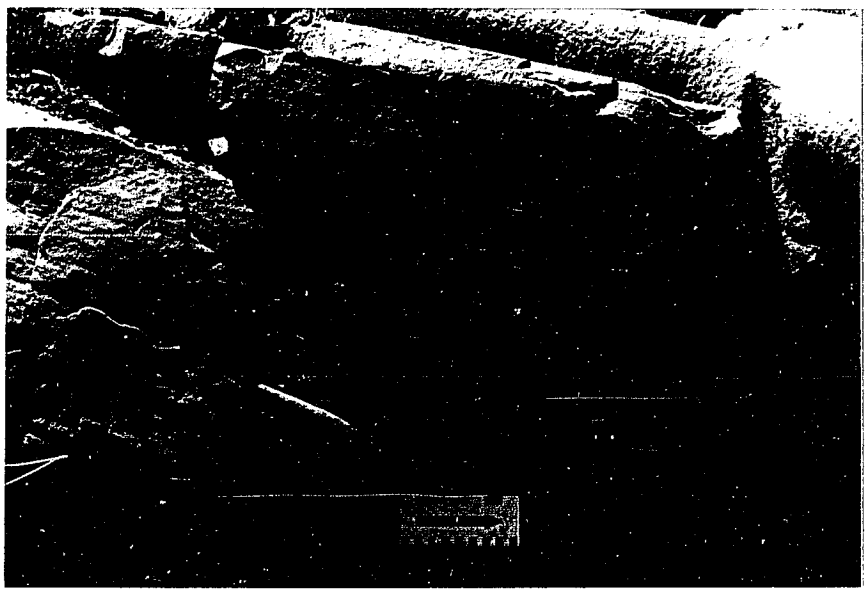

g: Interfingering relationship between bed type 4 (bt4) and bed type 1 (bt1). Scale is in inches and centimeters

h: Small-scale crossbed set with foresets dipping in direction opposite to that of underlying type 4 beds of master crossbed set. Scale is in inches and centimeters

commonly form foreset, toeset and pause bed laminations and distinct beds up to 1 inch (2.5 cm) thick. Vertical tube-like trace fossils with bulbous downward terminations of the ichnogenus Teredolites are locally found among mat-like sandy coal deposits (fig. 3.29). Specific petrologic aspects of the coal fragments are discussed in Chapter 3.

At Buckhorn Wash (Z-18) is a stream-cut exposing a complex megaripple coset 20 feet (6m) thick and an array of troughs and scoop-shaped scour pits with distinct intersections or ribs between adjacent scour pits (fig. 3.30). Some scour pits have been filled in with medium-scale trough crossbeds and others have been partially filled in with asymmetric ripples showing mainly bidirectional and some multidirectional trends. Straight- to sinuous-crested ripples are commonly associated with the shallower sides of the trough or pit while lunate ripples are associated wth the deeper trough axis. Mean ripple length is 4.5 inches (6.5 cm) amd mean height is 0.5 inches (1.5 cm). Gyrochorte and Planolites-like locomotion and grazing traces are associated with siltstone laminations which drape the ripple surface.

Ripples with draping siltstone laminations locally form discontinuities between successive foreset beds. In relation to master crossbeds upon which they occur, ripple symmetry and foresets indicate forward-, reverse-, and locally oblique- and parallel-flow suggesting a polymodal paleoflow (fig. 3.31). Reverse-flow ripples locally buried by and interbedded with grain flow foresets occur along lower bounding surfaces of some crossbed sets. Ripples and small megaripples form thin, cross-stratified beds (2.5 inches or 6 cm thick or less) directly above medium-scale crossbeds and show foreset dip azimuths exactly opposite to the underlying crossbeds (fig. 3.28) These beds may be

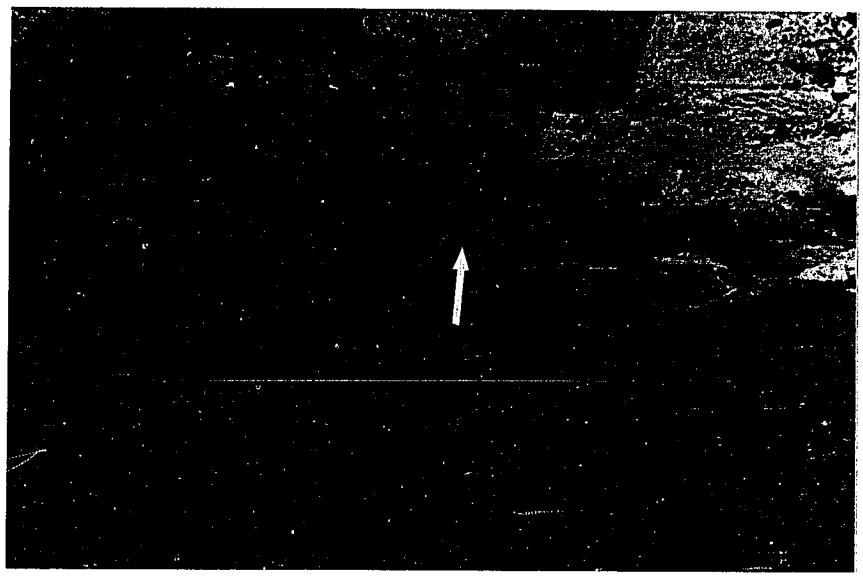

Figure 3.29. Thin beds composed of coalified plant matter (coal clasts) associated with crossbedded microsequences; locally developed Teredolites burrows (arrow) (San Rafael Swell West, Z-6)

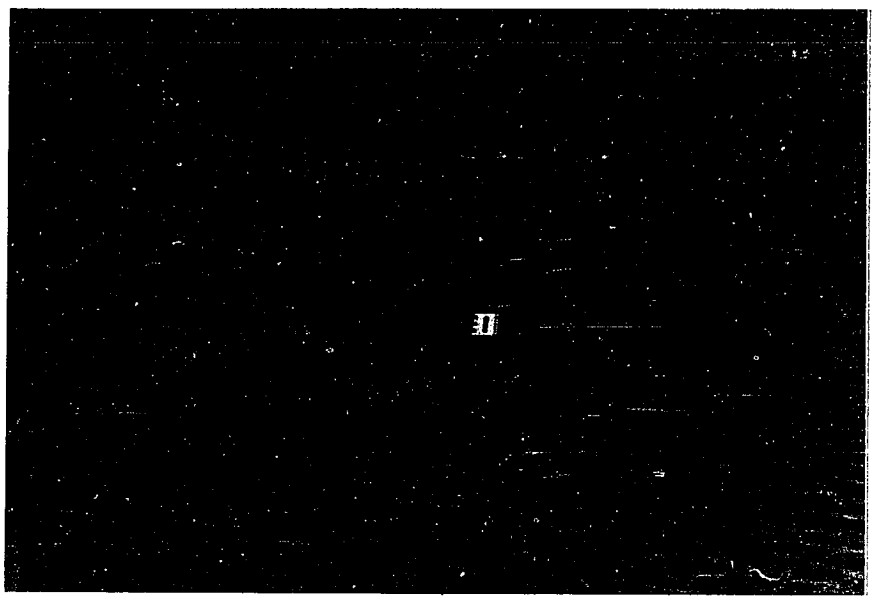

Figure 3.30. Trough-shaped scour pits filled with ripple fans; note pit intersections (ribs). Scale is in inches and centimeters (Buckhorn Wash, Z-18)

Figure 3.31. Megaripple beds with piggy-back ripples forming topset and foreset beds. Ripple-crest orientations are nearly parallel to migration direction of megaripple (North Salt Wash, Z-16)

considered the "ripple roof" of Boersma and Terwindt (1981).

Stratification ratio maps have been used by Smith (1970) and Peterson (1980) to demonstrate the downstream changes in stratification types and corresponding stream energies in modern and ancient braided stream deposits. The ratio is P/P+H where P is the total thickness of planar crossbeds and H is the total thickness of horizontal or plane laminations (Smith, 1970; Peterson, 1980). Figure 3.32 is a map showing percent of net crossbedded sandstone in the Curtis Formation. It is similar to a stratification ratio map in that it shows the increase or decrease in all crossbedding relative to the other sedimentary structures in the Curtis. The map reflects the ratio of cumulative thicknesses of crossbed sets to the total thickness of the Curtis measured in the field. The apparent horizontal beds of the parallel- and cross-bedded sandstone facies is complexly interstratified with plane- and ripple-laminations and crossbeds. Unless a bedding exposure reveals parting lineation, rib-and-furrow structures or crosslaminations, it is difficult to distinguish plane- from ripple-laminations in cliff exposures. Thus, it was not possible to employ the stratification ratio concept in the strictest sense.

By comparing figure 3.32 with isopach maps in figures 3.3, 3.4, and 3.6 similar patterns are observed. Values reflecting high percentages of crossbedding form a trough-like pattern that coincides with thick trends or troughs on isopach maps. Furthermore, the map shows that crossbedding increases in percentage or abundance in a westward and northwestward direction. It is replaced by other bedding to the south and east.

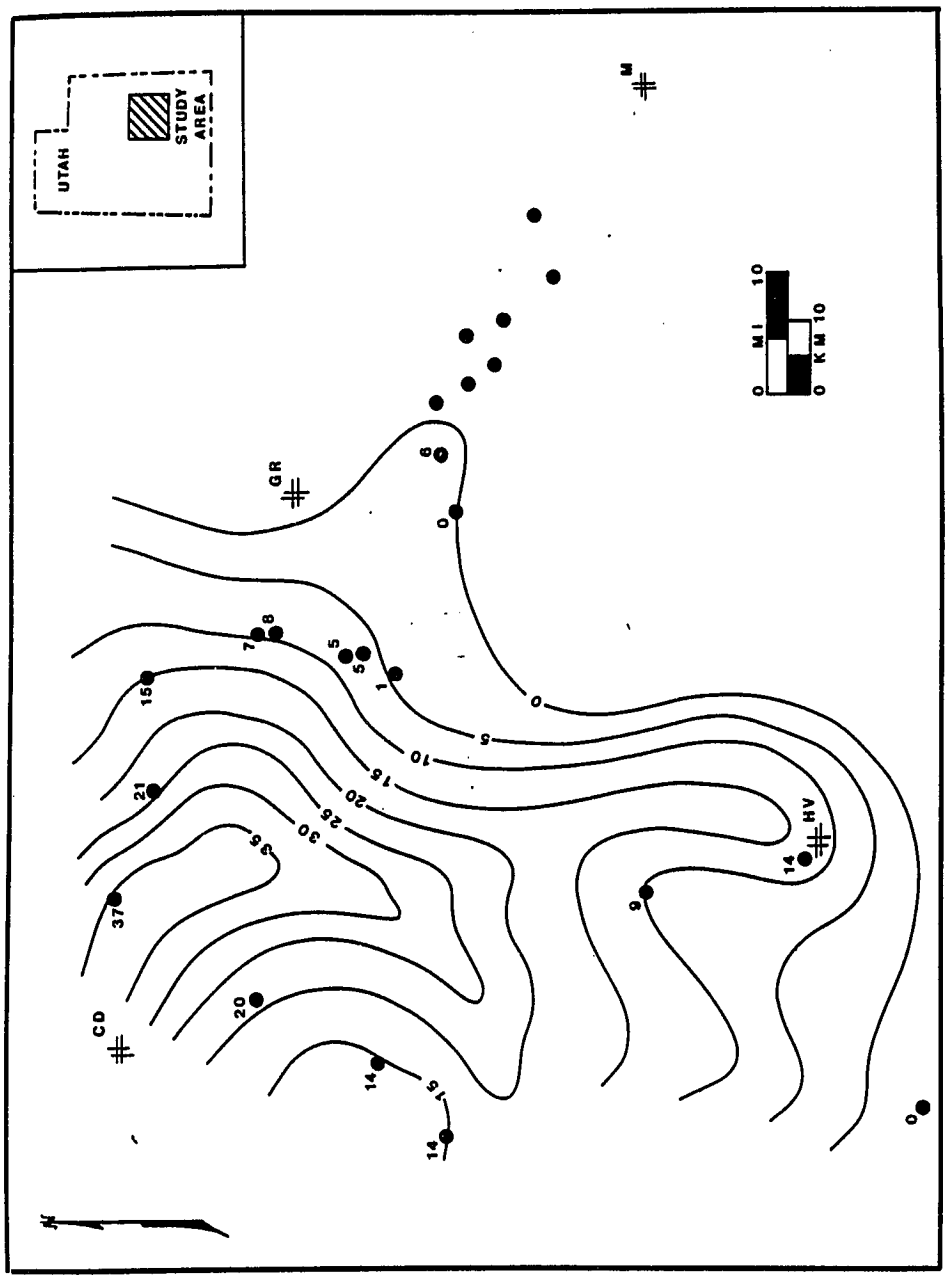

Figure 3.32. Percent net crossbedded sandstone in the Curtis Formation. Contour interval: 5%. Map symbols (table 1.3)

Parallel bedded microsequence. The parallel-bedded microsequence ranges in thickness from 4 inches (10 cm) to several tens of feet thick; often nearly as thick as the entire composite sandstone facies. The microsequence resembles a series of simple, flat, parallel, beds (fig. 3.33a), however the beds are internally stratified with small-scale, locally repetitive cycles. The cyclic beds are triplets composed of plane laminations, partial to complete ripple-form laminations, and siltstone or mudstone laminations, in ascending order, and are 1 to 1.5 inches (2 to 4 cm) thick (fig. 3.33b). In other intervals, this three-part cycle is replaced with amalgamated beds of varying thickness consisting of either plane laminations, ripple laminations or irregular intercalations of plane- and ripple laminations with local mudstone laminations. Broad discontinuities extend several feet laterally and create subtle angular discordances between these beds (fig. 3.34). This feature is common in most exposures of the facies all along the San Rafael Swell. In other places, laterally extensive truncation horizons are marked by extremely abrupt discontinuities, 0.5 to 2 feet (15 to 60 cm) of erosional relief, and lenses of mudstone intraclasts (fig. 3.35) (table 3.2).

A great variety of ripples is preserved in this interval. Lunate ripples are responsible for most of the ripple laminations in the triplet and are preserved as rib-and-furrow structures on exposed bedding surfaces. The furrows are 0.5 to 1.0 inch (1.5 to 2.5 cm) deep, 3 to 5 inches (7.5 to 12.5 cm) wide, and have been filled with delicate ripple foreset laminations (fig. 3.36). The crosslaminations indicate localized uni- and bimodal paleocurrents within an overall polymodal paleocurrent regime (Paleocurrent Trends, previous section, this

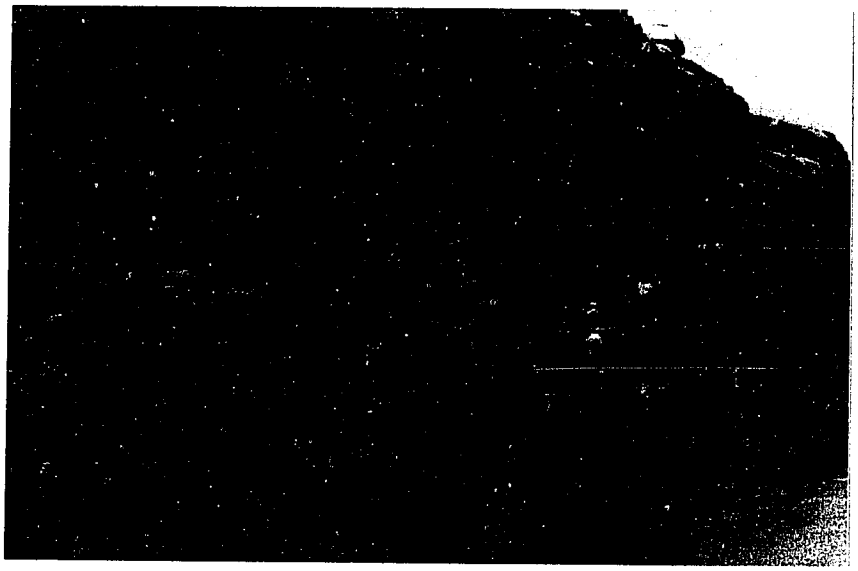

a:

b:

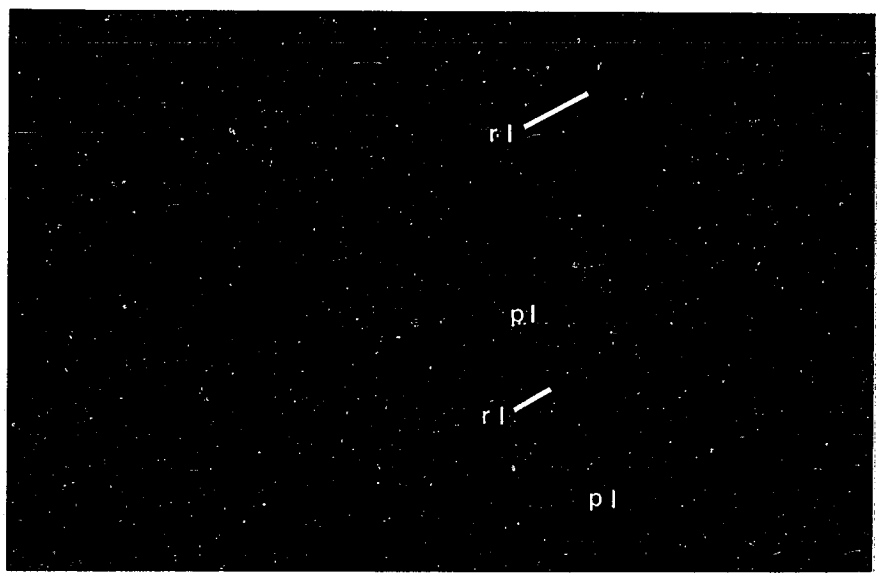

Figure 3.33. a: Apparent flat beds of the parallel-bedded microsequence, b: consisting of small-scale cycles of plane-laminations (pl), ripple laminations (rl), and locally developed siltstone laminations (not shown in photograph). Scale is in inches and centimeters (San Rafael Swell, Z-6)

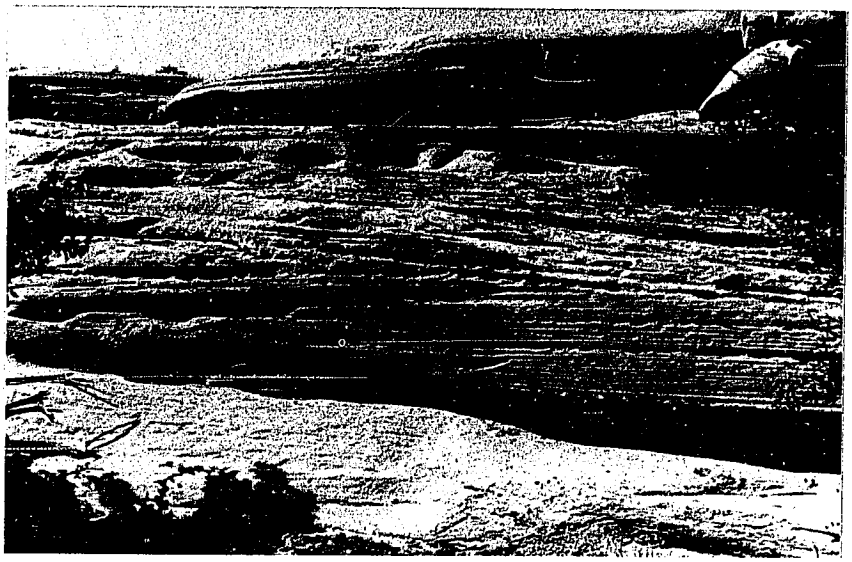

Figure 3.34. Subtle angular discordances within parallel-bedded microsequence. Scale is in inches and centimeters (near Lookout Point, Z-14)

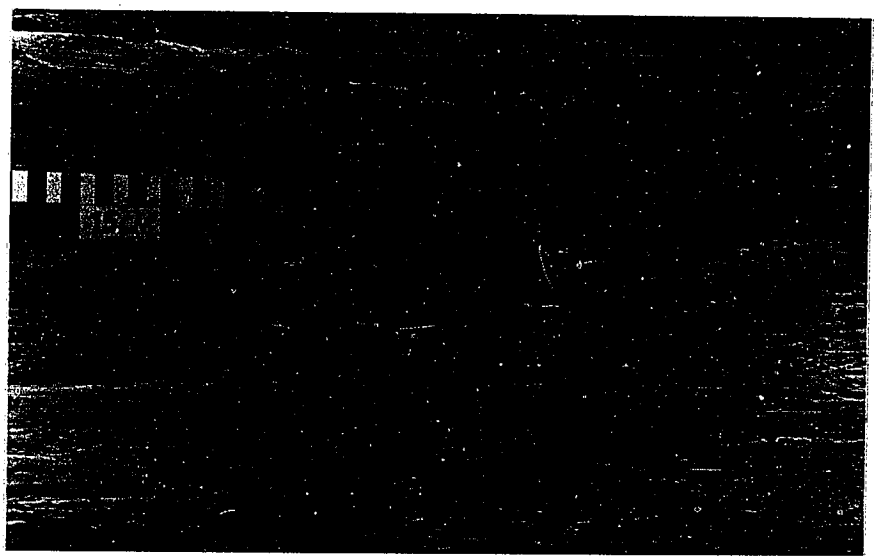

Figure 3.35. Erosional truncation and relief associated with mixed complex bundled and simple crosslamination sets (San Rafael Swell West, Z-6)

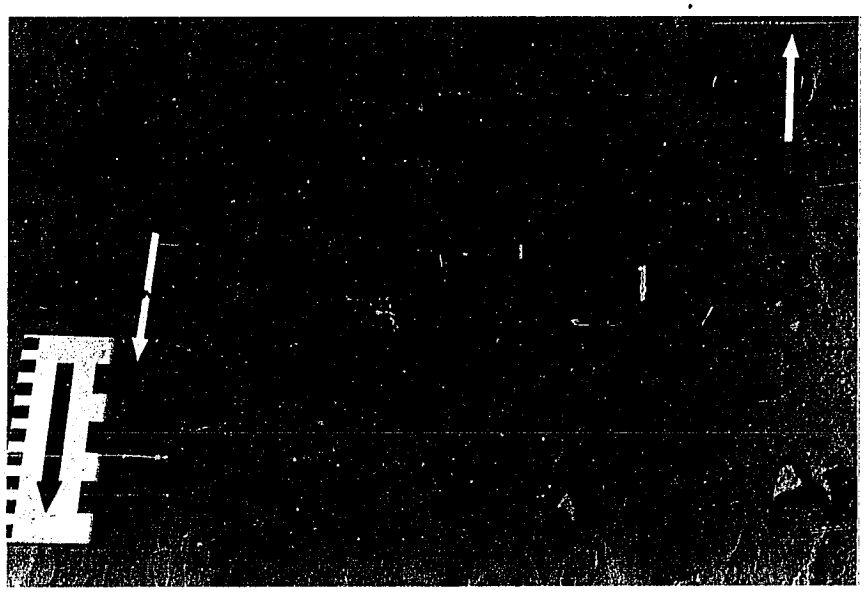

Figure 3.36. Rib-and-furrow structures associated with lunate ripples in parallel-bedded microsequence in the composite sandstone facies. Note bimodal rib-and-furrow pattern (arrows) and parting lineation (pl). Scale is in inches and centimeters

chapter). Linguoid ripples, which do not produce ribs-and-furrows because of the absence of a well-defined leeside scour and covex-downstream shape, can only be identified if complete bedforms are preserved and exposed on bedding surfaces. Linguoid ripples in this facies are 0.5 to 1.25 inches (1.5 to 3 cm) high. Interfering ripples are locally present.

Straight- to slightly sinuous-crested asymmetrical ripples display small-scale sedimentary features that are extremely useful for paleoenvironmental interpretations. With favorable bedding exposure, these ripples can be traced laterally for several feet. They are regularly spaced with mean length of 2 inches (5 cm) and mean height of 1.2 inches (3 cm) and may locally bifurcate. Ripples may show local rounded or flattened crests, ladder ripples, and local, well-preserved features which are herein named run-off tongues named herein, which point in a north-northwest ward direction (fig. 3.37). These features are restricted to exposures along the eastern San Rafael Swell. Straight-crested ripples are locally associated with climbing ripple-drift laminations. Other ripple beds were formed as complex foreset bundles characterized by uneven lower bounding surfaces, bundle upbuilding, and bidirectional lenses (fig. 3.38).

Plane laminations are either cyclically or irregularly interbedded with ripple laminations; they are clearly recognized by parting lineation on exposed bedding surfaces (fig. 3.39). As described earlier, the rhythmic beds consist of basal plane laminations overlain by ripple laminations and are repetitively interrupted by thin mudstone or siltstone laminations. Where exposed, these mudstone/siltstone drapes also preserve crawling and feeding trace fossils. One kind of

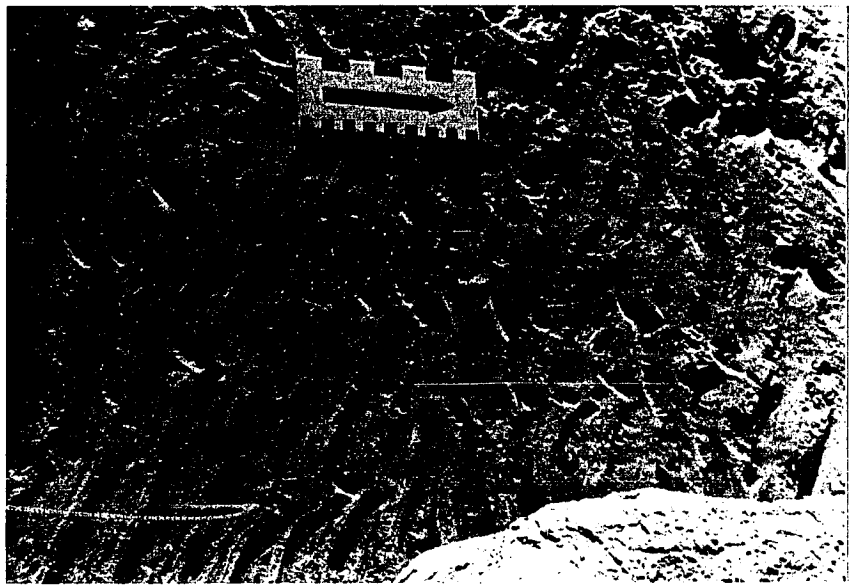

Figure 3.37. Straight-crested ripples and locally developed run-off tongues (rt) which point to the right. Scale is in inches and centimeters

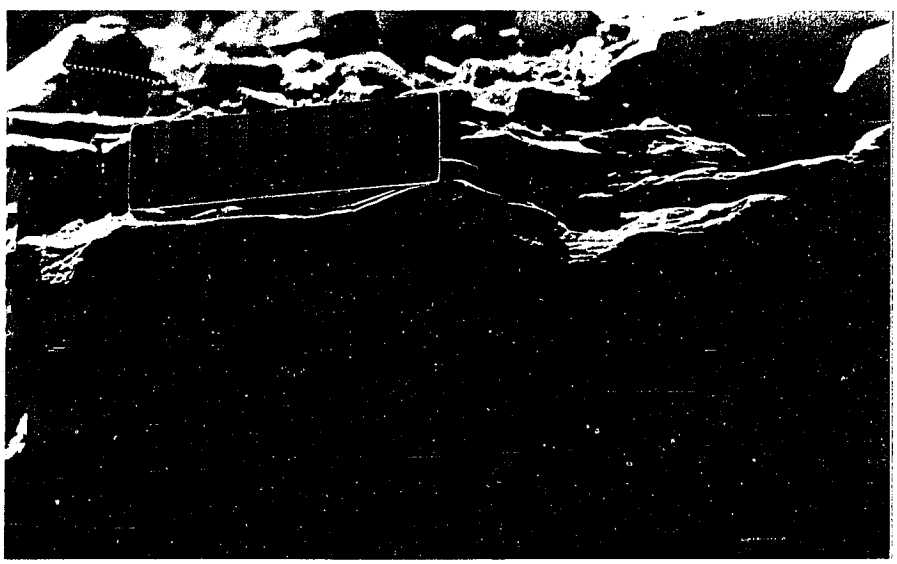

Figure 3.38. Complexly interwoven foreset bundles displaying uneven lower bounding surfaces (bs) (highlighted) and bidirectional lenses (bl) (San Rafael Swell West, Z-6)

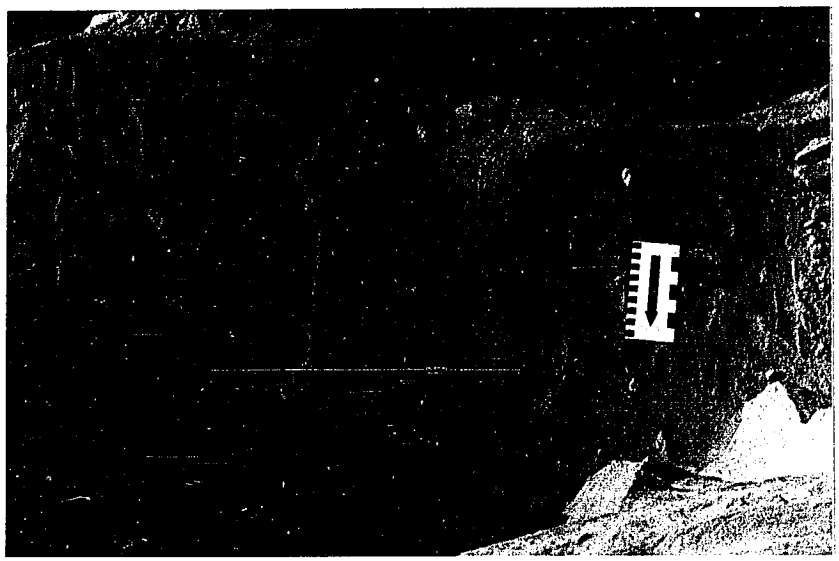

Figure 3.39. Parting lineation associated with plane laminations in parallel-bedded microsequence. Scale is in inches and centimeters

Figure 3.40 Sinuous, cylindrical, horizontal burrows developed in plane- or ripple-laminated sandstone in parallel-bedded microsequence (San Rafael Swell West, Z-6)

trace fossil occurs as long, sinuous single tubes 3 to 5 mm in diameter with backfill structures poorly preserved or absent. Another type of trace occurs as bilobed tubes with a median furrow; chevron backfill structures are locally visible. Often, these traces have formed on ripple- or plane-laminated surfaces in the absense of draping mudstone/siltstone laminations. Not only do the sinuous traces intersect, and cut across each other, they also disturb and truncate rib-and-furrowwstructures and plane laminations (fig. 3.40).

Rippled Silty Facies

The rippled silty facies is a ledge- and slope-forming light greenish-gray sandy siltstone or silty sandstone facies. It is recognized at the top of the Curtis Formation as a weathered gray slope between the composite sandstone facies and the Summerville Formation (figs. 2.9, 3.19). It comprises the entire Curtis Formation in the Henry Mountains area. In the Green River Desert area, it grades abruptly into the redbed facies (fig. 3.7). Microsequences are developed but stratification is more simplified relative to that in underlying facies. Because of the fine-grained texture and the low resistance to weathering, sedimentary features are not as well preserved or exposed, especially paleocurrent structures.

In general, this facies represents a transition from sandstones in lower facies to silty sandstones and siltstones in the overall upward-fining macrosequence in the upper half of the Curtis. Rocks finer than sandstone persist across the gradational Curtis-Summerville boundary and into the Summerville.

Two microsequences are present in the facies (table 3.4). Both are upward-fining, upward-thickening microsequences with distinct variations in stratification types and vertical sequences. Microsequence 1 is the dominant sequence and characterizes much of the facies around the San Rafael Swell area and northern Henry Mountains. Microsequence 2 is best expressed in the Green River Desert, particularly at Dellenbaugh Butte (Z-8), near the transition with the redbed facies.

Table 3.4. Sedimentary features of the rippled silty facies of the Curtis Formation

Sedimentary Features	Interpretation	Modern
1. Forms upward-fining sequence with underlying composite sandstone facies	Progradation of higher intertidal sand flat over lower intertidal and subtidal shoal and channel system during regression	Thompson
2. Ripples -straight to slightly sinuous-crested; asymmetrical, smooth lower bounding surfaces; critical-supercritical climbing; RI = 11.7 to 6.5	Current ripples; high net sedimentation rates; ripple drift lamination in dominant unidirectional currents	McKee (19 (1982)
-symmetrical to slightly asymmetrical; foreset bundles, bundle upbuilding, bidirecitonal lenses, uneven lower bounding surfaces; local bifurcating crests; runoff tongues pointing northwest	Asymmetrical ripple upbuilding by wave currents	Clifton
3. Local vertical/oblique burrow tubes	Few organisms able to tolerate environmental conditions on higher sand flats: higher salinity (evaporite polygon casts); sandy, unstable substrate; or greater degree of bioturbation overlooked as massive or cryptic bedding	Thompson and Hert
4. Upward-fining, upward-thickening microsequences c. cryptic-bdd, cross-lmtd or plane-lmtd slt, ms or cs w/ lenticular beds of vf (88-125 μ) ss and cryptic-bdd vf sandy slt in thin beds b. wavy-bdd vf sandy slt	Alternating sand and mud related to tidal rhythm; ebb- and flood-tidal currents on higher intertidal sand flats; unidirectional, wave-induced, shoreward directed currents	Hantzche (1954c, Singh (1 Elliott Weimer e

facies of the Curtis Formation

n	Modern	Ancient
of higher intertidal r lower intertidal shoal and channel regression	Thompson (1968, 1975)	Klein (1977b), Weimer et al. (1982)
es; high net sedimenta- ipple drift lamination nidirectional currents	McKee (1966a), Harms et al. (1982)	Chanda and Bhattacharyya (1974)
ripple upbuilding by	Clifton (1982)	de Raaf et al. (1977)
able to tolerate conditions on higher igher salinity (evapo- casts); sandy, unstable greater degree of overlooked as massive dding	Thompson (1968, 1975), Dorjes and Hertwick (1975)	Reif and Slatt (1979)
and and mud related to ebb- and flood-tidal igher intertidal sand ectional, wave-induced, ected currents	Hantzchel (1939), van Straaten (1954c, 1961), Reineck and Singh (1980), Reineck (1972), Elliott and Gardiner (1981), Weimer et al. (1982)	Reif and Slatt (1979)

Table 3.4. Continued

Sedimentary Features	Interpretation	Modern
4. Upward-fining, upward-thickening microsequences (cont.)		
a. plane-lmtd and cross-lmtd silty vf (62-125 μ) ss and vf sandy slt; local complete ripple foresets; ms flasers; local evaporite polygon casts		
units b or c only		
Alternating cryptic-bdd ms and flaser-bdd, wavy-bdd, or lenticular bdd cross-lmtd vf (62-88 μ) ss; silty; local chalcedony nodules after gypsum		Thompso

ation	Modern	Ancient
	Thompson (1968)	Reif and Slatt (1979)

Microsequence 1. Microsequence 1 seems to be a relic of microsequences in the composite sandstone facies in textural and bedding sequences. However, sequences are disorderly and unpredictable. Basal beds of this microsequence may be either plane- or ripple-laminated. Ripple foresets are well defined because of mudstone partings or flasers which have been removed by weathering. Complete ripple-form laminations are present; beds weather in a peculiar fashion by exfoliating along these ripple laminations (fig. 3.41). The rocks form an irregularly bedded sequence of silty very fine-grained sandstones and very fine sandy siltstones. Evaporite polygon cast are rare (fig. 3.42). These beds grade upward into wavy-bedded very fine sandy siltstones. The top of the microsequence is marked by a disorganized array of either cryptic-bedded (i.e. stratification is either non-existent or indeterminable), ripple-laminated, or plane-laminated siltstone, mudstone and local claystone.

Ripple-laminated ledge-forming sandstones from 1 inch to 1 foot (2.5 to 30 cm) thick protrude from the general weathered slope. These units are generally pure sandstones and are well cemented with calcium carbonate, clay, and iron oxide cements. The recess-forming units are often similar in textuue and bedding but are less cemented.

There are very localized features near the zone transitional with the Summerville Formation. These include thin micaceous (muscovite) sandstones, very calcareous sandstones or sandy sparites (i.e. a rock name used herein to denote a limestone with detrital siliciclastic grains, no fossils, and greater than 70 % cement as either microspar, pseudospar, neomorphic spar or normal spar), and wavy beds that may be

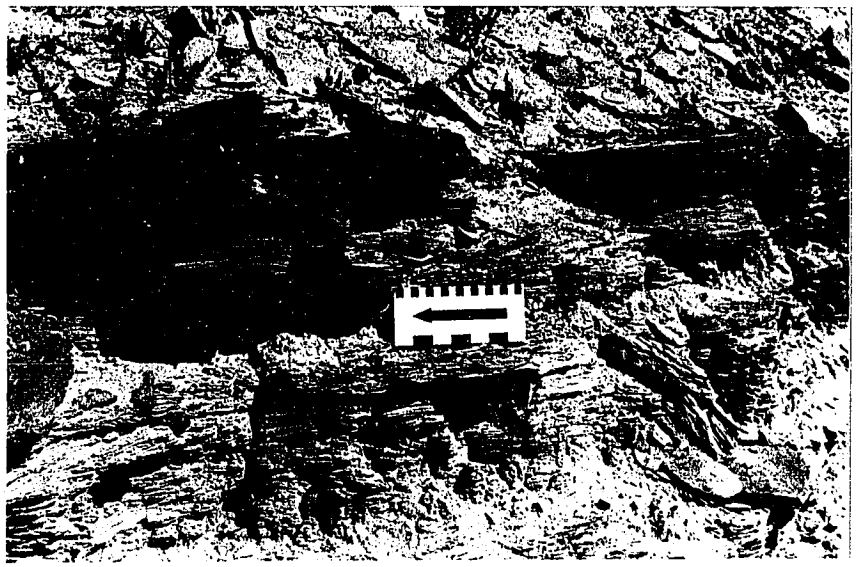

Figure 3.41. Weathering by exfoliation along ripple laminations in in microsequence 1 of the rippled silty facies. Scale is in inches and centimeters (Horse Bench, Z-12)

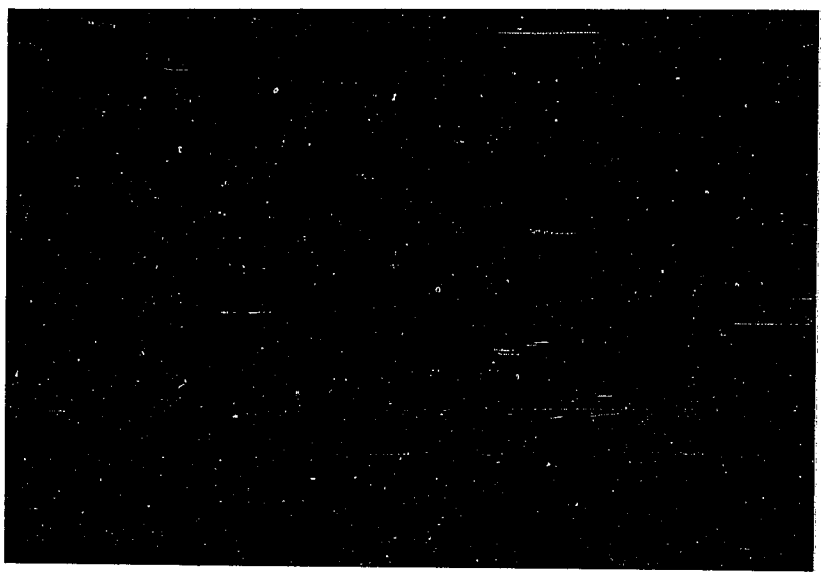

Figure 3.42. Rare evaporite polygon casts in very fine-grained sandstone of microsequence 1 in the rippled silty facies. Scale is six inches (15 cm) long (San Rafael Swell East, Z-2A)

stromatolitic (San Rafael Swell Northeast, Z-3A). Molds of mudstone intraclasts produced by weathering and shrinkage cracks are locally preserved at Hanksville (Z-4). Vertical and oblique burrows are very locally preserved.

Ripples are predominantly asymmetrical, varying from straight- and slightly sinuous-crested, lunate and interference ripples. Local runoff tongues are preserved on straight- and sinuous-crested, nearly symmetrical ripples and point to the northwest; crests are aligned northeast-southwest similar to those in the parallel- and cross-bedded sandstone facies.

Crosslaminated beds are 0.5 to 1 inch (1 to 2.5 cm) thick, exhibit smooth lower bounding surfaces and critical angles of climb (i.e. where apparent angle of bedform climb and the angle of the ripple stoss slope is about equal, Hunter, 1977a, b). In instances where supercritical angles of ripple climb have been achieved, the climb angle exceeds the general ripple stoss slope angle, and complete ripple-form laminations have been preserved. Cross-laminated sets are also laterally continuous for a few feet within cosets, and form tabular units between nearly parallel bounding surfaces. Relative to underlying facies, there are fewer ripple-laminated beds displaying complexly knitted foreset bundles, bidirectional lenses, bundle upbuilding and irregular lower bounding surfaces.

Microsequence 2. An upward-fining, upward-thickening microsequence is recognized by its chaotic internal stratification. Beds are 1 to 2 feet (30 to 60 cm) thick. Bedding sequences are typified by an irregular pattern of flaser-bedded, wavy-bedded, or lenticular-bedded cross-laminated very fine-grained silty sandstone interbedded with

cryptic-bedded mudstone. The sandstones form the base of each sandstone-mudstone doublet. Discoidal pebble- and cobble-sized chalcedony nodules locally interrupt bedding. The chalcedony has formed as a replacement of original gypsum (Chapter 3, Petrology).

Redbed Facies

The name, redbed facies, is assigned to a succession of dark orangish- and reddish-brown evenly bedded siltstone and sandstone beds that crop-out in the Green River Desert between Dellenbaugh Butte (Z-8) and Mill Canyon (Z-25). This distribution forms a northeast-southwest trending belt about 6 miles (10 km) wide (fig. 3.3). These beds comprise what has been referred to as the lower Summerville of earlier reports (McKnight, 1940; Baker, 1946; Wright el al., 1962; O'Sullivan, 1980a) because of the reddish-brown color and succession of uniform beds which are characteristic of the Summerville elsewhere in east-central Utah. In this study, field relations suggest that the ripple-laminated silty facies of the Curtis grades eastwardly into these redbeds which then form a marginal facies transitional between typical greenish-gray Curtis to the west and the sandstones of the Moab Tongue of Entrada to the east. Although these beds can be thought of as genetic facies of either the Curtis, Summerville or Moab, for simplicity, they are herein considered a facies of the Curtis. An orangish-brown color is, as yet, only one physical characteristic used to distinguish these beds from the overlying Summerville Formation.

The first complete exposure of the redbed facies is present at White Wash (Z-11), where, seen from a distance, the beds seem to form an uninterrupted succession of cliffs and slopes upward from the Beds at Goblin Valley to the Summerville (fig. 3.43). The redbed facies of the Curtis is distinguished from the Beds at Goblin Valley by the microsequences and the absense of hoodoo- or goblin-forming weathering features. A very subtle angular discordance can be observed at the contact between the Curtis and Entrada by trenching through the slope-

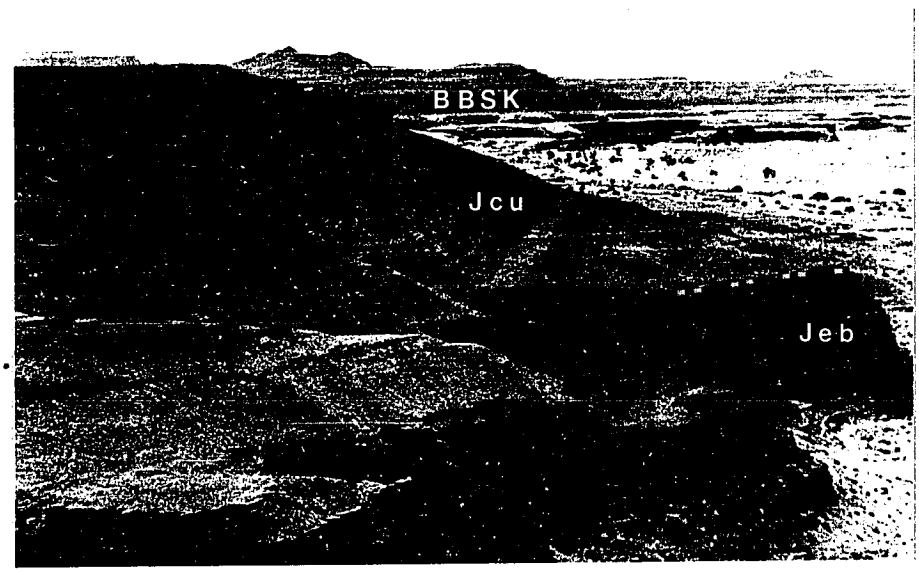

Figure 3.43. Redbed facies (Jcu) including Bed at Black Steer Knoll (BBSK) above the Beds at Goblin Valley (Jeb) at White Wash (Z-11). Exposure is 75 ft (22.5 m) thick. Slick Rock Member of Entrada Sandstone in background (Jes)

wash at White Wash.

From White Wash, where the redbed facies is 110 feet (33 m) thick, it begins to thin gently eastward, At both White Wash and Duma Point (Z-7), the normal succession of microsequences is punctuated by the appearance of a new microsequence comprising the Bed at Black Steer Knoll (O'Sullivan, 1980b), a stratigraphic marker described earlier. Farther eastward, at Tenmile Canyon South (Z-21), the redbed facies is clearly interrupted by the Moab Tongue of the Entrada Sandstone and forms upper and lower redbed sequences (cf. lower and upper beds of O'Sullivan, 1980a). From here, the Moab Tongue continues to increase in thickness at the expense of the Curtis redbeds until at Bartlett Flat (Z-22), the J-5 unconformity has completely removed the overlying Summerville and forms a poorly exposed horizon between overlying gray mudstones and wackestones in the Tidwell Member of the Morrison and the upper part of the redbeds. The unconformable relationship described by O'Sullivan (1980a) between the Morrison and Curtis is unclear at this locality.

At Mill Canyon, (Z-25), recent erosion has locally stripped back the Morrison and part of the Moab Tongue. O'Sullivan (1980a) has demonstrated that the upper part of the redbed facies has been removed by the J-5 unconformity, so that the Tidwell Member and Moab Tongue are now in contact. The lower part of the redbed facies persists between the Slick Rock and Moab Members of the Entrada and is only 4.5 feet (1.35 m) thick here.

The redbed facies of the Curtis can be described as an upward-coarsening, upward-thickening macrosequence. Individual, upward-fining, upward-thinning bedding packages or microsequences are developed that

are 1 to 4 feet (0.3 to 1.2 m) thick. Each microsequence generally thickens upward from the base of the facies yielding a greater net percentage of sandstone and siltstone beds near the top of the facies (fig. 3.44a). However, other intervals may be completely disorganized and heterolithic; consisting of ripple-laminated very fine-grained sandstone or siltstone interbeddd with structureless siltstone, mudstone, laminated purplish claystone, nodular calcareous siltstone or silty sparite and local beds of gravel-size mudstone intraclasts. Some siltstones and mudstones exhibit either a contorted structure from down-loading or may be completely disrupted from bioturbation(?).

Four upward-fining, upward-thinning microsequences are recognizeable; they are designated by number (table 3.5). In ascending order, microsequences 1 through 3 are preserved at White Wash (Z-11) and typify the vertical thickness and textural trends of the redbed facies. In the lower part of the redbed facies, microsequences 1 and 2 grade upward into microsequence 3 in the Bed at Black Steer Knoll. In outcrop, these upward-fining, upward-thinning microsequences form a regular arrangement of ledge-forming sandstones and recess-forming siltstones, mudstones and local claystones with pot-belly-like weathering profiles (fig. 3.44b).

1. Microsequence 1. Within the lower 20 feet (6 m) of the lower redbed facies are beds 1 to 3 feet (30 to 90 cm) thick characterized by basal cryptic- and crosslaminated very fine-grained sandstone or siltstone coupled with an overlying cryptic-bedded siltstone or mudstone. Within the next overlying 20-foot interval, bedding diversity gradually increases and the microsequence developes distinct basal very fine-grained sandstone beds characterized by cross-laminations with

a:

b:

Figure 3.44. a: Upward-coarsening, upward-thickening macrosequence (person for scale, arrow), b: composed of upward-fining, upward-thinning, sandstone-siltstone-mudstone microsequences (staff is in feet) (Tenmile Canyon South, Z-21)

Table 3.5. Sedimentary features of the redbed facies of the Curtis Formation

Sedimentary Features	Interpretation	Modern
Microsequences		
1. b. cryptic-bdd slt or ms; disrupted fabric from bioturbation (?) a. cross-lmtd or cryptic lmtd vf (62-88 μ) ss or slt; basal loads and wavy lams; local ms partings along foresets	Rhythmically alternating sandstone-siltstone-mudstone bedding deposited on upper intertidal to supratidal flat; vertically accreted spring-neap tide bundle: when sandstones are deposited during spring tides and siltstone and mudstone are deposited during neap tides; vertical cycles reflect decrease in current energy and decreasing transport of sand; non channelized flow on intertidal flat	Hantzsch Straaten Reineck Thompson Reineck Terwindt (1982)
2. (bedding units 1-4 ft (0.3-1-1.2 m) d. siltstone or mudstone with lenticular-bedded very fine (62-88 μ) sandstone; local horizontal burrows and tracks c. wavy-bedded very fine (62-88 μ) sandstone and siltstone b. cross-laminated very fine (62-88 μ) sandstone; flasers; basal load structures a. trough crossbeds: 1 ft (30 cm) thick or less; concave-upward foresets, tangential toesets; very coarse sand- and granule-size mudstone intraclasts along foresets	Similar in origin to microsequence 1. Megaripples on upper intertidal to supratidal flat; temporary introduction of coarser sand during storm- or wind-enhanced flood tidal currents or greater-than-normal spring tides	Inman e
3. Bed at Black Steer Knoll d. plane- or cryptic-laminated siltstone, mudstone or claystone; local lenticular-bedded very fine sandstone or siltstone; shrinkage cracks; local horizontal burrows and tracks c. wavy and lenticular-bedded very fine sandstone or siltstone with mudstone; local wavy- to ripple-foreset laminated siltstone with mudstone	Storm- or wind-enhanced flooding of upper intertidal-supratidal flat and subsequent modification by normal tidal currents; similar to washover processes	

of the Curtis Formation

	Modern	Ancient
lternating sandstone- tone bedding deposited tidal to supratidal ly accreted spring- le: when sandstones during spring tides and mudstone are ng neap tides; vertical decrease in current reasing transport of nelized flow on inter-	Hantzschel (1939), van Straaten (1954a, 1961), Reineck (1967, 1975), Thompson (1967, 1975), Reineck and Singh (1980), Terwindt (1981), Clifton (1982)	McCave (1973), Reif and Slatt (1979)
gin to microsequence 1.		
upper intertidal to ; temporary introduction during storm- or wind- tidal currents or rmal spring tides	Inman et al. (1966)	
enhanced flooding tidal-supratidal flat modification by normal similar to washover		

Table 3.5. Continued

Sedimentary Features	Interpretation	Modern
Microsequences (cont.)		
3. Bed at Black Steer Knoll b. cross-laminated very fine (62-88 μ) or siltstone a. plane-laminated or cross-laminated with complete ripple-form laminations; silty, very fine to fine (62-177 μ) sandstone; beds 0.5-3 ft (15-90 cm) thick or crossbedded fine-medium (177-500 μ) sandstone; mudstone granules and rippled siltstone partings along foresets; basal load structures; beds: 0.5-1 ft (15-30 cm) thick		
4. Irregular alternations of very thin beds of ripple foreset laminated or lenticular-bedded very fine sandstone with laminated mudstone or siltstone; local channel-form geometry Ripples: -straight-crested to slightly sinuous; local flattened, rounded crests; local run-off tongues -lunate-linguoid	Similar to microsequence 1 in origin; alternating sandstone, siltstone, and mudstone are fill- and bank-deposits associated with tidal or wadi channels	Hantzsche Wunderlich Singh (19 Glennie (Glennie a

	Modern	Ancient
rosequence 1 in ting sandstone, mudstone are fill- ts associated with hannels	Hantzschel (1939), Reineck and Wunderlich (1969), Reineck and Singh (1980)	Weimer et al. (1982)
	Glennie (1970), Glennie and Evans (1976)	Porter (1987)

mudstone partings. At the base of most sandstone beds are load structures which deform underlying mudstone beds and cause undulating or wavy contortions of overlying cross-laminated beds.

2. Microsequence 2. In the second microsequence, basal sandstone beds like those of microsequence 1 are locally underlain by small trough crossbedded sets 1 foot thick or less. Foresets are concave-upward with tangential toesets and are locally formed of very coarse sand- and granule-sized mudstone intraclasts. They grade upward into: a. cryptic- or wavy-bedded siltstone, mudstone, or very fine-grained sandstone with ripple foresets, and b. siltstone with cross-laminated, sandy, lenticular beds (table 3.5).

3. Microsequence 3. A more complicated succession of bedding and lithologic types within microsequence 3 comprises the stratigraphic marker Bed at Black Steer Knoll. Basal beds are 0.5 to 3 feet (15 t 90 cm) thick and are characterized by either plane laminations, complete or partial ripple-form laminations, or crossbedding (megaripple beds). Crossbeds are concave upward and tangential to lower bounding surfaces. They are associated with basal load and flame structures, contorted laminations, granule-sized mudstone intraclasts, and rippled siltstone laminations along foresets. The sandtones are very fine- to medium-grained. In ascending order, the following bedding succession is visible above the stratified sandstones: a. siltstone or very fine-grained sandstone with ripple foresets, b. very fine-grained sandstone, siltstone, or mudstone that is either ripple laminated, wavy-bedded, or lenticular bedded, c. siltstone, mudstone, or claystone with local sandy or silty cross-laminated lenticular beds. These uppermost silty and muddy beds locally preserve shrinkage cracks and subhorizontal

feeding and crawling trace fossils. Units b and d are superimposed when units b and c are absent (table 3.5).

Straight- to slightly sinuous-crested asymmetric ripples have been locally rounded and flattened and slightly modified with poorly developed run-off tongues. Cross-laminated beds are 5 feet (1.5 m) thick or less.

4. Microsequence 4. The regular occurrence of all the microsequences described above is locally interrupted by microsequence 4. Beds 1 to 3 feet (30 to 90 cm) thick contain irregular interbeds of thin, cross-laminated, very fine-grained sandstone, plane-laminated siltstone or mudstone, and cross-laminated lenticular beds of very fine-grained sandstone. These beds may locally enclose nodular sandy micritic sparites.

At Duma Point, microsequence 4 locally occurs as one channel-form body having a flat top and convex-downward base; it is about 3.5 feet (1.05 m) thick and 12 to 15 feet (3.6 to 4.5 m) wide. This microsequence is characterized by an irregularly bedded sequence of dark sandy siltstone, tan sandstone, whitish-green draping claystone laminations, and brown mudstone. The units occur in lenticular beds in which stratification is either plane- or cross-laminated, or obscure.

Interpretation of the Curtis Formation

General Interpretation

Collective primary bedding features (tables 3.1-3.5) in facies and microsequences of the Curtis, Summerville, and Moab Tongue suggest that the Curtis was deposited as an upward-shallowing, regressive or offlap sequence in nearshore marginal marine environments. A general upward-fining textural character is preserved in the Curtis within which are smaller-scale normally- and reversely-graded sequences. A local upward-coarsening, upward-shallowing macrosequence is preserved in the sandstone-mudstone facies, the lowermost Curtis facies, in which a basal gravelly microsequence preserves the earliest trangressive event during Curtis time. Stratigraphically higher microsequences in this facies and in the composite sandstone facies preserve features that indicate progressive upward-shallowing, a seaward-prograding shoreline, higher current energies corresponding with shallower water depths, and coarser sand transported as a complex of small- and medium-scale bedforms. The rippled silty facies, deposited near the end of Curtis time, indicates that the tidally controlled sand flat finally emerged, as finer sandy and silty deposits of higher intertidal flats prograded seaward.

Minor marine trangressive episodes are superimposed on the gross regressive episode. Secondary transgressive events are recorded in the lower and upper Curtis and secondary regressive events are recorded in the middle Curtis, Moab Tongue, and Summerville.

In the Green River Desert, the shoreline trend was approximately north-northeast to south-southeast based on the northeast-southwest

paleocurrent patterns preserved in facies of the Curtis, particularly the basal gravelly microsequence and crosslamination in other microsequences (fig. 3.3-3.12). The transition in facies and therefore a transition from terrestrial to marginal marine to nearshore marine is generally perpendicular to this inferred northeast-southwest shoreline trend. Paleocurrent patterns and lateral facies relationships in the southern San Rafael Swell and northern Henry Mountains areas suggest that the local shoreline was probably aligned more nearly east-west.

Marine conditions persisted throughout the deposition of the Curtis-Moab-Summerville. However, sedimentation in the Summerville records the last Jurassic marine event in southern Utah. Henceforth, the region was characterized by subaerial exposure and regional erosion along the J-5 unconformity.

Sandstone-Mudstone Facies

Sedimentary features in the sandstone-mudstone facies, particularly the heterogeneity of microsequences, suggest that it was deposited at or slightly above normal wavebase in a sandy subtidal nearshore marine environment influenced strongly by tide, wave, and wind currents (table 3.1). Equivalent parts of the composite sandstone facies, the rippled silty facies, and redbed facies were deposited as contemporary shoreward facies especially in the eastern San Rafael Swell and Green River Desert.

Basal gravelly microsequence. The basal gravelly microsequence in the San Rafael Swell area was an initial deposit of Curtis that was preserved as sea level rose rapidly and the shoreline migrated eastward into the Green River Desert area. A localized trace fossil assemblage is preserved at North Salt Wash (Z-16) in the Beds at Goblin Valley

(Entrada Sandstone) at the J-3 unconformity which was the marine depositional surface. The assemblage is similar to a Glossifungites ichnofacies (Frey and Pemberton, 1984) in which J-, U-, and tear-shaped dwelling traces were formed by suspension feeding organisms living in a firm but possibly unlithified substrate. The J- and U-shaped structures were the living structures of polychaete annelids (Warme and McHuron, 1978) and possibly small crustaceans. The tear-shaped structures were made by burrowing pelecypods. In these structures, the bulbous-downward terminations clearly suggest the dwelling chamber of a clam from which a tube structure, presumably a siphon, extended upward to the sediment-water interface for feeding. Vertical movements, either upward escape traces or normal downward burrowing are not evident; truncated and upturned laminations or backfill structures are poorly developed or absent. The traces are pre-depositional (Kern, 1980) becauue they have been truncated by sedimentary events related to the deposition of the gravelly microsequence and have been filled with sediment which is texturally and mineralogically similar to that in the overlying Curtis. The fact that all the burrows have been truncated and that some burrows physically extend across the J-3 contact into the Curtis suggests two conclusions. First, pre-burial marine conditions existed for a relatively short yet undefined time. Second, more than one sedimentary event occurred prior to the deposition of the gravelly microsequence.

Textural and mineralogic aspects of the deposit suggest the following ideas concerning the nature of the gravel. The deposit is a mixture of "Curtis-like" sediment, such as fine to coarse quartz-rich sand with local feldspar clasts (Chapter 3, Petrology) and fragments of

echinoderms and pelecypods which probably lived on the nearshore sea bottom during Curtis time. These clasts are mixed with very coarse sand and rounded granule-, pebble-, and cobble-size gravel clasts from an uncertain source terrane. The granules and small pebbles are lithoclasts of chert, silicified and dolomitized sparites and other limestones and local siltstone and sandstone fragments which were probably eroded from older, underlying strata. Larger pebble- and cobble-size clasts are texturally and mineralogically similar to the underlying Beds at Goblin Valley. These characteristics suggest that the gravels originated on the J-3 surface by processes acting before those of Curtis time. The sand became mixed with the older gravel clasts by processes active during Curtis time. Hence, the deposit is composed of palimpsest sediments (Emery, 1952, 1968b; McManus, 1975).

The exact timing and manner of emplacement of the relict sediment is uncertain. It could be a residue or regolith caused by physical and chemical weathering on the exposed Entrada surface. However, there are limestone clasts which are not related to texture and composition of the underlying Entrada. The presence of chert and exotic limestone clasts, and the general westward increase in size and abundance of gravel clasts suggests that they were derived from the west and quite possibly transported from that direction by eastward flowing alluvial systems. Preliminary studies of gravel clasts from older and younger Jurassic strata, as well as the Curtis-Summerville interval suggest an uplifted wetern source area that was strongly raised at the beginning of Curtis time (Peterson and Caputo, 1986). This uplift may have marked the onset of deformation in the Sevier orogenic belt and may have been significant enough to expose older Mesozoic and possibly Paleozoic rocks from which the chert and limestone fragments could have been

eroded. Furthermore, there is no evidence in facies deposited shoreward or eastward and southward to suggest the presence of streams flowing unobstructed from the east or south during deposition of the Curtis. The Circle Cliffs area, which lies south of Capitol Reef National Monument, southwest and outside of the study area, was a positive area during Curtis time (Peterson, USGS, Denver, Colorado, pers. comm., 1984; Peterson and Caputo, 1986). It is uncertain whether this uplift may have been severe enough to expose older Mesozoic and Paleozoic strata.

The geometry and distribution of the gravelly microsequence as suggested by the isopach map (fig. 3.4) is probably a relict feature. The distribution may have been controlled by local basin topography created during J-3 time. The southeasternmost or extreme shoreward edge of the microsequence is at least 18 miles (29 km) from the inferred approximate shoreline near Dellenbaugh Butte (Z-8). The gravels were initially reworked by shoreline processes as the sea transgressed over the J-3 surface. Relatively high-energy currents, possibly those generated by waves in a breaker zone, may have winnowed finer sediment from a residue of coarse sand and gravel as a transgressive lag (Clifton, 1981). Certain waves (Stokes waves) in shallow water are characterized by a forward orbital motion under wave crests that is shorter in duration but higher in velocity than that under the wave trough. The net effect is that pebbles and cobbles become selectively driven shoreward (Komar, 1976).

Following the redistribution of the relict sediment during sealevel rise, the gravelly sands were later reorganized by coastal currents in water depths at or slightly below wave base. Sediments

accumulating during Curtis time were mixed with the relict sediments by marine currents as suggested by echinoderm and mollusc fragments mixed with fine gravels.

The crossbedded nature of the deposit suggests traction transport by megaripple-scale transverse bedforms, especially gravel waves (Harms et al., 1982; Stride et al., 1982). Sandflow cross-strata which are contiguous and not separated by grainfall strata are usually formed by slipface deposition on subaqueous bedforms (Hunter, 1985b; Buck 1985; Hunter and Kocurek, 1986).

Draping siltstone laminations and fore- and back-flow ripples interrupting successive sandflow strata (table 3.1) suggest intermittent migration of the gravel waves. Stronger threshold current velocities, particularly during spring tide periods or enhanced by seasonal wind or storms, were required for migration of the gravel waves. Below threshold velocities, the gravel bedform remained relatively stationary, and sediment was transported by small-scale bedforms like ripples. Fore- and back-flow orientations of ripples on master foresets suggest eddy currents on the leeside of the master bedform. Siltstone laminations record suspension sedimentation during slack water periods. Burial of these laminations by successive sand flow strata suggests remobilization or reactivation (Collinson, 1970; Klein, 1977) of the master bedform.

The general northeastward paleo-transport direction indicated by sandflow azimuths (fig. 3.8) suggests uniform sand transport by a steady current. The paleocurrent direction also suggests transport away from the east-west trending southern shoreline in the south San Rafael Swell-northern Henry Mountains areas. In contrast, paleo-flow is shore-parallel in the Green River Desert, where the shoreline is thought to

be aligned nearly north-south.

Coastal currents are generated by tidal currents, wind-driven currents or by some other means and are parallel to the coast (Reineck and Singh, 1980). Tidal flow and sediment transport directions assume coast-parallel paths because of the semi-enclosed and elongate nature of the tidal basin of the English Channel and southern North Sea (Reineck, 1963; Stride, 1963; Reineck and Singh, 1982; Johnson et al., 1982; Swift and Niedoroda, 1985; Johnson and Baldwin, 1986). German Bay, a part of the North Sea, is bordered on the south by an east-west trending embayed shoreline of the Dutch and German coasts and on the east by a north-south trending embayed shoreline of the German and Danish coasts. The southern coast experiences shore-parallel tidal flow. In contrast, the eastern coast experiences shore-normal tidal currents (Reineck and Singh, 1980). This setting may be a modern analog to the Curtis seaway. Paleocurrent features, especially in the basal gravelly microsequence, suggest flow parallel to the eastern shoreline and flow away from or normal to the southern shoreline

McCave (1973) has described a similar setting for a middle Devonian transgressive sequence. Tillman and Martinsen (1984, 1985) interpret shore-parallel marine currents intensified during storms as a mechanism for shelf-ridge or bar complexes in the Cretaceous Shannon Sandstone of Wyoming.

Wind systems operate over different spatial and temporal scales: daily land-sea breeze systems, several-day mesoscale disturbances such as warm and cold fronts and cyclones, and seasonal, large-scale systems such as mid-latitude high pressure cells (Mooers, 1976; Johnson and Baldwin, 1986). Winds at these scales can exert shear stress on surface

water and create wind-driven currents which penetrate to depths of 50 to 80 meters with near bed velocities up to 80 cm/s (Smith and Hopkins, 1972) Such a current velocity is capable of transporting granules and small pebbles in form of 2-D and 3-D megaripples (extrapolated from size-velocity diagram in Harms et al. 1982).

Gravel waves up to 1 meter in height migrate by tidal currents in the English Channel and may be crossbedded, as suggested by the presence of leeslopes (Stride et al., 1982). Lag gravel is known to have been reorganized into gravel waves by storm-wave currents on ancient shelves (Wright and Walker, 1981). A similar origin for gravel waves has not been reported for modern shelves. Storm-related conglomerates are generally associated with hummocky cross-stratification (HCS), a sedimentary structure not observed in any Curtis or Summerville facies. The accepted origin of HCS is related to wave orbital currents of large waves created by stormy weather at sea (Harms et al., 1982; Swift, 1985).

Another mechanism capable of producing coast-parallel currents on modern and ancient shelves is wind set-up or wind-forcing (Swift et al., 1979; Swift et al., 1983; Walker, 1984b; Aigner, 1985; Swift and Niedora, 1985). Without citing examples, Walker (1984b) further described that such flows generate current ripples, megaripples and graded beds and that megaripples may appear in the geological record as medium-scale, angle-of-repose crossbedding.

Large waves with deeper-than-normal wavebase are created by storms at sea and and can generate bottom currents which are sufficiently competent to transport fine and medium gravel (Harms et al., 1982; Swift et al., 1979). However, storm deposits are usually recognized by distinct features such as hummocky cross-stratification and normally

graded bedding sequences from a basal shell or gravel conglomerate to HCS sandstone or siltstone overlain by a fair-weather mudshale (Reineck and Singh, 1972; Hamblin and Walker, 1979; Bourgeois, 1980; Kreisa, 1981; Hunter and Clifton, 1982). These features are absent in the gravelly microsequence. Leckie and Duke (1984) have descibed gravelly deposits as being coarse-grained equivalents of HCS produced by straight-crested symmetrical gravel dunes. In contrast, stratification in the gravelly microsequence appears as foreset beds which suggest avalanching or sandflow on the leeside of a transverse bedform. The probable mechanism is unidirectional traction transport and not wave-oscillation.

In conclusion, the origin of sedimentary features observed in the basal gravelly microsequence (table 3.1) are best explained by deposition and mixing of sediment by processes acting before and during Curtis time and remodification by coastal currents. It is likely that tidal currents were dominant and that sediment transport was amplified by high-energy, event-producing currents such as storm- or wind-driven currents causing the migration of subaqueous dunes alongshore. Characteristics of the microsequence are similar to those of the initial sandwave facies deposited during marine transgressions described by Nio (1976). Crossbeds in that facies are characterized by 1.5 m sets, tangential foresets, and mudstone laminations and ripples along foresets. These are similar features of the basal gravelly microsequence (table 3.1)

Mudshale microsequence. Sparse sedimentary features (table 3.1) and stratigraphic position relative to other microsequences and facies suggest that the mudshale microsequence is a locally preserved muddy

deposit that formed in somewhat restricted subenvironments in depths similar to upper offshore and transition zones below normal wavebase of mainland beaches (Masters, 1967; Reineck and Singh, 1971; Howard and Reineck, 1972a, b; Elliott, 1986).

The localized occurrence of mudshale at San Rafael Swell West (Z-6) and San Rafael Swell Northeast (Z-3) suggests deposition along the margins of the main sand thoroughfare of the main channel and shoal system preserved in the composite sandstone facies of the Curtis (later sections, this chapter). In this position, sand is less available and current energy is lower. This interpretation is also supported by isopach distribution of the sandstone-mudstone facies (fig. 3.5) and map showing percent net crossbedded sandstone in the Curtis (fig. 3.32). Mud settled from suspension in currents too calm to produce traction. It is possible that either seasonally high winds or storm activity generated deeper wavebase waves that impinged on the seafloor. Sand and silt might have been introduced into the system by storm- or wind-current enhanced ebb currents as suspension fall-out or as ripples migrating in from shallower depths. Tidal currents reworked the silt and sand in the form of isolated crosslaminated ripple forms. Migration ceased during slack water as isolated ripples were preserved in place by slowly settling mud in sand-starved conditions. Hence, the ripple-form crosslaminated lenses or starved ripples are locally encased in mudshale. Bidirectional crosslamination was not evident in the lenses. In modern subtidal sand facies, unidirectional ripple foresets are dominant and herringbone structures have not yet been reported (Terwindt, 1981). Sparse trace fossils such as horizontal and vertical burrowing suggest a slight resemblance to a Cruziana ichnofacies

characteristic of subtidal zones of sandy beaches (Seilacher, 1967; Chamberlain, 1978; Frey and Pemberton, 1984). The non-specific vertical tube-like traces were probably dwelling structures of worms. Horizontal traces may have been crawling or grazing marks of gastropods.

Upward-coarsening, upward-thickening microsequence. The upward-coarsening, upward-thickening microsequence was deposited by processes in an inshore (nearshore) subtidal environment. This sequence is developed directly above mudshale microsequences and represents the onset of the first minor regressive episode in the overall prograding sandy shoreline system of the Curtis. Sedimentary features, including trace fossils (table 3.1), suggest deposition by wave- and storm- or wind-enhanced currents at or above normal wavebase. The onset of upward-shallowing conditions are recorded in this microsequence.

The textural and bedding trends both reflect an upward increase in the availability of sand and intensity of currents. These trends are preserved in a vertical sequence beginning with lenticular-bedded sandstone and grading upward into wavy- and flaser-bedded (crosslaminated) sandstones with sand increasing and mud and silt decreasing upward. Crosslaminations show simple, climbing, undirectional laminasets deposited by unidirectional or non-wave, probably tidal currents. Complex interwoven foreset bundles with bidirectional lenses, bundled upbuilding and irregular lower bounding surfaces (table 3.1; fig. 3.15) are internal structures of ripples generated by wave orbital currents (de Raaf et al., 1977). Cotter (1985) described nearly identical microsequences of similar wave-current origin in Carboniferous marine bar sequences of Ireland. Hence, sand was transported in the form of asymmetrical and nearly symmetrical

ripples by wave- and tidal currents respectively.

The ripple foreset bundles suggest the first record of and probable motion of fairweather waves and therefore wavebase conditions. Wavebase is usually defined as the coastal water depth that is equal to one-half the wave length of fair weather solitary waves for a particular coast. It is the depth at which wave orbital currents first impinge on the sea bottom and sediment is moved as traction load, usually in the form of ripples (Shepard and Inman, 1950; Ingle, 1966; Clifton et al. 1971). This depth corresponds with the bottom of the transition zone, a zone that is transitional between shoreface (inshore or nearshore) and offshore zones.

Methods for estimating depth-to-wavebase and paleotidal range are given by Klein (1971, 1972, 1974). However, mean wavebase or tidal range were not determined from Curtis facies because of: 1. the difficulty in recognizing mean emergence levels in the Curtis facies, and 2. anomalously high values that may result from the effects of subsidence, compaction, and vertically stacked or amalgamated facies (Elliott, 1986).

Paleocurrent data (fig. 3.9) are interpreted as follows. At the six locations where ripple foreset azimuths were measured, two paleocurrent modes are indicated. One mode trends northeast-southwest and a second mode trends northwest-southeast. The weakly bimodal northeast-southwest trend is preserved in complex ripple foreset bundles which were formed by wave orbital currents. It is estimated that wave crests approached the shoreline obliquely and trended approximately 160-340 degrees azimuth. The bimodal northwest-southeast trend is preserved in non-wave formed asymmetric ripples and reflect flood- and ebb-tide flow.

Amalgamated crosslaminated sandstones interrupted by thin continuous mudstone laminations or discontinuous flasers in ripple troughs and crosslaminated wavy- and lenticular-bedded sandstones interbedded with mudstones are all forms of alternating bedding or rhthmic sand/mud bedding (Reineck and Singh, 1980). Interbedded mudstone and crosslaminated sandstones in microsequences of the sandstone-mudstone facies are one to several centimeters thick, particularly the sandstones, and are more specifically called coarsely interlayered bedding (Reineck and Singh, 1980). Rhythmic sand/mud bedding has been described from modern intertidal flats (Hantzschel, 1939; van Straaten, 1954a, 1961), especially mixed sand and mud intertidal flats (Reineck, 1967a; 1975) and modern nearshore subtidal environments (Terwindt, 1971a, 1981) but is not exclusive of tidal environments (de Raaf and Boersma, 1971; Reineck and Singh, 1980). Rhythmic sand/mud or silt beds are also deposited by storm currents (Reineck and Singh, 1972, 1980) and are thought to reflect alternating storm (sand) and fairweather (mud) conditions (Aigner, 1985; Cotter, 1985). Storm deposits are further characterized by normally graded beds with gravel or shells in basal beds and HCS (Hamblin and Walker, 1979; Bourgeois, 1980; Kreisa, 1981; Hunter and Clifton, 1982) These sedimentary features attributed to storms were not observed in the sandstone-mudstone facies. Rhythmically layered sandstone-mudstone suggests intermittent transport of sand by ripples between slack water periods when mud was deposited. The coarsely interlayered beds in the microsequence may reflect spring-neap tide cycles. More sand is transported and deposited during spring tides; more mud settles from suspension during neap tides (Terwindt, 1971a). During spring tides,

peak flood- and ebb-flow velocities are greatest because high- and low-tide levels are greatest.

Current velocities between 20 and 45 cm/s are needed to move very fine- and fine-grained sand in the form of small ripples to produce flaser- and wavy-bedded sandstones; mud settles out of suspension in velocities less than 20 cm/s to form interbedded mud layers (Reineck and Singh, 1980). These changes in current speeds are related to tidal cycles (table 3.1).

Some mudstones associated with wavy-bedding are less than 0.4 inches (1 cm) thick and could have been deposited during one slack water period between successive high and low tide reversals in a diurnal system. Several millimeter-thick mud layers can be deposited during a single tidal phase (Reineck and Wunderlich, 1969). Maximum thickness of a mud deposited during an exceptionally long slack water period of 3 hours is about 0.4 inches (1 cm) (Terwindt, 1981). Mud layers as thick as 2 cm have been deposited during a slack water period of 30 minutes in Jade Bay, North Sea (Wunderlich, 1978).

Load structures are absent in the soles of crosslaminated sandstones which overlie interbedded mudstones. The lack of such features suggests significant cohesive strength of and consolidation of mud in a brief period of time in subaqueous conditions. Laboratory experiments have shown that after 3 to 4 hours of initial consolidation, a mud layer only a few millimeters thick, was cohesive enough to support a sand layer 0.5 cm thick; consolidation was further enhanced by increasing the thickness of the sand layer (Terwindt and Breusers, 1972; Terwindt, 1981).

There are physical and biogenic structures in the soles of wavy-bedded sandstones that, by comparison to modern and ancient storm

deposits described by Aigner (1985), may be storm-related. Sole markings such as flutes, gutter casts and various tool marks (table 3.1) were produced by scouring by local eddies and impacting by saltating bedload and have been described from storm or distal tempestite deposits (Aigner, 1985).

The nature of preservation of hyporelief crawling and dwelling trace fossils suggests higher-energy sedimentation events. A great variety of hyporelief casts (table 3.1) are present in the soles of wavy-bedded sandstones. The assemblage belongs to the Cruziana ichnofacies (Seilacher, 1967; Chamberlain, 1971, 1978; Eldale et al., 1984; Frey and Pemberton, 1984) and includes arthropod dwelling structures, Thalassinoides (Howard, 1972; Howard and Frey, 1984) and various horizontal, cylindrical burrows that were probably made by arthropod or gastropod locomotion (table 3.1). They are preserved as hyporelief casts in the soles of crosslaminated sandstones and were originally formed in the previously deposited mud during slack water or fair-weather conditions by deposit-feeding organisms. Aigner (1985) described how such traces can be washed out to produce a mold in mud. The mold is later filled in as a hyporelief cast in the soles of sandy tempestites by storm waves. Trace fossils in this microsequence were made by deposit-feeding benthic organisms that locally built dwelling structures or mined the sediment for nutrients.

In the light of the preceding discussion, bedding features in the microsequence, such as alternating crosslaminated sandstones and mudstones, could have been deposited by storm wave-currents. However, in the absense of coarse graded beds and HCS, such an interpretation is weak. The sedimentary features in table 3.1 suggest that the

microsequence was deposited within normal wavebase depths by a combination of wave orbital currents and tide-influenced unidirectional currents under conditions similar to those in transition and lower shoreface subenvironments. Crosslaminated lenticular-, wavy- and flaser-bedded deposits are of mixed wave- and non-wave current origin. Wave currents are important in producing crosslaminated flaser- and lenticular-bedding (Reineck and Singh, 1980). Mudstones associated with lenticular- and wavy-bedding and flasers were related to paleo-tidal rhythm and were probably deposited during slack water periods between daily tides. Reverse textural grading and vertical change in stratification suggest accelerating currents up-section and may reflect a change in current strength from neap to spring tide (Terwindt, 1981). This ancient microsequence resembles the coarsening microsequence of Terwindt (1971a, 1981) deposited in weak to medium non-wave currents in a mesotidal subtidal environment along part of the coast of the Dutch North Sea. DeRaaf et al. (1977) described nearly identical wave- and non-wave formed structures and upward-coarsening and upward-fining (next section) sequences that were generated by temporary rough weather, storm, and post-storm conditions in an ancient subtidal deposit.

Upward-fining, upward-thinning microsequence. This microsequence grades from very fine-grained sandstones to mudstones and bedding style changes vertically from crosslaminations to wavy- and lenticular-bedding to laminated mudstones. Horizontal and vertical burrows are locally present. Small trough crossbedded sets form local basal beds.

Except for the different vertical arrangment, the texture and stratification patterns are nearly identical to those in the upward-coarsening, upward-thickening microsequence. Hence, both microsequences are genetically related and were both formed by tidal- and wave-currents in a subtidal nearshore environment within normal wavebase. The normal grading reflects decelerating currents and may be related to fluctuations in current strength between spring and neap tides (Terwindt, 1981).

Fine- to medium-grained megaripple crossbedding locally replaces very fine- to fine-grained crosslaminated sandstones in basal portions of the microsequence. This change was controlled by grain size. For the same velocity, medium-grained sand is transported as 2-D large ripples and very fine- and fine-grained sand is transported as ripples (size-velocity diagram, Harms et al., 1982).

Partially developed microsequences closely resemble fining-upward microsequences of Terwindt (1971a, 1981) generated by medium to weak non-wave currents in a subtidal environment along part of the North Sea coast. The upward decrease in sandstone records the decreasing availability of sand or decreasing ability of currents to move sand. In a tide-dominated nearshore subtidal environment, more transport and deposition of sand occurs during spring tide periods due to greater

high and low tide maxima and greater peak velocities. In like manner, relatively more mud settle during neap tide periods (Terwindt, 1981). Interbedded mudstones and crosslaminated wavy- and lenticular-bedded sandstones may closely correspond to neap-spring tide cycles. However, mudstone beds greater that 0.4 inches (1 cm) thick were probably deposited by currents too weak or calm to move sand during several consecutive slack water periods between high and low tides; sandy lenticular beds and perhaps wavy-beds, could have been deposited during one phase of a single tide (Terwindt, 1981). Nearly identical sandy microsequences have been described as subtidal bars in Carboniferous sandstones built by wave- and storm-processes (Cotter, 1985) and high-energy shoals at the mouth of a modern estuary (Greer, 1975).

The anomalously thick accumulation of sandstone-mudstone facies at Tidwell Draw (Z-9A,B) may record sedimentation in a local topographic basin inherited from subaerial exposure during J-3 time or controlled by active structures. During the marine transgression in early Curtis time, this topographic depression may have evolved into a locally deeper embayment or tide-dominated, non-fluvial estuary restricted from stronger marine currents by a subtidal sand bank or shoal seaward or westward of the local basin. Westward thinning of the facies and replacement by the composite sandstone facies at Cedar Mountain (Z-17) and Buckhorn Wash (Z-18) (fig. 2.5) supports this interpretation.

In general, the upward-coarsening and upward-fining microsequences of sandstone-mudstone facies mark the building of a subtidal sand shoal and channel complex that is fully developed in the composite sandstone facies.

Composite Sandstone Facies

The composite sandstone facies is characterized by sedimentary features (tables 3.2, 3.3) that suggest sedimentation in a tide-dominated nearshore environment equivalent to middle and upper shoreface and lower and middle foreshore or intertidal subzones of sandy beaches. The sand-grain size is the coarsest of all the Curtis facies. Primary sedimentary structures, including megaripple crossbedding and plane laminations, suggest the highest current velocities of all the sandy facies. Very thin mudstone laminations deposited in calm water interrupt ripple and megaripple beds. Along the eastern San Rafael Swell, these mudstone laminations are deformed by shrinkage cracks suggestive of emergent or subaerial conditions in this area during early to middle Curtis time. Hence, shoreline features are better developed and more recognizeable in this interval of Curtis.

Upward-fining microsequence. Upward-fining, upward-thinning microsequences in the composite sandstone facies represent sandier deposits that are transitional with similar microsequences in the sandstone-mudstone facies and reflect even greater availability of sand-size grains, consistently stronger current velocities, and shallower water depths (table 3.2).

Normal grading from fine- to medium-grained sandy trough crossbeds to sandstone-mudstone intercalations (table 3.2) suggest an upward decrease in transport velocity. Velocities of at least 50 to 60 cm/s are required to move fine- to medium-grained sand in the form of megaripples (2-D or 3-D megaripples) according to the size-velocity diagram (Harms et al., 1982) and observations on modern intertidal and subtidal megaripples (Boothroyd and Hubbard, 1975; Allen and Friend,

1976; Boersma and Terwindt, 1981: Terwindt, 1981); other observations indicate velocities as high as 65 to 70 cm/s (Terwindt, 1970).

The sandy crossbedded and flaser-bedded intervals reflect greater availability of sand and greater capacity for currents to transport sand especially during spring tide periods. Wavy- and local lenticular-bedded sanstones and mudstones may record sedimentation during periods between successive spring tides, particularly at neap tide and during daily tidal cycles. Toeset and foreset ripples are preserved on respective stoss- and leesides of larger megaripples (master bedforms). Orientation of ripple crests and migration directions of sttss side ripples are oblique to those of the master megaripple; corresponding orientations of leeside ripples are normal to the master megaripple. Small-scale bedforms, such as ripples occur superimposed on medium- and large-scale bedforms in both wind (Wilson, 1972b) and water (Allen, 1968c) environments, such as coastal and inland eolian dune, fluvial point bar, and tidal inlet environments (personal observations). Smaller superimposed bedforms with migration orientations opposed, transverse, or oblique to that of the master bedform usually indicate a pause or decrease in the migration rate of the larger bedform and that currents are swift enough to only move ripples (de Raaf and Boersma, 1971). Klein (1970b, 1975a, 1977a) and Swett et al. (1971) have described how such bedform relationships more specifically suggest slackening tidal flow or run-off during peak low tide when the tidal flat emerges. Indeed, a fluvial point bar may experience similar hydraulic and bedform relationships during emergence of the point bar at low river stage (personal observation). However, textural characteristics, internal stratification and lateral bedding

relations indicate that superimposed bedforms in this microsequence are not of either fluvial or eolian origin (table 3.2).

Mudstone or siltstone laminations interrupt and drape across either foreset beds or across superimposed ripples. Cylindrical, horizontal tunneling or crawling/feeding trails are associated with these mudstone laminations (table 3.2). Together with the ripples and trace fossils, they suggest waning current flow, a pause in megaripple migration, settling of mud, and feeding activity of either gastropods (Howard and Dorjes, 1972) or tunneling of worm-like organisms (Howard and Frey, 1984).

The origin of polygonal fractures associated with mudstone laminations and megaripple bedding is uncertain. They could be the result of subaqueous dewatering and shrinkage called synaeresis (Jungst, 1934) or subaerial exposure and dessication at the time of deposition. A third idea is that they are the result of recent weathering.

Synaeresis is a continuation of the process of clay flocculation (Potter et al., 1980) whereby fresh water enters marine water at an estuary and the contrast in salinity favors the aggregation of suspended clay particles. There is yet no sedimentary evidence in the Curtis to suggest synaeresis, clay flocculation, or ancient riverine estuaries. If the fractures are the result of desiccation, their formation is related to subaerial emergence and subsequent drying of the bedforms upon which they were deposited. If the megaripples had completely emerged, superimposed ripples would have displayed diagnostic features of falling water levels and run-off such as rounded and flattened crests, ladder ripples (Reineck and Singh, 1989), ripple fans (Elliott and Gardiner, 1981) or run-off tongues. None of these

features has been developed or preserved. It is most likely that the polygonal fractures are the result of recent weathering and mechanical disaggregation of the mudstone laminations.

Crossbedded and parallel-bedded microsequences.

Collective sedimentary features (tables 3.2, 3.3) of these two microsequences suggest sand-dominated nearshore sedimentation in a system of subtidal to intertidal shoals with shallow channels and berms. The two microsequences are composed of a complex macrosequence of interbedded crossbedded medium- to coarse-grained sandstones and thick sequences of very fine- to fine-sandy parallel beds (table 3.2). Some parallel beds exhibit cycles of normal grading from fine sandstone to siltstone or mudstone and a vertical change in stratification from plane laminations to ripple laminations. These vertical changes indicate cyclically-waning current strengths, an upward decrease in flow velocities, and a transition from traction sedimentation to suspension sedimentation. The crossbedding records the migration of medium-scale transverse bedforms (megaripples or sandwaves and dunes) across sand shoals during spring tides. Shoals nearest the seaward (western) part of the system may have been continuously submerged. Subaerial or emergent features such as modified ripple crests, ladder ripples, run-off tongues and dessication cracks were not observed in crossbed sets. Discontinuities with well-preserved ripple structures show diverse paleocurrent directions relative to master foresets and suggest waning tidal flow (Klein, 1970b, 1975a, 1977a; Swett et al., 1971).

In contrast, the cyclic and non-cyclic plane- and ripple-laminated beds record sedimentation on topographically higher berms on sand shoals. During high tides, either daily, spring or neap, the shoals became submerged and were built and eroded by tidal currents, wave currents and occasionally high wind-generated currents or storm currents. At low tides, landward shoals fully emerged as suggested by run-off tongues, ladder ripples and ripples with modified crests in microsequences along the eastern San Rafael Swell. Bedding relationships between the two microsequences may have originated in two ways. They may have been deposited by the collective lateral migration of channels and shoals with time and the burying of megaripples in tidal channels by shifting shoals.

An alternate mechanism is suggested by the vertical stacking of about four cycles consisting of basal trough crossbeds overlain by a succession of rhythmic beds at San Rafael Swell West (Z-6). Each cycle could represent a spring-neap tide cycle on an intertidal shoal setting similar to that described by Boersma and Terwindt (1981a), Westerscheld estuary, North Sea. Here, outer margins of a shoal border on estuarine channels and are characterized by high bedform activity. As the spring tide period approaches, current velocities across the shoal increase, dunes and sand waves are formed. Two days before and during neap tides, megaripples are replaced by small and medium ripples. Between successive spring tides, daily tides build rhythmic beds whose internal stratification suggests an increase, peak, and then decrease in current strength.

Figure 3.32 shows how the percent net crossbedding in the facies decreases to the south, the southeast, and east, in the directions of the inferred paleoshoreline. Likewise, percent crossbedding increases to the northwest. The patterns suggest that hydraulic conditions favoring the construction and migration of megaripples in tidal waterways was increasingly dominant to the northwest. In the same direction, the tidal waterways or arteries were probably broader which allowed a greater area for development of megaripples. Consequently, several intervals of megaripple beds are present in every stratigraphic section in the western San Rafael Swell. Toward the south and east, in the inferred shoreward direction, the tidal waterways probably became narrower and more restricted near the higher sand flats; the drainage system in this area was probably more like a system of run-off gullies or very shallow canals in which hydrodynamic conditions and grain size often did not favor the formation of megaripples. Consequently relatively few or no intervals of crossbeds are present in stratigraphic sections in the eastern San Rafael Swell and Green River Desert. In these areas, there is a high proportion of ripple laminations relative to plane laminations, a near absense of crossbedding and primary structures suggesting subaerial exposure.

Patterns suggested by the percent net sandstone map (fig. 3.2) and the isopach map of the composite sandstone facies (fig. 3.6) suggest major sand troughs or thoroughfares in the western San Rafael Swell mainly in the vicinity of San Rafael Swell West (Z-6) and Buckhorn Wash (Z-18, 23). These areas are interpreted as the deeper submerged portions of tidal channels and shoals where the greatest volume of water flowed and greatest volume of sediment was transported and deposited. Thickness patterns demonstrate sand-body thinning in a

general shoreward direction toward the south and east.

Excavations mainly from subtidal and intertidal deposits along the North Sea have shown sand body characteristics which lend support to the above conclusions (table 3.2, 3.3). In this area, channels and submerged bars and shoals characterize the subtidal portions of nearshore deposits. Maximum tidal current velocities, channel width, and channel depth are developed at the farthest seaward extensions of the channel-shoal complex and decrease shoreward in magnitude. Vertical sequences are typified by basal channel deposits successively buried by shoal and higher tidal flat deposits and decrease landward in thickness (van Straaten, 1961; Reineck and Singh, 1980).

Other sandy deposits affected by mainly tidal currents and subordinate wave- and storm-currents in nearhsore sandy shoal systems with active channels and berms are characterized by similar microsequences in modern (Oomkens and Terwindt, 1960; de Raaf and Boersma, 1971; Greer, 1975; Boersma and Terwindt, 1981a, b; Kohsiek and Terwindt, 1981; Terwindt, 1981) and ancient (Bosence, 1973; McCave, 1973; Johnson 1975, 1977; Roep et al., 1979; Levell, 1980b; Erikson et al., 1981; Bridges, 1982) settings.

1. Crossbedding. Single and composite sets of crossbeds in this microsequence were the result of medium-scale transverse bedforms (megaripples) both straight-crested (sandwaves or type 1 megaripples) bedforms. These bedforms were generated across sand shoals during spring tides in tidal waterways or broad, shallow channels coursing among and between topographically higher sand berms in upper subtidal to lower intertidal environments. Despite the lack of modified crests of superimposed ripples and other subaerial features, such as

dessication cracks or raindrop imprints, some megaripples may have been exposed at low tide, especially near the more shoreward reaches of the tidal pathways. In contrast, megaripples formed in the more seaward portions of the system, may have been constantly submerged.

Trough-shaped crossbedding especially with concave-upward foresets and tangential toesets is typically formed by migrating dunes (Harms et al., 1975, 1982), cuspate megaripples (Boothroyd and Hubbard, 1975; Boothroyd, 1978), type 2 megaripples (Dalrymple et al, 1975, 1978), 3-D ripples (Harms et al., 1982; Costello and Southard, 1981), lunate bars (Allen, 1963), or scroll bars over fluvial point bars (Cant, 1978). Regardless of name, the bedform possesses an arcuate or sinuous crest. The relationship between foreset geometry and bedform crest geometry is determined by flow conditions across the crest of the bedform (Jopling, 1965b; Boothroyd, 1978). As flow velocity increases, more grains are swept beyond the crest. As the grains descend through zone of flow separation, the fall trajectories allow them to settle farther downcurrent, near the base of the leeside slope. Just ahead of the dune, the flow becomes reattached to the substrate where intense erosion scours a moderately deep pit. Hence, an apron of tangential foresets or bottomsets is produced (Jopling, 1965a, b).

Tabular-planar crossbedding is usually generated by migrating sand waves (Harms et al., 1975, 1982), linear megaripples (Boothroyd and Hubbard, 1975; Boothroyd, 1978), type 1 megaripples (Dalrymple et al., 1975, 1978), 2-D megaripples (Costello and Southard, 1981), or transverse or linguoid bars (Collinson, 1970; Smith, 1970). They are distinguished from dunes by generally straight crests and lack of scour pit. Sandwaves arise from hydraulic conditions different from those

which produce dunes. In the lower flow regime, sand waves are considered intermediate bedforms between ripples and dunes (Jopling, 1965b; Harms et al., 1975, 1982; Boothroyd and Hubbard, 1975; Boothroyd, 1978). Straight-crested sandwaves form in velocities lower than those that generate dunes (Jopling, 1965b; Harms et al., 1975, 1982). Sandy sediment is transported as traction load or creep, probably resulting from saltation bombardment. Sediment creeps along the stoss side and accumulates near the brinkpoint of the sandwave, until the angle of yield (Allen, 1979) is attained, and a mass of sand avalanches down the leside as a grainflow (Bagnold, 1954) or sandflow (McKee et al., 1971; Hunter, 1977). Avalanching under these flow conditions produces planar slipface surfaces and foresets which apporoach the lower bounding surface at an acute angle (Jopling, 1965b). Hence, planar crossbedding is produced.

Tidal current- and velocity-asymmetry (Klein, 1970a) may affect the complexity of crossbed sets. Allen (1980) described a model in which dunes formed in mainly unidirectional currents (current asymmetry) which produced simple crossbeds bounded by first-order (E-1) surfaces and very minor second-order (E-2) surfaces. As reversing currents such as in a tidal environment, become more nearly equal in strength and duration (current symmetry) sand waves were produced with complex internal stratification. The complex stratification is a result of smaller, superimposed bedforms migrating in response to the reversing currents. Herringbone or bimodal cross-stratification with second- and third-order bounding surfaces is produced. Amalgamated sets or cosets of crossbeds, like those at Buckhorn Wash (Z-18, 23) and Lookout Point (Z-14) are similar to cross-strata formed by class IV A sandwaves (Allen, 1980) in which bed sets are deposited by superimposed

megaripples.

Crossbed foresets in these megaripple beds are composed of continuous sandflow strata characterized by both normal and reverse grading. Reverse grading is the expected texture resulting from grainflow because of the nature of grain-grain collisions and size sorting due to bed shear (Bagnold, 1954a). Normally graded sandflow beds are difficult to explain. The upward-fining character may reflect the presence of thin grainfall strata locally overlying successive sandflow beds. Grainfall sediments are generally finer than sandflow sediments (Hunter, 1977; Schenk, 1983). An alternative explanation is that grainflowage is sometimes an erosive mechanism. Perhaps successive grainflows partially eroded the upper few millimeters of underlying grainflow beds and incorporated the coarse grains there into the fresh grainflow.

Ripples with opposing crosslamination locally occur along lower set boundaries and are buried by sandflow strata. Because they are not developed along the entire length of the master toesets suggests that they were formed in front of the master bedform in the zone of reverse flow (Boersma, 1969; Jopling, 1965a).

Groups of foresets which display progressive downcurrent thickening and thinning in a crossbed set are usually separated by prominent discontinuities and are termed bundles. Boersma (1969) used the term and Visser (1980) and Kreisa and Moiola (1986) defined bundle as the lateral succession of cross-strata generated on the slipface of a bedform migrating during one dominant tide. Visser (1980), and Boersma and Terwindt (1981a, b) have described how relatively thicker foreset bundles are related to stronger velocity and duration of spring

tidal currents. Whereas, weaker currents of shorter duration during neap tide phase produce thinner bundles. A whole suite of sedimentary structures in tidal bundles related to neap and spring tide conditions has been described by Boersma and Terwindt (1981a, b), Kohsiek and Terwindt (1981), and Terwindt (1981). Tidal bundles were not measured in this study. However, Kreisa and Moiola (1986) have measured and described lateral variability of foreset bundles in one crossbed set in the Curtis at San Rafael Swell West (Z-6). They concluded that the cyclic, downcurrent thickening and thinning of foreset bundles and their internal stratification suggest the affect of spring and neap tidal currents.

Discontinuities between successive sand flows are accented by mudstone laminations or thin, rippled or crosslaminated beds with polymodal paleocurrent features. The discontinuities reflect a pause in the migration of the master bedform. Mudstone laminations suggest suspension sedimentation during slack water between daily high and low tides. Thin, discrete rippled intervals along nearly the entire length of master foresets suggest that ripples were generated during waning tidal flow or perhaps during late-stage run-off at low tide (Klein, 1970b, 1975a, 1977a; Swett et al., 1971; de Raaf and Boersma 1971).

Traces of coalified plant matter increase in abundance to the southwest as suggested by the relative increase in coal clasts in that direction and highest concentration at San Rafael Swell West (Z-6). It is thought that there were few isolated tree or plant forms growing near the shoreline at some indeterminate distance toward the southwest. For this to be so, fresh water conditions are required higher up on the coastal plain. Perhaps there were sparsely wooded, sandy areas associated with a fresh-water table such as in either raised or low

lying coastal mires (Bryer and McCabe, 1986). The coal clasts are all vitrinite (a maceral or inorganic unit originating in wood and bark tissues; Blatt, 1982) and the cell structure suggests that the material is of terrestrial plant origin (Mark Pawlewicz, USGS, Denver, Colorado, written comm., June, 1986). Fred Peterson (USGS, Denver, Colorado, pers. comm., 1986) has suggested that the coal clasts or wood fragments may have been derived from moister coastal highlands along the southwestern edge of the basin. Here, incipient crustal upwarping may have been related to Sevier deformation near the end of middle Jurassic time.

A variety of trees and plants grows on older Holocene beach- and dune-ridges associated with formerly prograding barrier islands and the Santee River delta plain on the South Carolina coast. Furthmore, the Santee River delta is presently undergoing local trangression and marine destruction. The shoreline is slowly transgressing landward, older Holocene shoreline sand deposits are being reworked by storm waves , and trees and plants are being uprooted. Older peat deposits are being exhumed in the foreshore, and together with uprooted trees and marsh grasses are redistributed alongshore by wave currents and into the back barrier system by tidal currents (pers. obs., March, 1984).

In the crossbedded microsequence, rounded, reworked mudstone clasts locally found on crossbed foresets are identified as intraclasts. They were derived from early consolidation of mud that formed in slack water during non-spring tide cycles when more mud settle from suspension (Terwindt, 1981). Mud layers up to 2 cm thick have accumulated in a slack water period of 30 minutes in Jade Bay of

the North Sea (Wunderlich, 1978) The mud layer represents a a pause or discontinuity during the migration of the megaripple. Later, it could have been eroded and transported as rip-up clasts in the opposing tidal current and deposited with sandflow foresets. That the clasts are aligned and seem to be locally concentrated near the top of sandflow strata suggests reverse grading from grain-grain collisions during the grainflow mechanism (Bagnold, 1954a).

The four bedding types (table 3.3) are interpreted as follows. Within foreset bundles produced by tidal current and spring-neap tide variations, is a lateral sequence of bedding structures that represent reactivated (accelerating), full-vortex, and slackening (decelerating) currents during one tidal phase, either ebb or flood, depending on tidal current asymmetry and the dominance of either flood or ebb currents (Boersma and Terwindt, 1981a, b; Kohsiek and Terwindt, 1981; Terwindt, 1981). Within this lateral sequence are thin siltstone laminations that represent discontinuities or pauses in the migration of the bedform.

Type 1 beds are beds of poorly sorted silty sandstones dipping at angles less than 20 degrees (table 3.3). They are interpreted as pause beds (pause plane of Boersma and Terwindt, 1981a) and reflect standstill periods in current activity when flow velocities are below the threshold for slipface migration (Terwindt and Brouwer, 1986). Low velocity conditions usually occur between successive spring tides especially during neap tide periods (de Raaf and Boersma, 1971) and these beds may represent parts or all of foreset bundles deposited around the time of neap tides. Slackening or waning currents are suggested by the poorly sorted silty texture. In comparison, bed types 3 and 4 which lie directly upcurrent were generated in higher flow

velocities and are composed of clean, coarser, well sorted sand. Pause planes (Boersma and Terwindt, 1981) or foreset discontinuities (Allen, 1980) are erosional or depositional and are usually buried by foresets similar to those beneath the discontinuity. Overlying foresets usually indicate resumption or reactivation of bedform migration (Collinson, 1970). Depositional pause planes are preserved as draping mudstone laminations or beds. The absence of a distinct mudstone drape in these pause beds suggests that either mud was not available in the system or that a previously deposited mud drape had been eroded by the subordinate reversing tidal current. Kreisa and Moiola (1986) have described and photographed one of the pause beds described in this report. They indicated two relatively darker laminations as distinct mudstone drapes and offered this as one line of evidence for tidal deposition in a subtidal environment. This interpretation is based on the idea of Visser (1980) who recognized two mud drapes which form a mud couplet from suspension sedimentation in the toesets of tidal bundles. A mud couplet is evidence for slack-water during high and low tide in subtidal environment; intertidal deposits have usually only one because the intertidal flat is only submerged during flood tide. Observations in this study suggest that neither mudstone singlets or couplets are present in the pause beds. The darker laminations in Kreisa and Moiola (1986) are made of very-fine to fine quartz and coal clasts, of which there may be up to 15 in one pause bed (fig. 3.28). Locally, there are thin rippled siltstone discontinuities within foreset bundles and may reflect fluctuating current speeds during daily tidal cycles.

Sedimentary structures of bed type 2 are gradational with those of bed type 1 (tables 3.3; fig. 3.28) and are suggestive of resumed or reactivated migration of bedforms in the dominant tidal current. They represent incipient bedform activity in currents too calm to produce fully developed, angle-of-repose avalanche beds. They are nearly identical to reactivation or acceleration structures of tidal bedforms associated with sand shoals in the North Sea estuarine coastline (Boersma and Terwindt, 1981a, b; Kohsiek and Terwindt, 1981; Terwindt, 1981).

Geometries and angular relations with lower bounding surfaces of foresets composing bed type 3 represent the full-vortex stage of a migrating bedform in the dominant tidal current. DDwncurrent, the foresets become more tangential with lower bounding surfaces presumeably as flow velocities increased. Sinuous-crested megaripples possess both barchanoid and linguoid elements of the crest (Boersma and Terwindt, 1981a; Elliott and Gardiner, 1981). Slightly concave-upward foresets may have been formed by the linguoid part of a megaripple just as concave-upward foresets are deposited by eolian parabolic dunes by nature of the convex-upward leeslopes (pers. obs., May, 1984, coastal dunes, Silver Lake State Park, southeast Lake Michigan). A wedge-shaped set of laminations dipping 9 to 13 degrees downcurrent are interpreted as full-vortex foresets. Topsets are formed in conjunction with full-vortex foresets in tidal megaripples and are generated under conditions where bedform geometry inhibits flow separation at the crest (Kohsiek and Terwindt, 1981). Foreset bundles within the same bed set may display mainly full-vortex foresets between pause beds and no reactivation structures (Lookout Point, Z-14, fig. 3.27). They are interpreted as features of tidal crossbedding formed between spring and

neap tides. During this time, bedding structures acquire characteristics that are intermediate between those of full spring- and full neap-tide. Typically, flow strength decreases, and vortex activity along the megaripple leeside is suppressed as the neap tide period is approached (Boersma and Terwindt, 1981a, b; Terwindt and Brouwer, 1986).

Foreset bed type 4 is nearly identical to sigmoidal foresets interpreted as slackening structures (Boersma and Terwindt, 1981a, b; Kohsiek and Terwindt, 1981; Terwindt, 1981). They represent the deceleration phase in the dominant tidal current where sediment having been swept into suspension during the full-vortex stage settles farther ahead of the bedform leeside. The reduced vortex activity is no longer able to move suspended sediment clouds from the leeside trough; deposition results in low-angle toesets (Boersma and Terwindt, 1981). As currents become slack, shear across the crest is insufficient to build up leeside slopes to the point of yield; avalanching is subdued.

Topset beds formed during the decelerating current stage are upcurrent extensions of sigmoidal foresets. They are characterized by rounded, more gradational brinkpoint intersections with sigmoidal foresets (fig. 3.28) and are interpreted as deceleration topsets (Kohsiek and Terwindt, 1981).

Crossbeds in one set of bundled foresets exposed at San Rafael Swell West (Z-6), dip uniformly to the west. Directly overlying these is a small-scale megaripple bed with foresets dipping to the east. The westward-dipping master foresets are interpreted as ebb-oriented sets. The overlying megaripple bed was deposited during the subordinate flood tide. Its restricted occurrence suggest that other similar beds were

probably deposited but were planed off during the next dominant ebb tide. This thin flood-tide deposit is equivalent to the ripple roof deposited during a subordinate ebb tide in neap-spring tide shoal sequences described from the North Sea (Boersma and Terwindt, 1981).

Other crossbedded sets, solitary simple or composite sets, also display unimodal paleocurrents. Taken collectively, crossbedding is primarily bimodal with tri- and polymodal components (fig. 3.11) Bimodality and polymodality of crossbedding is a common feature of tidal environments. However, bimodal or herringbone crossbeds have been identified in modern fluvial tributary mouth bar deposits (Alam et al., 1985). In the composite sandstone facies, solitary crossbed sets with unidirectional flow patterns are bimodal with respect to other unidirectional crossbeds preserved in different lateral vertical stratigraphic intervals. This relationship suggests ebb- and flood-tide and related bedform motion in different tidal courses or channels. Such behavior of tidal flow is the result of time-velocity asymmetry (Postma, 1967), where maximum flood and ebb current levels, do not occur at the midpoint of the tidal cycle, but usually at some time after mid-tide. In settings such as in tidal inlets, estuaries, and tidal flats (Hayes, 1975), it becomes necessary for tide waters to occupy different flow paths. In a tidal inlet, peak ebb-flow velocity is not attained until well after mid-ebb tide. So at the onset of high tide, ebb water is still flowing seaward through the ebb channel, and flood water is forced to migrate shoreward in different channels marginal to the main ebb channel (Hayes, 1975). Hence, during deposition of the composite sandstone facies, there were different channels to accomodate dominant ebb- and flood tide currents as indicated by crossbed patterns and complexity caused by velocity

asymmetry.

The above discussion is based on observations of modern subtidal and intertidal bedforms and stratification produced in tidal shoals and channels in estuaries along the South Carolina coast and the Dutch coast of the North Sea. In reference to sigmoidal foreset beds and their formation during slackening currents, it is important to note the following. Sigmoidal foreset beds have been described from delta-like deposits in laboratory flumes (Jopling, 1965b), linguoid ripples in flood deposits of ephemeral streams (Williams, 1971), hurricane washover deposits (Morton, 1978), ancient point bar deposits (Nami and Leeder, 1978), and ancient eolian deposits (pers. obs.), so they are not a feature produced exclusively in tidal environments. In contrast to their origin in decelerating currents (Boersma and Terwindt, 1981a, b), sigmoidal bedding has been generated in accelerating currents in the lower flow regime and is associated with the transition from linear bedforms to lunate bedforms (Jopling, 1965b). Saunderson and Lockett (1983) observed sigmoidal foreset beds as a transitional bedding phase between lower flow regime dunes and upper flow regime plane beds.

Because of the fine to slightly coarse-grained texture of the crossbed sets, current velocities of at least 50 cm/s are required to generate sandwaves and dunes (Harms et al., 1982) Flow velocities have been measured over dunes between 0.60 m/s and 0.80 m/s in a modern estuary (Boothroyd and Hubbard, 1975) and 0.4 m/s to 1.3 m/s on a modern tidal shoal (Kohsiek and Terwindt, 1981). Velocities related to sand wave migration are between 0.60 m/s and 0.70 m/s in a modern estuary (Boothroyd and Hubbard, 1975) and 0.30 m/s to 0.80 m/s (Reineck and Singh, 1980)

Parallel-bedding. Bedding aspects (table 3.2) and the relationship with the crossbedded microsequence suggests that the parallel-bedded microsequence was deposited on the lower and middle intertidal portions of shoals on topographically higher sand flats or berms. These areas became submerged at high tide but were fully exposed at low tide. Because of the higher percentage (fig. 3.32) and greater frequency of crossbedded sandstones toward the west, hydraulic conditions favoring the generation and migration of megaripples were greater there and became less so to the east. Toward the east, the interidal berms and flats became dissected by progressively narrower tidal channels and the interchannel berms were broader in extent.

In a study of modern tidal bedforms, Elliott and Gardiner (1981) described how extensive rippled surfaces were formed on topographically elevated sand flats of intertidal bars. Megaripples were relatively undeveloped in these areas because of the time-velocity asymmetry of tidal currents and the effect of scour lag (van Straaten and Keunen, 1958). By the time maximum ebb velocities were attained for megaripples to form, the higher sand flats were already exposed. While during maximum flood current velocities, the sand flats had not yet been inundated (Elliott and Gardiner, 1981).

Cyclic beds consist of plane laminated sandstone, ripple-laminated sandstone and locally developed siltstone or mudstone laminations, in ascending order. Vertical grain-size and stratification trends suggest an upward decrease in current energies. The highest current velocities are represented by the plane-laminated very fine to fine-grained sandstones. They were deposited as sheets or waves of sand grains (plane beds of upper flow regime) transported by currents flowing

between 60 and 120 cm/s (Harms et al., 1982). These beds represent the fine-sand equivalent of contemporary megaripples (crossbedded microsequence) that had migrated in similar current velocities (size-velocity diagram, Harms et al., 1982). Evenly laminated sand is deposited on the submerged parts of tidal sand bars, shoals and channel slopes in the North Sea from settling out of suspension clouds produced by shoaling waves (Reineck and Singh, 1980).

Overlying crosslaminated beds were deposited by symmetric lunate ripples, and by straight-crested or linear current ripples as flow velocities progressively decreased. Like megaripples, ripples also exhibit a change in external form and crest outline with changing velocities. Hayes (1976) demonstrated how linear ripples evolve into three-dimensional or cuspate ripples with increasing current strength.

Thin siltstone or mudstone laminations which drape over sandy rippled surfaces suggest that the ripples formed under water during slackwater and temporary standstill just before the reversing tide.

Sand flat emergence and exposure is indicated by modified ripples with flattened or rounded crests, run-off tongues and ladder ripples. These are common features of tidal flats and are formed during falling water stages and eventual emergence (Reineck and Singh, 1980; Elliott and Gardiner, 1981). During slackwater or emergent stages, benthic organisms roamed upon and mined the fresh sediment and left imprints of winding bilobed and cylindrical tracks and trails. The trace fossils suggest crawling and deposit-feeding activity and belong to the Cruziana ichnofacies.

A strong bimodal and slight polymodal paleocurrent patterns are indicated in nearly every stratigraphic section where data from rib-and-furrow structures and other ripple features were collected. Ribs-

and-furrows were generated by migrating lunate ripples. Distinct paleocurrent reversals are seen on bedding surfaces. Parting lineation trends, related to deposition of plane laminations, show correspondingly similar paleocurrent trends (fig. 3.10). By comparing rose plots of ripple data against crossbed data (figs. 3.10, 3.11), other paleocurrent relationships are indicated. Most ripple data show good correspondence with crossbed data. However, at Cedar Mountain (Z-17), ripple data show a strong northward component but crossbed data show a strong southward component. This relationship suggests that a dominant current flowed to the south and a subordinate reversing current flowed northward.

Other ripple data show trends that are oblique or perpendicular to crossbed trends. These relationships are used to identify megaripples migrating in submerged tidal channels where ripple migration is controlled by lower flow velocity during neap tides when megaripples are motionless (Terwindt and Brouwer, 1986). Cumulative paleocurrent data show a general strong northeast-southwest reversing paleocurrent pattern. This means that reversing tidal currents had flowed parallel to the shoreline in the San Rafael Swell area and perpendicular to the shoreline in the northern Henry Mountains area.

Rippled Silty Facies

Mostly current-rippled sandy and silty beds in the rippled silty facies (table 3.4) suggest sedimentary processes operating in an intertidal sand flat, analogous to modern lower sand flats of the German North Sea (Reineck, 1975). The very fine sandy and silty beds form a general upward-fining macrosequence with the underlying fine- and medium sandy composite sandstone facies. Lowermost beds in the facies in the Green River Desert area, especially at Dellenbaugh Butte (Z-8) and Horse Bench (Z-12) are laterally equivalent and contemporary with easternmost beds of the composite sandstone facies. Together with the redbed facies, a mantle of very fine sand, silt and mud was deposited farther eastward, and presmumeably southward, at higher levels on the intertidal-supratidal flat contemporary with coarser sand deposited seaward in a shoal and channel system. On modern tidal flats, sandier sediments are deposited at lower water levels where wave- and tidal-current strengths are greatest; mixed sand and mud characterize middle tidal flats (Reineck, 1975; Weimer et al., 1980). Muddier sediments tend to accumulate higher up on the flats mainly as a result of settling lag (Postma, 1961) and scour lag (van Straaten and Keunen, 1958) to form an extensive laterally-fining deposit (Hantzschel, 1939; van Straaten, 1954a; Thompson, 1968; Curray, 1969b). A similar laterally-fining relationship is demonstrated in figure 3.2 which is a map showing the variation of percent net sandstone in the Curtis Formation. Sandy beds decrease in percent toward the south and east in the inferred paleoshoreline directions. The pattern emphasizes the volumetric importance of sandstone accumulation in the western San

Rafael Swell area where shoal-channel systems were present.

Westward progradation of the higher sand flats over the lower channel and shoal system resulted in upward-fining macrosequence in this interval of the Curtis. The progradation is related to a major regression that began during late Curtis time and continued through deposition of the Summerville.

Bedding features such as run-off structures, very local evaporite polygon casts and lack of megaripple crossbedding suggest shallow water emergent conditions with exposure at levels on the sand flat higher than those interpreted for the composite sandstone facies. Near the contact with the Summerville at San Rafael Swell East (Z-3) are very locally preserved dessication cracks, undulating beds due to algal growth and preservation as stromatolites, and molds of reworked intraclasts of dried mud. These features may suggest deposition in higher intertidal or supratidal zones with greater degree of exposure. Complexly bundled crosslaminations suggest wave orbital currents.

Ripples of silt, very fine- and fine-sand are typically the dominant bedform of modern sand flats (Reineck and Singh, 1980) especially on topographically elevated berms on intertidal shoals (Gardiner and Elliott, 1981). Hydraulic conditions here do not favor the formation of megaripples because of time-velocity asymmetry (Klein, 1970a) in which peak flood- and ebb-current velocities occur some time before or after mid-tide cycle. When peak ebb velocities have been attained, the flats have not yet been flooded (Elliott and Gardiner, 1981). Formation of ripples in very fine- and fine-grained sand requires flow velocities of 5 cm/s and up to 60 cm/s (Harms et al., 1982). Reineck and Singh (1980) reported current velocities between 30 and 50 cm/s associated with ripples on North Sea sand flats. Thompson

(1968) reported velocities of 25 to 50 cm/s across intertidal flats associated with the Colorado River delta, Gulf of California.

The few paleocurrent measurements taken in this facies are probably of little use in recognizing specific paleocurrent mechanisms or processes. However, weak bimodal and polymodal trends (fig. 3.12) do indicate major paleoflow directions to the south and southeast, general onshore directions, and northeast, north and northwest polymodal patterns reflect run-off controlled by local topography during sand flat emergence.

The two upward-fining microsequences contain rhythmically interbedded sandstone and siltstone or mudstone beds. Each microsequence records an upward decrease in flow velocity, grain size, and availability and transport of sand. This vertical trend may represent higher current velocities and greater sand transport during spring tide periods and low flow velocity, low sand transport, and settling of mud during neap tide periods. Sandstone beds show variations from flaser- to wavy- and lenticular-beds where ripple-laminated sandstones indicate greater availability of sand and traction sedimentation in the form of water ripples. Interbedded wavy mudstones and mudstones containing lenticular beds or starved ripples indicate gentler currents and greater volume of mud settling out of suspension. Beds like these have been described from modern intertidal flats (Hantzchel, 1939; van Straaten, 1954c, 1961; Reineck and Singh, 1980; Weimer et al., 1982) especially in mixed sand and mud intertidal flats (Reineck, 1967, 1972, 1975). Tidal environments are subjected to daily, spring-neap, and seasonal fluctuations in current strengths which are occasionally enhanced during rain or wind storms. The ripple laminated

sandstones with flasers probably record vertical accretion of the sand flat during spring tides when a greater amount of sand is transported (Terwindt, 1981). Interbedded sandstone and mudstone was deposited during daily tidal fluctuations and during neap tide periods when significantly more mud settles from suspension (Terwindt, 1981), very similar to the origin described for an upward-fining, upward-thinning microsequence in the sandstone-mudstone facies. This comparison between two texturally and structurally similar microsequences emphasizes how similar processes can produce similar deposits in different environments or subenvironments.

Modern sandy tidal flats commonly exhibit greater degrees of sediment bioturbation in higher intertidal flats relative to lower parts where wave- and current energies are greater (Reineck and Singh, 1980; Weimer et al., 1982) Abundance of bioturbation features, especially trace fossils, is generally low relative to other modern and ancient shoreline sequences of comparable sedmentary conditions (Howard, 1972; Howard and Dorjes, 1972; Frey and Howard, 1982; Howard and Frey, 1984). Whole trace fossils are seemingly in lesser abundance in the rippled silty facies than in the composite sandstone facies. Trace fossils were either overlooked and not observed or were not formed or preserved because paleoecologic or preservational conditions may have been harsh. Perhaps, a greater degree of bioturbation in this facies is preserved in the beds described as cryptic-bedded siltstones and mudstones (table 3.4) in which physical bedding is not recognizeable.

Redbed Facies

Deposition of microsequences in the redbed facies represents two stages of marine transgression and eastward retreat of marginal marine environments during middle(?) and late Curtis time. Deposits of the first minor transgression are separated from those of the second by sandstones in the Moab Tongue, which accumulated during a minor regression and westward progradation of the shoreline. The general upward-coarsening macrosequence preserved below either the Bed at Black Steer Knoll or Moab Tongue reflects increasingly sandier conditions and advance and burial by wind-blown sand in the Moab Tongue. Individual upward-fining, upward-thinning microsequences compose the macrosequence and record mainly subaqeous sedimentation in a sandy coastal sabkha, upper intertidal-supratidal complex recurrently modified by wind- and storm-flooding and possibly wadi sedimentation. This interpretation is consistent with the mixed water- and wind-laid deposits and upward-drying conditions in the overlying wavy sandstone facies of the Moab Tongue.

Individual bedding units of the redbed facies are cyclic upward-fining, microsequences (microsequences 2 and 3) except for the disorganized, heterolithic intervals (microsequences 1 and 4) (table 3.5). There is a greater proportion of siltstone and mudstone beds in this facies relative to non-red facies in the middle and upper Curtis to the west. Thii textural relationship is consistent with the overall eastward lateral decrease in grain size described for the Curtis Formation. A shoreward-fining textural trend is a common feature of modern intertidal flats (Hantzschel, 1939; van Straaten, 1954a; van

Straaten and Keunen, 1958; Postma, 1961; Thompson, 1968; Curray, 1969b). The redbed facies was deposited in middle to upper intertidal and possibly lower supratidal environments further shoreward or eastward than contemporary deposits in the rippled silty facies. A change from gray-colored, sandy facies to reddish-brown sandy facies at a location approximately between Dellenbaugh Butte (Z-8) and White Wash (Z-11) represents an approximation of the shoreline or mean intertidal zone, at the time of deposition of these facies.

Basal trough crossbed sets in microsequences 2 and 3 are deposits of large subaqueous ripples or small megaripples as suggested by well-developed foreset laminations, and gravel-sized mudstone intraclasts along foresets. These beds may have formed in broad, shallow, current-dominated channels and may be remnants of small tidal creeks or gullies on the upper coastal plain. The tidal range and therefore currents associated with tidal range are controlling factors on the distribution of bedforms. In a mesotidal setting (tidal range 2 to 4 meters) surfaces of higher parts of the intertidal flats have well developed wave- and current-formed ripples; sandwaves and dunes form on the lowermost flats adjacent to large channels (Clifton, 1982). In a macrotidal (tidal range greater than 4 meters), as in the Bay of Fundy, megaripples are generated over much of the intertidal flat (Dalrymple et al., 1978).

Crosslaminated very fine- and fine-grained sandstones and siltstones with local mudstone flasers suggest transport of sand in current velocities between 25 to 50 cm/s as oberved on some sandy intertidal flats (Thompson, 1968; Reineck and Singh, 1980). Cross-laminated and trough crossbedded sandstones may represent the spring-tide portion of a vertically-accreted neap-spring tide bundle because

of their cyclic occurrence at the base of some microsequences (table 3.5). They may represent the spring-tide portion of a vertically-accreted neap-spring tide bundle. More sand is transported during spring tides and less so during neap tides (Terwindt, 1981). Very thin mud laminations are present assflasers formed by mud settling out of suspension during tidal reversals. Ripple migration is resumed during the next tide current and the mud drape or flaser is preserved as long as ripple-forming currents do not exceed the threshold for eroding mud (Terwindt, 1969, unpub., cited in Reineck and Singh, 1980). Progressively less sand was moved up on to the flat between successive spring or storm-enhanced tides as suggested by the overlying interbedded mudstone and siltstone with thin crosslaminated wavy-bedded sandstone beds. These constitute rhythmic sandstone-siltstone-mudstone interbeds which have modern counterparts in some modern middle and upper intertidal flats (Hantzschel, 1939; van Straaten, 1954a, 1961; Reineck, 1967, 1975) and owe their origin to the tidal rhythm (Reineck and Singh, 1980). Relatively thicker siltstone, mudstone, and claystone with crosslaminated ripple-form lenses were probably deposited by daily tides around neap tide period.

Local horizontal cylindrical burrows and tracks indicate feeding and crawling activity of benthic organisms during calm water periods. Shrinkage cracks in mudstones are interpreted as dessication features related to low tide emergence and exposure.

The Bed at Black Steer Knoll forms a traceable stratigraphic interval in the redbed facies. Correlations with equivalent bedding intervals in the Moab tongue are uncertain. It may correlate with the uppermost bed of the wrinkled sandstone facies at the top of the Moab

as suggested by O'Sullivan (1980a) (fig. 2.5). Nonetheless, beds in this microsequence were deposited rapidly by currents swifter than those that produced the other microsequences as indicated by plane laminations and fine- to medium-grained crossbedded sandstone (table 3.5). Underlying wet mudstones and siltstones were severely deformed by down-loading accompanied by shearing to produce flame structures. Rippled siltstone partings along foresets are discontinuities (Allen, 1980) and indicate intermittent bedform movement. The overlying vertical succession of wavy- and lenticular-bedded sandstone and siltstone and interbedded siltstone, mudstone and claystone record waning current conditions and deposition of the finest sediment. Crosslaminated silty and sand lentils enclosed in mudstone with dessication cracks record the last stages and final emergence of the subaqueous environment which deposited the microsequence.

Locally, the Bed at Black Steer Knoll is tabular in geometry but regionally it pinches out or grades into facies of the Moab Tongue. The microsequence shows affinities to sequences deposited in different kinds of environments. Similar vertical textural and bedding sequences are developed in fluvial point bars (Allen, 1964, 1970a; Leopold et al., 1964), tidal creek point bars (Howard and Frey, 1980), washover fans (Howard and Frey, 1980) and wadi deposits (Glennie, 1970). Both fluvial and tidal point bars are generally characterized by basal gravel beds, lateral accretion surfaces or longitudinal crossbedding (Reineck, 1967; Reineck and Singh, 1980; Weimer et al., 1982) and lenticular geometries. These features are absent in this microsequence. Lack of gravel in the microsequence suggests good sorting, unavailability of gravel, and low current strengths.

Washover fan deposits can be as thick as 4.3 feet (1.25 m), are wedge-shaped, preserve shoreward-dipping foresets, and are internally interrupted by numerous erosion surfaces from successive hurricane events (Andrews, 1970; Howard and Frey, 1980) Localized wedge-shaped beds and discrete multiple truncation surfaces are generally absent in the microsequence. Paleocurrent data is insufficient to discriminate shoreward, seaward, or shore-parallel flow.

Some wadi deposits typically resemble braided stream deposits (Reineck and Singh, 1980) and usually contain alternating wind-blown and subaqueous megaripple strata with gravels (Glennie, 1970). Diagnostic eolian features are not recognizeable in this microsequence. Crossbedding from flow in a wadi system should dip westward or seaward because wadi channels generally drain downslope or into interior basins (Glennie, 1970).

In light of the above discussion, the microsequence in the Bed at Black Steer Knoll, and other similar microsequences in the redbed facies, were probably deposited by wind- or storm-enhanced spring-tide flooding of a coastal plain sand flat. In process, it may have resembled a washover that was later modified by normal tidal currents.

Locally preserved lenticular, channel-form bodies are filled with interbedded siltstone, sandstone, and mudstone and were deposited in either tidal or wadi channels.

Glennie and Evans (1976) have described supratidal salt flats of coastal India which are annually flooded by seawater during monsoon and wind-enhanced spring tides. Numerous upward-fining sequences 20 to 30 cm thick grade vertically from sand to silt and clay. Between floods, the flat is exposed and desiccation and evaporation favor the

crystallization of halite and gypsum. Ephemeral streams or wadis drain seaward and bring in coarse sand and gravels from adjacent uplands. Absence of evaporites in the redbed facies suggests that either salinities were too low or original evaporites have been removed during diagenesis or weathering. The fine-grained texture of the channel-fill deposits suggests low velocity currents and lack of coarser sediment available for transport. Paleocurrent indicators are poorly preserved; sedimentary structures indicating bimodal paleocurrents were not observed.

Recognizeable, whole trace fossils are few yet extensive bioturbation may have been responsible for disrupted and unbedded mudstone and siltstone. Hantzschel (1939) observed that on some modern tidal flats (wattenschlick) sediment reworking and restratification occur so rapidly that burrowing animals do not have time to destroy bedding. Few traces of organisms in this microsequence may suggest an inhospitable environment, perhaps too hot and arid, as suggested by interbedded Moab facies of eolian origin. Salinity was probably high (local evaporite casts and nodules of chalcedony after gypsum in contemporary rippled silty facies to the west, table 3.5) but not high enough to allow thick gypsum to form as it did during Summerville time.

Significance of redbeds. The distinct color change from brownish-red in the redbed facies to a light greenish-gray color in all the other Curtis facies may be a useful feature in estimating the position of the paleoshoreline during Curtis time. The inferred color change occurs approximately between Dellenbaugh Butte (Z-8) and White Wash (Z-11). This geographic location may coincide with the approximate position of the shoreline, possibly between intertidal and supratidal

coastal zones during deposition of contemporary rippled silty facies and redbed facies. Thompson (1968) was able to distinguish different tidal zones in deposits of the Colorado River delta, Gulf of California. Here, brown colors in sediments in upper intertidal and supratidal zones are attributed to greater subaerial exposure and higher degree of iron-oxidation. Whereas, beds deposited in lower intertidal zones acquire a brownish-gray color due to greater submergence and partial iron-reduction. The red color in sedimentary rocks, mainly shales, is produced by oxidizing depositional or diagenetic environments and is strongly controlled not by the amount of iron present, but by the ratio of the oxidation states of iron, Fe^{3+}/Fe^{2+}, and the amount of organic carbon present (Potter et al., 1980). Red colored shales are associated with high ratios, gray and green colored shales with low ratios (McBride, 1974; Potter et al., 1980). The colors, and therefore, the oxidation states of iron are ultimately controlled by amount of organic matter present; even small amounts favor the reduced form of iron, Fe^{2+} (Potter et al., 1980) Although these ideas deal with the colors of shales, they may by applicable to the gray-red color difference between the Curtis and Summerville. All of the Curtis facies except for the redbed facies were deposited in subtidal to intertidal coastal subenvironments. The marine environment favors reduced iron Fe^{2+} and tends to produce drab red, gray, and green colored sediments as described Recent intertidal flat sediments; greater subaerial exposure in upper intertidal and supratidal flat sediments favors the oxidation of iron and the formation of dark brown or red sediments (Walker, 1967a; Thompson, 1968). Organic matter, mainly woody material in the form of coal clasts, was transported from another part of the southern or

southwestern shoreline and deposited with other sediments in the Curtis. The abundance of coal clasts is greatest among facies in the lower Curtis especially in the San Rafael Swell area. Coaly material is not observed in the redbed facies.

Hence, sealevel, and therefore shoreline position, and presence of coal clasts are factors controlling color in the gray Curtis facies in accordance with the observations of Thompson (1968) and Potter et al.(1980). However, the specific mineral origin for the iron staining in these rocks is yet uncertain.

Entrada Sandstone

Moab Tongue

The Moab Tongue of the Entrada Sandstone is composed of clean, light-tan or light whitish-gray sandstone facies which are contemporaneous with and, therefore stratigraphically equivalent to, the redbed facies and ripple-laminated silty facies in the Curtis Formation. As the thinnest, uppermost member of the Entrada Sandstone, it interfingers with beds of the Slick Rock Member of the Entrada to the east about 8 miles (13 km) west of the Colorado River in Fish Seep Draw (O'Sullivan, 1981b) and to the southeast along Dry Valley, south of La Sal Junction (O'Sullivan, 1980b; 1981a) (fig. 3.47). From these locations, it forms a wedge-shaped body of sandstone that is perched at the top of the Slick Rock Member and extends no farther northwest than Tenmile Canyon South (Z-21).

The Moab interfingers with the redbed facies of the Curtis and subdivides that facies into lower and upper parts between Mill Canyon (Z-25) and Duma Point (Z-7), in the Green River Desert. In this area, the Moab is present as a conspicuous tan and gray cliff-forming sandstone, inaccessible at most exposures, and displays a peculiar columnar weathering pattern related to vertical joints (figs. 3.45, 3.46). Southwest of Mill Canyon, where the Moab lies unconformably on the Slick Rock Member, the two sandstone members are nearly identical in texture and stratification, yet the Moab is still distinguishable by the tan and gray color and columnar weathering.

Figure 3.45. Moab Tongue (Jem) of the Entrada Sandstone interrupting sequence of redbed facies (Jcu) on ridge along Tenmile Canyon. Section Z-21 is at tip of ridge. Slick Rock Member of Entrada (Jes). Exposure is 145 ft (43.5 m) thick from top of Slick Rock Member

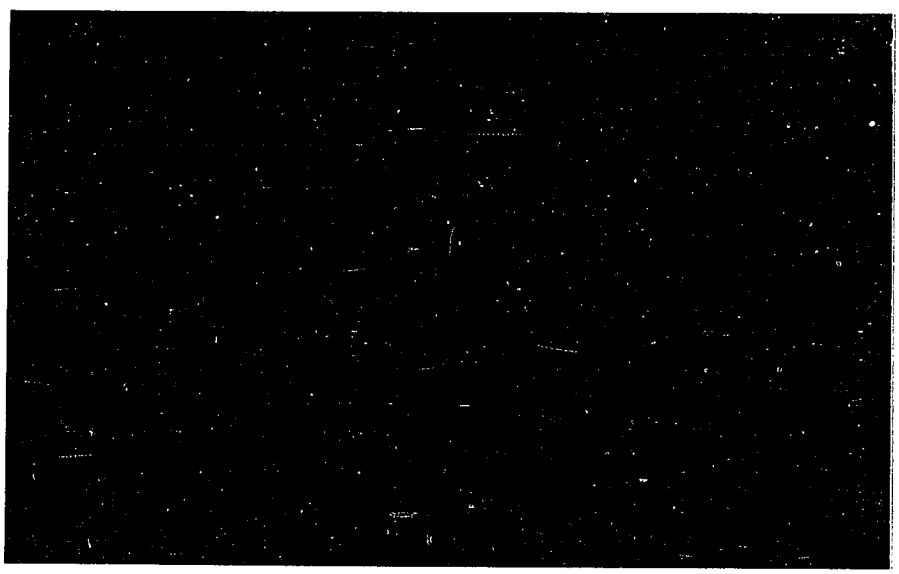

Figure 3.46. Columnar weathering pattern related to vertical joints in the Moab Tongue. Cliff-forming sandstone is 64 ft (19.2 m) thick (Dubinky Well, Z-19)

Three facies are recognized in the Moab Tongue. A wrinkled sandstone facies occurs as two distinct intervals interbedded within the crossbedded sandstone facies. The uppermost interval may be correlative with the Bed at Black Steer Knoll in the redbed facies of the Curtis. A crossbedded sandstone facies comprises the bulk of the Moab Tongue and a wavy sandstone facies forms an interval at the base and at the top of the Moab. Hence, from the top of the lower part of the Curtis redbed facies, a typical vertical succession of facies begins with a wavy sandstone facies overlain by a crossbedded sandstone facies which is locally interrupted by a wrinkled sandstone facies. At the top, the wavy-laminated sandstone facies reappears and grades upward into the basal upper part of the Curtis redbed facies (fig. 2.5).

Isopach Trends

Because of the thinness of the entire Moab interval itself, it was deemed unnecessary to map the distribution of individual facies contained therein. Instead, the spatial and stratigraphic relationships of the Moab facies are illustrated in figure 2.5.

Only four stratigraphic sections that included the Moab Tongue were measured and described in this report. They are Tenmile Canyon North and South (Z-20, 21), Dubinky Well (Z-19) and Bartlett Flat (Z-22) (figs. 1.1). The exposure of Moab at Mill Canyon is not measured and is only partially described. Figure 3.47 shows the thickness patterns and approximate area of outcrop of the Moab Tongue where data permit. Supplemental thickness data have been gathered from other sources (table 1.2). Contour lines are discontinuous south of the Green River, in the Canyonlands District. Here, the Moab and other Mesozoic

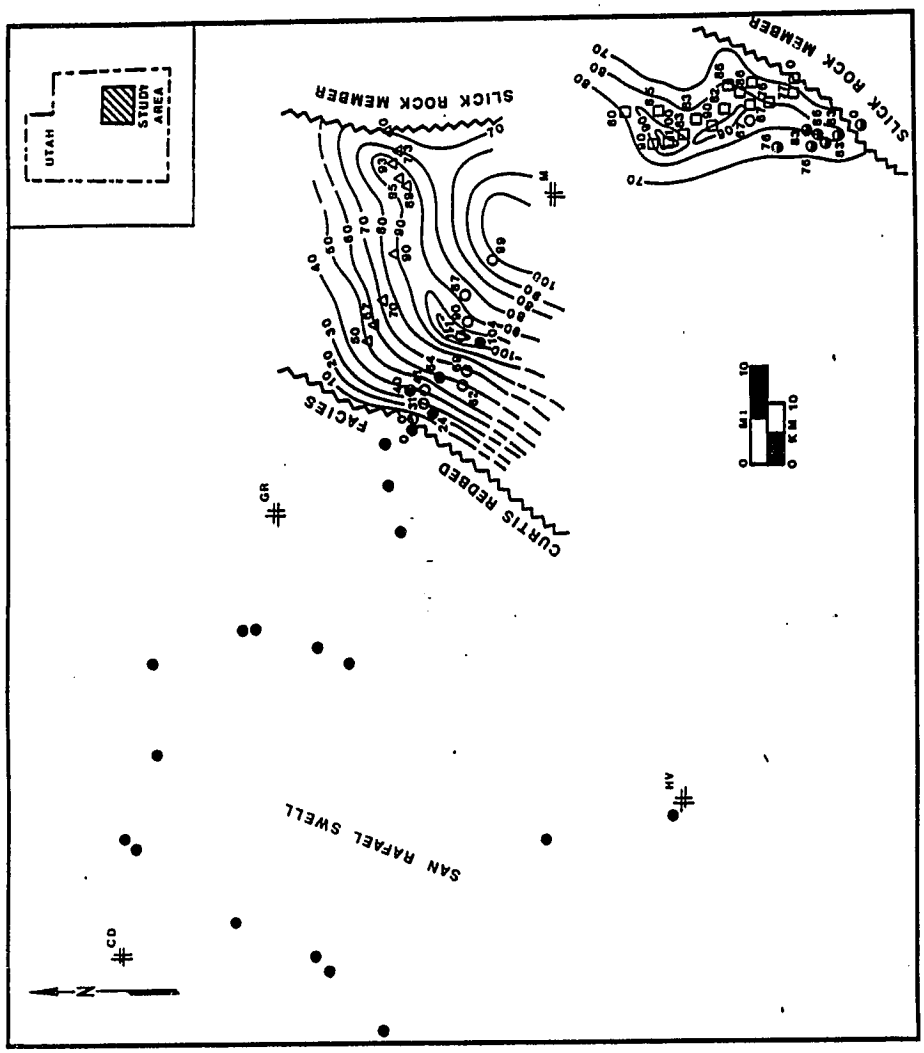

Figure 3.47. Isopach map of the entire Moab Tongue in east-central Utah. Contour interval: 10 ft (3 m). Map symbols (table 1.3)

strata are missing because of probable erosion related to movement of the Monument Uplift. The Moab Tongue would have possibly extended southwestward into this area to form a more continuous northeast-southwest trending belt of sandtone between the Curtis redbed facies and the Slick Rock Member. the isopach map shows fairly uniform thinning to the northwest and ultimate replacement by the redbed facies of the Curtis. Hummocky thickness patterns are developed in the Bartlett Flat are (Z-22) and just northwest of the Moab townsite (fig. 3.47) suggesting ridge-like sand build-ups or thicks with an approximate northeast-southwest trend. At these looations, thicknesses of greater than 90 feet (27 m) are attained.

Paleocurrent Trends

Sixty-two crossbed azimuths were measured in the crossbedded sandstone facies at four locations. The results of the statistical analysis are presented in figure 3.48. Note that only two measurements were recorded at Tenmile Canyon South because only two crossbed sets comprise the exposure of Moab there. The rose diagrams endicate average westerly paleocurrents. Moreover, the petals or wedge-sections of the roses also show multi-directional crossbed azimuths (also Fred Peterson, USGS, Denver, Colorado, 1985 and Gary Kocurek, Univ. Texas, 1986, pers. comm.). Moderate to low reliability indices between 25 and 52 suggest relatively high dispersion or non-uniformity of crossbed dip directions (table A.1, appendix)

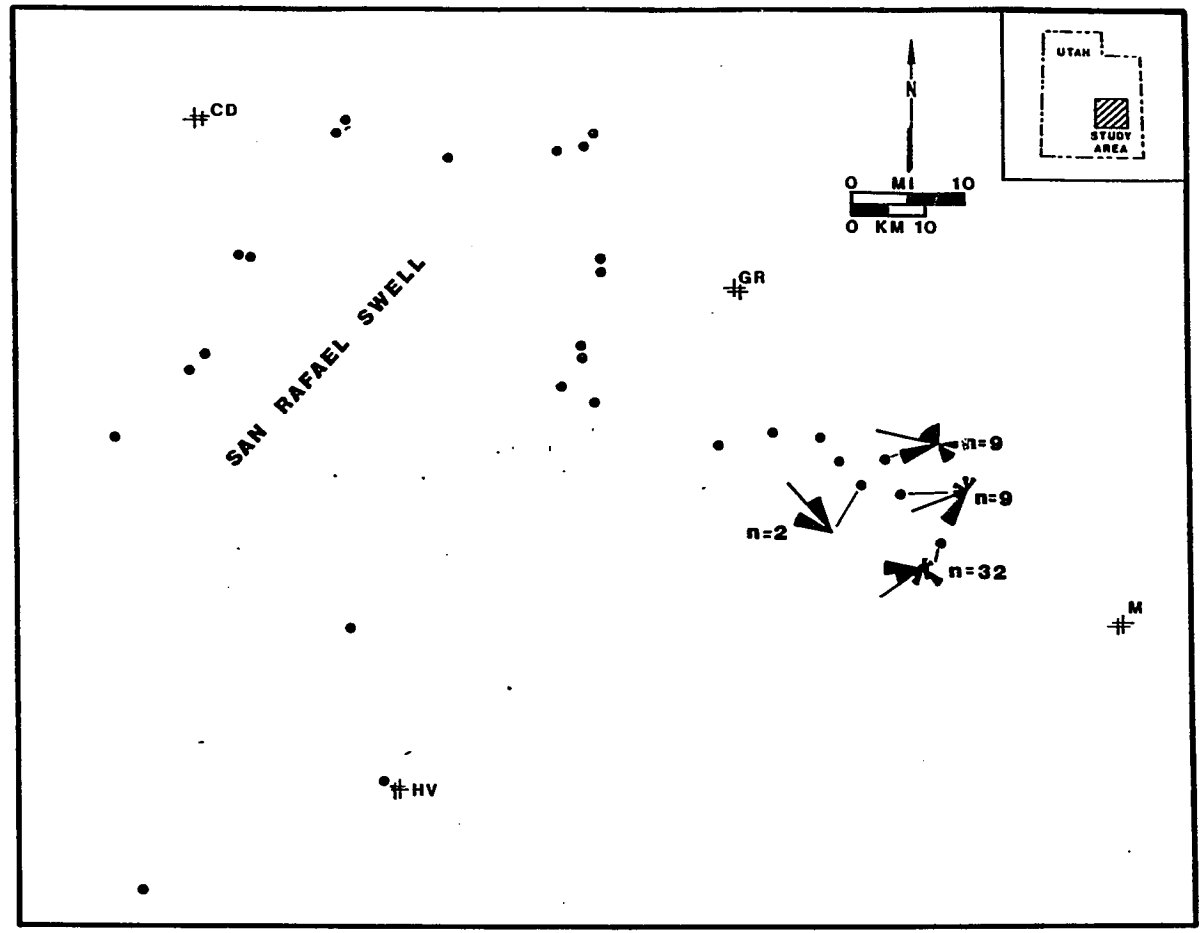

Figure 3.48. Paleocurrent patterns preserved in the crossbedded sandstone facies of the Moab Tongue; n = number of measurements; stick = mean paleocurrent vector. Map symbols (table 1.3)

Crossbedded Sandstone Facies

The crossbedded sandstone facies comprises 80 to 90% of the Moab Tongue and forms the straight, vertical or smooth, rounded slickrock cliffs so common among the other Jurassic quartzarenite sandstones (e.g. Navajo and Page Sandstones and Slick Rock Member of the Entrada Sandstone), particularly those of eolian origin. It is underlain and overlain by the wavy-laminated sandstone facies in all four stratigraphic sections and is locally interrupted by the wrinkle-bedded facies. The cross-bedded sandstone facies thins gradually to the northwest, as does the entire Moab Tongue.

The facies is composed solely of crossbedded sandstone beds, in which the grains are very fine to fine, well sorted, subrounded to rounded mostly quartz sand (Chapter 3, Petrology). Pores are 14% to 17% of the rock.

A white crossbedded sandstone bed about 6 feet (1.8 m) thick crops out at White Wash (Z-11) between the upper part of the Curtis redbed facies and the Tidwell Member of the Morrison Formation. Stratigraphic relations of the bed are unclear. It may be bed A (O'Sullivan, 1980a) at the base of the Morrison. However, it seems locally developed in the White Wash area and does not appear as laterally extensive as shown in the cross-section of O'Sullivan (1980a). An alternative explanation is that it is an isolated accumulation of a crossbedded sandstone facies related to that in the Moab Tongue. Therefore, it would be included as part of the Curtis-Moab interval and be considered as an anomalous bed at the top of the redbed facies.

Sedimentary featuree. In describing the small-scale stratification which internally makes up a cross-stratified set, the following terms are used. Foreset beds (Gilbert, 1885) or crossbeds (Rubin and Hunter, 1983) generally consist of both grainfall strata (Hunter, 1977a) or sandflow strata (McKee et al., 1971) or just sandflow strata. Toeset or bottomset (Gilbert, 1885) beds may be constructed of combinations of sandflow, grainfall, or climbing translatent strata, but usually the latter two. Avalanches (McKee et al., 1971) include slumps and sandflows where sandflows are a type of grainflow (Bagnold, 1954) Hence, the terms sandflow and grainflow are often used interchangeably.

Because of the nature and thickness of crossbed sets microsequences are not recognized in this facies. Sedimentary features are summarized in table 3.6 and in the following paragraphs.

Crossbeds are distinguished between simple and compound sets (table 3.6). Simple crossbed sets are 1 to 4 feet (0.30 to 1.2 m) thick and relatively thinner than the compound sets Each crossbed set is internally stratified with alternating thicker sandflow strata and thinner grain fall strata as foresets. Climbing ripple strata are absent or indistinct in toesets. Toesets of some crossbeds are contorted where they overlie beds in the wavy-laminated sandstone facies. Set geometries are mainly tabular and may be wedge-shaped in a laterally continuous exposures; other wedge sets are locally clearly evident. Upper and lower bounding surfaces are nearly horizontal and are identified as second-order (E-2) surfaces (Brookfield, 1977).

A compound (Harms et al., 1975) or composite (McKee and Weir,

Table 3.6. Sedimentary features of the crossbedded sandstone facies, Moab Tongue of the

Sedimentary Features	Interpretation
1. Texture: -very fine-fine (88-250 μ) sandstone	
2. Multidirectional paleowinds; mean paleowind direction: easterly	Wind directions varying daily, seasona or during storms; variable dune types multidirectional slipfaces such as rev parabolic, oblique dunes; dune type un
3. Bedding a. simple crossbeds: -1-16 ft (0.3-4.8 m) thick -foresets composed of alternating sandflow-grainfall strata -climbing ripple strata absent or indistinct in toesets; in sets less than 5 ft (1.5 m) thick -recognizeable second-order (E-2) bounding surfaces truncating local third-order (E-3) surfaces -tabular-and wedge-sets -locally deformed toesets which overlie redbed facies of the Curtis and wavy sandstone facies of Moab Tongue	Simple dunes; type uncertain; general occurrence at edge of Moab erg
-local, base-of-slope, crabbing scour pit	Product of erosional scour pit migrati along lee slope
b. compound crossbeds: -composed of simple sets -bounded by first-order (E-1) erosion surfaces and associated wrinkled sandstone facies -climbing ripple strata along toesets	General occurrence in central portion Moab erg
c. foresets: -sand flow strata 1-8 in (2.5-20 cm) thick -fine (177-250 μ) sandstone -inverse grading indistinct or not developed -sharp contacts highlighted by interstratified grainfall deposits -wedge- or tongue-shaped geometry in dip section; pinching-out into grainfall or ripple strata; lenticularity in strike sections, outlined by enclosing grainfall strata	Foreset beds produced by avalanching o flow on slip faces of eolian dunes

andstone facies, Moab Tongue of the Entrada Sandstone

erpretation	References
d directions varying daily, seasonally, during storms; variable dune types with tidirectional slipfaces such as reversing, abolic, oblique dunes; dune type uncertain	Bigarella et al. (1969), Hunter et al. (1983), Swift and Niedoroda (1985)
mple dunes; type uncertain; general currence at edge of Moab erg	McKee (1966, 1979), Brookfield (1977), Wilson (1972a, b), Kocurek (1981a)
oduct of erosional scour pit migrating ong lee slope neral occurrence in central portion of ab erg	Rubin and Hunter (1983)
reset beds produced by avalanching or grain- ow on slip faces of eolian dunes	Bagnold (1954), Sharp (1966), Middleton (1970), Hunter (1977a, b; 1981; 1985b), Kocurek and Dott (1981) Schenk (1983)

Table 3.6. Continued

Sedimentary Features	Interpretation
3. Bedding (cont.)	
c. foresets: -grainfall strata: very fine to fine (88-177 μ) sandstone; 0.12 in (3 mm) thick or less	Component of foresets of eolian dunes; produced in zone of flow separation in currents too calm to produce traction (ripples)
d. climbing ripple strata -even, cyclic thick laminations 0.4 in (1 cm) thick or less -locally and faintly developed foreset laminations -inversely graded beds: very fine (88-125 μ) to fine (125-177 μ) sandstone -occurrence mainly along foreset toes of crossbed sets greater than 5 ft (1.5 m) thick	Climbing translatent strata as a product of ripples generated by wind eddies alon dune leeside

erpretation	References
ponent of foresets of eolian dunes; duced in zone of flow separation in rents too calm to produce traction ples)	Hunter (1977a, b; 1981; 1985b), Kocurek and Dott (1981)
mbing translatent strata as a product ripples generated by wind eddies along e leeside	Hunter (1977a, b; 1981)

1953) crossbed, as observed in this study, is a coset of individual, simple crossbedded sets with extremely complex bedding surface relationships. These beds range in thickness from 2 to 16 feet (0.60 to 4.8 m) and internally are more complexly stratified. Sandflow strata are thicker than those in the simple crossbeds and are rarely interrupted by grainfall deposits. Crossbed geometries are tabular-, wedge- or trough-shaped.

Climbing translatent strata are locally recognizeable where they form tangential toesets of crossbeds (table 3.6). They appear as evenly-spaced, cyclic bands that are about 0.4 inches (1 cm) thick or less and are inversely graded from very fine- to fine-grained sand. This textural feature is usually difficult to observe and determine. Locally and faintly developed foresets are common. In dip-parallel exposures, the toeset beds can be followed up the foreset dip to where they become intricately interbedded among grain fall and grain flow strata (fig. 3.49).

There are localized crossbedded sets 1 to 2 feet (30 to 60 cm) thick that resemble trough sets. However, laterally successive trough surfaces intersect to form a rib or spur. In a strike-oblique section, a series of intersecting troughs produces a scalloped lower bounding surface. Hence, the structure is called scalloped crossbedding (Rubin and Hunter, 1983).

Sandflow beds (table 3.6) observed in this facies are 1 to 8 inches (2.5 to 20 cm) thick; most fall within a thickness range of 2 to 5 nches (5 to 12.5 cm). Along foreset dip sections, individual sandflows are thickest updip and gradually become tapered downdip into distinct wedge-shaped units that intertongue with grainfall and climbing translatent strata. They are locally enclosed by grainfall

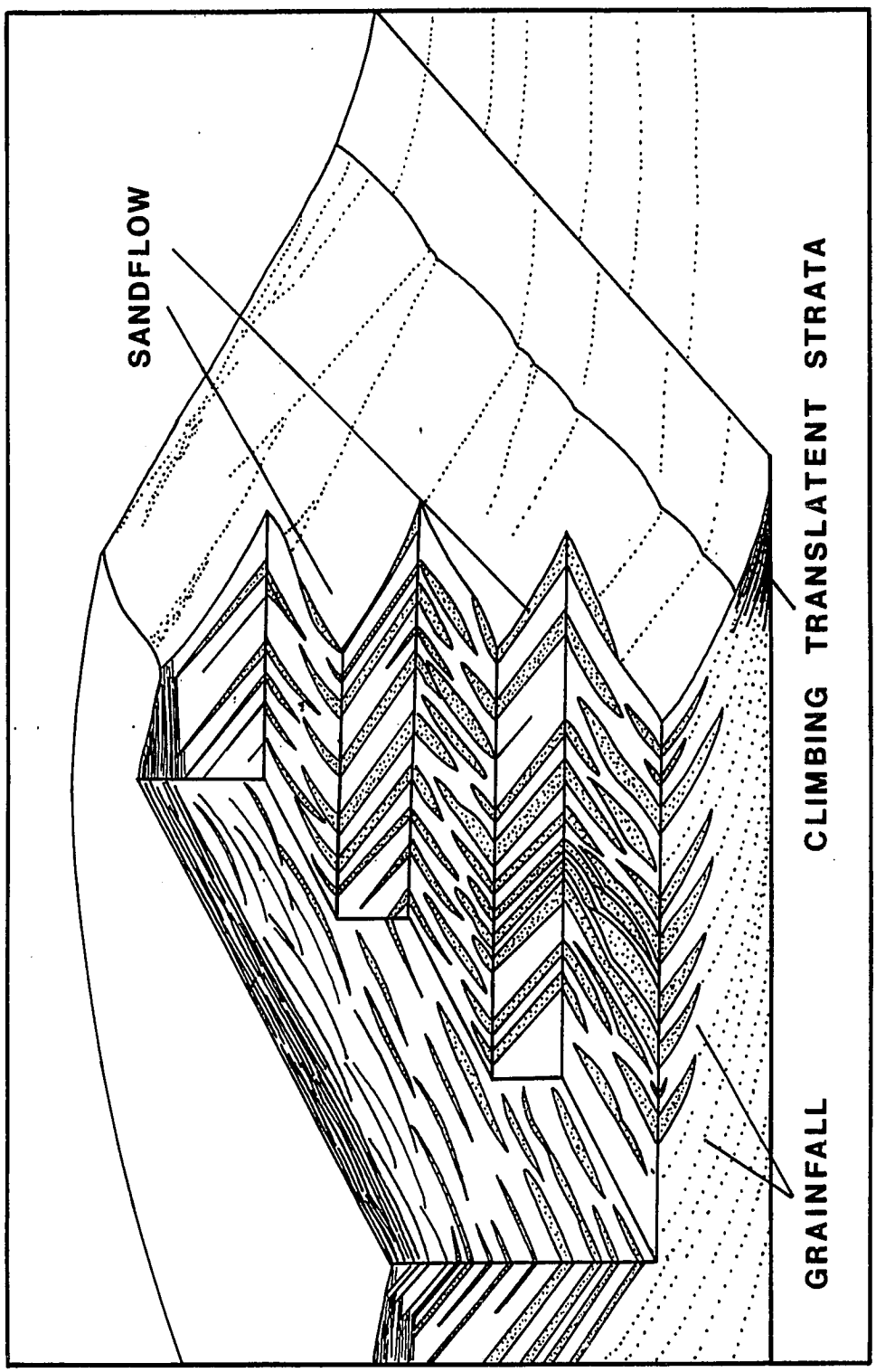

Figure 3.49. Relationship and distribution of stratification as locally preserved in crossbed sets in the Moab Tongue (after Hunter, 1977a)

strata in strike sections particularly in the thinner, simple crossbed sets (fig. 3.49).

Grainfall strata (table 3.6) comprise the second component of foreset beds, are usually 0.12 inches (3 mm) thick or less and are distinctly composed of very fine- to fine grained sand. As observed in dip-sections, they are usually interbedded with sandflow beds, tend to thicken down-dip while grading into and gradually being replaced by climbing translatent strata (fig. 3.49).

Simple and compound cross-stratification is distinguished by the degree of internal complexity characterized by the presence of second or third order bounding surfaces. Simple crossbedding of this facies is bounded by concave-upward second-order surfaces which locally truncate third-order surfaces (figs. 3.50, 3.51). Whereas with compound crossbedding, numerous truncation surfaces are tentatively identified as second order (E-2) surfaces (Brookfield, 1977) that successively truncate third and other second-order surfaces (fig. 3.50, 3.51). The entire crossbedded sandstone facies may be constructed by one or several thick cosets of complexly truncated crossbed sets. In general, simple crossbedding is present near the thin edge of the facies where it is exposed at Tenmile Canyon South (Z-21) (figs. 3.51). Compound crossbedding can be found in the thick central portion of the facies bounded by first-order (E-1) surfaces and related wrinkled sandstone facies.

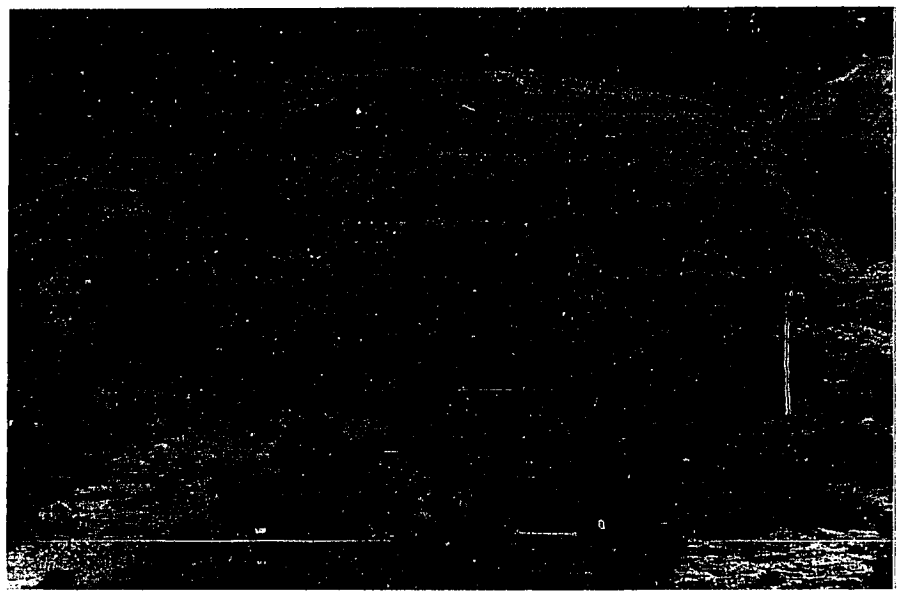

Figure 3.50. Complex bounding surface relationships within bed sets in the crossbedded sandstone facies of the Moab Tongue; first-order (E-1), second-order (E-2), bounding surfaces (Bartlett Flat, Z-22)

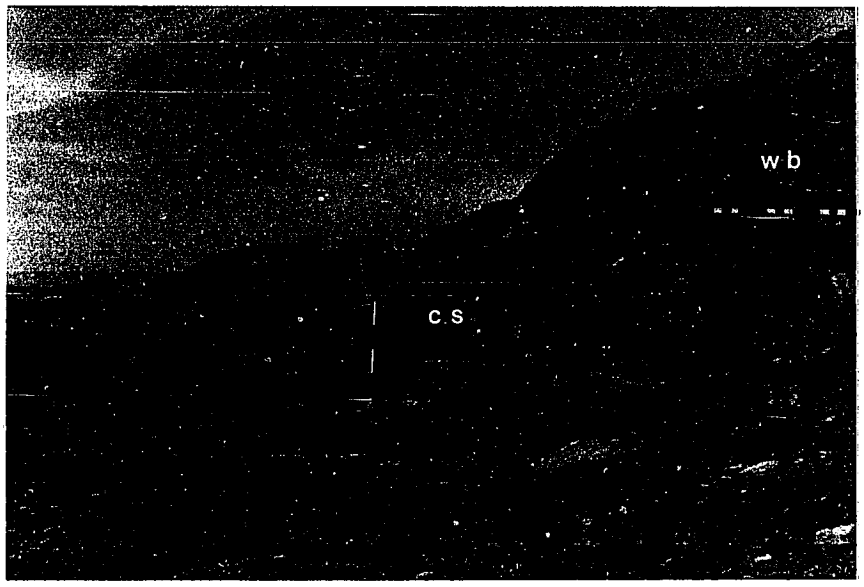

Figure 3.51. There are two simple crossbed sets preserved near the western margin of the Moab Tongue at Tenmile Canyon South (Z-21); only one can be seen in photograph. Staff is in feet. Crossbedded sandstone facies (csf); wavy-bedded sandstone facies (wb)

Wrinkled Sandstone Facies

The wrinkled sandstone facies occurs in units about 2 to 4 feet (0.6 to 1.2 m) thick which crop-out distinctively among large-scale crossbed sets of the crossbedded sandstone facies (fig. 3.52). The facies is composed of very fine- to fine-grained, well sorted, sandstone beds which are stratified with climbing ripple beds, wrinkled or crinkly very thin beds or laminations, crosslaminated beds, and wrinkled beds lacking foresets or any other discriminating stratification (table 3.7).

Bedding units of the facies occur in two local intervals enclosed within the crossbedded sandstone facies at Dubinky Well (Z-19) and Bartlett Flat (Z-22). It is preserved as a thin interval within the lower part of the crossbedded sandstone facies at Tenmile Canyon North (Z-20) and is completely undeveloped at Tenmile Canyon South (Z-21).

Sedimentary features. Sedimentary features are not described in terms of microsequences. However, because of the general thinness, the facies itself can be considered a microsequence.

A distinct type of stratification produced by ripples in sand is called climbing translatent stratification (cts)(Hunter, 1977a). Cts is recognized in Moab facies by even, cyclic beds less than 0.4 inches (1 cm) thick; local, faintly developed foresets; beds inversely graded from very fine- to fine sand; and subcritical, critical and supercritical angles of climb (table 3.7) (fig. 3.53).

Large-scale ripple-laminated beds are between 0.8 and 1.6 inches (2 to 4 cm) thick. These beds are distinguished from the climbing ripple strata by greater thickness and well developed concave-upward

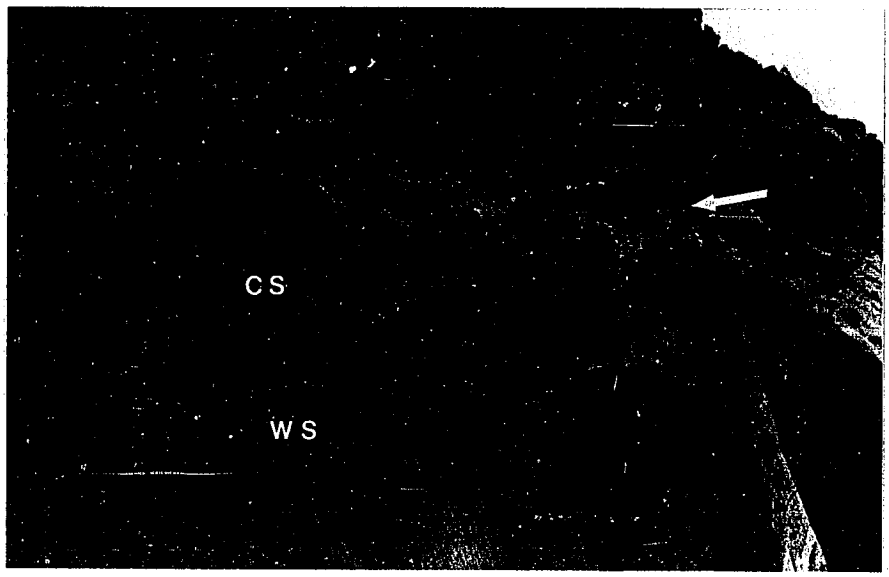

Figure 3.52. Tabular wrinkled sandstone facies (ws) interstratified with beds of the crossbedded sandstone facies (cs). Person for scale (arrow) (Dubinky Well, Z-19)

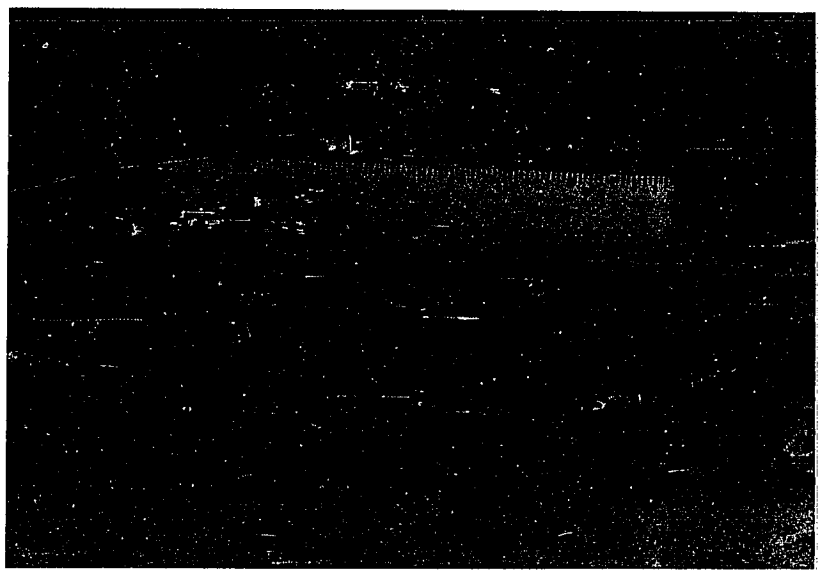

Figure 3. 53. Climbing translatent strata recognized by cyclically banded thick laminations less than 0.4 in (1 cm) thick, poorly developed foreset laminations, and inverse grading. Scale is 6 in (15 cm) long (Tenmile Canyon North, Z-20)

Table 3.7. Sedimentary features of the wrinkled sandstone facies, Moab Tongue of the En

Sedimentary Features	Interpretation
1. Texture: very fine to fine (125-250 μ) sandstone	
2. Occurrence as widespread lenticular units associated with first-order (E-1) bounding surfaces and interbedded with crossbedded sandstone facies	Sandy interdune deposits associated with first-order bounding surfaces; translatin down-wind with dune-draa system
3. Climbing ripple strata: -even, cyclic beds less than 0.4 (1 cm) thick -faintly developed foresets -subcritical climbing nature -inversely graded beds from very fine to fine (125-177 μ) sandstone	Climbing translatent strata (cts) deposit by wind ripples in interdune area
4. Undulating or wrinkled very thin beds of silty, fine (125-250 μ) sandstone, siltstone, and mudstone laminations	
5. Local large-scale cross-laminated fine (125-250 μ) sandstone; beds 1-2 in (2-4 cm) thick; unidirectional, well-developed foresets; smooth lower bounding surfaces; subcritical angles of climb	Subaqueous ripples
6. Undulatory beds of very fine-fine (88-177 μ) sandstone lacking foresets or any other discriminating stratification	
7. Broad scours or scoops filled with climbing ripple strata less than 0.4 in (1 cm) thick or thicker, larger scale cross-laminated beds	
8. Cylindrical concretions with central tube-like canal; vertical to slightly oblique; 0.8-1.6 in (2-4 cm) long; 0.4 in (1 cm) in diameter	Root casts or rhizoliths (rhizoconcretion of sparse plants growing in a wet or damp interdune area
9. Local interfingering with sandflow toesets of overlying beds in crossbedded sandstone facies	

andstone facies, Moab Tongue of the Entrada Sandstone

erpretation	References
dy interdune deposits associated with st-order bounding surfaces; translating n-wind with dune-draa system	McKee and Moiola (1975), Kocurek (1981b), Blakey and Middleton (1983), Middleton and Blakey (1983)
mbing translatent strata (cts) deposited vind ripples in interdune area	Hunter (1977a, b; 1981)
aqueous ripples	
casts or rhizoliths (rhizoconcretions) parse plants growing in a wet or damp rdune area	Sarjeant (1975), Loope (1985b)
	Blakey and Middleton (1983)

foresets and tangential toesets. These crosslaminated sets generally show unidirectional foresets, smooth lower bounding surfaces, and subcritical to critical angles of climb. Large-scale ripple beds and climbing ripple strata also occur together as composite beds filling in broad discordant scours or scoops (fig. 3.54).

Most of the sandstone beds in this facies display wavy or undulatory geometries and are clearly stratified with climbing ripple strata or large-scale crosslaminations. Other undulatory beds are merely deformed or wrinkled very thin sandstone beds or siltstone and mudstone laminations. There are locally occurring beds which lack any identifiable internal stratification.

Biogenic features associated with this facies are locally preserved vertical to slightly oblique sandstone cylinders or tubes that are 0.8 to 1.6 inches (2 to 4 cm) long and 0.4 inches (1 cm) in diameter. A central canal about 2 mm in diameter runs the length of the tube. These features are identified as root casts or rhizoconcretions (fig. 3.55).

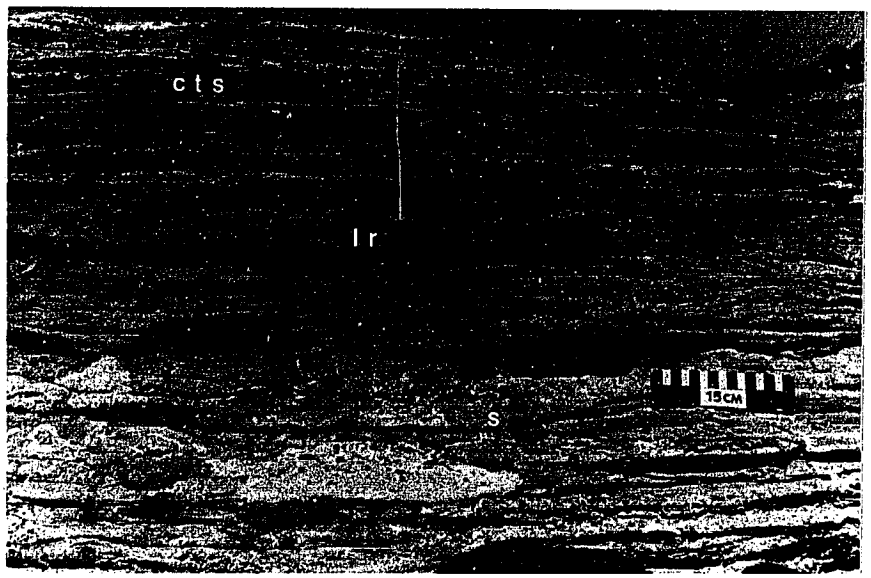

Figure 3.54. Wrinkled sandstone facies characterized by large-scale ripple beds (lr) filling in local scours (s), and climbing translatent strata (cts) (Bartlett Flat, Z-22)

Figure 3.55. Root casts in the wrinkled sandstone facies (Dubinky Well, Z-19)

Wavy Sandstone Facies

A wavy sandstone facies occurs in intervals 2 to 8 feet (0.60 to 2.4 m) thick. It is typified by cliff-forming, evenly bedded light tan or light whitish-gray, very fine- to fine grained sandstone restricted only to the lower- and uppermost levels in the Moab. Because of this stratigraphic position, it appears as a facies transitional between the lower redbed facies in the Curtis below and the crossbedded sandstone facies in the Moab above. It is developed again at the top of the Moab as a transitional sequence between the crossbedded sandstone facies below and the upper redbed facies in the Curtis above. The actual stratigraphic position in space where the Moab Tongue thins down to a few feet and is ultimately replaced by the Curtis redbed facies had been removed by erosion in a small canyon between Tenmile Canyon South (Z-21) and Duma Point (Z-7). At this location, the Moab Tongue would probably consist entirely of the wavy-laminated sandstone facies which would then form a facies laterally transitional between the crossbedded sandstone facies to the east and the Curtis redbed facies to the west.

This is the only facies of the Moab in which microsequences can be recognized. Two microsequences are identified. An upward-coarsening, upward-thickening microsequence is typical of the facies in the lower Moab and an upward-fining, upward-thinning microsequence is typical of the facies in the upper Moab (table 3.8).

Upward-coarsening, upward-thickening microsequence. The upward-coarsening, upward-thickening microsequence contains three beds which are characterized by distinct bedding features and occur in a regular vertical succession (table 3.8). Basal beds of the microsequence form ledges extending over recessed beds in the underlying Curtis redbed

Table 3.8. Sedimentary features of the wavy sandstone facies, Moab Tongue of the Entrad

Sedimentary Features	Interpretation
1. Texture: very fine-fine (62-250 μ) sandstone Conspicuous yellow limonite-cemented interval near contact with upper redbed facies of Curtis	
2. Occurrence: extreme lower and upper intervals of the Moab Tongue	
3. Microsequences a. Upward-coarsening, upward-thickening (lower Moab Tongue)	Upward-drying, wind-swept conditions on interdune-coastal plain (sabkha-tidal fl complex
3. simple wedge- and trough-crossbeds; 1-1.5 ft (30-45 cm) thick; fine (125-250 μ) sandstone; second-order (E-2) and local third-order (E-3) bounding surfaces; foresets composed of intercalated sandflow and grainfall strata with local wind ripple strata, locally deformed toesets	Incipient dunes migrating across moist interdune or supratidal coastal sabkha in overall upward-drying sequence
2. Cross-laminated fine (177-250 μ) sandstone; partial to complete ripple foreset laminations; subcritical, critical, supercritical angles of climb; locally developed convex-upward, crinkled foreset laminations	Climbing translatent strata generated by migrating wind ripples; locally developed adhesion wind ripples by wind blowing across moist sand
1. Wavy beds of alternating very fine-fine (62-250 μ) sandstone and siltstone; beds 0.2-0.6 in (o.5-1.5 cm) thick; basal load structures	

one facies, Moab Tongue of the Entrada Sandstone

rpretation	References
ard-drying, wind-swept conditions on erdune-coastal plain (sabkha-tidal flat) plex	
ipient dunes migrating across moist erdune or supratidal coastal sabkha overall upward-drying sequence	
mbing translatent strata generated migrating wind ripples; locally eloped adhesion wind ripples by l blowing across moist sand	Hunter (1977a, b; 1980, 1981), Kocurek and Fielder (1982)

Table 3.8. Continued

Sedimentary Features	Interpretation
3. Microsequences (cont.)	
b. Upward-fining, upward-thinning (upper Moab Tongue)	Upward-wetting conditions; storm- and wind-enhanced flooding of wind-tidal flat; marine reworking of decaying coastal erg margin
4. wavy siltstone-mudstone beds; plane- or cryptic-laminated	
3. wavy fine-medium (177-359 μ) sandstone; plane- or cryptic-laminated	
2. cross-laminated fine-medium (177-350 μ) sandstone; critically climbing ripple foresets	
1. small-scale trough crossbedded fine-medium (177-350 μ) sandstone; 4-12 in (10-30 cm) thick; local granule-size mudstone clasts along foresets; basal load structures	
or	
irregular sequences of units 1-2, 2-3, 2-4, or 3-4	

erpretation	References
ard-wetting conditions; storm- and d-enhanced flooding of wind-tidal :; marine reworking of decaying stal erg margin	

facies. Bed 1 consists of 0.2 to 0.6 inch (0.5 to 1.5 cm) silty fine-grained sandstone beds regularly interbedded with siltstone laminations. The wavy or undulatory nature of these strata is imparted by basal load structures which uniformly distort over- and underlying beds (fig. 3.56). The beds maintain their geometry and coarsen-upward to fine-grained sandstones which contain features that resemble adhesion ripples (fig. 3.57) because they exhibit foreset laminations which are sharply convex-upward and a ripple spacing of less than 0.8 inches (2 cm) (Ralph Hunter, USGS, Menlo Park, California, written comm., May, 1984).

Bed 2 is usually constructed entirely of climbing translatent strata (cts) in fine-grained sand. The cts is characterized by evenly-spaced beds less than 0.4 inches (1 cm), locally developed complete to partial ripple-foreset laminations, and subcritical, critical, and supercritical angles of climb (table 3.8).

Bed 3 is composed of simple and compound crossbedded sets of fine-grained sandstone in beds 1 to 1.5 feet (30 to 45 cm) thick. Toesets are locally deformed.

Upward-fining, upward-thinning microsequence. An upward-fining, upward-thinning microsequence ideally contains four beds in regular vertical succession. However, the microsequence is more commonly preserved as combinations of beds 1 and 2, 2 and 3, 3 and 4, or 2 and 4.

Basal bed 1 contains fine- to medium-grained sandstone in trough crossbedded sets 4 to 12 inches (10 to 30 cm) thick with well-developed foresets and local granule-sized mudstone intraclasts along foresets. Basal load structures are common. Foresets are composed of mostly

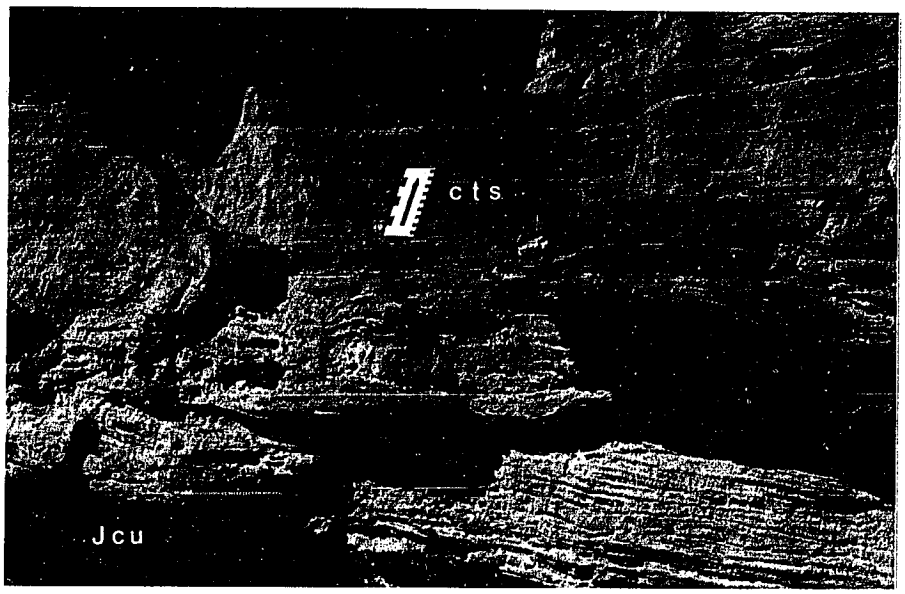

Figure 3.56. Wavy bedded units consisting of mostly of climbing translatent strata (cts) deformaed by loading down into striped beds of redbed facies of the Curtis Formation (Jcu). Scale is in inches and centimeters (Mill Canyon, Z-25)

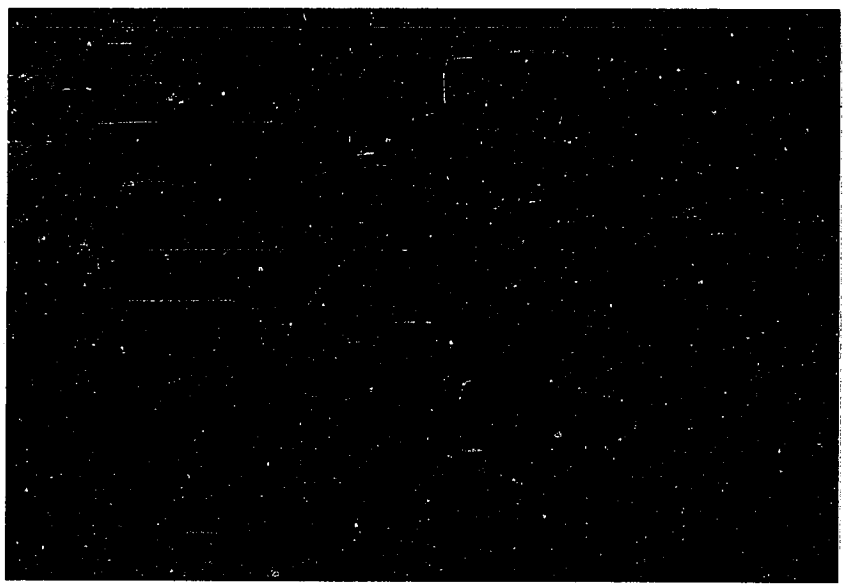

Figure 3.57. Finger is pointing to thin interval of ripple-forms which resemble climbing adhesion ripples because of short ripple-spacing and convex-upward foreset laminations in wavy sandstone facies of the Moab Tongue (Mill Canyon, Z-25)

sandflow strata. Nine measurements of foreset azimuth indicate paleocurrents flowing between N 5 E and N 70 E.

Bed 2 is a fine- to medium grained sandstone in which individual beds are completely crosslaminated in sets 2 inches (5 cm) thick and climb at critical angles. Complete ripple foresets are very well preserved with local mudstone partings or flasers between foresets (fig. 3.58).

Unit 3 consists of thin, wavy beds of plane- or cryptic-bedded fine- to medium-grained sandstone and siltstone; unit 4 is a mudstone of similar structure. These uppermost bench-forming units mark the top of the facies and the Moab Tongue itself and are in contact with the base of the upper redbed facies of the Curtis. They are locally stained whitish-yellow from a probable limonite or similar iron-oxide cement. There is also a localized accumulation of asphalt or "dead oil" in the same stratigraphic interval at Dubinky Well (Z-19).

The microsequence developed in the Bed at Black Steer Knoll is very similar to the upward-fining, upward-thinning microsequence in the wavy-laminated sandstone facies, and the two, therefore, may be genetically related. Moreover, the Bed may indeed be the northwestern-most remnant of the Moab Tongue.

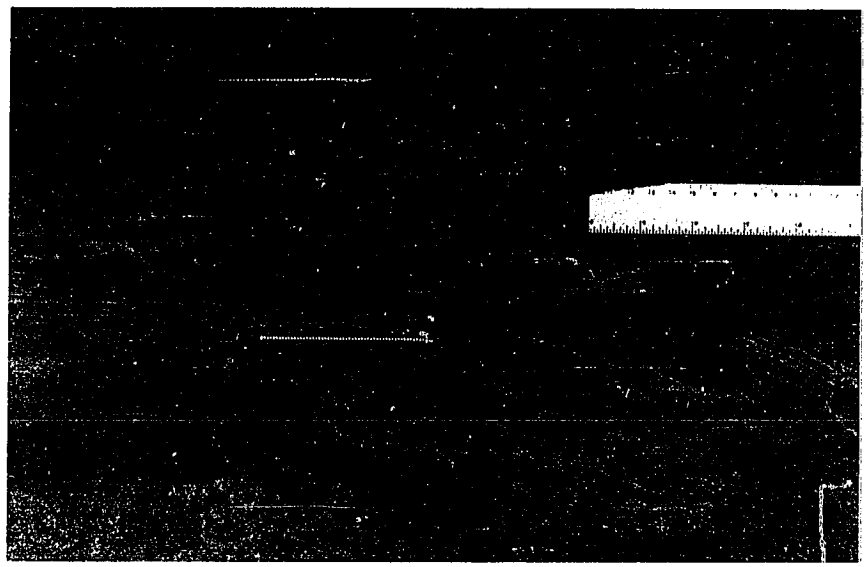

Figure 3.58. Nearly complete climbing ripple-form laminations in wavy sandstone facies in upper part of Moab Tongue. Scale is 6 in (15 cm) long (Bartlett Flat, Z-22)

Interpretation of the Moab Tongue of the Entrada Sandstone

General Interpretation

Sedimentation in the Moab Tongue of the Entrada Sandstone was contemporaneous with middle and upper parts of the Curtis Formation, namely the composite sandstone and ripple silty facies. Collective sedimentary features of Moab facies (tables 3.6, 3.7, 3.8) and lateral relationships with facies of marine origin in the Curtis to the west suggest a terrestrial eolian origin for the Moab. Specific stratification features are interpreted in the light of detailed observations made within the last ten years on bedforms and structures produced by wind: ripples and slipface deposits (Hunter, 1977a, b; 1980; 1981; Kocurek and Dott, 1981; Kocurek and Fielder, 1982), dunes (McKee and Bigarella, 1979b; McKee, 1979, 1982), interdunes (Ahlbrandt and Fryberger, 1981; Kocurek, 1981b); bounding surfaces (Brookfield, 1977; Kocurek, 1981b) and comparative subaqueous slipface deposits (Hunter, 1985b; Hunter and Kocurek, 1986).

Crossbedded Sandstone Facies

The scale and variety of crossbed sets, the occurrence of diagnostic small-scale bedding features (table 3.6), the close association with beds of distinct eolian interdune origin (wrinkled sandstone facies) suggest deposition by eolian processes in a small coastal sand sea (erg). Accumulation of the crossbedded sandstone facies coincides with a temporary regression and westward extension of the shoreline and dune

field. The change in sea level and westward shift of the shoreline may have been related to changes in global sea level eustatic) or changes in basin subsidence rate (tectonic).

First-order bounding surfaces (E-1) are well demarcated by flat-bedded interdune sandstones of the wrinkled sandstone facies. These are primary erosional or bedding surfaces (Brookfield, 1977; Allen, 1980) which represent truncation surfaces over which giant dunes called draas (Wilson, 1972a, b; 1973)) or compound dunes (McKee, 1979) migrated. In the hierarchy of eolian bedforms, the draa is the largest bedform composed of simple dunes, such as barchan or transverse dunes, as superimposed bedforms. Within a draa, second-order (E-2) discontinuity or erosion surfaces (Brookfield, 1977; Allen, 1980) are developed and reflect the migration of simple dunes. In simple dunes, third-order (E-3) (Brookfield, 1977) discontinuities reflect a periodic halt in the migration of the dune and may show reworking by wind ripples on temporarily immobile dune leesides (pers. obs., October, 1982, coastal dunes, Dillon Beach, Calif.) The mechanism is similar to that for reactivation surfaces on subaqueous bedforms (Collinson, 1970; Allen, 1980) which reflect the successive halt and resumption of active dune slipfaces. Hence, third-order (E-3) surfaces are truncated by and enclosed within second-order (E-2) surfaces which are truncated by and enclosed within first-order (E-1) surfaces.

The distribution of bounding surfaces in an eolian sand sea is controlled by the distribution of parent bedforms. Simple dunes, like transverse dunes usually form in the upwind portions of dune fields, usually along sand sea margins and often nearest the sand source (McKee, 1966, 1979). Barchan dunes are also simple dunes and are

characteristic of erg margins where sand cover is thin and sand availability is minimal. Good examples of this are barchan dunes forming in the Salton Sea basin, southern California, and in dry washes covered with alluvium in the Green River Desert, Utah (pers. obs.). Crossbeds of erg margin deposits should contain one or two orders of bounding surfaces (Kocurek, 1981a). Erg interiors are usually characterized by thick sand accumulation and draas, such as longitudinal and crescentic dunes (Wilson, 1972a; McKee, 1979) and crossbeds thereof should display 2 or more orders of bounding surfaces.

In the Moab Tongue, there are at least three intervals of draa-like dune-crossbedding preserved between the wrinkled and wavy sandstone facies (fig.2.5). The wrinkled sandstone facies is interpreted as an interval associated with first-order bounding surfaces. The crossbedded sandstone facies is bounded at the very base and top by the wavy sandstone facies deposited by processes similar to those in interdunes but actually represent constructive and destructive phases of the Moab erg. The uppermost interval is associated with first-order (E-1) surface because of truncation of underlying crossbeds and second-order (E-2) surfaces. However, where the facies directly overlies the lower redbed facies of the Curtis, the contact is abrupt and without clear evidence of truncation of underlying beds. Oakes (1983) and Kocurek and Oakes (1985) described the contact between the Moab Tongue and Slick Rock Member as a superbounding surface, which is a truncation surface generated by the migration of a whole erg. At Dubinky Well (Z-19) and Bartlett Flat (Z-22), where the Moab is thickest in the study area, crossbed cosets consist of amalgamated simple sets up to 16 feet (4.8 m) thick. Bounding surface relationships suggest deposition by draa-size dunes with large superimposed simple

dunes. Deposition of this facies may be analogous to deposition of the central erg facies recognized by Porter (1986, 1987).

Second-order bounding surfaces in the crossbedded sandstone facies are contained within intervals enclosed by first-order surfaces. This relation suggests simple dunes as components of draas bounded by interdune deposits in a central erg area. A similar interpretation was given for bounding surfaces and crossbed sets near the center of the distribution of the Slick Rock Member of the Entrada Sandstone (Kocurek, 1981a). Not only do the second-order surfaces bound simple crossbed sets but also display complex truncations of either third-order surfaces or other second-order surfaces. This bounding surface relationship suggests intersecting dunes migrating oblique or perpendicular to each other. Simple crossbeds in the facies are thinner relative to complex cosets, bounded by second-order surfaces, are locally interupted by third-order surfaces, and are considered deposits of simple dunes associated with the erg margins (Kocurek, 1981a). Simple crossbed sets are developed in the thinnest interval of Moab measured at Tenmile Canyon South (Z-21) and in the lowermost crossbed sets of the facies.

Fluid flow charactistics and grain and bedform behavior are very similar among wind and water bedforms, especially among ripples and large transverse bedforms as shown in laboratory studies by Jopling (1963, 1965b), Hunter (1985b), and Hunter and Kocurek (1986). Both wind and water tend to create similar sandflow and grainfall strata, similar angles-of-repose of foreset beds and a similar occurrence of ripples formed by leeside eddies and traction sedimentation near the bed in sandy megaripples (Allen, 1970; Hunter, 1985b; Hunter and Kocurek

1986). Both wind and water produce the same hierarchical system of bedforms from ripples to megaripples (dunes) and giant ripples (aqueous sandwaves or eolian draas) (Allen, 1968c; Wilson, 1972a).

Hunter (1977a,b; 1981, 1985b) has observed the details of small-scale, somewhat subtle structural and textural differences that are useful in distinguishing subaqueous cross-strata from eolian cross-strata. Climbing translatent strata (cts) are produced by wind ripples which migrate in response to grain impact during saltation and creep (Bagnold, 1954a). They are characterized by poorly developed crosslaminations in thin sets (less than 1 cm) and reverse textural grading (Bagnold, 1954a); Hunter, 1977a, b; 1981). Whereas, water ripples are higher amplitude bedforms (Collinson and Thompson, 1982) and tend to deposit thicker crosslaminated beds. Because of differences in settling velocities, effective grain densities and sorting abilities between water and wind, water ripples produce well-developed cross-laminated beds with normal textural grading (Hunter, USGS, Menlo Park, California, pers. comm., May, 1984; Kocurek and Dott, 1981). Grainflows of eolian bedforms are less continous so that sandflow strata tend to be enclosed in thin grainfall laminations. Grainflows among subaqeous bedforms are a more continuous phenomenon and produce contiguous sandflow strata interrupted locally by grainfall laminations (Buck, 1985; Hunter, 1985b, Hunter and Kocurek, 1986) Crossbed forsets in the crossbedded sandstone facies contain features such as sandflow tongues enclosed in grainfall laminations both of which may locally grade downcurrent into a toeset containing climbing translatent strata. These forset characteristics, bounding surface relationships and facies distribution support an eolian interpretation for the crossbedded sandstone facies.

Paleowinds. Paleocurrent data indicate multidirectional wind patterns with a dominant wind direction to the west (fig. 3.48). The pattern suggests fluctuating wind which may be related to seasons, storms, and regional and local topography. Onshore winds which shape parabolic dunes at Dillon Beach, California blow mainly from the northwest during summer and from the southwest during winter yet structures and bedform orientation indicate that the summer winds are dominant (Hunter, USGS, Menlo Park, California, pers. comm., October, 1982). Straight-crested dunes are transverse to and are controlled by mainly south-southwesterly winter storm winds and are oblique to and slightly modified by north-northwesterly summer winds (Hunter et al., 1983). Bigarella et al. (1969) described coastal dune crossbedding with apparent reversing dips related to slipface deposition all along the flanks of linguoid or parabolic dunes. They did describe daily and seasonal reversing wind patterns, but only the southeasterly winds were competent to transport sand. Perhaps, the polymodal paleowind pattern reflects the migration of either parabolic or oblique dunes in northerly winds. Parabolic dunes would show slipface or avalanche deposits dipping down-wind and perpendicular to the wind direction as a function of the parabolic or linguoid morphology of the dune. Alternatively, oblique dunes may have migrated in response to seasonally reversing, northerly and temporary southerly winds, to produce a polymodal paleocurrent pattern. Further, detailed study of the attitude of bounding surfaces and geometry of foresets and crossbed sets in the Moab Tongue is needed to help recognize specific dune types.

Crossbedding indicates northerly winds for the Early Jurassic Navajo Sandstone and equivalent strata (Poole, 1962; Kocurek and Dott, 1983), northeasterly winds for the Page Sandstone (Caputo, 1980, 1981), and northerly winds of the Slick Rock Member of the Entrada Sandstone (Kocurek and Dott, 1983). Poole (1962) stated that the western Colorado Plateau probably moved out of the northerly and northeasterly trade wind belt and into an easterly belt at the time of deposition of the Moab.

Wrinkled Sandstone Facies

Tabular to lenticular geometries. overall horizontal bedding, distribution within the crossbedded sandstone facies of eolian dune origin, and small-scale bedding features (table 3.7; fig. 2.5) indicate deposition of the wrinkled sandstone facies in an eolian interdune environment. A complex mixture of small-scale bedding features indicates local interdune conditions fluctuating from dry to wet. Features in this facies. which are amonn those of dry interdune areas, include climbing translatent strata (cts) scoured surfaces filled with cts; of damp interdunes include plant root structures; and of wet interdunes include wavy beds and well-developed large-scale crosslamination (Kocurek, 1981b) (table 3.7). Distinct adhesion structures were not observed. The facies forms two distinct, horizontally-bedded intervals deposited on first-order (E-1) bounding surfaces that formed by migration of interdune areas (Kocurek, 1981a; Blakey and Middleton, 1983; Middleton and Blakey, 1983). All of the sedimentary features observed in this facies have been described and interpreted as distinct features of modern (Ahlbrandt and Fryberger, 1981; Kocurek, 1981b) and ancient (Kocurek, 1981b; Blakey and Middleton, 1983; Middleton and Blakey, 1983) interdune areas.

Ripple crosslamination is clearly recognized as climbing tranlatent strata (cts) by general eveness and cyclic spacing of less than 0.4 inches (1 cm), poorly developed foresets because of good sorting, inversely graded beds, and subcritical angles of climb (Hunter, 1977a, b; 1981; Kocurek and Dott, 1981).

Lenticular sets of crosslaminated sandstones 1 to 2 inches (2 to 4 cm) thick are interpreted as water ripple deposits because of well-developed foresets and greater net bed thickness relative to wind-ripple (cts) deposits (Hunter, 1977a, b; 1981; Kocurek and Dott, 1981).

Because of the combination of sedimentary structures suggesting fluctuating dry and wet interdune conditions, there are two possible explanations for the localization and discontinuity of water ripple beds. One is to invoke occasional wetting and ponding of water during a heavy rainy season in the interdune basin. This setting has been oberved in modern coastal dune fields on Padre Island (Kocurek, 1981a), on the southeastern shore of Lake Michigan (pers. obs., May, 1984) and in the Slick Rock Member of eolian origin in the Entrada Sandstone (Kocurek, 1981a). Alternatively, low-lying interdune areas, especially in dune settings along coasts, may be periodically flooded by seawater during spring-tides, wind-enhanced spring tide, or wind- or storm-enhanced high tides (Inman et al., 1966). The lateral association with the redbed facies in the Curtis of supratidal origin may support a marine dune flooding mechanism. Storm or spring tide flooding of coastal interdunes was interpreted for normally graded and rippled sandstones in the Page Sandstone of eolian origin (Caputo, 1980, 1981).

Wavy Sandstone Facies

Sedimentary features of the upward-coarsening, upward-thickening microsequence in the wavy sandstone facies suggest upward-drying conditions, as wind processes become progressively dominant under interdune-like conditions of sedimentation. Features of the upward-fining, upward-thinning microsequence indicate upward-wetting conditions as wind processes are suppressed either by a second minor transgressive event or progradation of a wet backerg (Porter, 1986, 1987) or interdune sabkha (table 3. 8).

Interpretation of bedding units in the upward-coarsening microsequence is as follows. Irregular, undulating interbeds of very-fine to fine-grained sandstones and siltstones (unit 1) suggest a transition from wet sedimentation on a featureless sandy coastal sabkha or supratidal flat in the Curtis redbed facies to wind-swept conditions and reworking of subaqueously deposted sand into wind ripples. Mixed sandstones and siltstones suggest cyclic deposition by wind ripples, later gentle reworking and modification by distal tidal flooding, and ultimate burial by silt. The undulating beds and basal load structures of these units indicates sedimentation on a water-saturated bed and contemporaneous hydroplastic deformation by down-loading. Wind-adhesion ripple structures (Hunter, 1980; Kocurek and Fielder, 1982) suggest sand previously blowing across a moist surface, and building a small ripple-form facing upwind by ground-water capillarity and surface tension.

Rippled beds with ripple foreset to complete ripple-form crosslaminations in fine sandstone (unit 2) exhibit distinct features

of climbing translatent strata (Hunter, 1977a, b; 1981) and were deposted by wind.

Medium-scale crossbed sets of fine sand are bounded by second-order surfaces and locally third-order reactivation surfaces. These beds are distinguished from subaqueous crossbeds by tongue-shaped sandflow strata associated with thin grainfall strata, and wind-ripple strata (cts) (Hunter, 1977a, b; 1981) and are interpreted as small incipient dunes of the Moab erg. Bottomset beds and lower portions of foreset beds are contorted as a result of dune migration onto wet interdune or coastal sabkha sediments and penecontemporaneous loading and deformation. These may be the interdune dunes described and interpreted by Kocurek (1981a). This microsequence is buried by thick, simple and compound crossbed sets of the overlying crossbedded sandstone facies as wind-blown conditions and migrating sand dunes dominated the westward expanding coastal erg. Porter (1987) described a similar macrosequence consisting of basal siliciclastic sabkha deposits succeeded by eolian sand sheet and small dune deposits which were ultimately buried by a large dune/draa complex. Deposition of this microsequence may be analogous to depostion of the fore-erg facies recognized by Porter (1986, 1987).

The upward-fining, upward-thinning microsequence characterizes the wavy sandstone facies at the top of the Moab Tongue. It marks a change from eolian to subaqueous sedimentation. Large dune and draa deposits in the underlying crossbedded sandstone facies grade upward into beds deposited by large water ripples with well-developed foresets and granule-size mudstone intraclasts along foresets. Five measurements of foreset azimuths indicate approximate paleoflow to the northeast. Deposition of this microsequence marks the onset of several changes or

events: 1. eastward shoreline and erg-margin retreat possibly related to eustatic sealevel rise, diminished supply of sand available for wind reworking, or changes in wind regime, 2. a re-establishment of periodically wet or flooded conditions in wadis or spring floods on a coastal sabkha or supratidal flat, 3. a suppressing of wind sedimentation, and 4. a change in grain size from very fine to fine wind-blown sand to fine to medium water-laid sand.

Although lenticular, channel-form beds were not observed, the basal fine- to medium-grained sandstones (unit 1) with complete ripple-form crosslaminations were deposited by unidirectional currents, possibly in a wadi system. Wadis are ephemeral streams in desert environments. They are generally characterized by channelized, gravelly, sandy, muddy deposits with crossbedding, plane-bedding, and ripple bedding; similar to aspects of braided streams (Glennie, 1970; Reineck and Singh, 1980). Small-scale vertical sequences consisting of subaqueous ripple laminations and desiccated mud interbedded with eolian plane-laminations and low-angle cross-strata have been descibed from desert wadi and flat environments in north Africa (Glennie,1970). In the absence of distinguishable wadi deposits, the strata in this microsequence were most likely the result of storm- or wind-enhanced supratidal flooding and reworking of a decaying coastal erg margin. Overlying units 2 through 4 record alternating wind-ripple sedimentation and settling suspension in gentle currents from spring tide flooding onto the upper reaches of a supratidal flat. Sedimentation is similar to that interpreted for the upward-coarsening, upward-thinning microsequence and indicates a return of fore-erg (Porter, 1986) conditions.

Summerville Formation

The Summerville Formation is the last rock interval studied herein between the underlying Curtis and Moab strata and the overlying J-5 unconformity at the base of the Morrison Formation (fig. 2.1). Throughout the San Rafael Swell, Green River Desert, and northern Henry Mountains areas, the Summerville crops out as a uniformly banded interval consisting of laterally continuous light tan, whitish-red, whitish-green, dark reddish-brown, and dark brown, thin beds (fig. 3.59). Terrain weathered on the Summerville typically forms banded buttes and mesas mantled by light reddish-brown weathered slopes. These slopes are continuous with the weathered slopes of the ripple-laminated silty facies at the top of the Curtis (fig. 3.19). Gravelly sandstones in the Salt Wash Member of the Morrison Formation have been usually stripped back, especially on monoclinal ridges and separated from the Summerville by the slope- and ledge-forming Tidwell Member of the Morrison (fig. 2.1). A red- and brown-stained, cliff-forming gypsum bed 5 feet (1.5 m) thick or more usually marks the base of the Tidwell Member and the J-5 unconformity at the top of the Summerville (Stratigraphy, Chapter 2; fig. 2.15). This gypsum bed acts as an erosionally resistant stratum and protects the inaccessible, vertical Summerville cliffs below.

The Summerville Formation is composed mainly of siltstone and mudstone with sandstone, gypsum, claystone and sandy sparite in decreasing abundance.

Figure 3.59. Slope- and cliff-forming exposures of the Summerville characterized by uniformly banded dark siltstones and mudstones and light siltstones and gypsum beds

A subtle overall upward-thickening, upward-fining macrosequence is developed in the Summerville. The upward-fining textural trend has a corresponding laterally-fining trend from northwest to southeast. The textural pattern is illustrated in figure 3.60 which is a contour map showing the percent distribution of net siltstone and mudstone relative to sandstone in the entire Summerville. The thickness of gypsum was not used in determining the ratio. Rocks finer than sandstone increase to nearly 100% in a southeasterly direction.

Two facies in the Summerville are identified according to presence or absence of gypsum beds. They are a reddish-brown silty facies and a gypsiferous facies. A description of facies and microsequences contained therein begins with discussions on isopach and paleocurrent trends in the following sections.

Isopach Trends

Data collected in this study were combined with thickness data from other reports to construct isopach maps of the total Summerville interval. Figure 3.61 shows the isopach distribution of the total Summerville. From maximum thicknesses of 300 feet (90 m) or more recorded in the western San Rafael Swell, the interval becomes thinner gradually and uniformly toward the east up to about the Hatt Ranch area (Z-10A). South and east of this location, in the Green River Desert, thinning is more rapid as suggested by the narrow contour spacing. East of White Wash (Z-11), Tenmile Canyon North (Z-20), and Dubinky Well (Z-19), the Summerville is absent. The general eastward thinning trend is related to normal basin-edge thinning. However, the accelerated thinning and ultimate removal in the Green River area is related to erosion along the J-5 horizon.

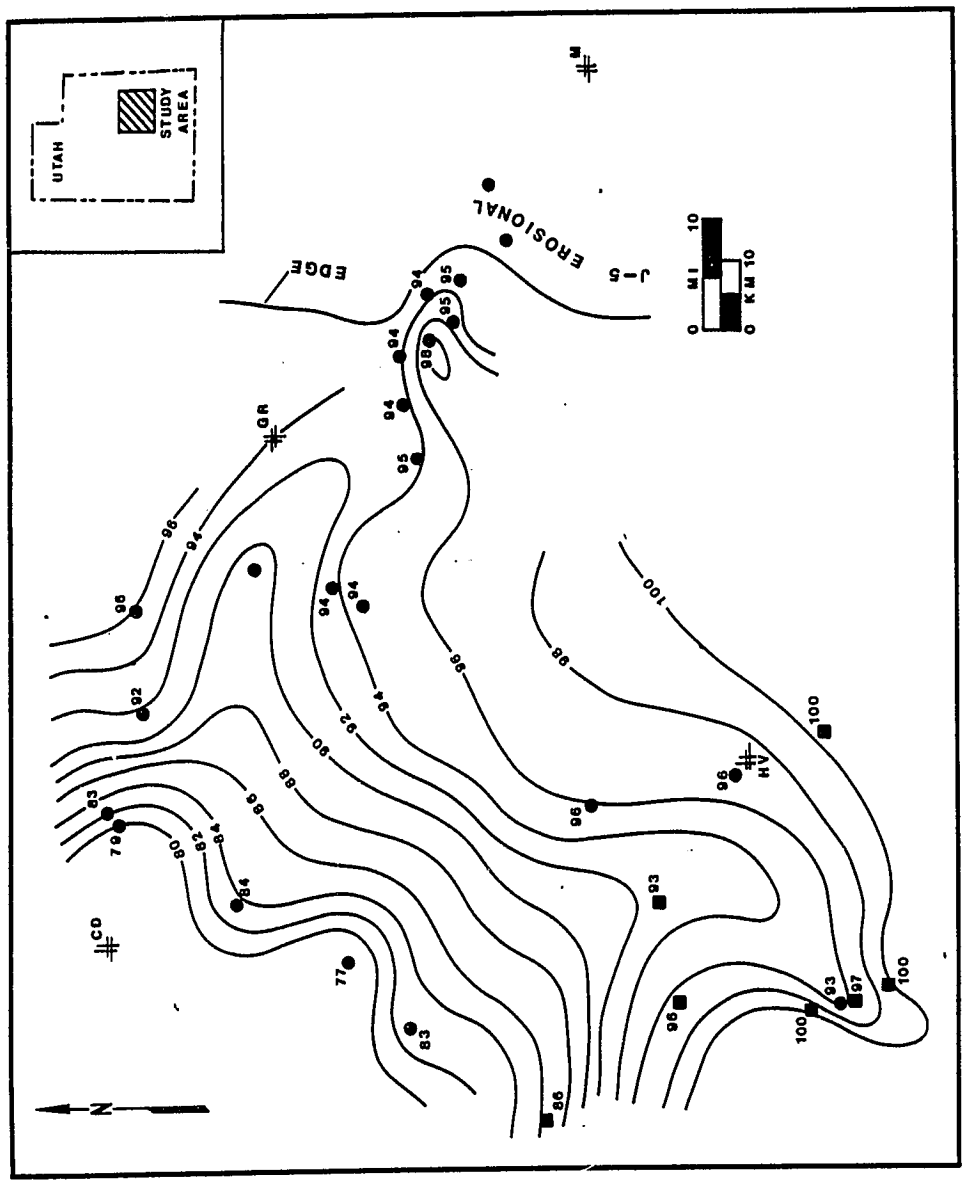

Figure 3.60. Percent net siltstone/mudstone in the Summerville Formation; based on thickness of detrital rocks and does not include gypsum. Contour interval: 2%. Map symbols (table 1.3)

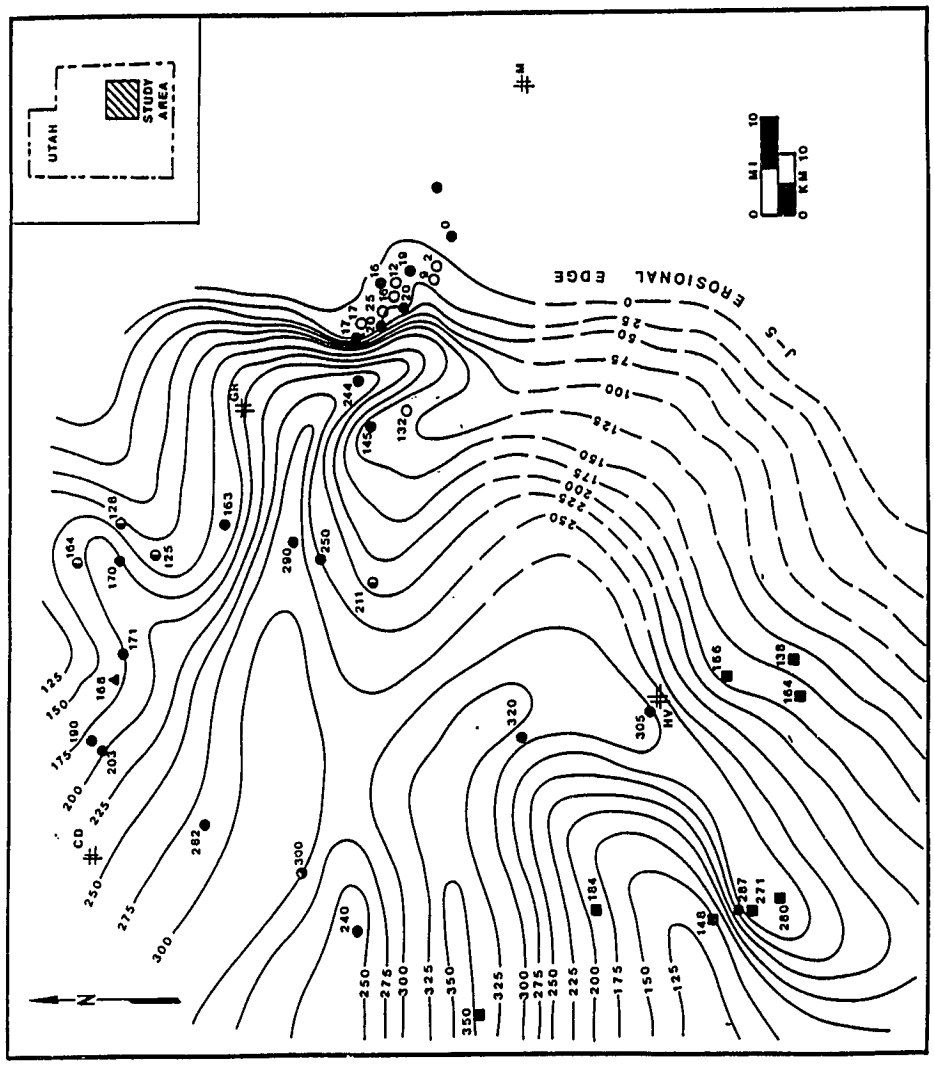

Figure 3.61. Isopach map of the Summerville Formation. Contour interval: 25 ft (7.6 m)
Map symbols (table 1.3)

Two linear thickness trends or depositional troughs are developed in the Summerville in the western San Rafael Swell area between Mussentuchit Wash (Z-24) and Buckhorn Wash (Z-18) and extend eastward into the central San Rafael Swell. The northern-most trough extends across the San Rafael Swell into the Green River Desert where data suggest an abrupt deflection toward the southeast in the vicinity of Dellenbaugh Butte (Z-8). The two depositional troughs seem to contribute to another main trough in the south-central San Rafael Swell. The axis of this prominent trough extends roughly south toward Hanksville (Z-5) where it shifts to the southwest toward Pleasant Creek (Z-4).

Paleocurrent Trends

Crossbedding is a poorly exposed and least abundant sedimentary structure in the Summerville. Crosslamination is moderately abundant and better exposed either as foreset laminations in cliff exposures or ripple marks and rib-and-furrow structures on bedding surfaces. The few directional properties of crosslamination and parting lineation that have been measured and recorded from each of the two Summerville facies are presented in figures 3.62 and 3.63. Paleocurrent patterns suggested by these few dat are interpreted with caution.

Crosslamination and parting lineation in the reddish-brown silty facies suggest dominant paleocurrents moving to the northeast (fig. 3.62). Mean paleocurrent azimuth may be biased because measurements less than ten were recorded at most locations; deceptive, high reliability indices also correspond with few measurements (table A.1, appendix). The shape of the rose diagrams for data collected at North Salt Wash (Z-16) and Lookout Point (Z-14) show indications of polymodal

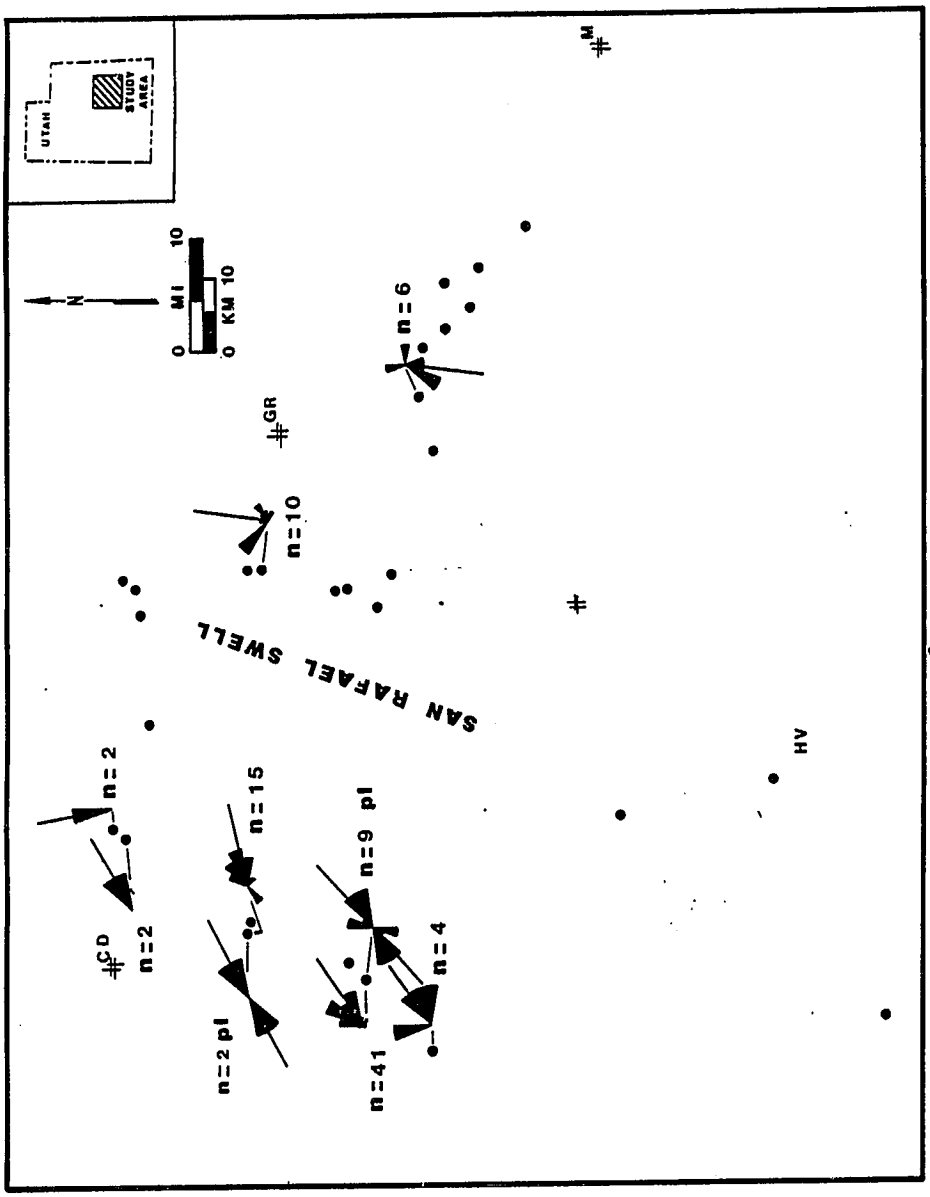

Figure 3.62. Paleocurrent trends indicated by crosslamination and parting lineation (pl) in the reddish-brown silty facies of the Summerville Formation; n = number of measurements; stick = mean paleocurrent azimuth. Map symbols (table 1.3)

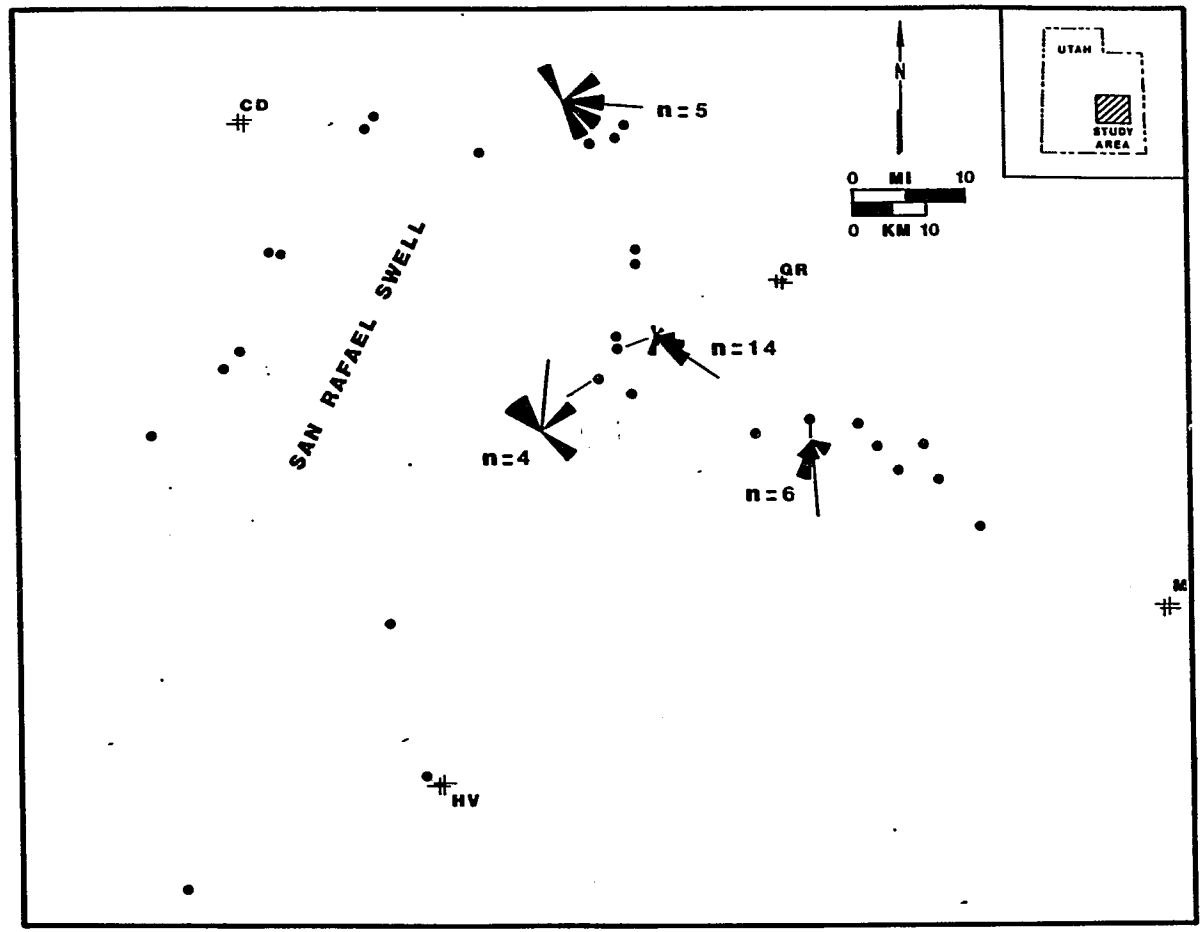

Figure 3.63. Paleocurrent trends indicated by crosslamination in the gypsiferous facies of the Summerville Formation; n = number of measurements; stick = mean paleocurrent azimuth. Map symbols (table 1.3)

trends. At these locations more than 15 measurements were taken and corresponding reliability indices are moderate with values between 66 and 79 (table A.1, appendix). The values suggest a more dispersive, less uniform paleocurrent with a persistant mean paleocurrent to the northeast. An exception is the plot for the Dellenbaugh Butte (Z-8) locality which is composed of only 6 measurements. It shows a mean paleocurrent azimuth in a south-southwest direction.

Even fewer measurements have been recorded from the gypsiferous facies. Rose diagrams of data collected from four locations are shown in figure 3.63. Mean paleocurrent azimuths and low to moderate reliability indices between 35 and 83 suggest polymodal paleocurrents.

Reddish-Brown Silty Facies

A reddish-brown silty facies volumetrically composes most of the Summerville. The absence of gypsum and the more ordered bedding arrangement of microsequences distinguish this facies from the gypsiferous facies. The facies is present in every exposure of Summerville; it comprises the entire Summerville section only in the Western San Rafael Swell area and the Green River Desert, east of Dellenbaugh Butte (Z-8). In the Green River Desert, it is presumed that most of the gypsiferous facies had been removed by erosion along the J-5 unconformity.

Exposures of the facies display alternating parallel light- and dark-colored beds consisting of thicker reddish-brown and dark brown mudstone and siltstone interbedded with thinner, light tan and whitish-green sandstone and siltstone characteristic of the Summerville. Two microsequences are distinguished by geometry and vertical textural and stratification changes. The microsequences are: 1. upward-fining,

upward-thinning, and 2. lenticular microsequenccs (table 3.9). All microsequences are irregularly interbedded in the Summerville of the western San Rafael Swell. However, in the eastern San Rafael Swell, the occurrence of lenticular microsequences diminishes and is wholly replaced by a variable combination of beds in the upward-thinning microsequence.

Upward-fining, upward-thinning microsequence. A complex upward-fining, upward-thinning microsequence is so named for the bedding sequences best developed in the western San Rafael Swell area. It comprises most of the reddish-brown silty facies and records a distinct vertical textural and lithologic change from sandstone to mudstone. A complete bedding sequence is herein described. However, most intervals are expressed by incomplete or partial microsequences consisting of mainly sandtone and mudstone or siltstone. These microsequences grade vertically and laterally into lenticular microsequences.

A complete microsequence begins with a basal unit a. This bed is commonly a fine- to very fine-grained silty sandstone, 0.4 to 12 inches (1 to 30 cm) thick, is crosslaminated by lunate and linguoid ripples. Beds are locally lenticular and show channel-form geometries. Crosslaminated sets display critical and supercritical angles of climb with corresponding complete ripple foresets and complete ripple-form laminations (fig. 3.64). Foresets may be planar or tangential. Local stratification features include plane laminations, oblique and horizontal burrows including Thalassinoides, and basal load and ball structures which deform underlying mudstones and produce overlying wavy laminations (table 3.9).

Table 3.9. Sedimentary features of the reddish-brown silty facies of the Summerville F

Sedimentary Features	Interpretation
Ripple Marks:	
1. asymmetrical: straight-crested; local bifurcating crests; planar foresets	Unidirectional wave orbital currents or non-wave currents; unrestricted flow; no ripple index data
2. sinuous-crested, in-phase crests; local run-off tongues; rounded-flattened crests	Non-wave currents; emergence and drainage of tidal flat
3. sinuous-crested, out-of-phase to linguoid	
4. lunate: rib and furrow structures	
Assorted features:	
1. parting lineation	
2. shrinkage cracks and crack casts	
Microsequences	
1. Upward-fining, upward-thinning (tabular and locally lenticular geometry)	Non-channelized and local channelized flow on upper intertidal flat and coastal sabkha; deposition along tidal channel margins and on interchannel areas; upward decrease in flow velocity and sand transport; vertically accret spring-neap tide bundles;
d. cryptic-bedded mudstone or claystone	
c. alternating cryptic-bedded mudstone and lenticular, cross-laminated very fine sandstone or siltstone; local shrinkage cracks	Exposure and desiccation
b. wavy-bedded cross-laminated very fine (62-88 μ) sandstone with siltstone or mudstone	
a. cross-laminated very fine to fine (62-135 μ) silty sandstone beds 0.4-12 in (1-30 cm) thick; complete ripple foreset laminations; flasers; lunate-linguoid ripple marks; local plane laminations; basal ball and load structures and associated deformed laminations	Contemporaneous sedimentation and hydroplastic loading on wet sediments
Or irregular combinations of units ac, bc, or d only	

wn silty facies of the Summerville Formation

ation	References
ional wave orbital currents or currents; unrestricted flow; index data currents; emergence and drainage of t	Reineck and Singh (1980) Harms et al. (1982)
elized and local channelized flow on ertidal flat and coastal sabkha; n along tidal channel margins and on nel areas; upward decrease in flow and sand transport; vertically accreted ap tide bundles;	Hantzschel (1939), Reineck (1967), Thompson (1968, 1975), Reineck and Wunderlich (1968b), Hereford (1977), Howard and Frey (1980), Reineck and Singh (1980)
and desiccation	
aneous sedimentation and tic loading on wet sediments	

Table 3.9. Continued

Sedimentary Features	Interpretation
Microsequences (cont.)	
Trace fossils: -local horizontal and oblique burrows -local large burrows with smooth walls nearly cylindrical, y-shaped branches	Thalassinoides: dwelling/feeding structure arthropods; Cruziana ichnofacies; harsh env mental conditions and scarcity of organisms
2. Lenticular microsequences d. alternating cryptic bedded mudstone and siltstone c. straight- and sinuous-crested ripple laminated silty, very fine (62-88 μ) sandstone; local run-off tongues, ladder ripples, flattened crests, interference ripples b. lunate ripple laminated very fine (62-88 μ) sandstone; local shrinkage cracks; local load structures a. medium-scale trough crossbedded fine (125-250 μ) sandstone; local granule-size clasts along foresets; local basal load structures	Upward decrease in sand availability and in transport and current velocity; megaripples migrating in shallow channels buried by cha margin and bank deposits
c. alternating mudstone and siltstone b. accretionary mudstone a. accretionary or longitudinal cross-bedded very fine to fine (88-177 μ) sandstone; mudstone laminations along accretionary bounding surfaces; mudstone granules; flaser-, wavy-, lenticular-bedded cross-laminated intrasets; extends across broad scours several meters wide	Meandering tidal creeks and fill by channel bank/margin deposits; laterally migrating creek channels with point bars

tation	References
noides: dwelling/feeding structure of ds; Cruziana ichnofacies; harsh environ- conditions and scarcity of organisms	Illing et al. (1965), Matter (1967), Thompson (1968), Heckel (1972), Frey and Pemberton (1984), Howard and Frey (1984)
ecrease in sand availability and in t and current velocity; megaripples g in shallow channels buried by channel nd bank deposits	van Straaten (1961), Reineck (1967), Reineck and Wunderlich (1969), Kellerhals and Murray (1969), Howard and Frey (1980), Reineck and Singh (1980)
ng tidal creeks and fill by channel- gin deposits; laterally migrating annels with point bars	Hantzschel (1939), van Straaten (1961), Reineck (1967), Kellerhals and Murray (1969), Reineck and Wunderlich (1969), Hereford (1977)

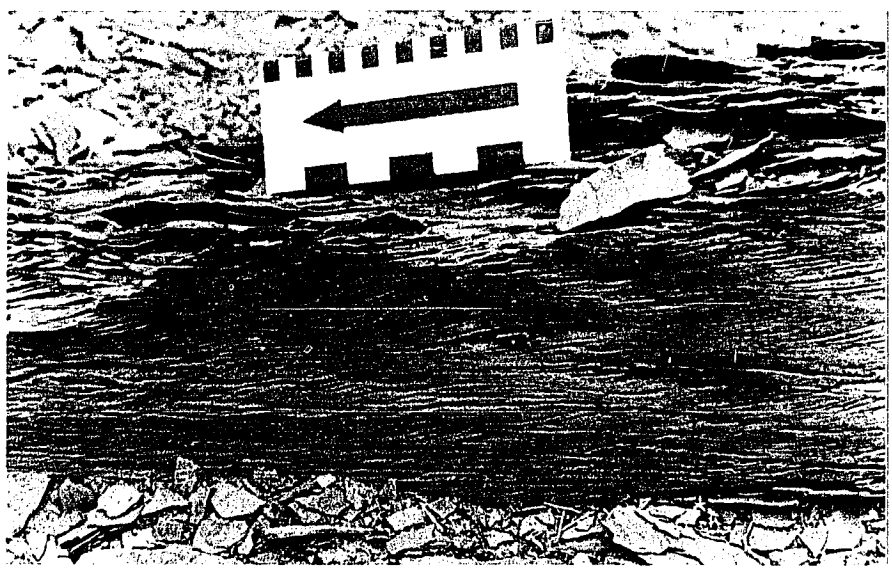

Figure 3.64. Climbing, complete ripple-form laminations in sandstone beds of upward-fining, upward-thinning and lenticular microsequences in the reddish-brown silty facies. Scale is in inches and centimeters (San Rafael Swell West, Z-6)

An overlying unit b may appear as a wavy-bedded, crosslaminated very fine-grained sandstone, siltstone or mudstone. Unit C consists of cryptic bedded mudstone alternating regularly with lenticular or tabular beds of very fine-grained sandstone or siltstone with local shrinkage cracks. Uppermost unit d is a cryptic bedded, dark brown mudstone.

Lenticular microsequences. Lenticular microsequences are interbedded with and locally truncate upward-fining, upward-thinning microsequences, show channel-form geometries, and show upward-fining textural and lithologic changes. Typical sequences are 1 to 5 feet (0.30 to 1.5 m) thick, approximatedly 7 to 25 feet (2.1 to 7.5 m) in width; length is not determinable.

A typical microsequence is usually lenticular, or channel-form in shape (fig. 3.67). Basal unit a is a medium-scale trough-crossbedded very fine- fine-grained sandstone that includes mudstone intraclasts along foresets and down-loading structures. This bed grades vertically and laterally into unit b, which is lunate or linguoid crosslaminated very fine-grained sandstone. The top of the microsequence is marked by unit c, an interbedded cryptic-bedded mudstone and siltstone (table 3.9).

A thinner version of the microsequence is 1 to 2 feet (0.30 to 0.60 m) thick and is characterized by basal very fine-grained sandstone that is crosslaminated by lunate ripples; rib-and-furrow structures are visible on bedding surfaces. Ripple-marked surfaces may be thinly covered with mudstone laminations broken by shrinkage cracks. Bed soles may have load structures which deform underlying scoured and truncated

mudstone beds. The lunate ripple beds are typically overlain by crosslaminated, silty very fine-grained sandstones produced by straight- and sinuous-crested ripples. Migration directions between successive ripple beds show divergent paleocurrents (fig. 3.65). Run-off tongues, ladder ripples, flattened and rounded ripple crests, and interfering ripples are common (table 3.9)(fig. 3.66). Uncommonly small ripples with mean length of 0.9 cm and height of 1 mm are very locally preserved.

Another variation of the microsequence forms a local simple, upward-fining sequence in lenticular or channel-form stratified bodies. Strata fill in convex-downward erosional depressions along which truncation of underlying beds is clearly visible. Scour-fill has been lateral or accretionary and resembles epsilon crossbedding (Allen, 1963b). The accretionary beds are very fine- to fine-grained sandstones consisting of flaser-, wavy-, and lenticular-bedded crosslaminated intrasets separated by mudstone bounding surfaces or pause planes. The completion of accretionary and scour-fill events is marked by dark brown mudstone and interbedded mudstone and siltstone (table 3.9) (fig. 3.67).

Gypsiferous Facies

A reddish-brown gypsiferous facies is developed in the upper one-half to two thirds of the Summerville in the eastern San Rafael Swell and northern Henry Mountains area. It is laterally confined by beds of the reddish-brown silty facies. In the Green River Desert, southeast of Dellenbaugh Butte (Z-8), it is presumeably removed, partially or completely by the J-5 erosion surface. The facies is characterized by generally upward-fining, upward-thinning microsequences similar to

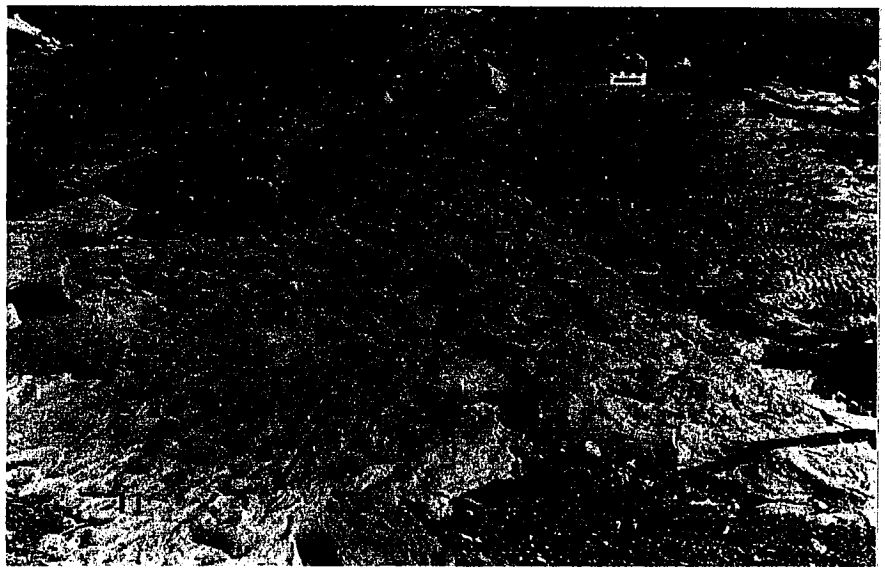

Figure 3.65. Ripple beds a few centimeters vertically apart show different ripple types and divergent migration directions; linguoid (li) and lunate (lu) ripples migrated away from viewer (arrow) and sinuous, long-crested (sl) ripples migrated to right (arrow on scale) in reddish-brown silty facies. Scale is in inches and centimeters (Lookout Point, Z-14)

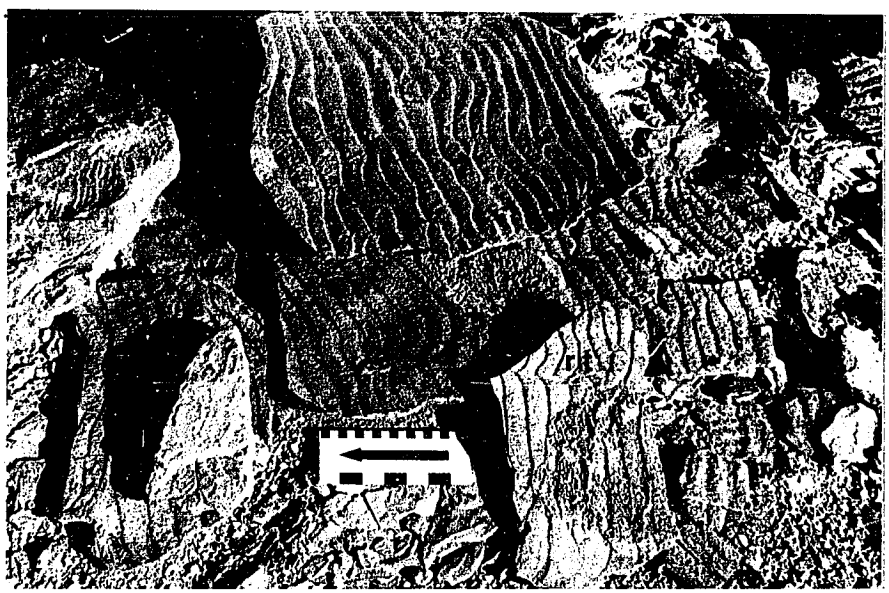

Figure 3.66. Long, sinuous-crested ripples with flattened and rounded crests, run-off tongues (rt) and ladder ripples developed on ripple stoss-sides. Scale is in inches and centimeters (Lookout Point, Z-14)

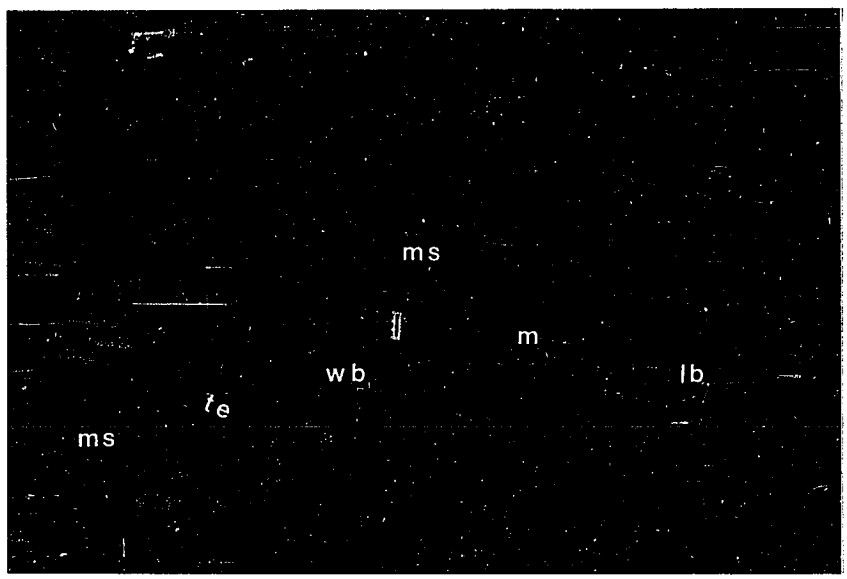

Figure 3.67. Truncation and erosional (te) scour filled in with tan, wavy-bedded, crosslaminated sandstone (wb), lenticular-bedded sandstone (lb), and mudstone (m) enclosed within interbedded brown mudstone, siltstone and thin beds of tan sandstone (ms). (Lookout Point, Z-14). Scale is in inches and centimeters.

those in the reddish-brown silty facies and the redbed facies in the Curtis. The separate distribution of cumulative gypsum in the Summerville is shown in figure 3.68 and delimits the extent of the gypsiferous facies. The facies is roughly confined to a northeast trending belt, the maximum thickness of which coincides with the maximum thickness of the Summerville Formation (cf. figs. 3.60 and 3.68).

Chaotic microsequence. Chaotic microsequences compose the entire gypsiferous facies with regularly occurring beds 1.5 to 3 feet (0.45 to 0.90 m) thick. Beds locally show distinct upward-fining, upward-thinning changes in vertical succession.

A complete microsequence is described in table 3.10. In such a microsequence, the base is typically marked by unit a, which is a tan, crosslaminated very fine sandstone or siltstone in lenticular beds 0.5 to 3 inches (1 to 3.75 cm) thick (fig. 3.69). Intrasets are constructed of complete lunate- and linguoid-ripple foresets or ripple-form laminae with local mudstone flasers. Ripple foresets may be either planar or tangential. Deformation of lowermost intraset and underlying mudstone is related to load structures. Plane laminations are commonly interbedded.

Unit b consists of light-tan, wavy or tabular beds of crosslaminated very fine sandstone or siltstone interbedded among brown cryptic-bedded mudstone. Unit b grades upward into unit c as mudstone increases in thickness; sandstone and siltstone beds are present as plane- or cross-laminated thin beds or lenses 0.4 to 1.5 inches (1 to 3.75 cm) thick (fig. 3.70). Units b and c locally form tabular units in which stratification resembles low-angle planar crossbedding and may be

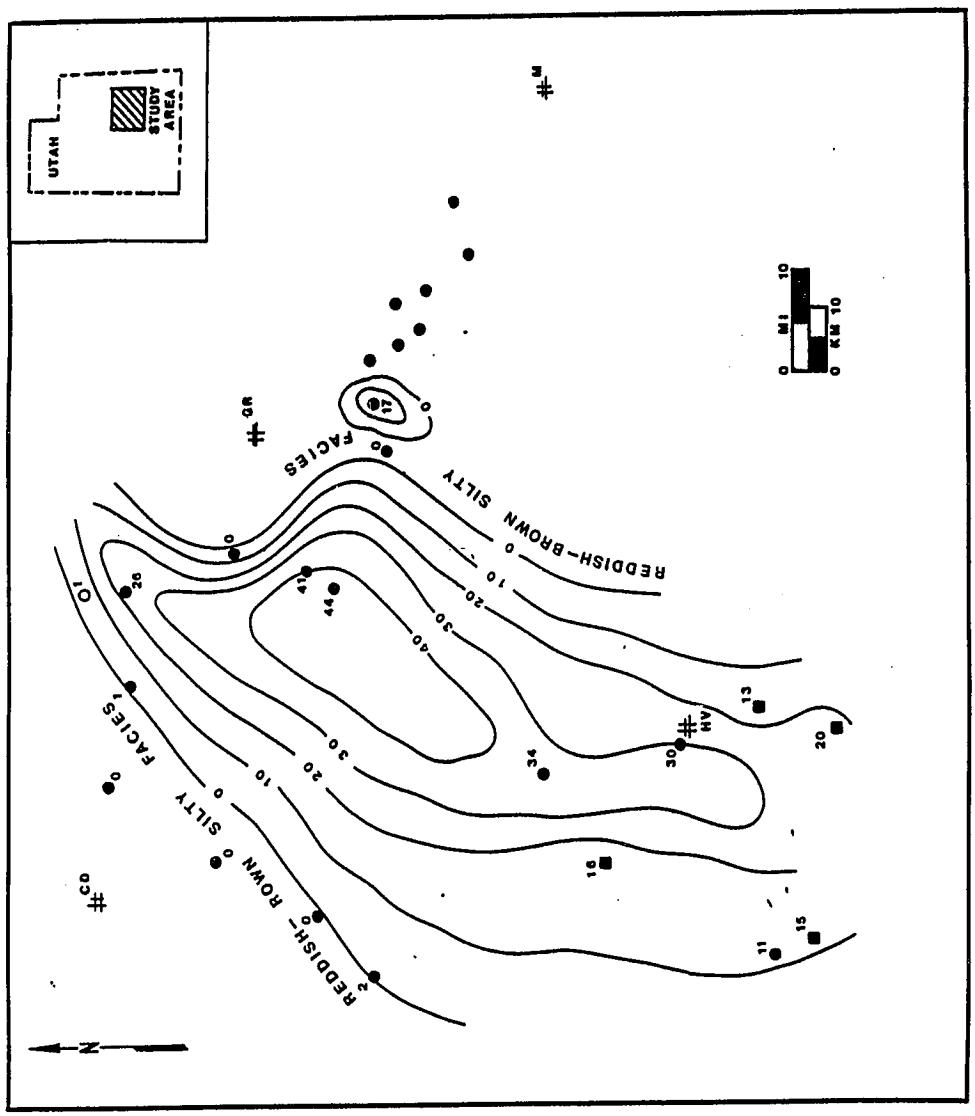

Figure 3.68. Isopach map of cumulative gypsum in the gypsiferous facies in the Summerville Formation. Contour interval: 10 ft (3 m). Map symbols (table 1.3)

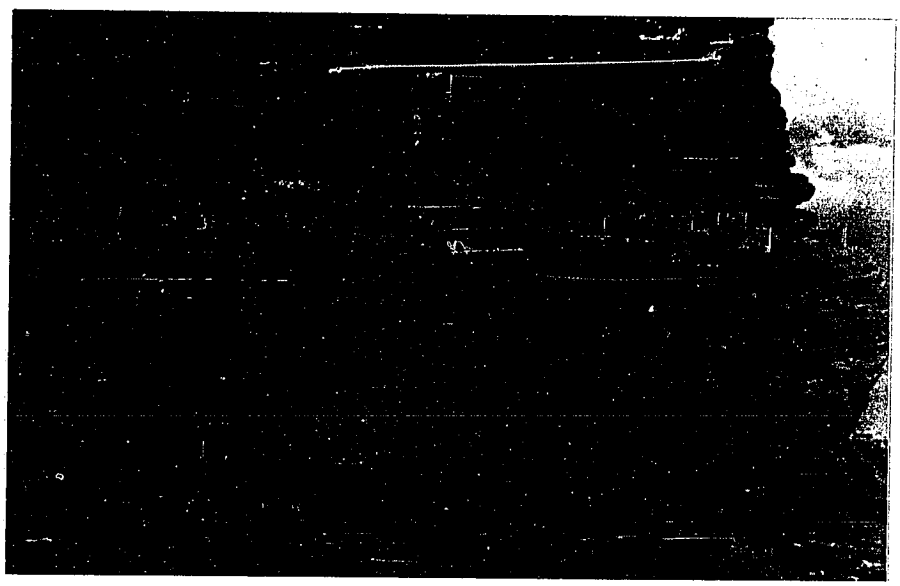

Figure 3.69. Climbing crosslaminations in lenses of very fine sandstone and siltstone surrounded by even beds of brown mudstone and siltstone in the chaotic microsequence of the gypsiferous facies. Bed is about 2 ft (0.6 m) thick (near San Rafael Swell East)

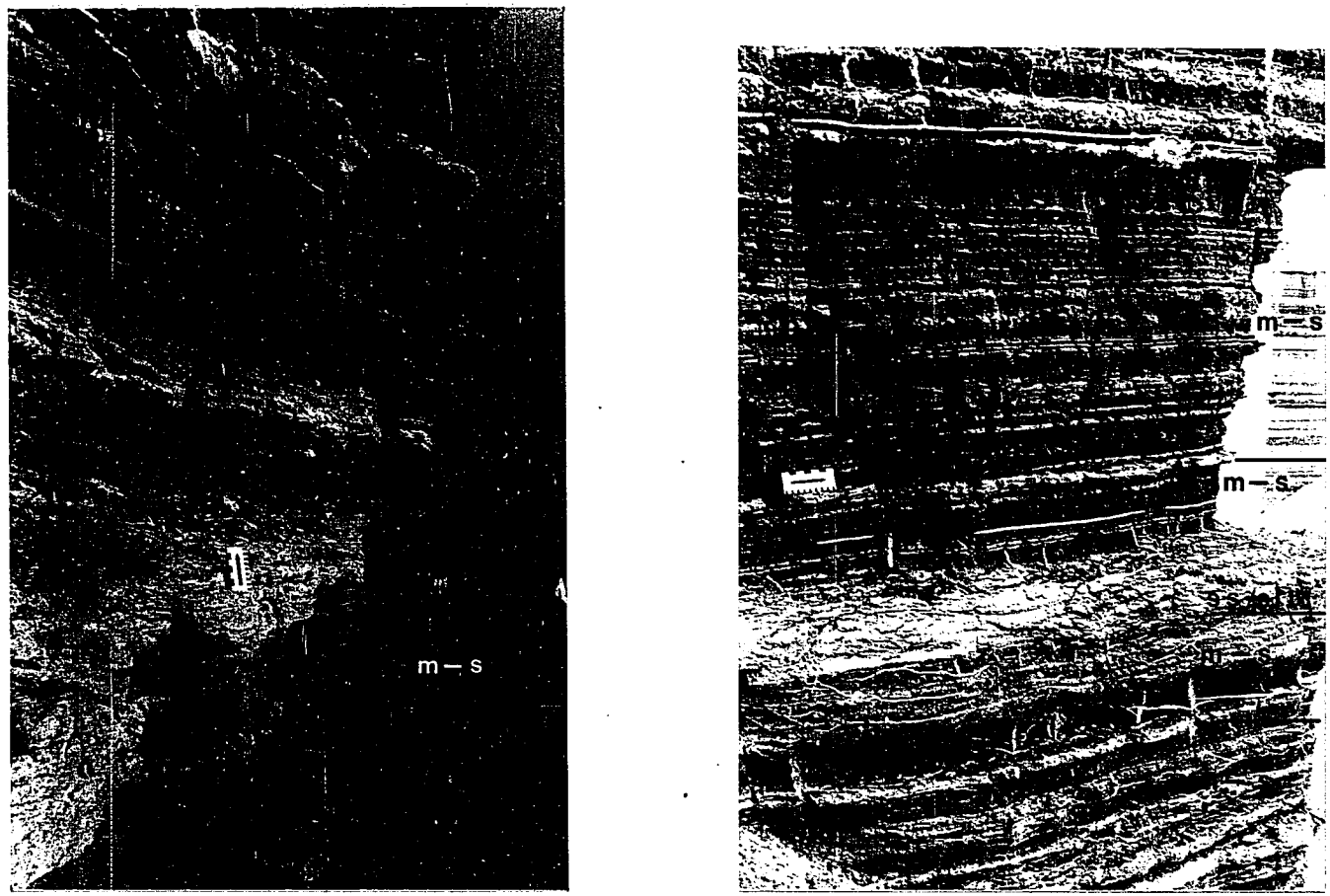

Figure 3.70. Partial chaotic microsequences (brackets) consisting of crosslaminated very fine sandstone or siltstone (ss/slt) and mudstone (m) with interbedded very thin beds of crosslaminated sandstone and siltstone (m-s). Scale is in inches and centimeters (a: San Rafael Swell Northeast, Z-3; b: Hanksville, Z-5)

accretionary or epsilon beds (fig. 3.71).

Unit d is either pure gypsum or a variation of unit c with gypsum nodules. The gypsum is characteristically white and is usually masked or encrusted by a greenish-white or reddish-brown weathering rind or stain. Occurrence is in two forms: either as lenticular nodules or lenticular beds. Nodules are present as compressed spheroids and other irregular shapes and are 0.2 to 6 inches (0.5 to 15 cm) along the longest dimension. Not only do they exhibit a displacive fabric among enclosing dark brown mudstone and whitish-green siltstone beds but there are vein-like inclusions of brown mudstone which give an internal "chicken wire" aspect to the nodules. (fig. 3.72a).

Gypsum beds seem tabuuar but are probably lenticular and range from 1 inch to 3 feet (2.5 to 90 cm) thick. Often, the gypsum beds form smooth, cliff- and bench-forming ledges. Other beds are extremely irregular and contorted and appear as a tabular cluster of amalgamated nodules. Such an outer texture is called enterolithic (Shearman, 1971, 1978) (fig. 3.72b). Much of the gypsum is composed of granular or sucrosic fine- to medium- sand (177 to 350 microns) size crystals. Thin sections show acicular and prismatic crystals forming mostly an irregular fabric with local radial, acicular crystals forming rosettes (Chapter 3, Petrology). Only two beds were observed at San Rafael Swell East (Z-2A) that were formed of gypsum grains reworked into ripples (fig. 3.72c) and crossbeds.

Noteworthy miscellaneous features in the microsequence include: straight- and sinuous-crested ripples with rounded or flattened crests and ladder ripples, molds and casts of evaporite polygons, casts of shrinkage cracks, raindrop impressions, wrinkle marks and interference ripples which locally resemble LLH stromatolites (Logan et al., 1964).

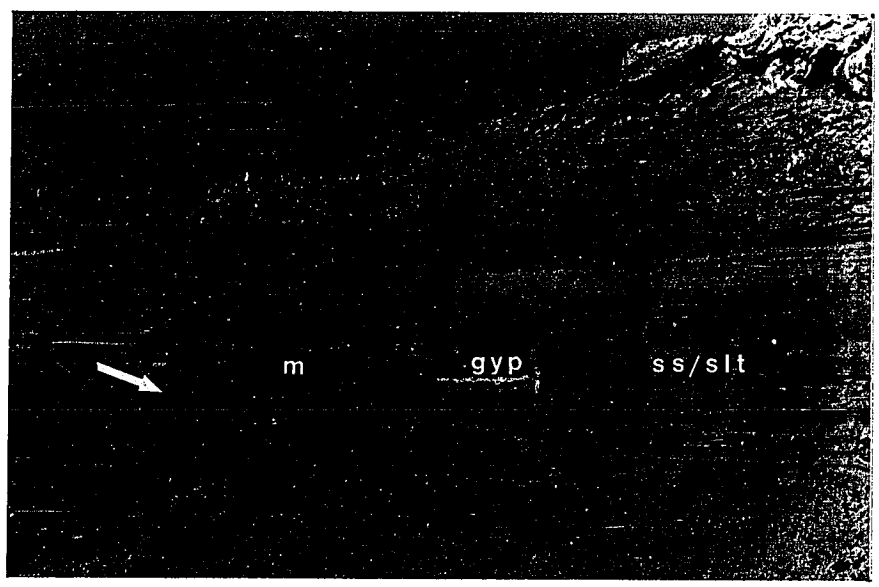

Figure 3.71. Interval of low-angle accretionary beds (arrow) consisting of chaotic microsequences of interbedded tan crosslaminated sandstone and siltstone (ss/slt), brown mudstone (m); nodular gypsum (gyp); gypsiferous facies. Interval is about 5 ft (1.5 m) thick (Hatt Ranch Hunting Farm, Z-10)

Figure 3.72. Nature of gypsum in the chaotic microsequence of the gypsiferous facies (a: San Rafael Swell West, Z-6; b: Hatt Ranch Hunting Farm, Z-10)

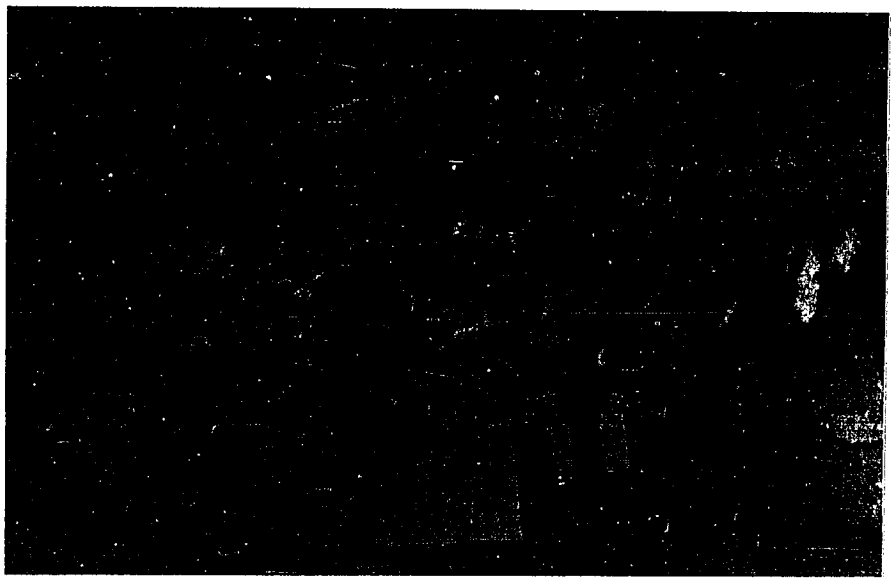

a: Small nodules of gypsum displacing and disrupting the fabric of brown mudstone

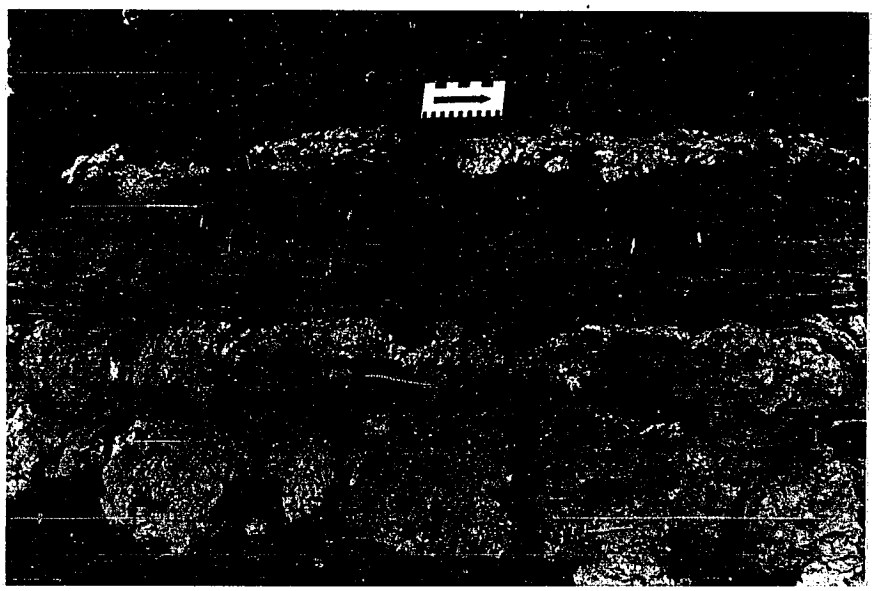

b: Larger nodules of gypsum coelesced to form enterolithic beds in brown siltstone and mudstone. Scale is in inches and centimeters

c: Locally occurring thin bed composed of rippled gypsum

These features are more diverse and abundant in the gypsiferous facies than in any other facies described herein (fig. 3.73a, b, c) (table 3. 10).

Figure 3.73. Common bedding-plane features preserved in the chaotic microsequence of the gypsiferous facies (San Rafael Swell East, Z-2)

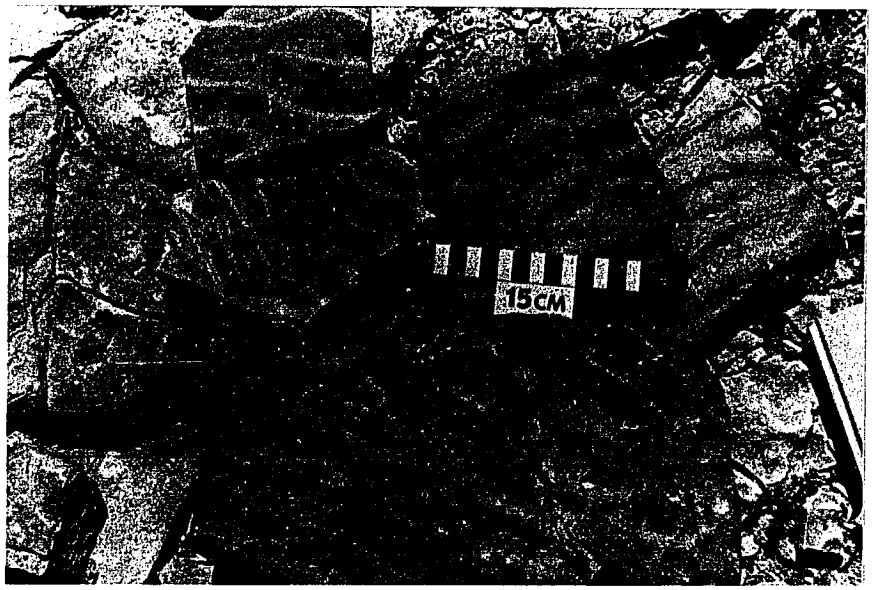

a: Sinuous, long-crested ripples with bifurcating, rounded and flattened crests

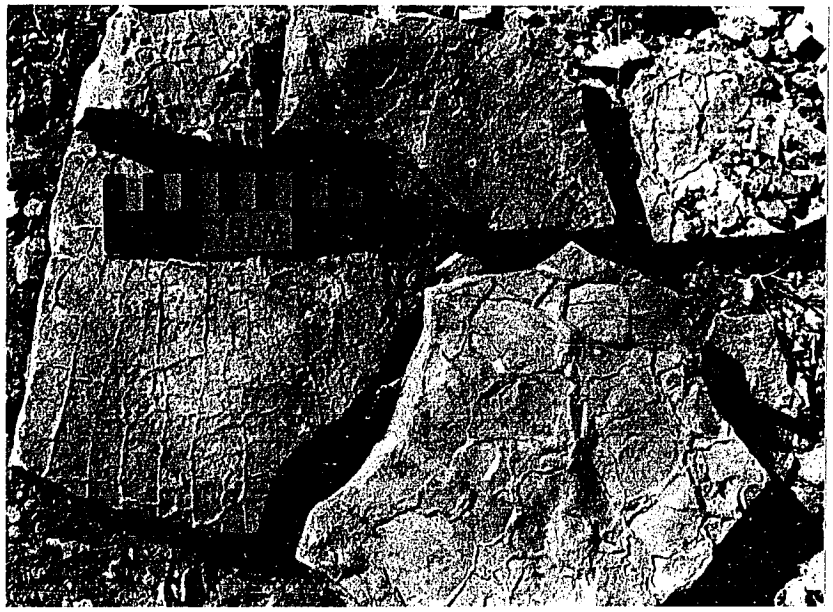

b: Sandstone casts of shrinkage cracks

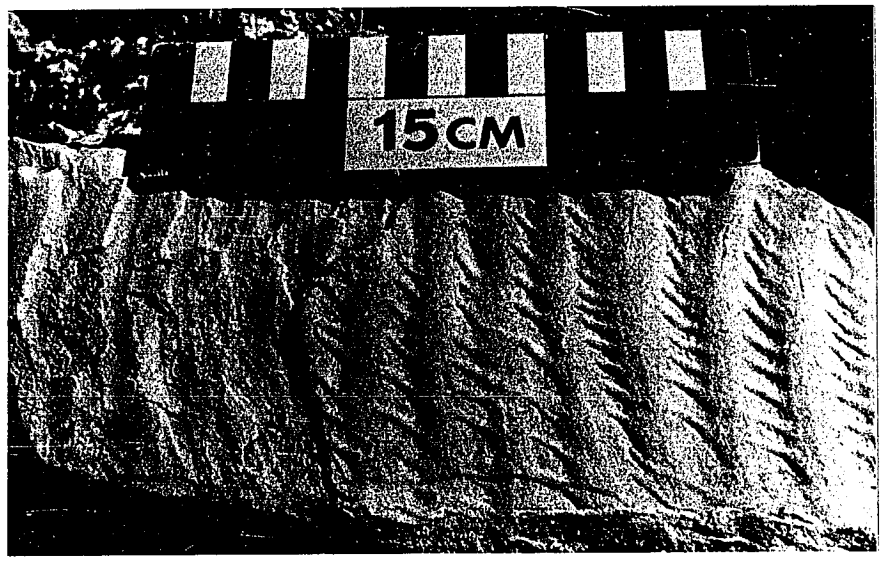

c: Linear ripples with rounded crests and ladder ripples

Table 3.10. Sedimentary features of the gypsiferous facies of the Summerville Formatio

Sedimentary Features	Interpretation
Assorted features	
1. Ripples -asymmetrical: straight- to sinuous-crested in-phase; locally bifurcating; rounded and flattened crests; local ladder ripples; RI = 6.2-8.9	Wave and non-wave currents; emergence drainage of tidal flat
2. Biogenic features rare or absent	Inhospitable arid, hypersaline conditi on sandy coastal sabkha
3. Local raindrop impressions, wrinkle marks, sandstone casts of desiccation cracks, evaporite polygons/molds	
Gypsum -white, weathers greenish white and reddish-brown	
-displacive nodules, pods, lenses in brown and reddish-brown mudstone and siltstone; locally thin to very thin discontinuous beds	Early diagenetic precipitate from inte stitial brines in phreatic and shallow marine-vadose zones of coastal sabkha
-enterolithic beds	Early diagenetic crystallizing and coelescing of gypsum lenses and nodule in sandy coastal sabkha
-granular/sucrosic texture; fine to medium sand-size crystals; -locally crossbedded and crosslaminated	Primary subaqueous precipitation and reworking by water (?) currents
-frequency and thickness of beds increases up-section	Prograding, regressive tidal flat-sabk sequence
Chaotic Microsequence d. gypsum nodules 0.2-6 in (0.5-15 cm) thick and enterolithic lenses and beds 1-36 in (2.5-90 cm) thick	Shallow tidal creeks and gullies fille with climbing ripple deposits; surroun by flat-bedded channel margin and inte channel deposits; early diagenetic cry lization of gypsum; local, ephemeral p or salinas and subaqueous precipitatio thicker gypsum beds; similar in origin
c. cryptic-bedded mudstone with lenses and beds of siltstone or very fine sandstone; plane- or cross-laminated; 0.4-1.5 in (1-3.75 cm) thick	lenticular microsequences in reddish-b silty facies
b. wavy-bedded, crosslaminated very fine (62-88 μ) sandstone or siltstone with mudstone; nodules and very thin beds of gypsum	

ıs facies of the Summerville Formation

terpretation	References
ve and non-wave currents; emergence and ainage of tidal flat	Klein (1970b, 1975a, 1977b), Reineck and Singh (1980)
hospitable arid, hypersaline conditions sandy coastal sabkha	Curtis et al. (1963), Illing et al. (1963), Thompson (1968)
rly diagenetic precipitate from inter-itial brines in phreatic and shallow-rine-vadose zones of coastal sabkha	Kerr and Thompson (1963), Murray (1964)
rly diagenetic crystallizing and elescing of gypsum lenses and nodules sandy coastal sabkha	Shearman (1971, 1978)
imary subaqueous precipitation and vorking by water (?) currents	Schreiber et al. (1982)
ograding, regressive tidal flat-sabkha quence	Thompson (1968, 1975), Lucia (1972), Klein (1977b), Warren and Kendall (1985)
allow tidal creeks and gullies filled h climbing ripple deposits; surrounded flat-bedded channel margin and inter-annel deposits; early diagenetic crystal-zation of gypsum; local, ephemeral ponds salinas and subaqueous precipitation of cker gypsum beds; similar in origin to ticular microsequences in reddish-brown ty facies	Thompson (1968, 1975), Shearman (1971, 1978), Voorhees (1978), Geesaman (1979), Reif and Slatt (1979), Blakey et al. (1983)

Table 3.10. Continued

Sedimentary Features	Interpretation
Chaotic Microsequence (cont.) a. cross-laminated very fine to fine (62-177 μ) silty sandstone or siltstone; 0.5-3 in (1.2-7.6 cm) thick; linguoid ripples; planar/tangential foresets; flasers; local plane laminations; local basal load structures; tabular or lenticular beds; local channel-form sandstone bodies composed of intrasets of climbing complete ripple-form laminations	Shallow wadi channels (?)

Interpretation	References
Shallow wadi channels (?)	Glennie (1970), Glennie and Evans (1976), Porter (1987)

Interpretation of the Summerville Formation

General Interpretation

The interpretation of facies and microsequences in the Summerville begins with a re-examination of the redbed facies in the Curtis. Assigning the redbed facies to the Curtis Formation is based on physical stratigraphic relationships recognized by O'Sullivan (1980a, 1981c) and other workers (Chapter 2). However, on the basis of color, mineral composition, texture, and microsequences examined in this report, it more closely resembles the Summerville in origin than the Curtis. The informal naming of the redbed facies as the "lower Summerville" by McKnight (1940) was valid.

During middle and late Curtis time, when the upper facies, including the redbed facies, in the Curtis, were deposited, the middle Jurassic marine transgression had reached a peak. Stillstand conditions prevailed and the shoreline remained fairly static as suggested by relatively thick amalgamated facies units in the Curtis (e.g. composite sandstone facies and rippled silty facies). However, there were small-scale shoreline fluctuations, minor transgressive (lower and upper redbed facies) and regressive (Moab Tongue) episodes. Summerville-like sedimentation is first recorded in the redbed facies of the Curtis, during stillstand conditions and onset of regression. This sedimentation style, consisting of subaerially exposed redbeds deposited in intertidal to supratidal environmerts, was dominant throughout the deposition of the Summerville in Callovian time.

Sedimentary facies and microsequences in the Summerville preserve a history of shoreline progradation during a relatively rapid regression. Siltstone and mudstone beds were deposited in higher intertidal and supratidal subenvironments. Shoreline environments prograded generally northward and westward as the Curtis-Summerville seaway receded to the north. Wave-agitated, tidal-circulating marine conditions during Curtis time evolved into more restricted, yet tide-influenced, hypersaline conditions during Summerville time. Thus, a complete upward-fining, upward-shallowing prograding shoreline sequence is preserved in subtidal to intertidal deposits in the Curtis and intertidal and supratidal deposits of the Summerville; a cycle typically formed in modern (Thompson, 1968,1975; Warren and Kendall, 1985) and ancient (Klein, 1970b, 1971, 1977) regressive tidal deposits.

The red color of the Summerville is probably related to high Fe^{3+}/Fe^{2+} ratios, little to no organic material (Potter et al., 1980) and greater degree of exposure at the shoreline favoring oxidation at the time of deposition (Thompson, 1968).

Reddish-Brown Silty Facies

Microsequences of the reddish-brown silty facies were deposited seaward of the gypsiferous facies in middle(?) and possibly upper intertidal subenvironments of a westward and northward prograding sandy coastal sabkha and intertidal system (table 3.9). The relationship between the upward-fining microsequence and the lenticular microsequences in this facies (fig. 2.5) is analogous to that between parallel-bedded and crossbedded microsequences in the composite sandstone facies in the, Curtis namely that the occurrence of crossbedding increases westward in the Curtis facies. The greater

thickness and abundance of crossbedding in the western San Rafael Swell is a reflection of sand transport by megaripples confined perhaps to tidal channels. Parallel bedded microsequences dominate the Curtis in the eastern San Rafael Swell and reflect rippled silt and sand accumulation on elevated intertidal flats and berms. In the reddish-brown silty facies, the frequency and thickness of interbedded lenticular microsequences is greater in the western San Rafael Swell. Lenticular channel-form siltstone and sandstone decrease in frequency and thickness toward the east and are gradually replaced by parallel-bedded and chaotic microsequences, especially in the gypsiferous facies. Hence, the lateral relationship between lenticular and parallel-bedded microsequences in the Summerville suggests the following: 1. higher-energy, silt and sand transport in tidal creeks and gullies in lower, more seaward flats in the western San Rafael Swell area, and 2. lower energy silt and mud transport and evaporation on a higher mud flats and coastal sabkha system in the eastern San Rafael Swell and Green River Desert. A lateral-fining textural relationship is shown in figure 3.60 in which the percentage of net siltstone and mudstone relative to sandstone increases eastwardly in the Summerville. This trend is developed in the Curtis facies and has been described from modern (Hantzchel, 1939; van Straaten, 1954a; Thompson, 1968; Curray, 1969b) and ancient (Caputo, 1980) tidal flat deposits.

Upward-fining, upward-thinning. Sedimentary features of upward-fining upward-thinning microsequences (table 3.9) are similar in texture and structure to those in the redbed facies of the Curtis. Vertical and lateral relationships with lenticular microsequences and

the general alternation of mudstone and sandstone suggest deposition along tidal channel margins and high portions of channel banks or interchannel areas. Crosslaminated sandstone was deposited by asymmetrical lunate, linguoid, and straight-crested ripples migrating in moderately low currents. At times, ripple-forming currents may have been restricted to shallow gullies or run-off channels as suggested by the locally developed lenticular geometries. The alternation of crosslaminated sandstone and siltstone interbedded with mudstone is comparable to bedding sequences produced on modern tidal flats by the rhythmic flow of tidal currents (Hantzschel,1939; Reineck and Wunderlich, 1968b; Howard and Frey, 1980; Reineck and Singh, 1980).

The greater thickness and volume of siltstone and mudstone relative to sandstone in the eastern San Rafael Swell and Green River Desert (fig. 3.60) suggests sedimentation in higher portions of tidal flats. Mixed sand flats and mud flats which are distinguished by the increase in mud content landward are deposited in middle and upper intertidal zones respectively and are a response to a shoreward decrease in current strength, and settling- and scour-lag (table 3.9). Most modern mixed and sandy intertidal flats have been reworkded by lateral migrating tidal channels (Reineck and Singh, 1980); related channel fill and contemporary channel bank deposits are commonly characterized by rhythmic alternations of sand and mud (Hantzschel, 1939; Reineck and Wunderlich, 969; Reineck and Singh, 1980).

More complete microsequences exhibit vertical transitions from crosslaminated, wavy-beds to lenticular beds and ultimately to mudstone or claystone. These variations indicated a decrease in current strength and greater settling of silt- and clay-size particles from suspension. The increase in mud deposition and decreasing current

strength may reflect the approach and arrival of neap tides (Terwindt, 1981).

Emergence and subaerial exposure is suggested by shrinkage cracks in mudstone, which are identified as dessication cracks; straight- to sinuous-crested ripples with rounded, flattened crests and locally developed run-off tongues are also emergent features. Few horizontal burrows characterized by branching galleries are examples of Thalassinoides, a dwelling trace fossil possibly constructed by arthropods in low energy environment (Howard, 1972; Howard and Frey, 1984).

Lenticular microsequences. The lenticular geometry, infilling strata, and paleocurrents to the northeast suggest that lenticular microsequences were deposited in shallow, coastal plain tidal channels. Van Straaten (1961) and Reineck and Singh (1980) have described how much of the sediment in intertidal flats undergoes multiple reworking by laterally migrating, meandering tidal channels. This is especially true for lower sand and mixed flats; channel migration in upper mud flats is somewhat retarded because of greater cohesion of mud. Meandering tidal channels also build laterally-accreting point bars (van Straaten, 1961; Howard and Frey, 1980; Reineck and Singh, 1980) which are similar to those formed in rivers (Allen, 1964, 1970a). Tidal and fluvial point bars may be differentiated by body and trace fossils assemblages (Pryor, 1967; Howard and Frey, 1980) and by paleocurrent structures. Point bar and channel-fill deposits in tidal and fluvial environments often contain basal gravels or shells. The absence of gravel in the lenticular microsequence expresses either the well-sorted nature of the sediment available for transport or the inability of

currents to transport available gravel. The absence of body fossils and rare trace fossils indicates that environmental conditions were too harsh to support diverse, abundant forms.

Trough crossbedding in fine grained sandstone indicates current velocities of at least 60 cm/s (Harms et al., 1982) Mudstone clasts along foresets support a subaqueous interpretation for these crossbeds. They represent mud reworked from pause beds and transported as cohesive intraclasts. Deformation due to loading in the basal crosslaminated sandstone suggests migration over and burial of water-saturated mud. Last stages of prograding channel-fill and possibly abandonment are recorded in crosslaminated fine- and very fine-grained sandstone and cryptic-bedded siltstone and mudstone in the uppermost part of the microsequence.

Low-angle bedding that locally fills in channel-form scours consists of crosslaminated flaser-, wavy-, and lenticular-bedding mixed with mudstone and is interpreted as accretionary bedding or longitudinal bedding (Reineck, 1967; Reineck and Wunderlich, 1969). In some intertidal deposits along the North Sea, meandering channels have been filled in with accretionary beds. These beds consist of intraclasts of rhythmic flaser-, wavy-, and lenticular- crosslaminated beds (van Straaten, 1961; Kellerhals and Murray, 1969) constructed by ripples migrating in the currents across the point bar flank. Successive mud laminations are deposited during slack water as pause beds enclose crosslaminated bundles formed during active current flow.

Along the eastern San Rafael Swell, thin sandstone and siltstone lenses are enclosed in mudstone and are built of intrasets of climbing ripple-form laminations (table 3.9). Complete ripple-form preservation

indicates moderately high sedimentation rate (Harms et al. 1982) probably in shallow tidal creeks. General thinness, dessication cracks, and isolated occurrence in mudstone, suggest a short-lived sedimentary event and ultimate burial in mud.

A fairly uniform paleocurrent trend to the northeast is suggested by plane- and cross-laminated beds in lenticular microsequences exposed along the western San Rafael Swell. Paleocurrent structures indicate northeastward drainage, presumably in a seaward direction or toward lower water-levels. This is consistent with a generally northward marine retreat of the Summerville seaway. Sedimentary structures indicating bimodal paleocurrents or shoreward paleocurrents were not observed. Therefore, paleo-drainage was primarily seaward and off the coastal plain.

Gypsiferous Facies

Chaotic microsequence. The near final events in the history of sedimentation in the Summerville are preserved in the gypsiferous facies. The interior seaway was probably more narrow and restricted as it continued to recede roughly northward during Summerville time. Shoreline retreat is reflected in the northeast-trending belt of the gypsiferous facies as evaporative, hypersaline conditions dominated and a coastal plain sabkha complex prograded northward. Ordered and chaotic microsequences with gypsum beds are of tidal origin and represent sedimentation in uppermost intertidal flat and supratidal sabkha (table 3.10). Irregular alternations of gypsum and detrital beds reflect alternating periods between clastic sedimentation during abnormal spring tides, enhanced perhaps by wind or storms, and periods of exposure and evaporation, perhaps during neap tide periods.

There are significantly more bedding features herein that suggest emergence and subaerial exposure than in other facies in the Summerville or Curtis (table 3.10) and include ladder ripples, straight- to sinuous-crested ripples with rounded and flattened crest, sandstone casts of shrinkage cracks, molds of evaporite polygons, local raindrop impressions and wrinkle marks.

The nature and occurrence of gypsum as lenses, nodules and discrete tabular beds is a strong characteristic indicating an origin in a supratidal sabkha environment (table 3.10). The distribution of the gypsiferous facies (fig. 3.68) suggests a belt of evaporation trending parallel to the coastline of the Summerville seaway. The thickest part of the trend closely coincides with the thickest part of the entire Summerville (compare figs. 3.61 and 3.68) and suggests that the locus of subsidence in the eastern and southeastern San Rafael Swell persisted throughout deposition of the entire Summerville.

The belt of gypsiferous facies is about 45 miles (72 km) wide. Some modern coastal sabkhas are between 6 and 9 miles (10 and 15 km) wide (Butler et al., 1982; Warren and Kendall, 1985). Westward progradation of the facies with time during regression accounts for the difference in width. This interpretation is consistent with the overall westward prograding nature of the entire Curtis-Moab-Summerville interval.

There are modern examples of sequences similar to that of the chaotic microsequence. Discontinuous beds of silt and mud interrupted with gypsum are described from upper intertidal to supratidal zones of the tide-dominated Colorado River delta (Thompson, 1968, 1975). The twisted and distorted nature of gypsum beds in this facies is referred to as an enterolithic texture. The crystallization of gypsum to form

lenses, nodules, and coelesced enterolithic beds is a characteristic feature of evaporites formed in coastal sabkhas (Shearman, 1971, 1978). Similar redbed sequences with gypsum deposited in ancient coastal sabkha or salina environments are preserved in the Triassic Moenkopi Formation in southern Nevada (Reif and Slatt, 1979) and in the Middle Jurassic Carmel Formation of southwestern Utah (Voorhees, 1978; Geesaman, 1979; Blakey et al., 1983).

Nodular and lenticular gypsum exhibits a displacive character within the contorted and disrupted reddish-brown mudstone and siltstone. A displacive origin within enclosing sediments suggests that the gypsum was an early diagenetic precipitate from interstitial brines (Kerr and Thompson, 1963; Murray, 1964) in phreatic and shallow marine-vadose zones of a coastal sabkha (Kendall, 1984). However, local thick, tabular beds, and localized ripple-marked gypsum suggest primary deposition in a subaqueous sedimentary environment (Schreiber et al., 1976; Warren and Kendall, 1985) probably from temporarily ponded water, similar to a coastal salina, related to wind- or storm-enhanced spring tides.

Paleocurrent data collected from crosslaminated beds in this facies are too few to make reliable interpretations. Nonetheless, a weak polymodal pattern in the ripples (fig. 3.63) may reflect unconfined or non-channelized currents on the coastal sabkha.

CHAPTER 4

PETROLOGY

Methods

Sixty-six representative samples of bedding units in each of the facies in the Curtis-Moab-Summerville interval were systematically collected, prepared, and studied under a polarizing microscope. Three hundred points were counted on each thin section. Selected samples were stained using alizarin red-S to distinguish calcite cement from dolomite cement and cobaltinitrate stain to help distinguish orthoclase from quartz and other feldspars. Petrographic characteristics including percentage of mineral and other framework grains, matrix and cement are summarized in table 4.1. Complete petrographic data of each sample are included in the appendix as table A.2. Nine samples from different localities and stratigraphic positions within facies contain matrix clay minerals which are poorly distinguishable in thin section and positively identified by x-ray diffraction analysis. The less-than-2 micron clay fraction was separated and analyzed by Richard Pollastro (July-August, 1987; USGS, Denver) and the results are summarized in table 4.2

Sandstone Classification of Facies in the Curtis-Moab-Summerville Interval

All of the samples studied in thin section are characterized by framework grains greater than 0.062 mm in diameter and are sandstones. Collective samples from each facies are assigned rock clan names according to the sandstone classification of Folk (1974). The ternary diagram of which is reproduced in figure 4.1a. Point-count percentages of all quartz (monocrystalline and polycrystalline), feldspars (orthoclase, plagioclase, microcline) and rock fragments (sedimentary and igneous rock fragments, and chert) were recalculated and normalized to 100 percent and plotted on the ternary diagram (fig. 4.1a).

Most sandstones contain greater than 80% quartz and are classified as subarkoses (composite sandstone facies of the Curtis; gypsiferous facies of the Summerville), sublitharenites (rippled silty and redbed facies of the Curtis) and quartzarenites (Moab facies) with few exceptions. Sandstones studied in the reddish-brown silty facies of the Summerville contain equal percentages of rock fragments and feldspar and therefore fall on the boundary between subarkose and sublitharenite. Sandstones in the wavy- and crossbedded sandstone facies of the Moab plot along the boundary between quartzarenite and sublitharenite. Sandstone composition of the sandstone-mudstone facies of the Curtis is strongly influenced by the rock fragment assemblage in the basal gravelly microsequence and therefore falls within the lithic arenite field.

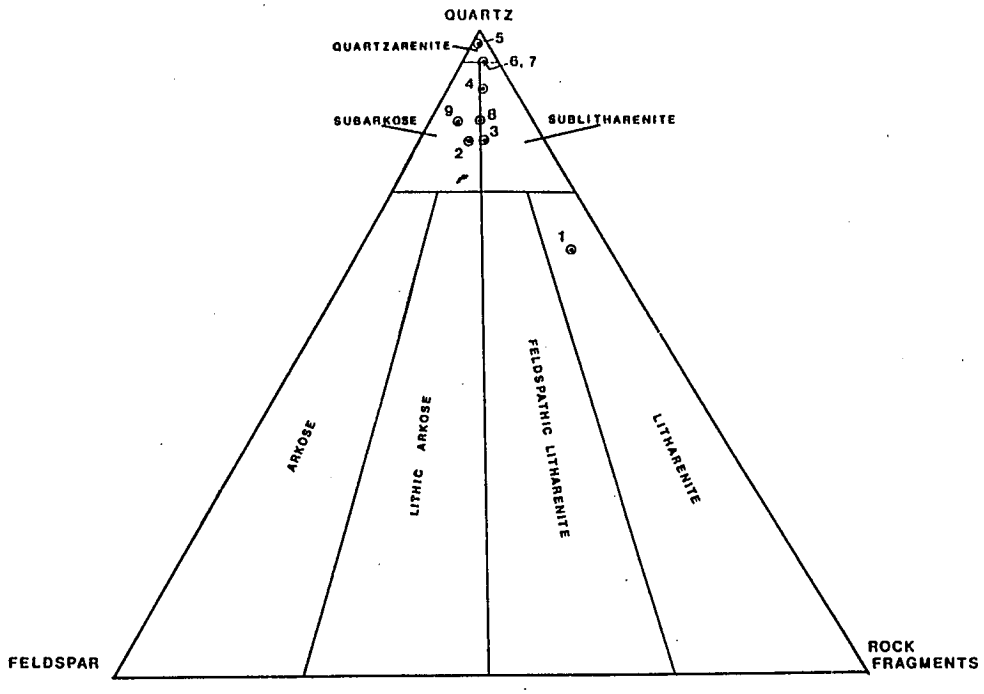

A

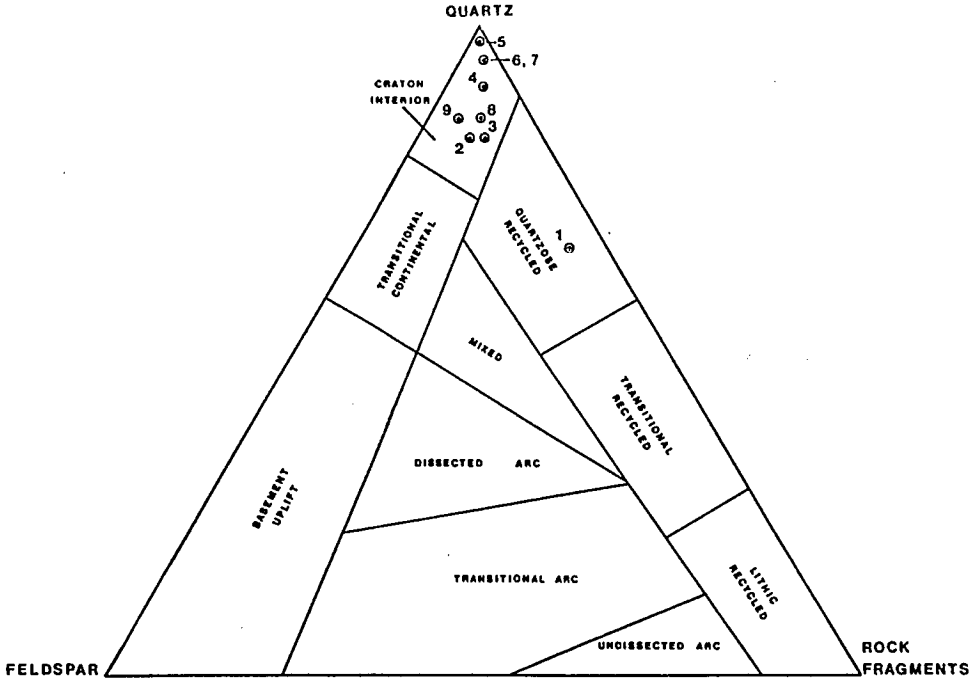

B

Figure 4.1. A: Composition and classification of sandstones in facies of the Curtis- scheme abbreviated from Folk et al., 1970); B: provenance types of sandstones in the determined from the three framework modes, quartz, feldspar, and total lithic fragmen et al., 1983)

SAMPL

Curti
1. Sa
2. Co
3. Ri
4. Re

Moab
5. Wr
6. Wa
7. Cr

Summe
8. Re
9. Gy

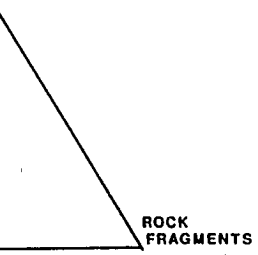

SAMPLES AND CORRESPONDING FACIES

Curtis Formation
1. Sandstone-mudstone facies
2. Composite sandstone facies
3. Rippled silty facies
4. Redbed facies

Moab Tongue
5. Wrinkled sandstone facies
6. Wavy sandstone facies
7. Crossbedded sandstone facies

Summerville Formation
8. Reddish-brown silty facies
9. Gypsiferous facies

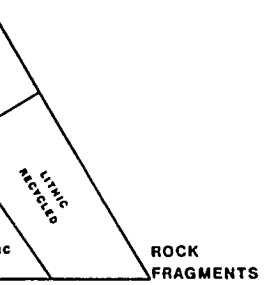

sandstones in facies of the Curtis-Moab-Summerville interval (classification
ovenance types of sandstones in the Curtis-Moab-Summerville interval as
, feldspar, and total lithic fragments (Q_mFL_t) (adapted from Dickinson

Provenance

Dickinson et al. (1983) and Dickinson (1985) have shown how the composition of modern sands based on the relative abundances of monocrystalline quartz, lithic or rock fragments, and feldspars may reflect origin from different tectonic terranes. The different compositional fields reflecting different tectonic settings are built into a ternary diagram which is reproduced in figure 4.1b. The quartz, lithic, and feldspar composition of sandstones in facies of the Curtis-Moab-Summerville interval is characterized by greater than 80% monocrystalline quartz and 10% or less of feldspars and lithic fragments with the exception of beds in the sandstone-mudstone facies in which lithic fragments are as much 25% of the rock. The percentage value of total monocrystalline quartz is plotted as total quartz with 2% polycrystalline quartz being neglible. The framework composition of these sandstones suggests a provenance type characterized by tectonic quiescence such as on a cratonic interior or cratonic shelf with little to no relief. Long and intense weathering and reworking of probably second-cycle sediment by wind and marine currents was required to concentrate quartz and reduce labile components such as feldspar and rock fragments.

The source for the "Great Sand Pile" which accumulated in ancient shoreline and eolian environments throughout the late Paleozoic and Mesozoic Eras in the western Colorado Plateau still remains a puzzle. Stanley et al. (1971) proposed that the sand deposited in the Western Interior during Jurassic time came from beyond and suggested early Jurassic erosion of upper Paleozoic and Triassic sedimentary rocks in Montana and southern Alberta, Canada. Sand deposited along ancient

shoreline and eolian environments in the Carmel Formation and Page Sandstone may have been redistributed southward from this area by southward-flowing winds and longshore currents (Caputo, 1980). It is now tentatively thought that the Page Sandstone represents temporary deflation and redistribution of sand from the eolian sand sea of the Navajo Sandstone (research in progress). Active volcanism in the western magmatic arc contributed detrital sediment in the Utah-Idaho trough during deposition of the Carmel and Page Formations (Caputo, 1980; Chapman, 1986).

Data in this report do not indicate a positively identifiable source area for the sand in the Curtis-Moab-Summerville interval. The middle Jurassic marine basin was locally restricted by eroded Ancestral Rocky Mountains uplifted to the east and volcanic highlands intermittently active in the Mogollon area to the south. Yet, stratigraphic and petrologic data suggest that these areas contributed little to no sediment into the basin during middle Jurassic time (Caputo, 1980; Peterson, 1987; this report).

The Moab Tongue is contemporaneous with and grades into the upper part of the Slick Rock Member of the Entrada Sandstone south and east of the Moab townsite (O'Sullivan, 1980a). Furthermore, the Moab Tongue is texturally, mineralogically, and genetically similar to the Slick Rock Member and was deposited by dominantly easterly winds. These characteristics suggest that sand in the Moab Tongue may have been derived from sand in the Slick Rock and may represent a short-lived reactivation of the Slick Rock erg. The origin of sand in the Curtis and Summerville is still uncertain.

Lithic fragments in the sandstone-mudstone facies strongly influence the sandstone composition of that facies and suggest

recycling of quartz-rich sediment partially modified by detritus shed from a fold-thrust system (fig. 4.1b). This is consistent with the westward increase in abundance of lithic clasts toward the locus of incipient crustal deformation in the Sevier orogenic belt during middle Jurassic time (Peterson and Caputo, 1986). The lithic fragments are gravel-size lithoclasts composed of chert and a variety of limestone types including partially to completely dolomitized sparite, vuggy microsparite, biomicrosparite, oopelmicrite, dolomitized biopelmicrite, microdolomite, and sandy dolosparite (sample Z-6, S-1; table A-2). Fossils in the biomicrosparite and biopelmicrite clasts are fragments of recrystallized, locally dolomitized or silicified pelecypod valves and gastropods. The above lithoclasts do not resemble rocks in either the Curtis-Moab-Summerville interval or the underlying Entrada Sandstone. The lithoclasts may have been eroded from older sedimentary rocks, possibly the older middle Jurassic Carmel Formation or other Mesozoic and Paleozoic strata uplifted in the Sevier orogenic belt.

Trace amounts of volcanic rock fragments are identified with uncertainty (table 4.1). Their extremely low abundance suggests that either volcanism was dormant at this time or that active volcanism contributed few clasts to the marine basin and currents did not transport them to the eastern shoreline.

Descriptive Mineralogy

This section of petrology provides a summary of petrographic characteristics of mineral grains observed in sandstones of the Curtis-Moab-Summerville facies.

Quartz

Quartz is the most abundant detrital framework component. It occurs as subangular to well rounded grains which are first-order gray under crossed nicols. In plane polarized light, quartz is colorless to partially cloudy due to bubble inclusions. Other inclusions are acicular, prismatic and fibrous crystals of apatite and rutile. Less than five grains were observed with abraded, optically continuous quartz overgrowths.

Degree of mineralogic maturity or abundance of quartz is greatest in facies of the Moab Tongue and decreases approximately westward in laterally adjacent facies in the Curtis, namely the redbed facies, rippled silty facies, composite sandstone facies and sandstone-mudstone facies (table 4.1). This mineralogic trend suggest that the quartz in the Curtis-Moab interval was perhaps derived ultimately from the east, from the Slick Rock Member, in which the origin of the sand is uncertain. The westward decrease in percent abundance of quartz possibly reflects distance away from source and dilution by other detrital components such as rock fragments. A similar but less pronounced trend is exhibited in the Summerville facies (table 4.1). Quartz is slightly more abundant, by 2%, in the more shoreward gypsiferous facies, than it is in the more seaward reddish-brown silty

facies.

Feldspars

Feldspars rank second in abundance with rock fragments. Orthoclase and undiffentiated plagioclases are present in subequal amounts; microcline is least abundant.

Orthoclase. Orthoclase produces first-order gray olors under crossed nicols and is distinguished from similar gray quartz by staining, biaxial negative optical sign and large 2V. In plane polarized light, orthoclase exhibits a dull, brown cloudiness due to partial alteration to clay minerals, possibly kaolinite.

Plagioclase. Plagioclase grains are colorless under uncrossed nicols and are distinguished from other minerals with low birefringence under crossed nicols by extinction patterns produced by Carlsbad and albite twin lamellae.

Microcline. Microcline grains are recognized by polysynthetic twinning which produces as gridiron or quadrille extinction pattern under crossed nicols.

Rock Fragments

Rock or lithic fragments are present in subequal amounts with feldspars. They are considered as lithoclasts reworked from older strata in the underlying Entrada Sandstone and uncertain older Jurassic, Triassic and possibly Paleozoic strata which might have been uplifted during early deformation in the Sevier orogenic belt (Chapter 5, Paleogeography). Rock fragments are chert and sedimentary rock fragments including rare siltstone and sandstone fragments and gravel-size clasts of limestone. Siltstone and sandstone fragments were

probably eroded from the underlying Entrada Sandstone. A diverse suite of gravel clasts is preserved mainly in the basal gravelly microsequence in the sandstone-mudstone facies and are granule- and small pebble-size clasts of well-rounded chert and limestone. The limestone gravels are pieces of vuggy microsparite, biomicrosparite, oopelmicrite, silicified mollusc biosparite, dolomitized biopelmicrite, microdolomite, sandy dolosparite, and dolomitized sparite. Sparite is an informal term used in this report to designate a calcareous rock consisting of less than 30% framework grains supported by a neomorphic or early diagenetic cement. Microsparite implies a similar fabric in micrrspar, a neomorphic cement.

Fossil fragments within biopelmicrite and biomicrosparite clasts have been replaced by either chert, chalcedony, dolomite, or calcite and can only be approximately identified as either pelecypod, gastropod and possibly brachiopod fragments. Uplifted parent rocks are probably lower Mesozoic and upper Paleozoic strata.

The origin of the clasts is still uncertain. The general westward increase in size and abundance of clasts in the basal Curtis suggests an uplifted source terrane to the west. Similar clasts are scarce in Jurassic rocks older than Curtis and increase in size and abundance in the Curtis, Summerville, Morrison and Cretaceous strata. Furthermore, the petrologic trend suggests that crustal deformation and uplift may have been strongly active at the beginning of Curtis sedimentation and persisted significantly throughout late Jurassic and younger Cretaceous time (Peterson and Caputo, 1986; Peterson, 1987).

Chert is counted as a lithic fragment. It is present as subrounded to subangular sand-size grains exhibiting low birefringence, first-

order gray colors, and irregular extinction under cross nicols. Chert clasts form 3 to 12% of the sandstones studied in facies of the Curtis-Moab-Summerville interval. They are most abundant in the basal gravelly mirosequence and exhibit an approximate decrease in abundance vertically through the Curtis and Summerville and eastwardly through the Curtis and Moab.

Fossils and Other Allochemical Grains

Allochemical framework grains comprise 3% or less of the sandstones in all the Curtis facies and less than 1% in the gypsiferous facies and 0% in the reddish-brown silty facies of the Summerville Formation (table 4.1). They generally decrease in percent abundance upward through the Summerville and laterally toward the east in the redbed facies of the Curtis. Such clasts were not observed in sandstones of the Moab Tongue.

Allochemical grains include rounded and abraded fragments of echinoderms, pelecypods, and gastropods, and whole peloids, and ooids in order of decreasing abundance. Echinoderm fragments are recognized by uniform extinction patterns, syntaxial overgrowths of coarse-crystalline calcite, and pores filled with authigenic glauconite. Ooid nuclei are usually smaller fragments of echinoderms or unidentifiable fossil fragments. Peloids may be true fecal pellets or highly micritized ooids or fossil fragments.

Heavy Minerals

Heavy minerals are present in the Curtis and Summerville facies and comprise 2% or less of the sandstones examined. They include zircon, tourmaline, biotite, and muscovite in order of decreasing abundance.

Gypsum

Gypsum occurs as nodules, pods, lenses, enterolithic masses and massive beds and locally as a cement in sandstones adjacent to gypsum beds in the gypsiferous facies of the Summerville Formation. In hand specimen, fine to medium sand-size (125-350 microns) crystals of gypsum form a white granular, sucrosic mass. In thin section, gypsum crystals appear as an irregular array of euhedral prismatic to fibrous crystals characterized by low birefringence and first-order gray colors under crossed nicols. Certain crystals exhibit either partial alteration to or incomplete alteration from anhydrite as suggested by zones of higher optical relief and first-order yellow colors (sample Z-1, S-1, table A.2).

A thin section from a locally occurring nodule of red chalcedony (jasper) in the rippled silty facies of the Curtis (sample Z-8, S-1, table A-2) shows both unaltered gypsum crystals and gypsum replaced by chalcedony. The original gypsum formed as radial prismatic to fibrous crystals arranged as small spherulites or rosettes within the nodule and as cavity linings around the inside rim of the nodule. Local replacement of gypsum crystals by chalcedonic quartz is suggested by the pseudomorphic crystal habit, and the length-slow and uniaxial positive optical properties.

Glauconite

Glauconite occurs as rounded to well-rounded pellet-like grains in all sandy facies in the Curtis and Summerville Formations and is absent in facies of the Moab Tongue. The grains appear bright apple-green, yellowish-green and dull brownish-green in polarized light;

birefringent colors are masked by the greenish color under crossed nicols and so the mineral exhibits a birdseye-like extinction pattern with green and locally yellow birefringent colors.

Glauconite forms 7% of the sandstones examined in the rippled silty facies, 3% of the composite sandstone facies and less than 1% of the sandstone-mudstone facies. This is a puzzling relationship because most of the organic activity as suggested by trace fossil variety and abundance is preserved in the sandstone-mudstone facies. A greater amount of glauconite is expected in this facies because glauconite formation is related to presence of fecal pellets (Pryor, 1975; Pettijohn et al., 1987). Perhaps the fecal material deposited in the sandstone-mudstone facies was isolated from glauconite-forming chemical conditions by rapid burial during traction sedimentation. Glauconite has also locally filled in pores of echinoderm fragments preserved in the basal gravelly microsequence of the sandstone-mudstone facies.

Glauconite is known to form as a syndepositional or early diagenetic mineral phase. It forms in response to a reducing microenvironment related to decaying organic material, mainly fecal pellets, in a marine environment (Pryor, 1975; Pettijohn et al., 1987).

Coal Clasts

Local laminations and thin beds of coalified plant matter form parts of beds in the mudshale microsequence in the sandstone-mudstone facies and in upward-fining and crossbedded microsequences in the composite sandstone facies. Coaly material was isolated and prepared for microscopic examination and analysis by vitrinite reflectance (Mark Pawlewicz, USGS, Denver, June, 1986). Six samples were studied and indicate that the coal particles are all vitrinite. Vitrinite is the

maceral or organic component of the coal type vitrain (Pettijohn, 1975). The vitrinite group of macerals originates in wood and bark (Blatt, 1982). The open cell structure of the coal clasts suggests immature coals and that the organic material either underwent low burial compaction or that other material was not available to fill in the cells. The immaturity of the coals suggests low-heat, shallow burial diagenetic or coal-forming conditions of short duration (Pawlewicz, pers. comm., June, 1986).

Clay Minerals

Clay minerals are locally recognizeable in thin section but are difficult to separate and count as a separate entity within the interstitial complex of clay minerals and cements. Eight samples were chosen for analysis by x-ray diffraction to identify clay minerals observed in thin section. The results of the analysis are summarized in table 4.2. Fifty-three to sixty-nine percent of the less than 2 micron clay fraction in samples of the composite sandstone facies is an iron-chlorite clay. Pelletoid grains indentified as glauconite under the microscope are sometimes identified as iron-chlorite by x-ray diffraction (W. A. Pryor, Univ. Cincinnati, pers. comm., September, 1987).

Two general relationships between facies and clay minerals are suggested by the data in table 4.2. The first relationship is that the deeper-water shoreline deposits in the sandstone-mudstone facies and composite sandstone facies in the Curtis are richer in iron-chlorite (glauconite) and mixed-layer illite-smectite clays. The second relationship is that the shallower-water, higher intertidal deposits in the rippled silty facies in the Curtis and the reddish-brown silty

facies in the Summerville are richer in smectite.

Cements

Cements in all samples examined petrographically are extremely heterogeneous and suggest a complex diagenetic history. Coarse, equant, sparry calcite is a consistently dominant cement in all samples. It forms a complex with clay minerals and other cements such as neomorphic microspar, neomorphic spar, micrite, dolomite, hematite, silica and gypsum in approximate order of decreasing abundance.

Table 4.1. Summary of petrographic analysis of sandstone samples from facies in the C

FACIES	Quartz		Feldspar			Rock fragments			
	Monocrystalline	Polycrystalline	Orthoclase	Plagioclase	Microcline	Chert	Carbonate	Sandstone-siltstone-shale	Igneous
Curtis Formation									
sandstone-mudstone facies	64.0	2.0	3.0	2.0	0.4	12.0	12.0	0.2	0.3
composite sandstone facies	78.0	2.0	7.0	3.0	0.2	4.0	1.0	0.1	--
rippled silty facies	75.0	0.7	5.0	2.0	0.1	7.0	0.1	0.6	--
redbed facies	90.0	1.0	3.0	1.0	--	4.0	--	--	--
Moab Tongue									
wrinkled sandstone facies	96.0	2.0	--	--	--	--	--	--	--
wavy sandstone facies	94.0	0.5	2.0	0.5	--	3.0	--	--	--
crossbedded sandstone facies	94.0	1.0	2.0	--	--	3.0	--	--	--
Summerville Formation									
reddish-brown facies	83.0	0.4	5.0	2.0	--	7.0	--	--	--
gypsiferous facies	85	1.0	8.0	2.0	--	3.0	--	--	--

ıdstone samples from facies in the Curtis-Moab-Summerville interval

ldspar		Rock fragments										
Plagioclase	Microcline	Chert	Carbonate	Sandstone-siltstone-shale	Igneous	Fossils and other allochemical grains	Glauconite	Heavy minerals	Evaporite	Matrix	Cement	Number of samples
2.0	0.4	12.0	12.0	0.2	0.3	3.0	0.6	0.5	--	0.1	34.0	15
3.0	0.2	4.0	1.0	0.1	--	1.5	3.0	0.2	--	1.0		12
2.0	0.1	7.0	0.1	0.6	--	0.2	7.0	2.3	--	--	48.0	11
1.0	--	4.0	--	--	--	0.4	0.1	0.5	--	--	62.0	8
--	--	--	--	--	--	--	--	--	--	17.0	19.0	1
0.5	--	3.0	--	--	--	--	--	--	--	17.0	16.0	1
--	--	3.0	--	--	--	--	--	--	--	--	0.5	2
2.0	--	7.0	--	--	--	--	0.8	1.8	--	--	60.0	10
2.0	--	3.0	--	--	--	0.6	--	0.4		--	63.0	6

Table 4.2. Percentage of matrix clay minerals as determined from x-ray diffraction analysis of the less than 2 micron clay fraction in selected samples from the Curtis-Moab-Summerville interval. Analysis and data provided by R. Pollastro (USGS, Denver)

LOCATION	FACIES	SAMPLE	Illite	Illite/smectite	Smectite	Iron-chlorite	Kaolinite	Percent of bulk rock
Tidwell Draw (Z-9)	sandstone-mudstone	Z-9B, S-2	31.0	67.0	--	2.0	--	11.0
Tidwell Draw (Z-9)	sandstone-mudstone	Z-9, S-2	18.0	73.0	--	9.0	--	12.0
San Rafael Swell-Northeast (Z-3)	composite sandstone	Z-3A, S-4	3.0	28.0	--	69.0	--	16.0
San Rafael Swell-West (Z-6)	composite sandstone	Z-6, S-1b	15.0	32.0	--	53.0	--	7.0
Wild Horse Creek (Z-13)	rippled silty	Z-13, S-4	9.0	--	86.0	5.0	--	13.0
Lookout Point (Z-14)	rippled silty	Z-14, S-2	19.0	75.0	--	6.0	--	6.0
Lookout Point (Z-14)	rippled silty	Z-14, S-3	2.0	--	97.0	1.0	--	24.0
Mussentuchit Wash (Z-24)	reddish-brown silty	Z-24, S-8	7.0	--	91.0	2.0	--	10.0

CHAPTER 5

PALEOGEOGRAPHY

Summary of Late Middle Jurassic Depositional Systems

The history of middle Jurassic sedimentation in east-central Utah is recorded in the complexly stratified detrital rocks of the Curtis-Moab-Summerville interval. During the second and final trangressive-regressive cycle in late middle Jurassic (Callovian) time, tide-, wave-, and occasional storm-currents deposited crossbedded, crosslaminated, and flat-bedded sandstone, siltstone, and mudstone in intertidal and shallow subtidal zones along a wind-swept coastal plain. Prograding sandy, muddy shoreline zones were established in the south in the northern Henry Mountains area and to the east in the Green River Desert area.

A dominant sandy tidal system is interpreted for facies in the Curtis and Summerville Formations based on the detailed descriptions and interpretations given in Chapter 3. Locally preserved physical sedimentary features indicate the occasional effects of wave-, wind-, and storm-currents. At the eastern edge of a supratidal sabkha, sand was reworked by variable winds to form a localized sand sea composed of dunes and draas in the Moab Tongue which was contemporary with middle and upper parts of the Curtis. Table 5.1 is a synthesis of the paleoenvironmental interpretations of facies and microsequences presented in chapter 3. Figure 5.1 shows the stratigraphic and spatial distribution of facies and their respective origins in the Curtis-Moab-Summerville interval.

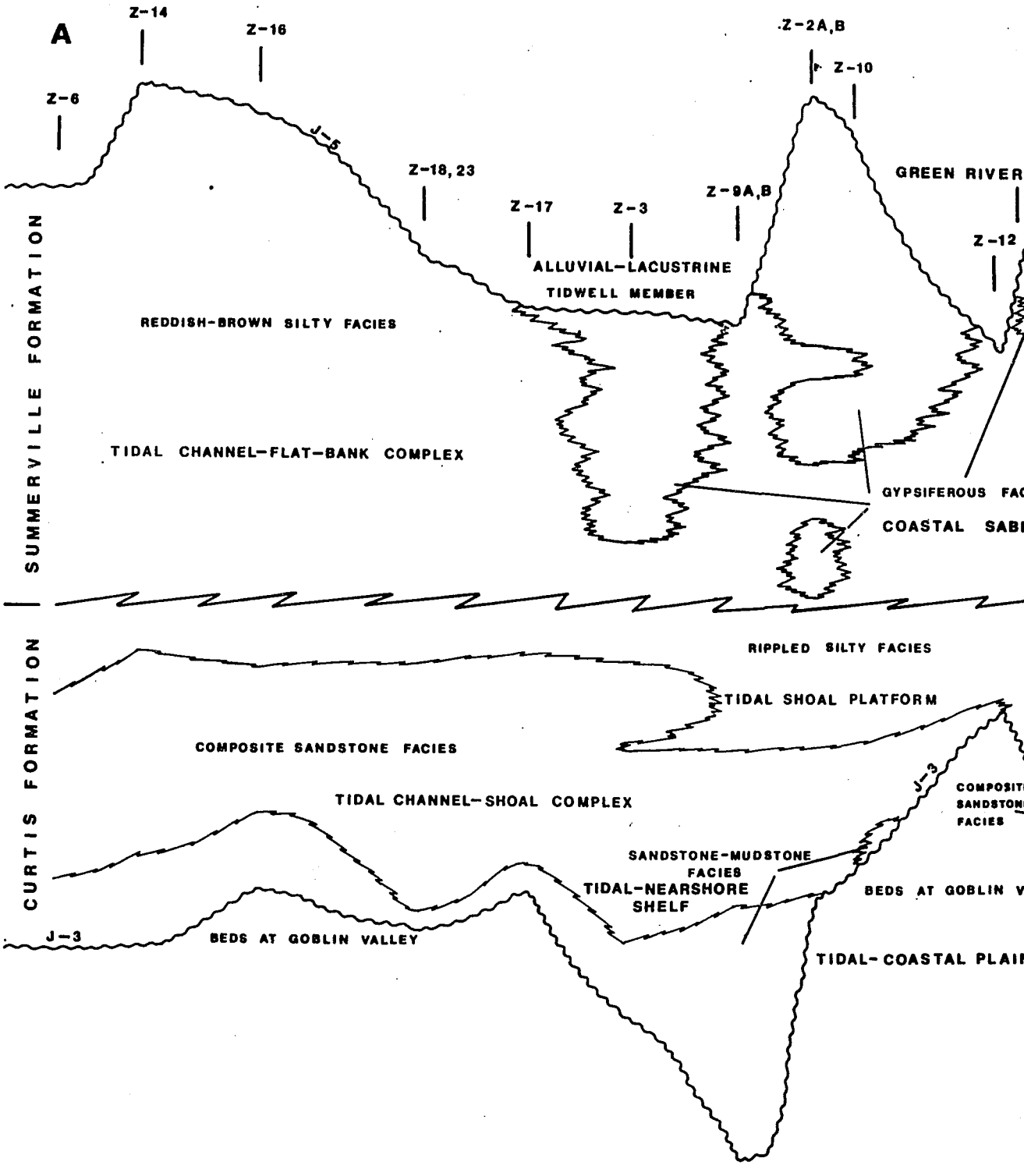

Figure 5.1. Distribution of facies and sedimentary origins thereof in the Curtis-Moab-S
(table 1.1 for names and locations of stratigraphic sections)

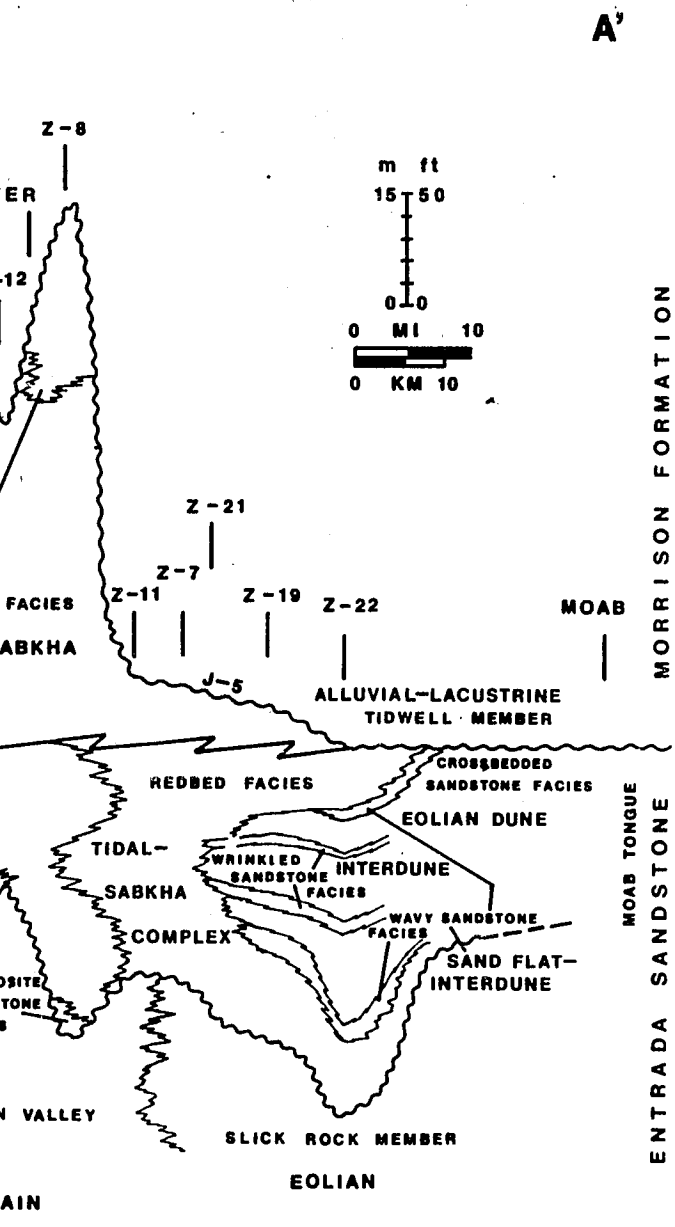

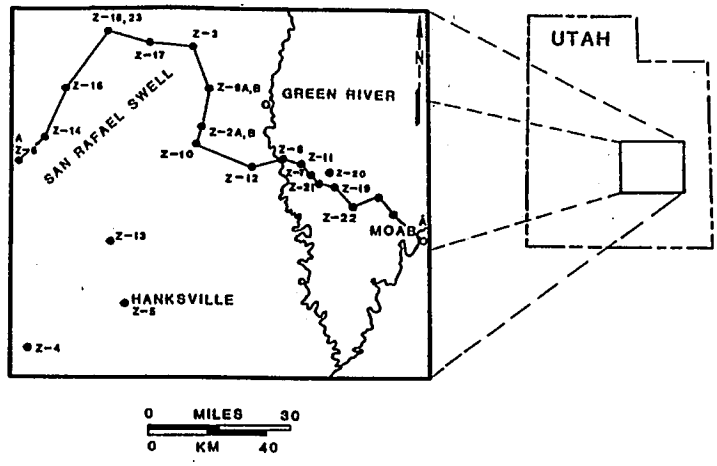

b-Summerville interval of east-central Utah

Table 5.1. Summary of late Middle Jurassic (Callovian) depositional systems of east-central Utah

Stratigraphic Interval	Facies and Microsequences	Depositional Environment
Summerville Formation	Reddish-brown silty facies upward-fining, upward-thinning microsequence	Upper intertidal-supratidal sand flat-tidal channel-channel bank; influenced by storm- and wind-enhanced tidal flooding; regressive
	lenticular microsequence	
	Gypsiferous facies chaotic microsequence	Upper intertidal-supratidal sandy coastal sabkha/salina; regressive
Entrada Sandstone Moab Tongue	Crossbedded sandstone facies	Coastal eolian dune and draa complex
	Wrinkled sandstone facies	Mixed wet-dry interdune
	Wavy sandstone facies upward-coarsening, upward-thickening micro-sequence	Eolian sandflat, interdune, fore-erg complex
Curtis Formation	Redbed facies upward-fining, upward-thinning microsequences	Upper intertidal-supratidal sandy coastal sabkha influenced by storm- and wind-tidal flooding; minor transgressive-regressive
	Rippled silty facies	Middle(?)-upper(?) intertidal shoal plat-form/berm influenced by tidal and minor wave currents

Table 5.1. Continued

Stratigraphic Interval	Facies and Microsequences	Depositional Environment
Curtis Formation (cont.)		
	Composite sandstone facies crossbedded microsequence parallel-bedded microsequence	Shallow subtidal to intertidal sandy shoal and channel complex influenced by tidal- and wave-currents; maximum transgression, incipient regression
	Sandstone-mudstone facies upward-fining, upward-thinning microsequence upward-coarsening, upward-thickening microsequence mudshale microsequence basal gravelly microsequence	Shallow nearshore shelf; influenced by tide- and wave-currents; initial transgression

Paleogeographic Reconstructions

Callovian Paleogeography and Tectonic Setting of the Western Interior

A reconstruction of regional paleogeography for the Western Interior during late middle Jurassic (Callovian) time (fig. 5.2) is based on paleoenvironmental reconstructions in this report and stratigraphic and tectonic studies in other reports (Dickinson, 1976, 1981b; Allmendinger and Jordan, 1981; Imlay, 1980; Kocurek and Dott, 1983; Bilodeau, 1986).

During Callovian time, east-central Utah was positioned at about 18 degrees north latitude (fig. 5.2). An arm of the main proto-Pacific ocean extended into southern Utah from southwestern Canada and the Pacific Northwest and also covered parts of Idaho, Wyoming, and Colorado. Plate tectonic reconstructions suggest that volcanoes associated with a trench-subduction system near western California (Hamilton, 1969a, 1978) were present as either a Japanese-type island arc or Andean-type magmatic arc complex as early as late Paleozoic (Rogers et al., 1974). Regional tectonic studies have suggested that magmatic arc volcanism occurred throughout the Mesozoic in various parts of eastern California and Nevada (Dickinson, 1976, 1981b; Burchfiel, 1981). Stratigraphic studies and the recognition of reworked volcanic rock fragments have shown that volcanoes were contemporary sediment sources during deposition of the Triassic Chinle Formation (Blakey and Gubitosa, 1983; Stewart et al., 1986), the early Jurassic Nugget-Aztec-Navajo Sandstone (Marzolf, 1986), and the Middle Jurassic (Bajocian-Bathonian) Carmel Formation (Caputo, 1980, 1981; Chapman, 1986). The rarity or absense of volcanic rock fragments in the Curtis-

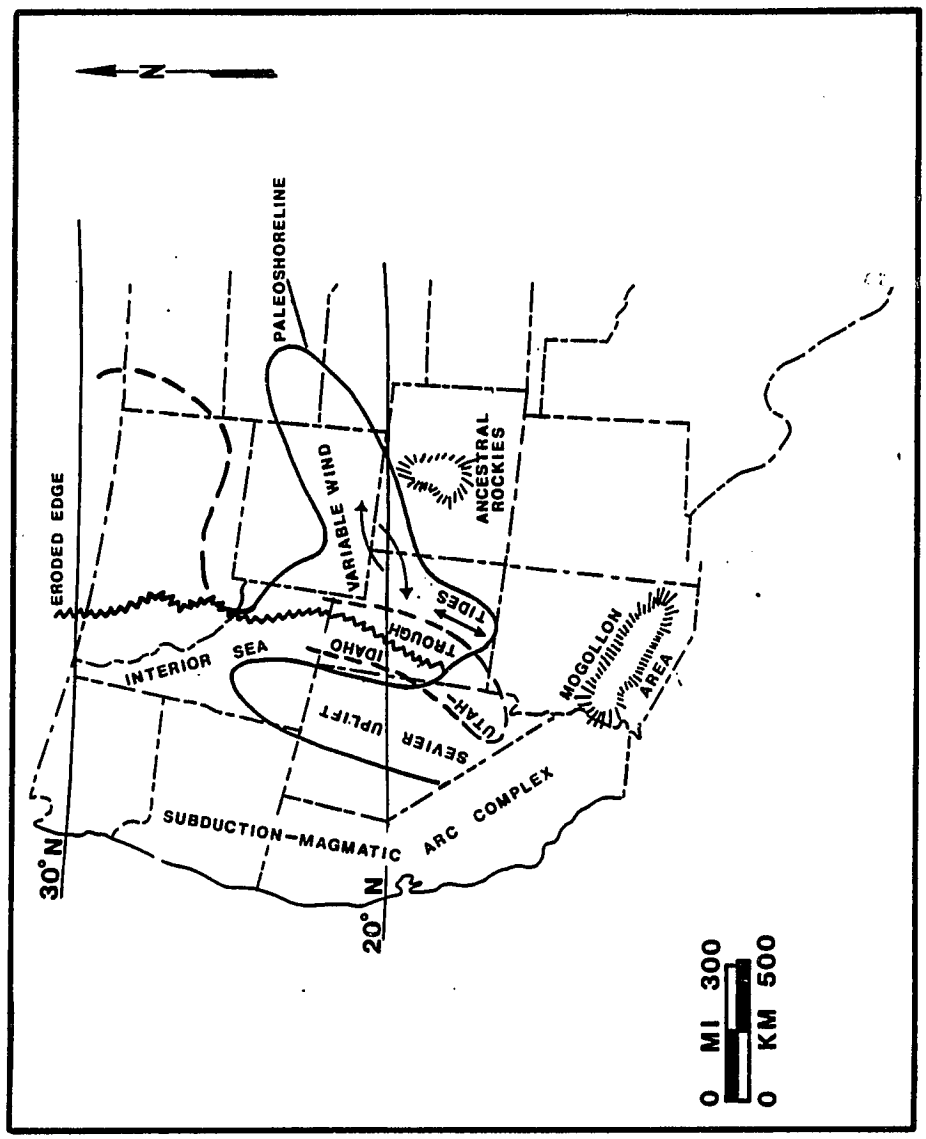

Figure 5.2. Regional paleogeographic and tectonic setting for the Western Interior during late middle Jurassic time (modified from Dickinson, 1976, 1981b; Imlay, 1980; Kocurek and Dott, 1983; Peterson, 1987)

Moab-Summerville interval suggest that volcanoes were either temporarily inactive or were separated from the marine basin to the east by a subtle physiographic barrier (fig. 5.2).

The interior seaway was restricted on the west by a gentle crustal uplift produced by folding and thrusting, events related to incipient deformation in the Sevier orogenic belt (Allmendinger and Jordan, 1981; Peterson and Caputo, 1986). The Mogollon region of southern Arizona has been considered a site of uplift and potential source terrane for Triassic (Blakey and Gubitosa, 1983) and some Jurassic rocks. It has been inferred as a physiographic barrier preventing interior seaways from extending further south during middle Jurassic time (Caputo, 1980; Blakey et al., 1983; Kocurek and Dott, 1983). It is still uncertain whether or not there were direct sediment sources for the Jurassic basin to the west.

In western Utah, all Jurassic rocks have been removed by erosion along the sub-Cretaceous (K-1) unconformity (Peterson and Pipiringos, 1979) and the paleogeographic configuration of the western shoreline is an inferred restoration.

Early Callovian (Entrada) Paleogeography

The epicontinental seaway, along which the Carmel Formation and contemporaneous Page Sandstone were deposited, partially withdrew form the Western Interior in early Callovian time. An expansive sandy desert extended across the southeastern one-third of Utah as deflationary winds swept across the generally northward prograding coastal plain (Kocurek and Dott, 1983). Crossbedded sandstones of the Slick Rock Member of the Entrada Sandstone were deposited in a dune-draa-interdune complex concurrent with Beds at Goblin Valley and earthy facies in the

Entrada which were deposited in sandy, silty, muddy tidal flat and local alluvial systems. Other contemporary strata in the Twin Creek Limestone, Arapien Shale, and Preuss Sandstone record siliciclastic and local carbonate sedimentation in and around a foundering, restricted seaway in north-central Utah (fig. 5.3).

The association of crossbedded eolian sandstones, coastal plain redbeds and marginal marine evaporites suggests a warm, dry climate. Paleowinds were generally northerly and northeasterly trade winds; sand transport was southward and southwestward (Poole, 1962; Kocurek, 1981a; Kocurek and Dott, 1983). Marginal marine environments experienced restricted hypersaline conditions which favored the precipitation of evaporites. Sedimentary and climatic conditions were suitable to only a few tolerant organisms along the shoreline. Deeper in the basin, normal marine conditions fostered the growth of diverse molluscan communities (Imlay, 1948, 1957, 1967; Sohl, 1965). Complete withdrawal of the seaway during middle Callovian time was followed by widespread deflation and erosion and gentle crustal upwarping associated with the J-3 unconformity (Pipiringos and O'Sullivan, 1978).

Middde and Late Callovian (Curtis-Moab) Paleogeography

Although uncertain, it is likely that combined eustatic and tectonic (allocyclic and autocyclic) changes within the central Utah basin were associated with renewed marine trangression during late middle Callovian time. This would be the final, cyclic marine invasion into the Western Interior, particularly southern Utah, during Jurassic time.

The nearly syndepositional Curtis and Moab sandstones and related Summerville beds were deposited by nearshore shelf and coastal plain

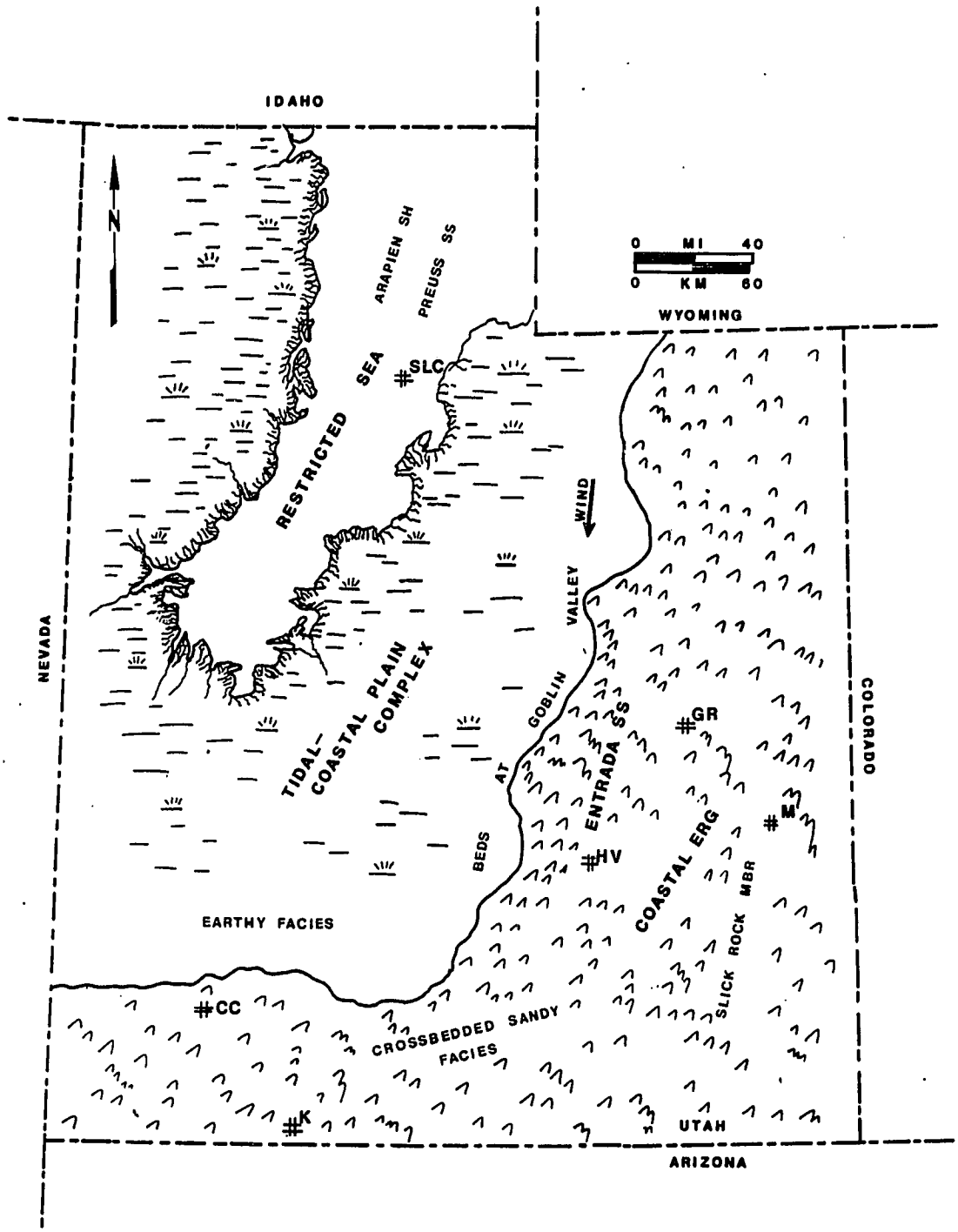

Figure 5.3. Early Callovian paleogeographic setting during deposition of the Entrada Sandstone and related strata in Utah (modified from Kocurek and Dott, 1983). Towns: Salt Lake City: SLC; Cedar City: CC; Kanab: K; Green River: GR; Moab: M. Hanksville: HV

processes during the final Jurassic transgressive-regressive cycle (fig. 5.4). The three stratigraphic units comprise a genetic sequence of middle Jurassic rocks bounded by regional unconformities. Marine and non-marine sedimentary strata in the Curtis and Entrada Formations, respectively, are sharply juxtaposed along the J-3 unconformity.

The initial transgressive events are preserved in the sandstone-mudstone facies of the Curtis. Within this facies, sedimentary features of the basal gravelly microsequence suggest the reworking of relict and newly eroded gravelly lithoclasts by mostly shoreline tidal currents aided by wave- and possibly storm- or wind-enhanced marine currents. The relict gravels were mixed with Curtis sediment and fashioned into dune-like bedforms which migrated predominantly northeastward in uniformly flowing marine currents. The presence of these gravels may signal incipient deformation during the Sevier orogeny, a confirmed Cretaceous event, previously unrecognized in Jurassic strata. Mudshale, upward-coarsening, upward-thickening and upward-fining, upward-thinning microsequences record full marine conditions at depths at or near normal wave base. Peak flood- and ebb-tidal currents and slackwater currents were infrequently abetted by wave-orbital currents and higher-energy currents influenced by surface storms or wind. Sand was intermittently transported in the form of ripples and megaripples. The feeding and crawling activity of soft-bodied worms, crustaceans, and possibly gastropods was recorded in the soft, somewhat cohesive mud and silt which was slowly settling during slackwater periods.

Near the southern shoreline, which extended into the northern Henry Mountains area, and the eastern shoreline which was developed in the Green River Desert, contemporary facies of the composite sandstone, rippled silty and redbed facies were deposited by mostly tidal and

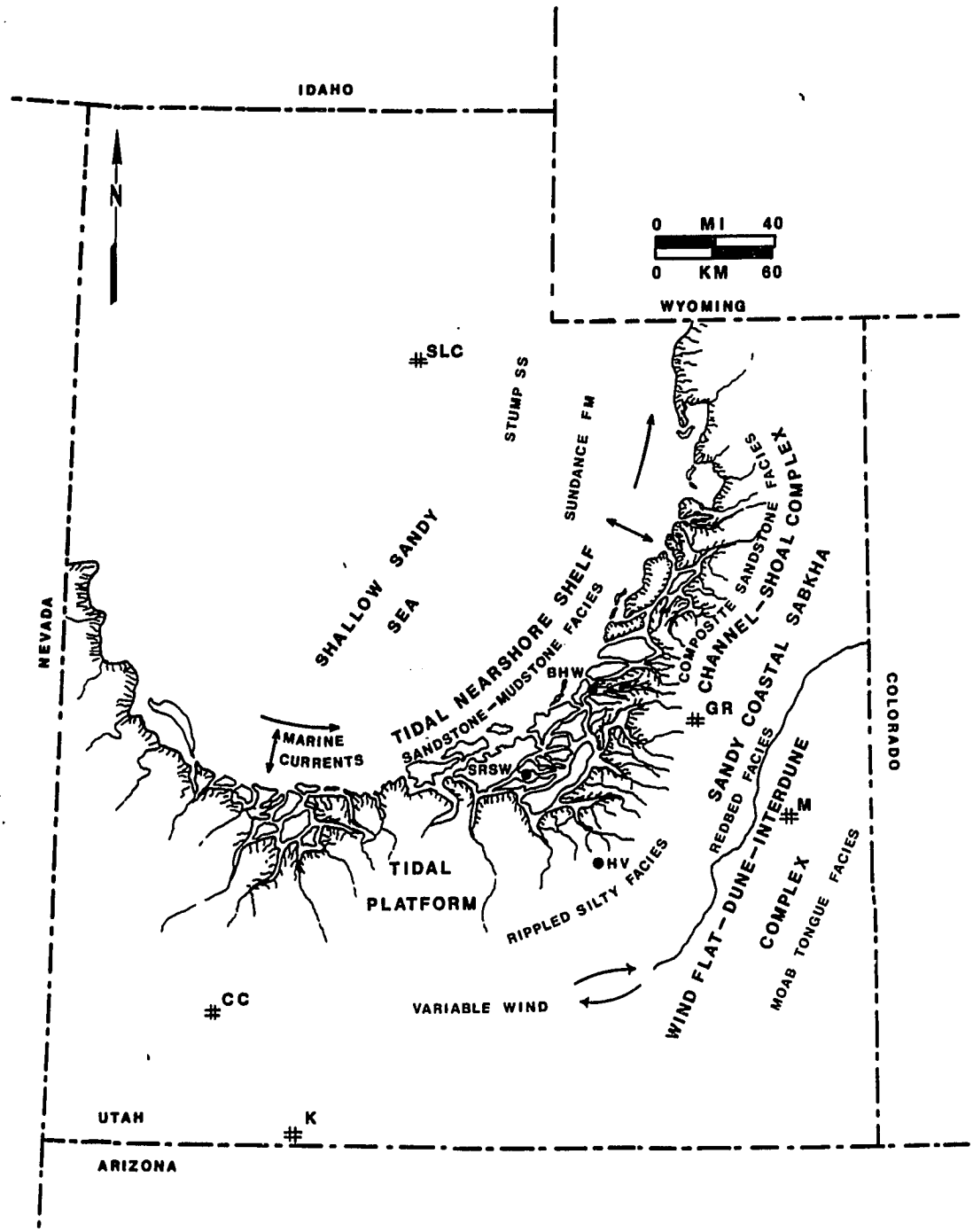

Figure 5.4. Middle and late Callovian paleogeographic setting during deposition of the Curtis-Moab interval and related strata in Utah (modified from Caputo and Peterson, 1986). Towns: Salt Lake City: SLC; Cedar City: CC; Kanab: K; Green River: GR; Moab: M. Stratigraphic sections: Buckhorn Wash: BHW; San Rafael Swell West: SRSW; Hanksville: HV

minor wave-currents in progressively higher parts of an intertidal and supratidal muddy, silty, sand flat. Marine circulation was largely controlled by tidal flow which was roughly north-south and parallel to the eastern shoreline. This general shore-parallel flow was locally modified by uniform shore-normal tidal exchange in channels and multidirectional paleoflow during unrestricted run-off and tidal flat emergence. In the upper subtidal to lower intertidal shoreline zones, the highest tidal- and wave-current energies constantly reworked very fine to medium grained sand in a network of tidal passes coursing through and around topographically elevated, more emergent sand shoals and berms. Some channels were flood-dominated others were ebb-dominated and the whole complex of channels and shoals constantly shifted laterally with time and built an amalgamated mass of crossbedded and parallel-bedded sandstone. The coastal plain was very sparsely overgrown with shore grasses and trees which may have become more dense to the west.

A higher intertidal sand flat was a rippled platform which formed a mantle around the shoreline and passed approximately through the Green River townsite. It was constantly awash in gentle tidal- and wave-currents. This rippled platform and interchannel shoal and berm system became fully emergent at low tide and were delicately reworked by foraging intertidal organisms. Only the highest spring tide floods and occasional storm- and wind-enhanced spring tide floods deposited sand, silt and mud in beds of the redbed facies. Between floods, this supratidal coastal sabkha environment was dry and biologically barren. Salinities were too low to favor the precipitation of evaporites.

The position of the shoreline remained relatively stable in the

Green River Desert area at this time except for minor fluctuations and small-scale transgressions during deposition of the redbed facies.

Variable daily and seasonal winds with a strong westward component reworked sand from a deflated dune field of the Slick Rock Member (Entrada Sandstone) in extreme eastern Utah. Infrequent coastal storms may have caused temporary, eastward, onshore-blowing winds but uniform easterly or seaward-blowing winds favored the westward progradation of a small coastal erg of the Moab Tongue. Small incipient dunes and wind-rippled sand flats built a foundation over the progressively drying sandy coastal sabkha of the redbed facies.

Simple barchan, transverse or oblique dunes advanced seaward and deposited a relatively thin margin of sand around a thicker interior erg where complex draas were constructed of mobile simple dunes. Broad interdune areas were periodically wetted during rain storms or periodically flooded during storm-enhanced spring tides. Very few plants and animals thrived in the interdunes which became ultimately buried by a westward prograding draa complex of the central erg.

The development of the Moab erg culminated in early late Callovian time. Further development of eolian sedimentation was suppressed by a decreased area of sand available for entrainment and trannport by wind. The sand-starved conditions were caused either by renewed marine transgression and eastward retreat of the shoreline-eolian system or erg burial by a westward prograding backerg, interdune sabkha. Periodic meteoric or tidal flooding again controlled sedimentation on a supratidal coastal sabkha at the end of Curtis time.

Late Callovian (Summerville) Paleogeography

Higher-energy, sand-dominated tidal flats in the Curtis evolved, with time, into relatively lower-energy, sandy mud- and silt-dominated flats in the Summerville. The interior seaway became narrow and restricted as it began to recede northward; the surrounding prograding coastal plain followed this general northward path of retreat (fig. 5.5).

The Summerville coastal plain was a broad, featureless platform with no vegetation and few organisms tolerating aridity, long periods of exposure and hypersaline, evaporative conditions. Sedimentation was controlled by rhythmic tidal flooding, laterally shifting tidal creeks and gullies, interstitial crystallization of gypsum and subaqueous precipitation of gypsum in local salinas or ponds on a coastal sabkha. At the shoreline, the intertidal flat was dissected by a dense network of ebb-dominated tidal channels and gullies with paleoflow directions mainly to the northeast.

Topographic relief in the form of low mountains, which were initially uplifted during Curtis time along the western shoreline, may have been more fully developed during Summerville time as a result of continuing deformation in the Sevier orogenic belt. Eolian sedimentation is recorded in the Romana Sandstone as a very localized coastal erg which accumulated near the southern tip of the Summerville seaway. Paleowind directions for the Romana erg were eastward (Peterson, 1987).

Sedimentation during Summerville time represents the final gasp of marine sedimentation in the Western Interior, mainly southern Utah, during Jurassic time. Middle Jurassic marine-eolian sedimentary associations were first established in the contemporary Carmel and Page

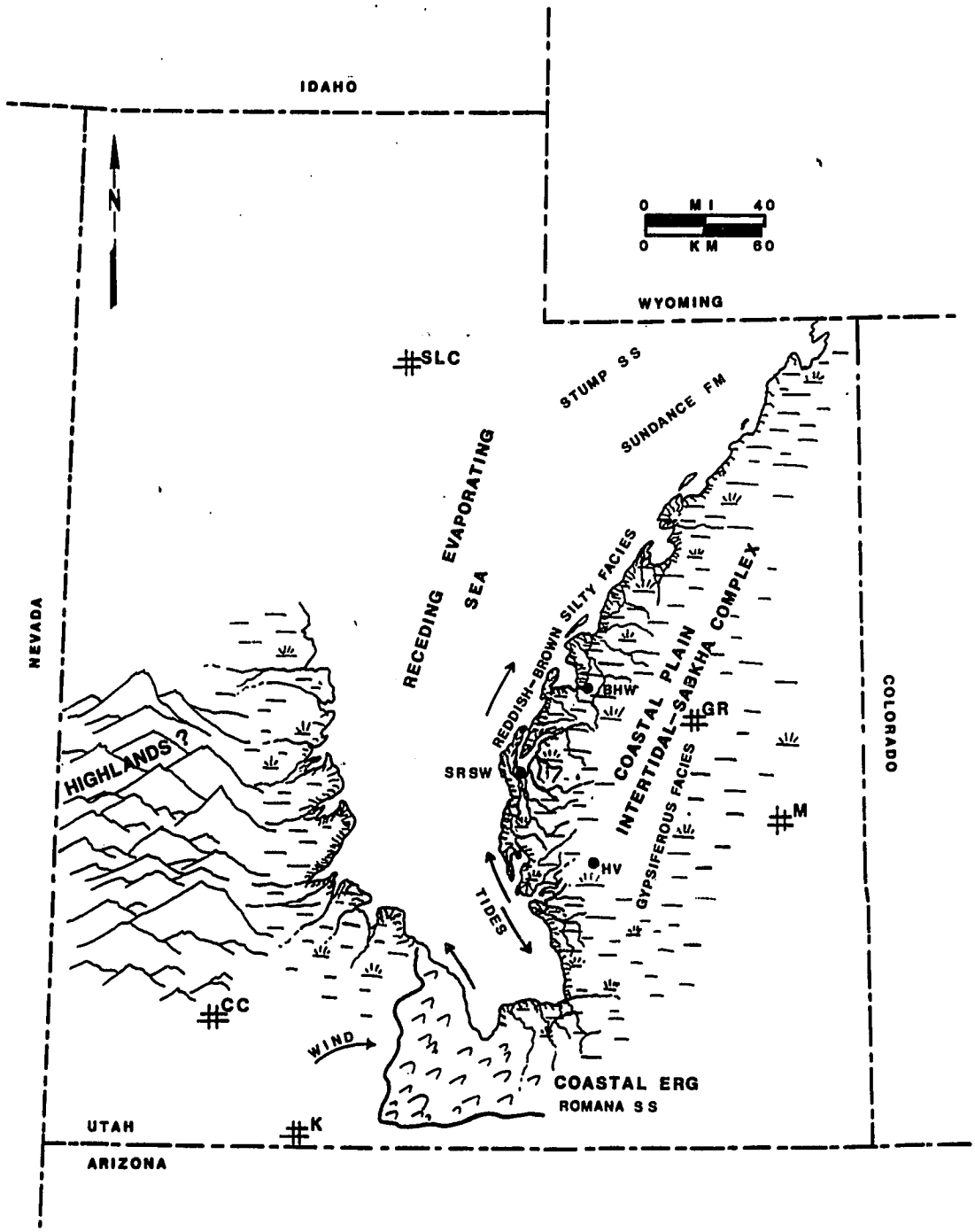

Figure 5.5. Late Callovian paleogeographic setting during deposition of the Summerville Formation and related strata in Utah (modified from Caputo and Peterson, 1986; Peterson, 1987). Towns: Salt Lake City: SLC; Cedar City: CC: Kanab: K; Green River: GR; Moab: M. Stratigraphic sections: Buckhorn Wash: BHW; San Rafael Swell West: SRSW; Hanksville: HV

Formations and persisted in facies of the Entrada Sandstone. The Curtis-Moab-Summerville interval preserves the last Jurassic marine-eolian sedimentary association in southern Utah. Following widespread erosion and truncation of strata in the Summerville, Curtis, and Moab, the late Jurassic sedimentary and tectonic history of southern Utah is preserved in widespread alluvial, paludal, and lacustrine deposits of the Morrison Formation.

Callovian Tectonic Setting of East-Central Utah

The Western Interior of the United States, mainly the Colorado Plateau province, had, until recently, been considered a relatively undeformed and tectonically stable portion of cratonic crust throughout the Triassic and Jurassic Periods. Development of domal and monoclinal flexures was attributed to late Jurassic and Cretaceous events such as the Nevadan, Sevier, and Laramide orogenies which involved complex subduction, magmatism and island-arc accretion in the California-Nevada region (Dickinson, 1976, 1981b; Schweickert and Cowan, 1975). Slight but noteworthy positive and negative structural elements were actively controlling sedimentation and distribution of facies throughout the Jurassic period (Peterson, 1987). Stratigraphic data for the upper San Rafael Group in east-central Utah confirm such a tectonic influence on the distribution of facies during late middle Jurassic (Callovian) time.

The prominent structural elements in east-central Utah are the northeast-trending axis of the San Rafael Uplift, the north-trending axis of the Henry Basin, and the northeast-trending axis of the Monument Uplift (fig. 1.1). Sedimentologic data and stratigraphic relationships in the San Rafael Swell and Green River Desert areas

indicate that the orientation of the eastern paleoshoreline and boundaries between contemporary facies in the Curtis follow a northeastward trend which is parallel to the axis of these structural elements.

The total isopach distribution of the Curtis-Moab-Summerville interval is shown in figure 5.6. A general pattern is one of stratigraphic thickening to the west. This is a pattern similar to that in mapped intervals in the lower San Rafael Group, namely parts of the Carmel and Page Formations (Voorhees, 1978; Caputo, 1980; Peterson, 1987). This westward thickening of strata is consistent with two regional crustal relationships in the Colorado Plateau region during Jurassic time. One is the interpretation of a regional Utah-Idaho trough in western Utah and eastern Nevada (fig. 5.2) which had been tectonically active during early middle Jurassic time (Peterson, 1987). The second is that during deposition of the San Rafael Group, there was westward regional tilting of the Colorado Plateau region (Peterson, 1987; Blakey, in press). Observations made in this study along the Water Pocket Monocline indicate local tilting to the south. Here, units of the Entrada Sandstone beneath the J-3 unconformity dip to the south and the J-3 unconformity truncates progressively down-section to the north. This structural relationship may reflect the presence of the northern edge of the Henry Basin.

A prominent depositional trough follows a northeastward trend and is nearly coincident with the axis of the San Rafael Uplift (cf. figs. 1.1, 5.6). Furthermore, the wider contour spacing in the central San Rafael Swell area is contrasted with narrower contour spacing on the east side of the Swell. The wide contour spacing in the central San

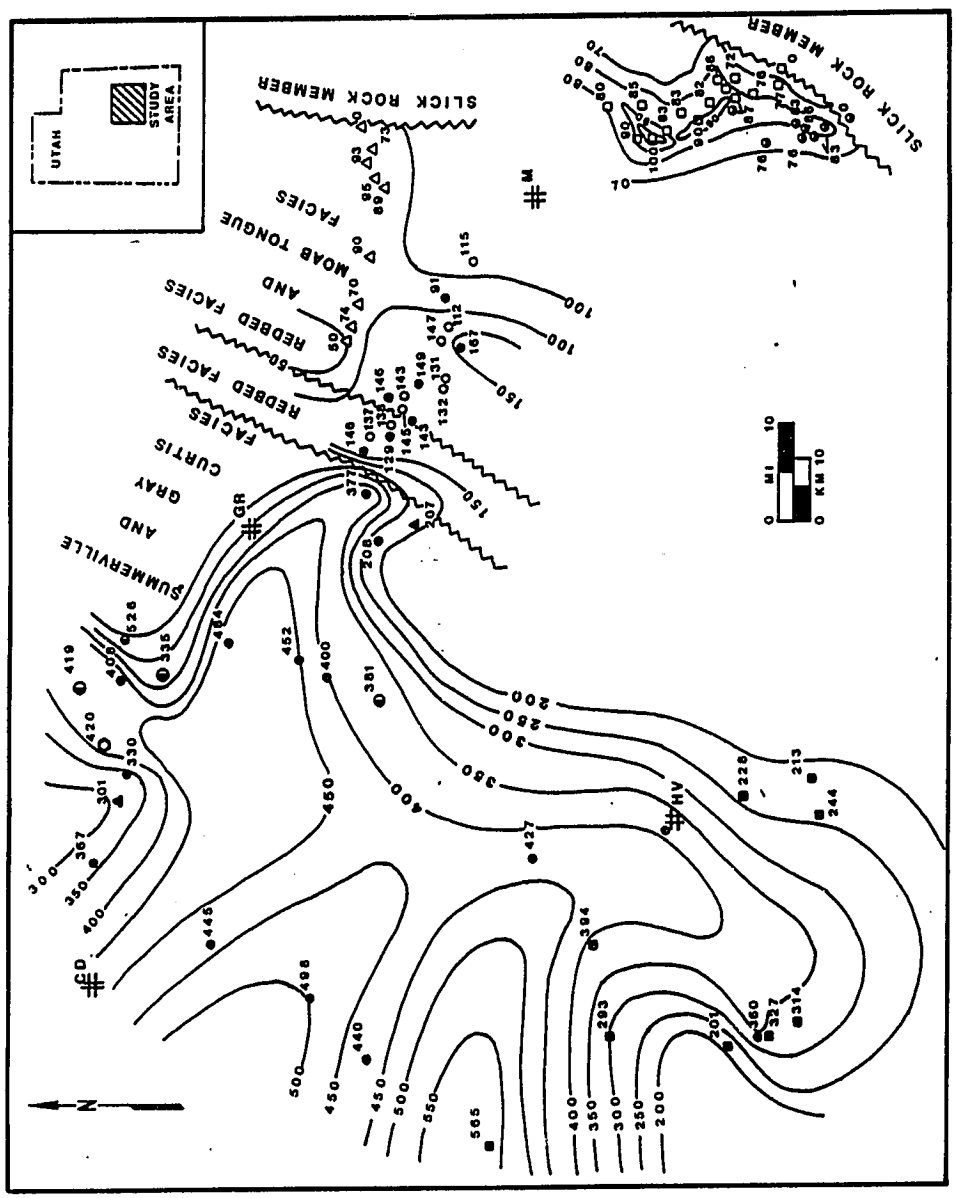

Figure 5.6. Isopach map of the total Curtis-Moab-Summerville interval in east-central Utah. Contour interval: 50 ft (15 m). Map symbols (table 1.3)

Rafael Swell may be apparent and may be related to removal of strata by uplift and erosion. If the interpretation is real, then the San Rafael Uplift may have been active as a gentle structural bench during middle Jurasic time. The southward-extending depositional trough is best developed in the northern Henry Mountains area near Hanksville and is suggestive of subsidence in the Henry trough at that time. This is consistent with the interpretations of Peterson (1987).

The northeast trend of the Curtis paleoshoreline, the facies boundaries in the Curtis and eastward thinning of the Curtis (fig. 3.3) suggest a control on the distribution of facies by active but subtle uplifts in the Monument region in middle Jurassic time. Peterson (1987) has interpreted the Monument region as a structural bench that influenced sedimentation throughout the Jurassic Period.

Stratigraphic data for the Moab Tongue suggest that its distribution may have been confined to a subtle regional down-warping of the crust between the gentle San Rafael Swell and Monument Uplifts (cf. figs. 1.1, 3.41).

CHAPTER 6

SUMMARY AND CONCLUSIONS

Stratigraphic, Sedimentologic, and Tectonic Summary

The upper part of the Middle Jurassic San Rafael Group is exposed along the flanks of domal uplifts and monoclinal ridges in east-central Utah, namely in the San Rafael Swell, Green River Desert and northern Henry Mountains areas. It consists of the Curtis Formation, Moab Tongue of the Entrada Sandstone, and the Summerville Formation, in ascending order. These stratigraphic intervals comprise a genetic sequence bounded by the regional Jurassic unconformities J-3 at the base and the J-5 at the top. Field data indicate that the Curtis Formation unconformably overlies the Beds at Goblin Valley of the Entrada Sandstone along the J-3 horizon. This unconformity may partially extend across the Slick Rock Member as a super bounding surface beneath the Moab Tongue. Beds at the top of the Summerville Formation are truncated by the J-5 unconformity beneath the Tidwell Member of the Morrison Formation.

The first middle Jurassic transgressive-regressive cycle is preserved in the lower San Rafael Group of east-central Utah and consists of the Carmel, Page, and Entrada Formations. The Carmel seaway partially withdrew from southern Utah as eolian desert, coastal plain and shoreline environments prograded northward and westward. A residue of gravelly sediments remained after erosion and deflation along the Entrada surface. The initial transgression of the Curtis seaway reworked and mixed this residue with other Curtis sediments which

became the basal gravelly microsequence in the basal facies of the Curtis, the sandstone-mudstone facies. Successive heterolithic microsequences in the sandstone- mudstone facies record rhythmic sedimentation of sand, silt, and mud by tidal currents, burrowing of benthic organisms during slackwater or neap tide, upward-shallowing conditions, and greater availability and transport of sand. Contemporaneous composite sandstone facies, rippled silty facies, and redbed facies represent sedimentation in higher intertidal and supratidal environments. Maximum transgression, stillstand, and incipient regression is recorded in the composite sandstone facies. A network of subtidal and intertidal channels scoured by ebb- or flood-dominated currents and buried by crossbedded sandwave and dune strata was developed at the shoreline. Complex tidal courses migrated around elevated sand shoals and berms which were constructed by ripples and plane beds at high tide and were exposed at low tide. The higher sand flat was less dissected with channels and gullies and evolved as a smooth rippled platform during deposition of the rippled silty facies. Crossbedding indicates uni- and bidirectional tidal currents in channels; crosslaminations indicate multidirectional current patterns produced by low-tide emergence and run-off.

Marine influence by wind- or storm- enhanced spring tidal flooding extended into the Green River Desert area where mostly ripple laminated and some crossbedded strata of the redbed facies interfinger with strata of the Moab Tongue. Deposition of the Moab Tongue represents a temporary regression of the shoreline as a localized coastal erg prograded westward. Erg margin deposits are mixed with subaqueous ripple and megaripple beds and wind-stratified deposits in the wavy sandstone facies because of infrequent storm- and tidal-current

flooding of the upper supratidal flat and erg margin. Complex draa and dune strata were deposited in the erg interior and comprise the crossbedded sandstone facies. These dune deposits are interrupted by the wrinkled sandstone facies which was deposited by water- and wind-ripples in a fluctuating wet and dry interdune environment. Wind directions were variable but an easterly component was dominant.

The complete regression of the middle Jurassic seaway from southern Utah is indicated by stratification sequences in the Summerville Formation. Restricted, hypersaline conditions on a coastal sabkha favored the early crystallization of gypsum which displaced and disrupted bedding in sandy, muddy chaotic microsequences of the gypsiferous facies. Gypsum crystals were locally reworked to form crossbedded and crosslaminated gypsum beds that were probably deposited in ephemeral coastal ponds or salinas. The reddish-brown silty facies was deposited in a system of shallow intertidal channels, channel banks, and interchannel flats at the shoreline. Sand, silt, and mud were rhythmically deposited by mostly ripples migrating with the tidal currents.

The Curtis-Moab-Summerville interval preserves the last Jurassic marine-eolian sequence in southern Utah. Arid, windy conditions of a northern trade-wind belt combined with probable eustatic and minor tectonic changes around the marine basin favored the cyclic occurrence of sandy, shallow-marine platform deposits with coastal plain eolian deposits. Following uplift and erosion along the J-5 unconformity, the sedimentologic and paleogeographic setting for most of the Western Interior during late Jurassic time was characterized by widespread alluvial and lacustrine sedimentation in the Morrison Formation.

Regional stratigraphic features of the Curtis-Moab-Summerville interval suggest struccural control of sedimentation during Callovian time. The northeast trending axes of the San Rafael and Monument Uplifts are roughly parallel to the trend of the paleoshoreline in the Green River Desert area and the trend of the boundaries between facies in the Curtis, Moab, and Summerville. Furthermore, general isopach patterns of individual facies and the entire Curtis-Moab-Summerville interval exhibit eastward thinning and pinching-out toward the Monument Uplift. These relationships suggest that the San Rafael and Monument Uplifts were significant enough to control sedimentation patterns and facies distribution.

Deformation, including crustal uplift and thrust faulting, in the Sevier orogenic belt in eastern Nevada and western Utah is usually considered a Cretaceous event. Petrologic data in this report combined with other recent data supports a new idea that gentle but noteworthy uplift in the Sevier Orogeny may have occurred as early as the middle Jurassic during deposition of the Curtis. Eastward thrust faulting did not develop until Cretaceous time after deposition of the Morrison Formation (Peterson, pers. comm., November, 1987).

Suggestions For Future Studies

The general study of local stratigraphic relations and the origin of facies is meant to serve as a basis for future work to examine specific stratigraphic, sedimentologic, and petrologic aspects within the Curtis-Moab-Summerville interval. The following are topics which require additional field investigation.

Comparison Between Water- and Wind-Laid Foreset Beds

Features of crossbedding in the composite sandstone facies of the Curtis can be compared with those of the crossbedded sandstone facies in the Moab Tongue. Systematic comparisons can be made between crossbed set thicknesses, angle-of-repose foresets, sandflow thicknesses, bounding surface relationships, and distribution of small-scale bedding features such as ripple crosslaminations and mudstone or siltstone laminations. Differences and/or similarities between bedform type and sediment transport mechanisms among subaqueous and eolian systems can be demonstrated.

Tidal Bundle Sequences

Thicknesses of foreset bundles were not measured in crossbedded sandstone units in the Curtis Formation. Recognition and measurement of bundled foreset sequences may help distinguish between spring and neap tide currents and perhaps identify smaller-scale differences in current strengths related to inequality of daily tides.

Expanded Facies Analysis

The study of the origin of facies in the Curtis-Moab-Summerville interval can be expanded to include facies of equivalent strata near

the Uinta Basin in northeastern Utah, and in the Henry Mountains and Circle Cliffs area in southern Utah to improve interpretations on ancient shoreline geography. Equivalent strata in central and north-central Utah should preserve contemporary offshore shelf deposits.

Bedforms and Bedform Hierarchies in Eolian Sandstones

A refinement of bounding surface relationships and bounding surface attitudes in the crossbedded sandstone facies of the Moab Tongue may more clearly indicate dune type and direction of dune migration with respect to wind direction as indicated by crossbedding.

Paleowind Analysis

Crossbedding in the entire Moab Tongue north and south of the Moab townsite should be measured and analyzed to more accurately explain the variable wind direction, determined in this study, and the paleogeographic conditions which may have caused the variable winds at that time.

Petrologic Studies

The relationship between sedimentary facies and the occurrence of clay minerals can be refined by analysis of other clay-bearing samples in the Curtis and Summerville Formations. A comparison may be made with the occurrence and distribution of clay minerals as controlled by chemical and physical factors in modern shoreline environments.

Further analysis of gravel-sized lithoclasts of chert and sedimentary rock fragments in equivalent strata to the southwest, in the Henry Mountains and Circle Cliffs area, is required to accurately determine a source direction for the gravel lithoclasts. The exact location, timing, and style of deformation and the relationship to

detrital sedimentation in the Jurassic marine basin is not entirely known.

There are interesting diagenetic relationships and paragenetic sequences which are observable in thin section but are not described in this report. A combined study of sandstone diagenesis, clay mineralogy, and coal petrography would generate ideas on depth and duration of burial. The results may be useful in constructing a diagenetic model for tide-dominated shoreline sandstones.

REFERENCES CITED

Ahlbrandt, T. S., and Fryberger, S. G., 1981, Sedimentary features and significance of interdune deposits, in: Ethridge, F. G., and Flores, R. M., (eds.), Recent and ancient nonmarine depositional environments: Models for exploration: Soc. Econ. Paleontologists Mineralogists Spec. Pub. no. 31, p. 293-314.

Aigner, T., 1985, Storm depositional systems- dynamic stratigraphy in modern and ancient shallow-marine sequences, Lecture notes in earth sciences no.3: Berlin, Springer-Verlag, 174 p.

Alam, M.M., Crook, K.A.W., and Taylor, G., 1985, Fluvial herringbone cross-stratification in a modern tributary mouth bar, Coonamble, New South Wales, Australia: Sedimentology, v. 32, no. 2, p. 235-244.

Allen, J.R.L., 1963b, the classification of cross-stratified units. With notes on their origin: Sedimentology, v. 2, p. 93-114.

_____, 1964, Studies in fluviatile sedimentation: six cyclothems from the Lower Old Red Sandstone, Anglo-Welsh Basin: Sedimentology, v. 3, p. 163-198.

_____, 1968c, The nature and origin of bedform hierarchies: Sedimentology, v. 47, p. 173-185.

_____, 1970a, Studies in fluviatile sedimentation: a comparison of fining upwards cyclothems, with special reference to coarse-member composition and interpretation: Jour. Sedimentary Petrology, v. 40, p. 298-323.

_____, 1979b, Physical processes of sedimentation, an introduction: London, George Allen and Unwin, 248 p.

_____, 1980, Sand waves: a model of origin and internal structure: Sedimentary Geology, v. 26, p. 281-328.

_____, and Friend, P.F., 1976, Changes in intertidal dunes during two spring-neap cycles, Lifeboat Station Bunk, Wells-Next-the-Sea, Norfolk, England (England): Sedimentology, v. 23, p. 329-347.

Allmendinger, R. W., and Jordan, T. E., 1981, Mesozoic evolution, hinterland of the Sevier orogenic belt: Geology, v. 9, p. 308-313.

Andrews, P. B., 1970, Facies and genesis of a hurricane washover fan, St. Joseph Island, central Texas coast: Bur. Econ. Geology, Univ. Texas, Austin, Rep. Invest. 67, p. 1-147.

Averitt, P., 1962, Geology and coal resources of the Cedar Mountain Quadrangle, Iron County, Utah: U.S. Geological Survey Prof. Paper 389, 71 p.

_____, Detterman, J. S., Harshbarger, J. W., Repenning, C. A., and Wilson, R. F., 1955, Revisions in correlation and nomenclature of Triassic and Jurassic formations in southwestern Utah and northern Arizona: Am. Assoc. Petroleum Geologists Bull., v. 39, p. 2515-2524.

Baars, D. L., and Molenaar, C. M., 1971, Geology of Canyonlands and Cataract Canyon: Four Corners Geol. Soc. Sixth Field Conf., Cataract Canyon River Expedition, 99 p.

Bagnold, R. A., 1954a, The physics of blown sand and desert dunes: London, Methuen, 265 p.

Bagshaw, L. H., 1977, Paleoecology of the lower Carmel Formation of the San Rafael Swell, Emery County, Utah: Brigham Young University Geol. Studies, v. 25, p. 51-62.

Baker, A. A., 1933, Geology and oil possibilities of the Moab district, Grand and San Juan Counties, Utah: U. S. Geol. Survey Bull. 841, 42 p.

_____, 1946, Geology of the Green River Desert-Cataract Canyon region, Emery, Wayne and Garfield Counties, Utah: U. S. Geological Survey Bull., 951, 122 p.

_____, Dane, C. H., and Reeside, J. B., Jr., 1936, Correlation of the Jurassic formations of parts of Utah, Arizona, New Mexico, and Colorado: U. S. Geological Survey Prof. Paper 183, 66 p.

_____, Dane, C. H., and Reeside, J. B., Jr., 1947, Revised correlation of Jurassic formations of parts of Utah, Arizona, New Mexico, and Colorado: Am. Assoc. Petroleum Geologists Bull., v. 31, no. 9, p. 1664-1668.

_____, Dobbin, C. E., McKnight, E. T., and Reeside, J. B, Jr., 1927, Notes on the stratigraphy of the Moab region, Utah: Am. Assoc. Petroleum Geologists Bull., v. 11, p. 785-808.

Bigarella, J. J., Becker, R. D., and Duarte, G. M., 1969, Coastal dune structures from Parana (Brazil): Marine Geology, v. 7, p. 5-55.

Bilodeau, W. L., 1986, Mesozoic paleogeography and tectonics of the Mogollon region, central Arizona (abs.): Geol. Soc. Am. Abs. with Programs, v. 18, no. 5, p. 342.

Bissel, H. J., 1954, The Kaiparowits region, in Guidebook, fifth ann. field conf: Intmtn. Assoc. Petroleum Geologists, p. 63-70.

Blakey, R. C., 1970, Geology of the Paria northwest Quadrangle, Kane County, Utah, unpubl. M. S. thesis, Dept. Geol., Univ. of Utah, 171 p.

_____, 1984, Marine sand wave complex of the Permian of central Arizona: Jour. Sed. Petrology, v. 54, no. 1, p. 29-51.

_____, in press, Triassic and Jurassic geology of the southern Colorado Plateau, Ariz. Geological Soc.

_____, and Gubitosa, R., 1983, Late Triassic paleogeography and depositional history of the Chinle Formation, southern Utah and northern Arizona, innReynolds, M. W., and Dolly, E. D., eds., Mesozoic paleography of the west-central United States, Rky. Mtn. Paleogeog. Symp. 2: Rocky Mtn. Sect. Soc. Econ. Paleont. Mineral., p. 57-76.

_____, and Middleton, L. T., 1983, Permian shoreline-eolian complex in central Arizona: dune changes in response to cyclic sealevel changes, in Brookfield, M. E., and Ahlbrandt, T. S., eds., Eolian sediments and processes: Amsterdam, Elsevier Publishers, p. 551-581.

_____, Peterson, F., Caputo, M.V., Geesaman, R.C., and Voorhees, B.J., 1983, Paleogeography of middle Jurassic continental, shoreline, and shallow marine sedimentation, southern Utah: in Reynolds, M.W., and Dolly, E.D., eds., Mesozoic Paleogeography of West-Central United States: Rocky Mtn Section, Soc. Econ. Paleont. Mineral., p. 77-100.

Blatt, H. 1982, Sedimentary petrology: San Francisco, Freeman and Co., 564 p.

Boekschoten, G.J., 1966, Shell borings of sessile epibiontic organisms as palaeoecological guides (with examples from the Dutch coast: Palaeogeog. Palaeoclimat., Palaeoecol., v. 2, p. 333-379.

Boersma, J.R., 1969, Internal structures of some tidal megaripples on a shoal in the Westerschelde estuary, the Netherlands; report of a preliminary investigation: Geol. en Mijn., v. 48, p. 409-414.

_____, and Terwindt, J.H.J., 1981a, Neap-spring tide sequences of intertidal shoal deposits in a mesotidal estuary: Sedimentology, v. 28, no. 2, p. 151-170.

_____, and Terwindt, J.H.J., 1981b, Berms on an intertidal shoal: shape and internal structure, in Nio, S.-D., Shuttenhelm, R.T.E., and van Weering, Tj.C.E., eds., Holocene marine sedimentation in the North Sea Basin, Spec. Pub. 5, Int. Assoc. Sedimentologists: Oxford, Blackwell Sci. Pubs., p. 39-50.

Boothroyd, J.C., 1978, Mesotidal inlets and estuaries, in Davis, R.A.,Jr., ed., Coastal sedimentary environments: New York, Springer-Verlag, p. 287-360.

_____, and Hubbard, D.K., 1975, Genesis of bedforms in mesotidal estuaries, in Cronin, L.E., ed., Estuariane Research: New York, Academic Press, v. 11, p. 217-235.

Bourgeois, J., 1980, A transgressive shelf sequence exhibiting hummocky stratification: the Cape Sebastian Sandstone (Upper Cretaceous), southwestern Oregon: Jour. Sed. Petrology v. 50 no. 3, p. 681-702.

Breyer, J.A., and McCabe, P.J., 1986, Coals associated with tidal sediments in the Wilcox Group (Paleogene), south Texas: Jour. Sed. Petrology, v. 56, no. 4, p. 510-519.

Bromley, R.G., 1970, Borings as trace fossils and Entobia cretacea Portlock, as an example, in Crimes, T.P., and Harper, J.C., eds., Trace Fossils: Liverpool, Seel House Press, p. 49-90.

_____, 1975, Trace fossils at omission surfaces, in Frey, R.W., ed., The study of trace fossils: New York, Springer-Verlag, p. 399-428.

_____, Pemberton, G., and Rahmani, R.A., 1984, A Cretaceous woodground: the Teredolites ichnofacies: Jour. Paleont., v. 58, no. 2, p. 488-498.

Brookfield, M. E., 1977, The origin of bounding surfaces in ancient aeolian sandstone: Sedimentology, v. 24, p. 303-332.

Buck, S.G., 1985, Sand-flow cross-strata in tidal sands of the Lower Greensand (Early Cretaceous), southern England: Jour. Sed. Petrology, v. 55, no. 6, p. 895-906.

Bullock, L. R., 1965, Paleoecology of the Twin Creek Limestone in the Thistle, Utah area, Brigham Young Univ. Geol. Studies, v. 12, p. 121-147.

Burbank, W. S., 1930, Colorado Sci. Soc. Proc., v. 12, p. 172.

Burchfiel, B. C., 1981, Geologic history of the central western United States, reprinted in Burchfiel, B. C., 1981, structural evolution of western North America and tectonics of marginal fold and thrust belts: Am. Assoc. Petroleum Geologists Cont. Ed. Course, Montana Geol. Soc., p. 1-11.

Butler, B. S., Loughlin, G. F., Heikes, V. C., and others, 1920, Ore deposits in Utah: U.S. Geol. Survey Prof. Paper 111, p. 608-610.

Butler, G. P., Harris, P. M., and Kendall, C. G. St. C., 1982, Recent evaporites from the Abu Dhabi coastal flats, in Handford, C. R., Loucks, R. G., and Davies, G. R., eds., Depositional and diagenetic spectra of evaporites-a core workshop: Soc. Econ. Paleont. Mineral., core workshop no. 3, p. 33-64.

Cant, D.J., 1978, Development of facies model for sandy braided river sedimentation: comparison of the South Saskatchewan River and Battery Point Formation in Miall, A.D., ed., Fluvial sedimentology: Can. Assoc. Petroleum Geologists, Mem. 5, p. 627-640.

Caputo, M. V., 1980, Depositional history of middle Jurassic shoreline sequences in southwestern Utah: unpub. M.Sc. thesis, Northern Ariz. Univ., 203 p.

_____, 1981, Stratigraphy and depositional history of the Thousand Pockets Tongue of the Page Sandstone and Crystal Creek Member of the Carmel Formation (Middle Jurassic) in southwestern utah (abs.): Am. Assoc. Petroleum Geologists Bull., v. 65, no. 3 p. 556.

_____, 1987, Middle Jurassic San Rafael Group of southwestern and east-central Utah: cyclic sedimentation on an epicontinental marine shelf (abs.): Miss. Geol. Soc., v. 34, no. 8, p. 5-6.

_____, and Peterson, F., 1986, Curtis and Summerville Formations and Moab Member of the Entrada Sandstone (Middle Jurassic): Sedimentation on tide- and wide-swept shoreline, east-central Utah (abs.): Geol. Soc. Am. Abs. with Prog., v. 18, no. 5, p. 345.

Cashion, W. B., 1967, Carmel Formation of the Zion Park region, southwestern Utah--a review, U.S. Geol. Survey Bull., 1244j, 9 p.

Casshyap, S.M., and Kumar, A., 1987, Fluvial architecture of the upper Permian Raniganj coal measure in the Damodar Basin, eastern India: Sedimentary Geology, v. 51, p. 181-213.

Chamberlain, C.K., 1971, Bathymetry and paleoecology of Ouachita geosyncline of south-eastern Oklahoma as determined from trace fossils: Am. Assoc. Petroleum Geologists Bull., v. 55, p. 34-50.

_____, C.K., 1978, Trace fossil ichnofacies of an American flysch, in Chamberlain, C.K., ed., A guidebook to the trace fossils and paleoecology of the Ouachita Geosyncline, SEPM Field Trip guidebook: Soc. Econ. Paleont. Mineral., p. 23-3

Chanda, S. K., and Bhattacharyya, A., 1974, Ripple-drift cross lamination in tidal deposits: examples from the Precambrian Bhander Formation of Maihar, Satna District, Madhya Pradesh, India: Geol. Soc. Am. Bull., v. 85, p.1117-1122.

Chapman, M. G., 1986, Composition, deposition and origin of volcanogenic clasts within the Jurassic Carmel Formation, southern Utah (abs.): Geol. Soc. Am. Abs. with Prog., v. 18, no. 5, p. 345.

Clifton, H.E., 1981, Progradational sequences in Miocene shoreline deposits, southeastern Caliente Range, California: Jour. Sed. Petrology, v. 51, no. 1, p. 165-184.

_____, 1982, Estuarine deposits, in, Scholle, P. A., and Spearing, D., eds., Sandstone depositional environments: Am. Association Petroleum Geologists Mem. 31, p. 179-190.

_____, Hunter, R.E., and Phillips, R.L., 1971, Depositional structures and processes in the non-barred high energy nearshore: Jour. Sedimentary Petrology, v. 41, p. 651-670.

Collinson, J.D., 1970, Bedforms of the Tana River, Norway: Geogr. Annaler., v. 52, p. 31-55.

_____, and Thompson, D.B., 1982, Sedimentary structures: London, George Allen and Unwin, 194 p.

Costello, W.R., and Southard, J.B., 1981, Flume experiments on lower-flow-regime bed forms in course sand: Jour. Sedimentary Petrology, v. 51, p. 849-864.

Cotter, E., 1985, Gravel-topped offshore bar sequences in the lower Carboniferous of southern Ireland: Sedimentology, v. 32, no. 2, p. 195-214.

Craig, L. C., and Cadigan, R. A., 1958, the Morrison and adjacent formations in the Four Corners area, in Sanborn, A. F., ed., Guidebook to the geology of the Paradox Basin, ninth ann. field conf.: Intmtn. Assoc. Petroleum Geologists, p. 182-192.

_____, and Dickey, D. D., 1956, Jurassic strata of southeastern Utah and southwestern Colorado, in, Geologic economic deposits of east-central Utah, guidebook, seventh ann. field conf: Intmtn. Assoc. Petroleum Geologists, p. 93-104.

_____, and Freeman, V. L., 1959, Last Chance Creek section, Sevier County, Utah, measured in 1950, 11 p. in: Craig, L. C., Measured sections of the Morrison Formation and adjacent formations: U.S. Geol. Survey open file rept. 1720.

_____, Holmes, C. N., Cadigan, R. A., Freeman, V. L., Mullens, T. E., and Weir, G. W., 1955, Stratigraphy of the Morrison and related formations, Colorado Plateau region-a preliminary report: U.S. Geological Survey Bull., 1009-E, p. 125-168.

Craig, L. C., and Shawe, D. R., 1975, Jurassic rocks of east-central Utah, in, Canyonlands Country, eighth field conf.: Four Corners Geol. Soc., p. 157-165.

Cross, W., 1988a, Telluride folio: U.S. Geol. Survey, Geological Atlas of the U.S. folio 57.

Curray, J. R., 1969b, Lecture 3. Estuaries, lagoons, tidal flats, and deltas, in Stanley, D. J., convener, The new concepts of continental margin sedimentation, application to the geological record, short course lecture notes: Washington, Am. Geol. Inst., p. 1-30.

Curtis, R., Evans, G., Kinsman, D. J. J., and Shearman, D. J., 1963, Association of dolomite and anhydrite in the Recent sediments of the Persian Gulf: Nature, v. 197, p. 679-680.

Dake, C. L., 1919, The horizon of the marine Jurassic of Utah: Jour. Geology, v. 27, p. 634-646.

Dalrymple, R. W., Knight, R. J., and Lambiase, J. J., 1978, Bedforms and their hydraulic stability relationships in a tidal environment, Bay of Fundy, Canada: Nature, v. 275, p. 100-104.

_____, Knight, R. J., and Middleton, G. V., 1975, Intertidal sand bars in Colequid Bay (Bay of Fundy), in Cronin, L. E. ed., Estuarine Research: New York, Academic Press, v. 11, p. 293-308.

Dane, C. H., 1935, Geology of the Salt Valley Anticline and adjacent areas, Grand County, Utah: U.S. Geol Survey Bull. 863, 184 p.

Derr, M. E., 1974, Sedimentary structure and depositional environment of paleochannels in the Jurassic Morrison Formation near Green River, Utah: Brigham Young Geology Studies, v. 21, no. 3; p. 3-39.

Dickey, D. D., and Wright, J. C., 1959, Semiannual reports to AEC on San Rafael (Entrada) studies, in: Geologic investigations of radioactive deposits-semiannual progress report, June 1 to November 30, 1958: U.S. Geol. Survey TEI-750, p. 59-65.

Dickinson, W. R., 1976, Sedimentary basins developed during evolution of Mesozoic-Cenozoic arc-trench system in western North America: Con. Jour. Earth Sci., v. 13, no.9, p. 1161-1185.

_____, 1981, Plate tectonic evolution of the southern Cordillera: Ariz. Geol. Soc. Digest, v. 14, p. 113-135.

_____, 1985, Interpreting provenance relations from detrital modes of sandstones, in Zuffa, G.G., ed., Provenance of arenites: Dordrecht-Boston-Lancaster, D. Riedel Pub. Co., p. 333-361.

Dickinson, W. R., Beard, L.S., Brackenridge, G.R., Erjavec, J.L., Ferguson, R.C., Inman, K.F., Knepp, R.A., Lindberg, F.A., and Ryberg, P.T., 1983, Provenance of North American Phanerozoic sandstones in relation to tectonic setting: Geol. Soc. Am. Bull., v. 94, p. 222-235.

Doelling, H. H., 1975, Geology and mineral resources of Garfield county, Utah: Utah Geological Mineral Survey, Bull. 107, 175 p.

Dorjes, J., and Hertweck, G., 1975, Recent biocoenoses and ichnocoenoses in shallow-water marine environments, in Frey, R. W., ed., The study of trace fossils: New York, Springer-Verlag, p. 459-492.

_____, and Howard, J. D., 1972, Animal-sediment relationships in two beach-related tidal flats: Sapelo Island, Georgia: Jour. Sed. Petrology, v. 42, no. 3, p. 608-623.

Dover, R. J., 1969, Paleoecology of the lowermost part of the Jurassic Carmel Formation, San Rafael Swell, Emery County, Utah: unpublished M.S. thesis, Utah State Univ., 73 p.

Dutton, C. E., 1880, Report on the geology of the high plateaus of Utah, with atlas: U.S. Geographical and Geological Survey of the Rocky Mountain region, 339 p.

_____, 1885, Mount Taylor and the Zuni Plateau: U.S. Geol. Survey 6th Ann. Rept., p. 136-137.

Ekdale, A. A., Bromley, R. G., and Pemberton, S. G., 1984, Ichnology: the use of trace fossils in sedimentology and stratigraphy: SEPM Short Course no. 15, 317 p.

Eldridge, G. H., 1896, Mesozoic geology, in Emmons, S. F., Cross, W., and Eldridge, G. H., Geology of the Denver Basin in Colorado: U.S. Geological Survey Mono. 27, p.51-150.

Elliot, T., 1986, Siliciclastic shorelines, in Reading, H. G., Sedimentary environments and facies, 2nd ed., Oxford, Blackwell Scientific Pubs., p. 155-188.

_____, and Gardner, A. R., 1981, Ripple, megaripple and sandwave bedforms in the macrotidal Loughor Estuary, South Wales, U. K., in Nio, S.-D., Shuttenhelm, R.T.E., and van Weering, Tj. C. E., eds., Holocene Marine Sedimentation in the North Sea Basin, Spec. Pub. 5: Int. Assoc. Sedimentologists, p. 51-64.

Emery, K. O., 1952, Continental shelf sediments of southern California: Geol. Soc. Am. Bull., v. 63, p. 1105-1108.

_____, 1968b, Relict sediments on continental shelves of the world: Am. Assoc. Petroleum Geologists Bull., v.52, p. 445-464.

Emery, W. B., 1918, the Green River Desert section, Utah: Am. Jour. Sci., 4th ser., v. 46, p. 551-577.

Eschner, T. B., and Kocurek, G. A., 1982a, A transgressive tidal sand bar complex-Jurassic Curtis Formation, northeastern Utah (abs.), Abstracts, Eleventh Int. Cong. Sedimentology, Hamilton, Out., Can: Int. Assoc. Sedimentologists, p. 98.

_____, and Kocurek, G. A., 1982b, Marine destruction of an eolian sand sea - Jurassic Curtis Formation, northeastern Utah (abs.), Abstracts, Eleventh Int. Cong. Sedimentology, Hamilton, Ont., Can: Int. Assoc. Sedimentologists, p. 163.

_____, and Kocurek, G., 1986, Marine destruction of eolian sand seas: origin of mass flows: Jour. Sed. Petrology, v. 56, no. 3, p. 401-411.

Evans, G., 1965, Intertidal flat sediments and their environments of deposition in the Wash.: Quar. Jour. Geol. Soc. London, v. 121, p. 209-241.

Fischer, R. P., 1942, Vanadium deposits of Colorado and Utah: U. S. Geological Survey Bull., 936-p, p. 363-394.

Folk, R.L., Andrews, P.B., and Lewis, D. W., 1970, Detrital sedimentary rock classification and nomenclature for use in New Zealand: New Zealand Jour. Geology and Geophys., v. 13, p. 937-968.

Forrester, J. B., 1918, A general survey of the Jurassic in southeastern Utah: Utah Acad. Sci. Trans., v. 1, p. 33.

Freeman, W. E., 1976, Regional stratigraphy and depositional environments of the Glen Canyon Group and Carmel Formation (San Rafael Group), in Hill, J. G., ed., Geology of the Cordilleran Hingeline: Rocky Mtn. Assoc. Geologists, p. 247-259.

Frey, R. W., and Howard, J. D., 1982, Trace fossils from the upper Cretaceous of the Western Interior: potential criteria for facies models: Mountain Geologist, v. 19, no. 1, p. 1-10.

_____, and Pemberton, S. G., 1984, Trace fossil facies models, in Walker, R. G., ed., Facies models, second edition: Geoscience Canada, Reprint Series 1, p. 189-207.

Fritz, T. R., 1977, the depositional environments of the Jurassic Carmel Formation of northeastern Utah, unpublished M. S. thesis in geology, Fort Hayes State Univ, 100 p.

Gard, L. M., Jr., 1976, Geology of the north end of the Salt Valley anticline, Grand County Utah: U. S. Geological Survey Open-File Report 76-303, 35 p.

Geesaman, R. C., 1979, Sedimentary facies of the Carmel Formation, southeastern Utah: unpub. M. Sc. thesis, Northern Ariz. Univ., 96 p.

Gilbert, G. K., 1875a, Part I, Report on the geology of portions Nevada, Utah, California and Arizona examined in the years 1871 and 1872 in Report upon Geographical and Geological Explorations and Surveys West of the One Hundredth Meridian, Engineer Dept., U. S. Army, v. 111-Geology: Washington, U. S. Govt. Printing off., p. 17-187.

_____, 1875b, Geology of portions of New Mexico and Arizona, explored and surveyed in 1873, in Report on Geographical and Geological Explorations and Surveys West of the One Hundredth Meridian, Engineer Dept., U. S. Army, v. 111 - Geology, p. 503-567.

_____, 1880, Report on the geology of the Henry Mountains: U. S. Geographical and Geological Survey of the Rocky Mountain Region: Washington, U. S. Govt. Printing Off., 170 p.

_____, 1885, the topographic features of lake shores: Ann. Report, U. S. Geological Survey, v. 5, p. 75-123.

Gilluly, J., 1929, Geology and oil and gas prospects of part of the San Rafael Swell and some adjacent areas in eastern Utah: U. S. Geological Survey Bull. 806-c, p. 69-130.

_____, and Reeside, J. B., Jr., 1928, Sedimentary rocks of the San Rafael Swell and some adjacent areas in eastern Utah: U. S. Geological Survey Prof. Paper 150-D, p. 59-110.

Glennie, K. W., 1970, Desert sedimentary environments: Amsterdam, Elsevier, Developments in Sedimentology 14, 222 p.

_____, and Evans, G., 1976, A reconnaissance the Recent sediments of the Ranns of Kutch, India: Sedimentology, v. 23, p. 625-647.

Goldman, M. I., and Spencer, A. C., 1941, Correlation of Cross' La Plata Sandstone, southwestern Colorado: Am. Assoc. Petroleum Geologists Bull., v. 25, no. 9, p. 1748-1762.

Gould, L. M., 1927, the geology of La Sal Mountains of Utah: Michigan Acad. Sci. Papers, v. 7, p. 64-77.

Grater, R. K., 1948, Some features of the Navajo Formation in Zion National Park, Utah: Am. Jour. Sci., v. 246, no. 5, p. 311-318.

Greensmith, J. T., and Tucker, E. V., 1975, Dynamic structures in the Holocene chenier plain setting of Essex, England, in Hails, J., and Carr, A., eds., Nearshore sediment dynamics and sedimentation: London, John Wiley, p. 251-272.

Greer, S. A., 1975, Sandbody geometry and sedimentary facies at the estuary-marine transition zone, Ossabaw Sound, Georgia: a stratigraphic model: Senckenbergiana Maritima, v. 7, p. 105-135.

Gregory, H. E., 1916, the Navajo country - a geographic and hydrographic reconnaissance of parts of Arizona, New Mexico, and Utah: U. S. Geological Survey Water Supply Paper 380, 219 p.

_____, 1917, Geology of the Navajo country-a reconnaissance of parts of Arizona, New Mexico, and Utah: U. S. Geological Survey Prof. Paper 93, 161 p.

_____, 1938, the San Juan country, a geographic and geologic reconnaissance of southeastern Utah: U. S. Geological Survey Prof. Paper 188, 123 p.

_____, 1948, Geology and geography of central Kane County, Utah: Geol. Soc. Am. Bull., v. 59, p. 211-247.

_____, 1950a, Geology and geography of the Zion Park region, Utah and Arizona: U. S. Geological Survey Prof. Paper 220, 200 p.

_____, 1950b, Geology of eastern Iron County, Utah: Utah Geol. Mineral Survey Bull., 37, 153 p.

_____, 1951, Geology and geography of the Paunsaugunt region, Utah: U. S. Geological Survey Prof. Paper 226, 116 p.

_____, and Moore, R. C., 1931, the Kaiparowits region, a geographic and geologic reconnaissance of parts of Utah and Arizona: U. S. Geological Survey Prof. Paper 164, 161 p.

_____, and Noble, L. F., 1923, Notes on a geologic traverse from Mojave, California to the mouth of the San Juan: Am. Jour. Sci., v. 5, p. 229-238.

_____,Moore, R. C., Gilluly, J., and Reeside, J. B., 1926, U. S. Geol. Survey Press Bull. 606-A.

Hague, A., and Emmons, S. F., 1877, Report of the Geological Exploration of the Fortieth parallel: Descriptive Geology, Professional papers of the engineer department, U.S. Army, v. 11: Washington, U.S. Govt. Printing Office, 890 p.

Hamblin, A. P., Duke, W. L., and Walker, R. G., 1979, Hummocky cross-stratification-indicator of storm-dominated shallow marine environment (abs.): Am. Assoc. Petroleum Geologists Bull., v. 63, p. 460-461.

Hamilton, W., 1969a, Mesozoic California and the underflow of Pacific mantle: Geol. Soc. Am. Bull., v. 80, no. 12, p.2409-2429.

Hamilton, W., 1978, Mesozoic tectonics of the Western United States, in Howell, D. G., and McDougal, K. A., eds., Mesozoic paleogeography of the western United States: Pacific Section, SEPM, Paleogeography Symposium, p. 33-70.

Hantzschel, W., 1939, Tidal flat deposits (Wattenschlick), in Trask, P. D., ed., Recent marine sediments: Tulsa, Soc. Econ. Paleont. Mineral., p. 195-206.

Harms, J. C., Southard, J. B., Spearing, D. R., and Walker, R. G., 1975, Depositional environments as interpreted from primary sedimentary structures and stratification sequences, short course no. 2: Dallas, Soc. Econ. Paleont. Mineral., 161 p.

_____, Southard, J. B., and Walker, R. G., 1982, Structures and sequences in clastic rocks: Tulsa, Soc. Econ. Paleont. Mineral., Short Course no. 9, 249 p.

Harshbarger, J. W., Repenning, C. A., and Jackson, R. L., 1951, Jurassic stratigraphy of the Navajo country, in Smith, C. T., and Silver, C., eds., Guidebook of the San Juan Basin, New Mexico and Arizona: New Mex. Geol. Soc., p. 95-99.

_____, Repenning, C. A., and Irwin, J. H., 1957, Stratigraphy of the uppermost Triassic and the Jurassic rocks of the Navajo country (Colorado Plateau): U.S. Geological Survey Prof. Paper 291, 74 p.

Hayes, M. O., 1975, Morphology of sand accumulation in estuaries: an introduction to the symposium, in Cronin, L. E., ed., Estuarine Research, v. II. Geology and Engineering: London, Academic Press, p. 3-22.

_____, 1976, Part I, Lecture notes, in Hayes, M. O., and Kana, T. W., eds., Terrigenous clastic depositional environments, some modern examples: Am. Assoc. Petroleum Geologists Short course notes, Univ. So. Carolina Tech. Rept. no. 11-CRD, p. 1-14.

Heckel, P. H., 1972, Recognition of ancient shallow marine environments, in Rigby, J. K., and Hamblin, W. K. eds., Recognition of ancient sedimentary environments: Soc. Econ. Paleont. Mineral., Spec. Pub. 16, p. 226-286.

Hereford, R., 1977, Deposition of the Tapeats Sandstone (Cambrian) in central Arizona: Geol. Soc. Am. Bull., v. 88, p. 199-211.

Hinman, E. E., 1957, Jurassic Carmel-Twin Creek facies of northern Utah: Compass, v. 34, p. 102-119.

Hintze, L. F., 1973, Geologic history of Utah: Brigham Young Univ. Geology Studies, v. 20, pt. 3, p. 54-58.

_____, Geological highway map of Utah: Brigham Young University Geology Studies, Spec. Pub. 3.

Howard, J. D., 1972, Trace fossils as criteria for recognizing shorelines in the stratigraphic record, in Rigby, J. K. and Hamblin, W. K., eds., Recognition of ancient sedimentary environments, S.E.P.M., Spec. Pub. 16, p. 215-225.

_____, and Dorjes, J., 1972, Animal-sediment relationships in two beach-related tidal flats: Sapelo Island, Georgia: Jour. Sedimentary Petrology, v. 42, p.608-623.

_____, and Frey, R. W., 1980, Holocene depositional environments of the Georgia coast and continental shelf, in Howard, J. D., DePratter, C. B., and Frey, R. W., eds., Excursions in southeastern geology, the archeology-geology of the Georgia coast: Geol. Soc. Am., Guidebook 20, p.66-134.

_____, and Frey, R. W., 1984, Characteristic trace fossils in nearshore to offshore sequences, upper Cretaceous of east-central Utah: Can. Jour. Earth Sci., v. 21, p. 200-219.

_____, and Reineck, H.-E., 1972a, Georgia coastal region, Sapelo Island, U.S.A., sedimentology and biology, IV. Physical and biogenic sedimentary structures of the nearshore shelf: Senckenbergiana Maritima, v. 4, p. 81-123.

_____, and Reineck, H.-E., 1972b, Georgia coastal region, Sapelo Island, U.S.A., sedimentology and biology, VIII, conclusions: Senckenbergiana Marit. v. 4, p. 81-123.

Howell, E. E., 1875, Geology of portions of Utah, Nevada, Arizona, and New Mexico, explored and surveyed in 1872 and 1873, in Report on Geographical and Geological Explorations and surveys West of the One Hundredth Meridian, Engineer Dept., U.S. Army, v. 111-Geology, p.237-301.

Hubbard, D. K., and Barwis, J. H., 1976, Discussion of tidal inlet sand deposits: examples from the South Carolina coast, in Hayes, M. O., and Kana, T. W., eds., Terrigenous clastic depositional environments: Dept. Geol., Univ. So. Carolina, Tech Rept. No. 11-CRS, p. II-128 - II-142.

Hunt, C. B., Averitt, P., and Miller, R. L., 1953, Geology and geography of the Henry Mountains region, Utah: U.S. Geological Survey Prof. Paper 228, 234 p.

Hunter, R. E., 1977a, Basic types of stratification in small eolian dunes: Sedimentology, v. 24, p. 361-387.

_____, 1977b, Terminology of cross-stratified sedimentary layers and climbing-ripple structures: Jour. Sed. Petrology, v. 47, p. 697-706.

_____, 1980, Quasi-planar adhesion stratification - an eolian structure formed in wet sand: Jour. Sed. Petrology, v. 50, no. 1, p. 263-266.

Hunter, R. E., 1981, Stratification styles in eolian sandstones: some Pennsylvanian to Jurassic examples from the western interior U.S.A., in Ethridge, F. G., and Flores, R. M., eds., Recent and ancient nonmarine depositional environments: models for exploration: SEPM Spec. Pub. 31, p. 315-330

_____, 1985b, Subaqueous sand-flow cross-strata: Jour. Sed. Petrology, v. 55, no. 6,, p. 886-894.

_____, and Clifton, H. E., 1982, Cyclic deposits and hummocky cross-stratification of probable storm origin in upper Cretaceous rocks of the Cape Sebastian area, southwestern Oregon: Jour. Sed. Petrology, v. 52, no. 1, p. 127-143.

_____, and Kocurek, G., 1986, An experimental study of subaqueous slipface deposition: Jour. Sed. Petrology, v. 56, no. 3, p. 387-394.

_____, Richmond, B. M., and Alpha, T. R., 1983, Storm-controlled oblique dunes of the Oregon coast: Geol. Soc. Am. Bull., v. 94, p. 1450-1465.

Illing, L. V., Wells, A. J., and Taylor, J. C. M., 1963, Penecontemporary dolomite in the Persian Gulf, in Pray, L. C., and Murray, R. C., eds., Dolomitization and limestone diagenesis-a symposium: Soc. Econ. Paleont. and Mineral. Spec. Pub. no. 13, p. 89-111.

Imlay, R. W., 1948, Characteristic marine Jurassic fossils from the Western Interior of the United States: U.S. Geological Survey Prof. Paper 214 B.

_____, 1952a, Correlation of the Jurassic formations of North America, exclusive of Canada: Geol. Soc. Am. Bull., v. 63, p. 953-992.

_____, 1952b, Marine origin of Preuss Sandstone of Idaho, Wyoming, and Utah: Am. Assoc. Petroleum Geologists Bull., v. 36, p. 1735-1753.

_____, 1957, Paleoecology of Jurassic seas in the western interior of the United States, in Ladd, H.S., ed., Treatise on Marine Ecology and Paleoecology: Geol. Soc. Am. Mem. 67, p. 469-504.

_____, 1964, Marine Jurassic pelecypods from central and southern Utah: U.S. Geological Survey Prof. Paper 483-c, 42 p.

_____, 1967, Twin Creek Limestone (Jurassic) in the western interior of the United States, U.S. Geol. Survey Prof. Paper 540, 105 p.

_____, 1980, Jurassic paleobiogeography of the conterminous United States in its continental setting: U. S. Geol. Survey Prof. Paper 1062, 134 p.

Ingle, J. C., Jr., 1966, the movement of beach sand, Developments in sedimentology, v. 5, Amsterdam, Elsevier Sci. Pub. Co., 221 p.

Inman, D. L., Ewing, G. C., Corliss, J. B., 1966, Coastal sand dunes of Guerrero Negro, Baja California, Mexico: Geol. Soc. Am. Bull., v. 77, p. 787-802.

Johnson, H. D., and Baldwin, C. T., 1986, Shallow siliciclastic seas, in Reading, H. G., ed., Sedimentary Environments and Facies: Oxford, Blackwell Sci. Pub., p. 229-282.

Johnson, I., 1957, A detailed stratigraphic and environmental analysis of the San Rafael Group (Jurassic) between Black Mesa, Arizona and the southern Kaiparowitz Plateau, Utah: unpub. Ph.D. dissert., Univ. of Ariz., 510 p.

Johnson, M. A., Kenyon, N. H., Belderson, R. H., and Stride, A. H., 1982, Sand transport, in Stride, A. H., ed., Offshore tidal sands, processes and deposits: London, Chapman and Hall, p. 58-94.

Jopling, A. V., 1963, Hydraulic studies on the origin of bedding: Sedimentology, v. 2, p. 115-121.

_____, 1965b, Hydraulic factors controlling the slope of laminae in laboratory deltas: Jour. Sed. Petrology, v. 35, p. 777-791.

Jungst, H., 1934, Geologic significance of synaeresis: Geologische Rundschau, v. 23, p. 321-325.

Kamola, D. L., 1984, Trace fossils from marginal-marine facies of the Spring Canyon Member, Blackhawk Formation (Upper Cretaceous), east-central Utah: Jour. Paleont., v. 58, no. 2, p. 529-541.

Kellerhals, P., and Murray, J. W., 1969, Tidal flats at Boundary Bay Fraser River Delta, British Columbia: Bull. Can. Petroleum Geologists, v. 17, no. 1, p. 67-91.

Kendall, A. C., 1984, Evaporites, in Walker, R. G., ed., Facies models, second edition: Geol. Assoc. Canada, Geoscience Canada, Reprint Series 1, p. 259-296.

Kent, D.V., and Gradstein, F.M., 1985, A Cretaceous and Jurassic geochronology: Geol. Soc. Am. Bull., v. 1419-1427.

Kern, J. P., 1980, Origin of trace fossils in Polish Carpathian flysch: Lethaia, v. 13, p. 347-362.

Kerr, S. D., Jr., and Thomson, A., 1963, Origin of nodular and bedded anhydrite in Permian shelf sediments, Texas and New Mexico: Am. Assoc. Petroleum Geologists Bull., v. 47, p. 1726-1732.

King, C., 1878, Report of the geological exploration of the fortieth paralled: systematic geology, Professional papers of the engineer department, U.S. Army, v.1, 803 p., (Jurassic p. 285-295.)

Klein, G. deV., 1967, Paleocurrent analysis in relation to modern marine dispersal patterns: Am. Assoc. Petroleum Geologists Bull., v. 51, p. 366-382.

_____, 1970a, Depositional and dispersal dynamics of intertidal sand bars: Jour. Sedimentary Petrology, v. 40, p. 1095-1127.

_____, 1970b, Tidal origin of a Precambrian quartzite-the lower fine-grained Quartzite (Dalradian) of Islay, Scotland: Jour. Sed. Petrology, v. 40, p. 973-985.

_____, 1971, A sedimentary model for determining paleotidal range: Geol. Soc. Am. Bull., v. 82, p. 2582-2592.

_____, 1972, Determination of paleotidal range in clastic sedimentary rocks: Proc. 24th Int. Geol. Congress, v. 24, no. 6, p. 397-405.

_____, 1974, Estimating water depths from analysis of barrier island and deltaic sedimentary sequences: Geology, v. 2, no. 8, p. 409-412.

_____, 1975a Paleotidal range sequences, middle member, Wood Canyon Formation (Late Precambrian), eastern California and western Nevada, in Ginsburg, R. N., ed., Tidal Deposits: New York, Springer, p. 145-151.

_____, 1977a, Tidal circulation model for deposition of clastic sediments in epeiric and mioclinal shelf seas: Sedimentary Geology, v. 18, p. 1-12.

_____, 1977b, Clastic tidal facies: Champaign, Ill., Continuing Education Pub. Co., 149 p.

Kocurek, G., 1981a, Erg reconstruction: the Entrada Sandstone (Jurassic) of northern Utah and Colorado: Paleogeog., Paleoclim., Paleoecol., v. 36, p. 125-153.

_____, 1981b, Significance of interdune deposits and bounding surfaces in aeolian dune sands: Sedimentology, v. 28, no. 6, p. 753-780.

_____, and Dott, R. H., Jr., 1981, Distinctions and uses of stratification types in the interpretation of eolian sand: Jour. Sed. Petrology, v. 51, no. 2, p. 579-595.

Kocurek, G., and Dott,, R. H., Jr., 1983, Jurassic paleogeography and paleoclimate of the central and southern Rocky Mountains regions, in Reynolds, M. W., and Dolly, E. D., eds., Mesozoic Paleogeography of West-Central United States: Rocky Mtn. sec., Soc. Econ. Paleont. Mineral., p. 101-116.

_____, and Fielder, G., 1982, Adhesion structures: Jour. Sed. Petrology, v. 52, no. 4, p. 1229-1241.

_____, and Oakes, C., 1985, Migration of dunes and ergs bounding surfaces revisited (abs.): Abstracts: SEPM Ann. Mdyr. Mtg. Golden, CO, p. 50.

Kohsiek, L. H. M., and Terwindt, J. H. J., 1981, Characteristics of foreset and topset bedding in megaripples related to hydrodynamic conditions on an intertidal shoal, in Nio, S.-D., Shuttenhelm, R. T. E., and van Weering, Tj. C. E., eds, Holocene marine sedimentation in the North Sea Basin, Spec. Pub. 5, Int. Assoc. Sedimentologists: Oxford, Blackwell Sci. Pubs., p. 27-38.

Komar, P. D., 1976, Beach processes and sedimentation: Englewood Cliffs, New Jersey, Prentice-Hall, 429 p.

Kreisa, R. D., 1981, Storm-generated sedimentary structures in subtidal marine facies with examples from the Middle and Upper Ordovician of southwestern Virginia: Jour. Sed. Petrology, v. 51, no. 3, p. 823-849.

_____, and Moiola, R. J., 1986, Sigmoidal tidal bundles and other tide-generated sedimentary structures of the Curtis Formation, Utah: Geol. Soc. Am. Bull., v. 97, no. 4, p. 381-387.

Leckie, D. A., and Duke, W. L., 1984, Origin of hummocky cross-stratification, part I, straight-crested symmetrical gravel dunes-the coarse-grained equivalent of hummocky cross-stratification (abs.): Can. Soc. Petroleum Geologists Shelf Sands and Sandstones Symp., Prog. and Abs., p. 51.

_____, and Walker, R. G., 1982, Storm- and tide-dominated shorelines in Cretaceous Moosebar-lower Gates interval-outcrop equivalents of deep basin gas trap in western Canada: Am. Assoc. Petroleum Geologists Bull., v. 66, no. 2, p. 138-157.

Lee, W.T., 1908, The Iron county coal field, Utah: U.S. Geol. Survey Bull. 316, p. 362-365.

_____, W.T., Gilluly, J., Boyer, W. Wy, Baker, A. A., Mcknight, E. T., Dobbin, C. E., and Reeside, J.B., Jr., 1927, Geology and oil in southeastern Utah: U. S. Dept. Interior Press Mem., July 29, 1927.

Leopold, L. B., Wolman, M. G., and Miller, J. P., 1964, Fluvial processes in geomorphology: San Francisco, Freeman and Co., 522 p.

Lessentine, R. H., 1965, Kaiparowits and Black Mesa basins-Stratigraphic synthesis: Am. Assoc. Petroleum Geologists Bull., v. 49, no. 11, p. 1997-2019.

Lewis, G. E., Irwin, J. H., and Wilson, R. F., 1961, Age of the Glen Canyon Group (Triassic and Jurassic) on the Colorado Plateau: Geol. Soc. Am. Bull., v. 72, no. 9, p. 1437-1440.

Logan, B. W., Rezak, R., and Ginsburg, R. N., 1964, Classification and environmental significance of algal stromatolites, Jour. Geol., v. 72, p. 68-83.

Longwell, C. R., Miser, H. D., Moore, R. C., Bryan, K., and Paige, S., 1923, Rock formations in the Colorado Plateau of southeastern Utah and northern Arizona: U. S. Geological Survey Prof. Paper 132-A, 23 p.

Loope, D. B., 1984b, Discussion: origin of extensive bedding planes in aeolian sandstones: a defense of Stokes' hypothesis: Sedimentology, v. 31, no. 1, p. 123-125.

_____, 1985a, Episodic deposition and preservation of eolian sands: a late Paleozoic example from southeastern Utah: Geology, v. 13, no. 1, p. 73-76.

_____, 1985b, Recognition and significance of rhizoliths in eolian sandstones (abs.): SEPM Ann. Midyear Mtg., v. 2, p. 56.

Lord, G. D., and Picard, M. D., 1984, Cyclic deposition and sea level changes: record in Twin Creek Limestone (Jurassic), northern Utah (abs.): Am. Assoc. Petroleum Geologists Bull., v. 68, no. 7, p. 941.

Lowrey, R. O., 1976, Paleoenvironment of the Carmel Formation at Sheep Creek Gap, Dagget County, Utah, Brigham Young Univ. Geol. Studies, v. 23, p. 173-203.

Lupton, C. T., 1914, Oil and gas near Green River, Grand County, Utah: U. S. Geological Survey Bull. 541, p. 115-133.

Mackin, J. H., 1954, Geology and iron ore deposits of the Granite Mountain area, Iron County, Utah: U. S. Geological Survey Min. Inv. Field Studies Map MF-14.

Marvine, A. R., 1875, Part II, Geology of route from Saint George, Utah, to Gila River, Arizona, in Report upon Geographical and Geological Explorations and Surveys West of the One Hundredth Meridian, engineer Dept., U. S. Army, v. 111, Geology: Washington, U. S. Govt. Printing Office, p. 189-225.

Marzolf, J. E., 1986, Nugget - Navajo - Aztec Sandstones: interaction of eolian sand sea with Andean-type volcanic arc (abs.): Am. Assoc. Petroleum Geologists Bull., v. 70, no. 5, p. 616.

Masters, C. D., 1967, Use of sedimentary structures in determination of depositional environments, Mesaverde Formation, William Fork Mountains, Colorado: Am. Assoc. Petroleum Geologists Bull., v. 51, p. 2033-2043.

Matter, A., 1967, Tidal flat deposits in the Ordovician of Maryland: Jour. Sed. Petrology, v. 37, p. 601-609.

McBride, E. F., 1974, Significance of color in red, green, purple, olive brown and gray bbds of Difunta Group, northeastern New Mexico: Jour. Sedimentary Petrology, v. 44, p. 760-773.

McCane, I. N., 1973, the sedimentology of a transgression: Portland Point and Cooksburg Members (Middle Denonian), New York State: Jour. Sed. Petrology, v. 43, no. 2, p. 484-504.

McKee, E. D., 1966a, Significance of climbing-ripple structure: U.S. Geological Survey Prof. Paper 550-D, p. D94-D103.

McKee, E. D., 1979, Introduction to a study of global sand seas, chapter A, in McKee, E. D., ed., a study of Global Sand Seas: U.S. Geological Survey Prof. Paper 1052, p. 1-19.

_____, and Bigarella, J. J., 1979b, Sedimentary structures in dunes-with sections on the Lagoa Dune Field, Brazil, Chapter E, in: McKee, E. D., (ed.), A study of Global Sand Seas: U.S. Geol. Survey Prof. Paper 1052, p. 83-133.

_____, Douglass, J. R., and Rittenhouse, S., 1971, Deformation of lee-side laminae in eolian dunes: Geol. Soc. Am. Bull., v. 82, p. 359-378.

_____, and Moiola, R. J., 1975, Geometry and growth of the White Sands dune field, New Mexico: U.S. Geol. Survey Jour. Res., v. 3, p. 59-66.

_____, 1982, Sedimentary structures in dunes of the Namib Desert, southwest Africa: Geol. Soc. Am. Spec. Paper 188, 64 p.

McKnight, E. T., 1940, Geology of the area between Green and Colorado Rivers, Grand and San Juan Counties, Utah: U. S. Geological Survey Bull., 908, 147 p.

McManus, D. A., 1975, Modern versus relict sediment on the continental shelf: Geol. Soc. Am. Bull., v. 86, no.8, p. 1154-1160.

Middleton, L. T., and Blakey, R. C., 1983, Processes and controls on the intertonguing of the Kayenta and Navajo Formations, northern Arizona: eolian-fluvial interactions, in Brookfield, M. E., and Ahlbrandt, T. S. eds., Eolian sediments and processes: Amsterdam, Elsevier Pub., p. 613-634.

Miller, J. A., 1975, Facies characteristics of Laguna Madre wind-tidal flats, in Ginsberg, R. N., ed., Tidal Deposits, a casebook of Recent and fossil Counterparts: New York, Springer-verlag, p. 67-73.

Miser, H. D., 1924, the San Juan Canyon, southeastern Utah: U. S. Geol. Survey Water-Supply Paper 538, p. 34, 38-39.

Molenaar, C. M., 1971, Mesozoic stratigraphy of Canyonlands National Park and adjacent areas in Baars, D. L., and Molenaar, C. M., authors, Geology of Canyonlands and Cataract Canyon, 6th field conf., Four Corners Geol. Soc., p. 49-60.

_____, 1981, Mesozoic stratigraphy of the Paradox Basin; an overview, in Wiegand, D. L., ed., Geology of the Paradox Basin: Rocky Mtn. Assoc. Geol., p. 119-127.

Mooers, C. N. K., 1976, wind-driven currents on the continental margin, in Stanley, D. J., and Swift, D. J. P., eds., Marine sediment transport and environmental management: New York, John Wiley and Sons, p. 29-52.

Moore, P. S., 1982, Ripple-mark analysis of a fine-grained epeiric-sea deposit (Cambrian, South Australia): Jour. Geol. Soc. Aust., v. 29, p. 71-81.

Moore, R. C., 1922, Stratigraphy of a part of southern Utah: Am. Assoc. Petroleum Geologists Bull., v. 6, p. 199-227.

Morton, R. A., 1978, Large-scale rhomboid bedforms and sedimentary structures associated with hurricane washover: Sedimentology, v. 25, p. 183-204.

_____, 1981, Formation of storm deposits by wind-forced currents in the Gulf of Mexico and the North Sea, in Nio, S.-D., Shuttenhelm, R. T. E., and van Weering, Tj. C. E., eds., Holocene Marine sedimentation in the North Sea Basin, Int. Assoc. Sedimentologists Spec. Pub. 5: Oxford, Blackwell Sci. Pubs., p. 385-396.

Murray, R. C., 1964, Origin and diagenesis of gypsum and anhydrite: Jour. Sedimentary Petrology, v. 34, p. 512-523.

Nami, M., and Leeder, M. R., 1978, Changing channel morphology and magnitude in the Scalby Formation (M. Jurassic) of Yorkshire, England, in Miall, A. D., ed., Fluvial sedimentology: Can. Soc. Petroleum Geologists, Mem. 5, p. 431-440.

Nio, S.-D., 1976, Marine transgressions as a factor in the formation of sandwave complexes: Geol. en Mijn., v. 55, p. 18-40.

Northrop, S. A., 1973, Lexicon of stratigraphic names of the Monument Valley-Four Corners region, in James, H. L., ed., Guidebook of Monument Valley and Vicinity, Arizona and Utah: New Mex. Geological Soc. Twenty-fourth Field Conf., p. 157-176.

Oakes, C., 1983, Environmental significance of variations in first-order bounding surfaces in eolian deposits: Entrada Sandstone, southeastern Utah: unpub. M.Sc. thesis, Dept. Geol. Sci., Univ. Texas, Austin,

Oomkens, E., and Terwindt, J. H. J., 1960, Inshore estuarine sediments in the Haringvliet (Netherlands): Geol. en Mijn., v. 39, p. 701-710.

O'Sullivan, R. B., 1978, Stratigraphic sections of Middle Jurassic San Rafael Group from Lohali: Point, Arizona to Bluff, Utah: U. S. Geol. Survey Oil and Gas Inv. Chart OC-77.

_____, 1980a, stratigraphic sections of Middle Jurassic San Rafael Group and related rocks from the Green River to the Moab area in east-central Utah: U. S. Geological Survey Misc. Field Studies MF-1247.

_____, 1980b, Stratigraphic sections of Middle Jurassic San Rafael Group from Wilson Arch to Bluff in southeastern Utah: U. S. Geol. Survey Oil and Gas Inv. Chart OC-102.

_____, 1981a, Stratigraphic sections of some Jurassic rocks from near Moab, Utah to Slick Rock, Colorado: U. S. Geological Survey Oil and Gas Inv. Chart OC-0107.

_____, 1981b, Stratigraphic sections of Middle Jurassic Entrada Sandstone and related rocks from Salt Valley to Dewey Bridge in east-central Utah: U. S. Geological Survey Oil and Gas Inv. Chart OC-0113.

_____, 1981c, the Middle Jurassic San Rafael Group and related rocks in east-central Utah, in Epis, R. C., and Callender, J. F., eds., Western Slope Colorado, guidebook, 32nd field conf.: New Mex. Geol. Soc., p. 89-95.

_____, 1984a, Stratigraphic sections of Middle Jurassic San Rafael Group and related rocks from Dewey Briige Utah to Uravan, Colorado: U. S. Geological Survey Oil and Gas Inv. Chart OC-0124.

_____, 1984b, the base of the Upper Jurassic Morrison Formation in east-central Utah: U. S. Geological Survey Bull. 1561, 17 p.

_____, and Craig, L. C., 1973, Jurassic rocks of northeast Arizona and adjacent areas, in James, H. L., ed., Guidebook of Monument Valley and vicinity, twenty-fourth field conf.: New Mex. Geol. Soc., p. 79-85.

O'Sullivan, R. B. and Pierce, F. W., 1983, stratigraphic diagram of Middle Jurassic San Rafael Group and associated formations from the San Rafael Swell to Bluff in southeastern Utah: U. S. Geological Survey Oil and Gas Inv. Chart OC-0119.

_____, and Pipiringos, G. N., 1983, stratigraphic sections of Middle Jurassic Eutrada Sandstone and related rocks from Dewey Bridge, Utah to Bridgeport, Colorado: U. S. Geological Survey Oil and Gas Inv. Chart OC-0122.

Otto, E. P., and Picard, M. D., 1975, stratigraphy and oil and gas potential of Eutrada Sandstone (Jurassic), Northeastern Utah: Rocky Mtn. Assoc. Geol. 1975 Symposium, Deep Drilling Frontiers of the Central Rocky Mtns., p. 129-139.

Pemberton, S. G., and Frey, R. W., 1985, the Glossifungites ichnofacies: modern examples from the Georgia coast, U. S. A., in Curran, H. A., ed., Biogenic structures: their use in interpreting depositional environments: SEPM Spec. Pub. no. 35, p. 237-260.

Peterson, F., 1974, Correlation of the Curtis, Summerville and related units (Upper Jurassic) in south-central Utah and north-central Arizona (abs.): Geol. Soc. Am. Abs. with Prog., v. 6, no. 5, p. 466-467.

_____, 1978, Measured sections of the lower member and Salt Wash Member of the Morrison Formation (Upper Jurassic) in the Henry Mountains mineral belt of southern Utah: U. S. Geological Survey Open-File Report 78-1094, 95 p.

_____, 1980, Sedimentology as a strategy for uranium exploration: concepts gained from analysis of a uranium-bearing depositional sequence in the Morrison Formation of south-central Utah, in Turner-Peterson, C. E., ed., Uranium in sedimentary rocks: application of the facies concept to exploration: Rocky Mtn Sect., EMP, p. 65-126.

_____, in press, stratigraphy and nonenclature of middle and upper Jurassic rocks, western Colorado plateau, Utah and Arizona: U. S. Geol. Survey Bull. 1633-B.

_____, 1987, Jurassic paleotectonics in the west-central part of the Colorado Plateau, Utah and Arizona, in Peterson, J. A., ed., Paleotectonics and sedimentation in the Rocky Mountain region, United States: Am. Assoc. Petroleum Geologists, Mem. 41, p. 563-596.

_____, and Caputo, M. V., 1986, the Middle Jurassic Summerville-Curtis interval; a time of transition on the western Colorado Plateau (abs.): Geol. Soc. Am. Abs. with Prog., v. 18, no. 5, p. 402.

Peterson, F., Cornet, B., and Turner-Peterson, C. E., 1977, New data bearing on the stratigraphy and age of the Glen Canyon Group (Triassic and Jurassic) in southern Utah and northern Arizona (abs.): Geol. Soc. Am. Abs. with Programs, v. 9, p. 755.

_____, and Pipiringos, G. N., 1979, Stratigraphic relationships of the Navajo Sandstone to Middle Jurassic formations southern Utah and northern Arizona: U. S. Geological Survey Prof. Paper 1035-B, 43 p.

_____, and Waldrop, H. A., 1965, Jurassic and Cretaceous stratigraphy of south-central Kaiparowits Plateau, Utah, in Goode, H. D., and Robison, R. A., eds., Guidebook to the geology of Utah, no. 19, Geology and resources of south-central Utah: Utah Geol. Soc.; Int-mtn. Assoc. Petroleum Geologists, p. 47-70.

Pettijohn, F.P., 1975, Sedimentary rocks, third edition: New York, Harper and Row Pub., 628 p.

Phoenix, D. A., 1963, Geology of the Lees Ferry area, Coconino County, Arizona, U. S. Geol. Survey Bull. 1137, 86 p.

Pipiringos, G. N., and O'Sullivan, R. B., 1975, Chert pebble unconformity at the top of the Navajo Sandstone in southeastern Utah: Four corners Geol. Soc. Guidebook, 8th Field Conf., p. 149-156.

_____, and O'Sullivan, R. B., 1978, Principal unconformities in Triassic and Jurassic rocks, western interior United States -a preliminary survey: U. S. Geological Survey Prof. Paper 1035-A, 29 p.

Poole, F. G., 1962, Wind directions in late Paleozoic to middle Mesozoic time on the Colorado Plateau: U.S. Geological Survey Prof. Paper 450-D, p. D147-D151.

Porter, M. L., 1986, Sedimentary record of erg migration: Geology, v. 14, no. 6, p. 497-500.

_____, 1987, Sedimentology of an ancient erg margin: the Lower Jurassic Aztec Sandstone, southern Nevada and southern California: Sedimentology, v. 34, p. 661-680.

Postma, H., 1961, Transport and accumulation of suspended matter in the Dutch Wadden Sea: Netherlands Jour. Sea Res., v. 1, p. 148-190.

Postma, H., 1967, Sediment transport and sedimentation in the estuarine environment, in Lauff, G. A., ed., Estuaries: Washington, D. C., Am. Assoc. Adv. Sci., no. 83, p. 158-179.

Potter, P. E., Maynard, J. B., and Pryor, W. A., 1980, Sedimentology of shale: study guide and reference source: New York, Springer-Verlag, 310 p.

Powell, J. W., 1876, Report on the geology of the eastern portion of the Uinta Mountains and a region of country adjacent thereto, with atlas: U. S. Geographic and Geologic Survey of the Territories, 1876, Washington, U. S. Govt. Printing off., 218 p.

Prommel, H. W. C., 1927, Geology and structure of portions of Grand and San Juan Counties, Utah: Am. Assoc. Petroleum Geologists Bull., v. 7, p. 384-399.

Pryor, W. A., 1967, Biogenic directional features on several recent point bars: Sedimentary Geology, v. 1, p. 235-245.

de Raaf, J. F. M., and Boersma, J. R., 1971, Tidal deposits and their sedimentary structures: Geol. en Mijn., v. 50, p. 479-504.

_____, Boersma, J. R., and van Gelder, A., 1977, wave-generated structures and sequences from a shallow marine succession, lower Carboniferous, County Cork, Ireland: Sedimentology, v. 24, p. 451-483.

Reeside, J. B., Jr., 1923, Notes on the geology of Green River Valley between Green River, Wyoming and Green River, Utah: U. S. Geological Survey Prof. Paper 132, p. 35-50.

_____, and Bassler, H., 1922, Stratigraphic sections in southwestern Utah and northwestern Arizona: U.S. Geol. Survey Prof. Paper 129, p. 63-64.

Reif, D. M., and Slatt, R. M., 1979, Redbed members of the Lower Triassic Moenkopi Formation, southern Nevada: Sedimentology and paleogeography of a muddy tidal flat deposit: Jour. Sedimentary Petrology, v. 49, no. 3, p. 869-890.

Reineck, H. -E., 1967a, Layered sediments of tidal flats, beaches and shelf bottoms of the North Sea, in Lauff, G. D., ed., Estuaries: Am. Assoc. Adv. Sci., no. 83, p. 191-206.

_____, 1972, Tidal flats, in Rigby, J. K., and Hamblin, W. K., eds., Recognition of ancient sedimentary environments: Soc. Econ. Paleont. Mineral. Spec. Pub. 16, p. 146-160.

_____, 1975, German North Sea tidal flats, in Ginsburg, R. N., ed., Tidal deposits, a casebook of Recent and fossil counterparts: New York, Springer-Verlag, p. 5-12.

_____, 1978, the tidal flats on the German North Sea Coast: Die Kuste, Archive for research and technology on the North Sea and Baltic Coast, v. 32, p. 69-85.

_____, and Singh, I. B., 1967, Primary sedimentary structures in the Recent sediments of the Jade, North Sea: Marine Geology, v. 5, p. 227-235.

Reineck, H. -E., and Singh, I. B., 1971, Der Golf von Gaeta/ Tyrrhenisches Meer, 3, die gefuge von vorstrand-und schelfsedimenten: Senckenbergiana Marit., v. 3, p. 185-201.

_____, and Singh, I. B., 1972, Genesis of laminated sand and graded rhythmites in storm-sand layers of shelf mud: Sedimentology, v. 18, p. 123-128.

_____, and Singh, I. B., 1980, Depositional sedimentary environments, 2nd ed.: Berlin, Springer-Verlag, 549 p.

_____, and Wunderlich, F., 1968b, Classification and origin of flaser and lenticular bedding: Sedimentology, v. 11, p. 99-104.

_____, and Wunderlich, F., 1969, Die entstehung von schichten und schicht banken im Watt: Senckenbergiana Marit.: v. 1, p. 85-106.

Richards, H. G., 1958, Cyclic deposition in the Jurassic Carmel Formation of eastern Utah: Jour. Sed. Petrology, v. 28, p. 40-45.

Rigby, J. K., 1964, Some observations on stratigraphy and paleoecology of the Carmel and Twin Creek Formations in the Uinta Mountains, in Guidebook to the geology and mineral resources of the Uinta Basin: Intermountain Assoc. Petroleum Geologists, p. 109-114.

_____, 1978, Mesozoic and Cenozoic sedimentary environments of the northern Colorado Plateau: Brigham Young University Geology Studies, v. 25, p. 47-65.

_____, 1986, Shallow water facies in the Jurassic Carmel Formation in the Beaver Dam Mountains of southwesternmost Utah (abs.): Rocky Mtn. Sect. Geol. Soc. Am., Abs. with Prog., v. 18, no. 5, p. 406.

Rogers, J. J. W., Burchfiel, B. C., Abbott, E. W., Anepohl, J. K., Eweng, A. H., Koehnken, P. J., Novitsky, J. M., and Tulukdar, S. C., 1974, Paleozoic and Lower Mesozoic volcanism and continental growth in the western United States: Geol. Soc. Am. Bull., v. 85, no. 12, p. 1913-1924.

Rubin, D. M., and Hunter, R. E., 1982, Bedform climbing in theory and nature: Sedimentology, v. 29, p. 121-138.

Sarjeant, W. A. S., 1975, Plant trace fossils, in Frey, R. W., ed., the study of trace fossils: New York, Springer-Verlag, p. 163-180.

Saunderson, H. C., and Lockett, F. P. J., 1983, Flume experiments on bedforms and structures at the dune-plane bed transition, in Collinson, J. D., and Lewin, J., eds., Modern and ancient fluvial systems: Int. Assoc. Sedimentologists Spec. Pub. 6, p. 49-60.

Schreiber, B. C., Friedman, G. M., Decima, A., and Schreiber, E., 1976, Depositional environments of Upper Miocene (Messinian) evaporite deposits of the Sicilian Basin: Sedimentology, v. 23, p. 729-760.

_____, Roth, M. S., and Helman, M. L., 1982, Recognition of primary facies characteristics of evaporites and the differentiation of these forms from diagenetic overprints, in Handford, C. R., Loucks, R. G., and Davies, G. R., eds., Depositional and diagenetic spectra of evaporites-a core workshop: Soc. Econ. Paleont. Mineral. Core Workshop no. 3, p. 1-32.

_____, Tucker, M. E., and Till., R., 1986, Arid shorelines and evaporites, in Reading, H. G., ed., Sedimentary environments and facies: Oxford, Blackwell Sci. Pub., p. 189-228.

Schweickert, R. A., and Cowan, D. S., 1975, Early Mesozoic tectonic evolution of the Western Sierra Nevada California: Geol. Soc. Am. Bull., v. 86, no. 10, p. 1329-1336.

Seilacher, A., 1967, Bathymetry of trace fossils: Marine Geology, v. 5, p. 413-428.

Sellwood, B. W., 1972, Tidal flat sedimentation in the Lower Jurassic of Bornholm, Denmark: Paleogeog., Paleoclim., Paleoecol., v. 11, no. 2, p. 93-106.

_____, 1978, Jurassic, in McKerrow, W. S., ed., The ecology of fossils, an illustrated guide: Cambridge, Mass., MIT Press, p. 204-279.

Shearman, D. J., 1971, Marine evaporites: the calcium sulfate facies: Alberta Soc. Petroleum Geology seminar, Univ. Calgary, 65 p.

_____, 1978, Evaporites of coastal sabkhas, in Dean, W. E., and Schreiber, B. C., eds., Marine evaporites: Soc. Econ. Paleont. Mineral. short course notes no. 4, p. 6-42.

Shepard, F. P., and Inman, D. L., 1950, Nearshore water circulations related to bottom topography and wave refraction: Am. Geophys. Union Trans, v. 31, p. 196-212.

Smith, D. J., and Hopkins, T. S., 1972, Sediment transport on the continental shelf of Washington and Oregon in light of recent current measurements, in Swift, D. J. P., Duane, D. B., and Pilkey, O. H., eds., Shelf sediment transport: Process and pattern: Stroudsbourg, Dowden, Hutchinson, and Ross, p. 143-180.

Smith, L. S., 1976, Paleoenvironments of the Upper Eutrada Sandstone and the Curtis Formation on the west flank of the San Rafael Swell, Emery County, Utah: Brigham Young Univ. Geol. Studies, v. 23, pt. 1, p. 113-171.

Smith, J. F., Jr., Huff, L. C., Hinrichs, E. N., and Luedke, R. G., 1963, Geology of the Capitol Reef area, Wayne and Garfield Counties, Utah: U. S. Geol. Survey Prof. Paper 363, 102 p.

Smith, N. D., 1970, the braided stream depositional environment: Comparison of the Platte River with some Silurian clastic rocks, north-central Appalachians: Geol. Soc. Am. Bull., v. 81, p. 2993-3014.

Sohl, N. F., 1965, Marine Jurassic gastropods, central and southern Utah: U.S. Geological Survey Prof. Paper 503-D, p. 1-29.

Sprinkle, D. A., and Waanders, G. L., 1984, Correlation of Twin Creek Limestone with Arapien Shale in Arapian Embayment, Utah-preliminary appraisal (abs.): Am. Assoc. Petroleum Geologists Bull., v. 68, no. 7, p. 950.

Stanley, K. O., Jordan, W. M., and Dott, R. H., Jr., 1971, New hypothesis of early Jurassic paleogeography and sediment dispersal for western United States: Am. Assoc. Petroleum Geologists Bull., v. 55, no. 1, p. 10-19.

Stanton, R. G., 1976, the paleoenvironment of the Summerville Formation on the west side of the San Rafael Swell, Emery County, Utah: Brigham Young Univ. Geol. Studies, v. 22, pt. 4, p. 37-73.

Steiner, M. B., 1986, Rotation of the Colorado Plateau: Tectonics, v. 5, no. 4, p. 649- 660.

Stokes, W. L., 1944, Morrison and related deposits in and adjacent to the Colorado Plateau: Geol. Soc. Am. Bull., v. 55, no. 8, p. 951-992.

_____, 1949, Triassic and Jurassic rocks of Utah, in Hansen, G. H., and Bell, M. M., eds., oil and gas possibilities of Utah: Utah Geol. Mineral Survey, p. 79-89.

_____, 1952, Uranium-vanadium deposits of the Thompsons area, Grand County, Utah-with emphasis on the origin of carnotite ores: Utah Geological and Mineralogical Survey Bull. 46, 51 p.

_____, 1954. Stratigraphy of the southeastern Utah uranium region, in Stokes, W. L., ed., Guidebook to geology of Utah, no. 9, uranium deposits and general geology of southeastern Utah: Utah Geol. Soc., p. 16-47.

_____, 1957, Jurassic system of the southern flank of the Uinta Mountains, in Seal, O. G., ed., Guidebook to the geology of the Uinta Basin, eigth ann. field conf.: Intmtn. Assoc. Petroleum Geologists, p. 92-96.

_____, 1963a, Triassic and Jurassic formations of southwest Utah, in Guidebook to geology southeast Utah, 12th Ann. Field Conf.: Intermtn. Assoc. Petroleum Geologists, p. 60-64.

Stokes, W. L., 1963b, Triassic and Jurassic Periods in Utah, in oil and gas possibilities, re-evaluated: Utah Geol. Mineral Survey Bull., v. 54, p. 109-121.

_____, 1957, Jurassic system of the southern flank of the Uinta Mountains, in Seal, O. G., ed., Guidebook to the geology of the Uinta Basin, Eighth Ann. Field Conf.: Intmtn. Assoc. Petroleum Geologists, p. 92-96.

_____, 1972, Stratigraphic problems of the Triassic and Jurassic sedimentary rocks of central Utah, in Baer, J. L., and Callaghan, E., eds., Plateau-Basin and Range Transition zone, central Utah, 1972: Utah Geol. Assoc. Pub. 2, p. 21-28.

_____, 1980, Stratigraphic interpretations os Triassic and Jurassic beds, Henry Mountains area, in Picard, M. D., ed., Henry Mountains symposium: Utah Geol. Assoc., Pub. 8, p. 113-122.

_____, and Holmes, C. N., 1954, Jurassic rocks of south central Utah, in Guidebook to the geology of the high plateaus, central and south central Utah: Intermtn. Assoc. Petroleum Geologists, 5th ann. field conf., p. 34-38.

van Straaten, L. M. J. U., 1953, Megaripples in the Dutch Wadden Sea and in the basin of Arcachon: Geol. en Mijn., v. 15, p. 1-11.

_____, 1954a, composition and structure of Recent marine sediments in the Netherlands: Leidse Geol. Mededel., v. 19, p. 1-110.

_____, 1961, Sedimentation in tidal flat areas: Jour. Alberta Soc. Petroleum Geologists, v. 9, no. 7, p. 203-226.

_____, and Keunen, P. H., 1958, Tidal action as a cause of clay accumulation: Jour. Sedimentary Petrology, v. 28, p. 406-413.

Stride, A. H., 1963, Current-swept sea floors near the southern half of Great Britain: Quart. Jour. Geological Soc. London, v. 119, p. 175-197.

Swett, K., Klein, G. de V., and Smit, D. E. 1971, A Cambrian tidal sand body-the Eriboll Sandstone of northwest Scotland: an ancient-Recent analog: Jour. Geology, v. 79, p. 400-415.

Swift, D. J. P., 1985, Response of the shelf floor to flow, in Tillman, R. W., Swift, D. J. P., and Walker, R. G., eds., shelf sands and sandstone reservoirs, short course notes no. 3: Tulsa, SEPM, p. 135-241.

_____, Figueiredo, A. G., Jr., Freeland, G. L., and Oertel, G. F., 1983, Hummocky cross-stratification and megaripples: a geological double standard?: Jour. Sed. Petrology, v. 53, no. 4, p. 1295-1317.

Swift, D. J. P., Freeland, G. L., and Young, R. A., 1979, Time and space distribution of magaripples and associated bedforms, middle Atlantic Bight, North American Atlantic shelf: Sedimentology, v. 26, p. 389-406.

_____, and Niedoroda, A. W., 1985, Fluid and sediment dynamics on continental shelves, in Tillman, R. W., Swift, D. J. P., and Walker, R. G., eds., Shelf sands and sandstone reservoirs, short course notes no. 13, SEPM, p. 47-134.

Stride, A. H., Belderson, R. H., Kenyon, N. H., and Johnson, M. A., 1982, offshore tidal deposits: sand sheet and sand bank facies, in Stride, H. H., ed., Offshore tidal sands: London, Chapman and Hall, p. 95-125.

Talbot, M. R., 1985, Major bounding surfaces in aeolian sandstones- a climatic model: Sedimentology, v. 32, no. 2, p. 257-266.

Tanner, W. F., 1967, Ripple mark indices and their uses: Sedimentology, v. 9, p. 89-104.

Taylor, D. W., 1981, Carbonate petrology and depositional environments of the limestone member of the Carmel Formation near Carmel Junction, Kane County, Utah: Brigham Young Univ. Geol. Studies, v. 28, pt. 3, p. 117-133.

Terwindt, J. H. J., 1970, Observation on submerged sand ripples with heights ranging from 30 to 200 cm occurring tidal channels of S. W. Netherlands: Geol. Mijn., v. 48, no. 6, p. 489-501.

_____, 1971a, Litho-facies of inshore estuarine and tidal inlet deposits: Geol. Mijn., v. 50, no. 3. p. 515-525.

_____, 1981, Origin and sequences of sedimentary structures in inshore mesotidal deposits of the North Sea, in Nio, S.-D., Shuttenhelm, R. T. E., and van Weering, Tj. C. E., eds., Holocene marine sedimentation in the North Sea Basin, Spec. Pub. 5, Int. Assoc. Sedimentologists: Oxford, Blackwell Sci. Pubs., p. 4-26.

_____, and Breusers, H. N. C., 1972, Experiments on the origin of flaser, lenticular, and sand-clay alternating bedding: Sedimentology, v. 19, p. 85-98.

_____, and Brouwer, M. J. N., 1986, the behavior of intertidal sandwaves during neap-spring tide cycles and the relevance for paleoflow reconstructions: Sedimentology, v. 33, no. 1, p. 1-32.

Thomas, C. R., McCann, F. T., and Ramon, N. D., 1945, Mesozoic and Paleozoic stratigraphy in northwestern Colorado and northeastern Utah: U. S. Geological Survey Oil and Gas Inv. Chart OC-16, 2 sheets.

Thompson, A. E., and Stokes, W. L., 1970, Stratigraphy of the San Rafael Group, southwest and south central Utah: Utah Geol. Mineral Survey Bull., 87, 50 p.

Thompson, R. W., 1968, Tidal flat sedimentation on the Colorado River delta, northwestern Gulf of California: Geol. Soc. Am. Mem. 107, 133 p.

_____, 1975, Tidal-flat sediments of the Colorado River delta, northwestern Gulf of California, in Ginsburg, R. N., ed., Tidal deposits, a casebook of Recent and fossil counterparts: New York, Springer-Verlag, p. 57-65.

Tillman, R. W., and Martinsen, R. S., 1984, the Shannon shelf-ridge sandstone complex, Salt Creek anticline area, Powder River Basin, Wyoming, in Tillman, R. W., and Siemers, C. T., eds., Siliciclastic Shelf Sediments: Soc. Econ. Paleont. Mineral., Spec. Pub. no. 34, p. 85-142.

_____, and Martinsen, R. S., 1985, Upper Cretaceous Shannon and Haystack Mountains Formation Field Trip, Wyoming, Guidebook for field trip no. 11: Rocky Mtn. Sect., Soc. Econ. Paleont. Mineral., 97 p.

Van Hinte, J. E., 1976a, A Jurassic time scale: Am. Assoc. Petroleum Geologists Bull., v. 60, no. 4, p. 489-497.

Visser, M. J., 1980, Neap-spring cycles reflected in Holocene subtidal large-scale bedform deposits: a preliminary note: Geology, v. 8, p. 543-54

Voorhees, B. J., 1978, Stratigraphy and facies of the lower Carmel Formation (Middle Jurassic), southwestern Utah: unpub. M. Sc. thesis, Northern Ariz. Univ., 161 p.

Walker, R. G., 1984b, Shelf and shallow marine sands, in Walker, R. G., ed., Facies models, second edition, reprint series 1: Geoscience Canada, p. 141-170.

Walker, T. R., 1967a, Formation of redbeds in modern and ancient deserts: Geol. Soc. Am. Bull., v. 78, p. 353-368.

Warme, J. E., 1970, Traces and significance of marine rock borers, in Crimes, T. P., and Harper, J. C., eds., Trace fossils, Liverpool, Seel House Press, p. 515-526.

Warme. J. E., and McHuron, E. J., 1978, Marine borers: trace fossils and geological significance, in Basan, P. B., ed., Trace fossil concepts: SEPM Short Course no. 5, p. 67-118.

Warren, J. K., and St. C. Kendall, C. G., 1985, Comparison of sequences formed in marine sabkha (subaerial) and salina (subaqueous) settings - modern and ancient: Am. Assoc. Petroleum Geologists Bull., v. 69, no. 6, p. 1013-1023.

Weeks, F. B., 1907, stratigraphy and structure of the Uinta Range: Geol. Soc. Am. Bull., v. 18, p. 427-448.

Weimer, R. J., Howard, J. D., and Lindsay, D. R., 1982, Tidal flats and associated tidal channels, in Scholle, P. A., and Spearing, D., eds., Sandstone depositional environments: Am. Assoc. Petroleum Geologists Mem. 31, p. 191-246.

Whitman, C., 1907, Stratigraphic results of reconnaissance in western Colorado and eastern Utah: Jour. Geology, v. 15, p. 644.

Williams, G. E., 1971, Flood deposits of the sand-bed ephemeral streams of central Australia: Sedimentology, v. 17, p. 1-40.

Williams, N. C., 1952, Jurassic stratigraphy of southwest Utah, in Guidebook to the geology of Utah, Cedar City, Utah to Las Vegas, Nevada: Intermtn. Assoc. Petroleum Geologists Guidebook to the geology of Utah, no. 7, p. 61-68.

Wilson, I. G., 1972a, Aeolian bedforms - their development and origins: Sedimentology, v. 19, p. 173-210.

_____, 1972b, Universal discontinuities is bedforms produced by the wind: Jour. Sed. Petrology, v. 42, p. 667-669.

_____, 1973, Ergs: Sedimentary Geology, v. 10, p. 77-106.

Wilson, R. F., 1965, Triassic and Jurassic strata of southwestern Utah, in Goode, H. D., and Robison, R. A., eds., Guidebook to the geology of Utah, no. 19, Geology and resources of south-central Utah: Utah Geol. Soc.; Intmtn. Assoc. Petroleum Geologists, p. 31-46

Woodruff, E. G., 1912, Geology of the San Juan oil field, Utah: U. S. Geol. Survey Bull. 471, p. 80, 88-89.

Wright, J. C., 1978, Four maps showing lithologic distributions of selected parts of the Jurassic San Rafael Group, Utah, Colorado, Arizona, and New Mexico: U. S. Geological Survey Open-File Rept. 78-572, 9 p.

_____, and Dickey, D. D., 1957, Semiannual report to AEC on San Rafael (Entrada) studies, in: Geologic investigations of radioactive deposits-semiannual progress report, Dec. 1, 1956 to May 31, 1957: U. S. Geol. Survey TEI-690, p. 351-354.

_____, and Dickey, D. D., 1958a, Semiannual report to AEC on San Rafael (Entrada) studies, in: Geologic investigations of radioactive deposits-semiannual progress report, Dec. 1, 1957 to May 31, 1958: U. S. Geol. Survey TEI-740, p. 139-146.

Wright, J. C., and Dickey, D. D., 1958b, Pre-Morrison Jurassic strata of south eastern Utah, in Sanborn, A. F., ed., Guidebook to the geology of the Paradox Basin: Intermtn. Assoc. Petroleum Geologists, ninth ann. field conf., p. 172-181.

_____, and Dickey, D. D., 1959, Semiannual reports to AEC on San Rafael (Entrada) studies, in: Geologic investigations of radioactive deposits-semiannual progress report for Dec. 1, 1958 to May 21, 1959: U. S. Geol. Survey TEI-751, p. 61-66.

_____, and Dickey, D. D., 1963a, Relations of the Navajo and Carmel Formations in southwestern Utah and adjoining Arizona, U. S. Geol. Survey, Prof. Paper 450E, p. E 63-E 67.

_____, and Dickey, D. D., 1963b, Block diagram of the San Rafael Group and underlying strata in Utah and part of Colorado: U. S. Geological Survey Oil and Gas Inv. Chart OC-63.

_____, and Dickey, D. D., 1978a, East-west cross sections of the Jurassic age San Rafael Group rocks from western Colorado to central and western Utah: U. S. Geological Survey Open-File Rept. 78-784.

_____, and Dickey, D. D., 1978b, North-south cross-sections of the Jurassic San Rafael Group in Utah and western Colorado: U. S. Geological Survey Open-File Rept. 78-965, one sheet.

_____, and Dickey, D. D., 1978c, Miscellaneous cross sections of the Jurassic San Rafael Group in southern Utah: U. S. Geological Survey Open-File Rept. 78-966.

_____, Dickey, D. D., and Snyder, R. P., 1979a, Stratigraphic sections of Jurassic San Rafael Group and adjacent rocks in Wayne County, Utah: U. S. Geological Survey Open-File Rept. 79-1126, 106 p.

_____, Dickey, D. D., and Snyder, R. P., 1979b, Measured stratigraphic sections of Jurassic San Rafael Group and adjacent rocks in Kane County Utah: U. S. Geological Survey Open-File Rept. 79-1373.

_____, and Dickey, D. D., 1979c, Stratigraphic sections of Jurassic San Rafael Group and adjacent rocks in Grand County, Utah: U. S. Geological Survey Open-File Rept. 79-1127, 44 p.

_____, and Dickey, D. D., Snyder, R. P., Craig, L. C., and Cadigan, R. A., 1979, Measured stratigraphic sections of Jurassic San Rafael Group and adjacent rocks in Emery and Sevier Counties, Utah: U. S. Geological Survey Open-File Rept. 79-1317, 157 p.

_____, Dickey, D. D., and Snyder, R. P., 1980, Stratigraphic sections of Jurassic San Rafael Group and adjacent rocks in Garfield County, Utah: U. S. Geological Survey Open-File Rept. 80-308, 84 p.

Wright, J. C., Shawe, D. R., and Lohman, S. W., 1962, Definition of members of Jurassic Entrada Sandstone in east-central Utah and west-central Colorado: Am. Assoc. Petroleum Geologists Bull., v. 46, no. 11, p. 2057-2070.

_____, and Snyder, R. P., and Dickey, D. D., 1979, Stratigraphic sections of Jurassic San Rafael Group and adjacent rocks in Iron and Washington Counties, Utah: U. S. Geological Survey Open-File Rept. 79-1318, 55 p.

Wright, M. E., and Walker, R. G., 1981, Cardium Formation (Upper Cretaceous) at Seebe, Alberta-storm-transported sandstones and conglomerates in shallow-marine depositional environments below fair-weather wave-base: Can. Jour. Earth Sci., v. 18, p. 795-809.

Wunderlich, F., 1978, Deposition of mud in the giant ripples of inner Jade, German Bight, North Sea: Senckenbergiana Marit., v. 10, p. 257-267.

Young, R. G., 1978, Depositional systems and dispersal patterns in uraniferous sandstones of the Colorado Plateau: Utah Geol., v. 5, no. 2, p. 85-102.

APPENDIX 1

Table A.1

Paleocurrent Data

Table A.1. Summary of paleocurrent analysis for facies in the Curtis-Moab-Summerville interval. Presentation format: X, Y, Z, where X = number of measurements, Y = mean vector in degrees (o) azimuth, Z = reliability index. Data on ripple foresets include: ripple asymmetry and ribs-and-furrows

Stratigraphic Section	Crossbedding	Ripple Foresets	Parting Lineation	Imbrication
Curtis Formation				
Sandstone-mudstone facies				
Z-6		10, 335°, 19		15, 236°,84
	Crossbedding	Ripple Foresets	Parting Lineation	Ripple Crests
Z-3A	9, 37°, 87	34, 70°, 35		10, 358°, 73
Z-14		10, 49°, 43		
Z-16	7, 104°,70			
Z-18	6, 275°, 77			
Z-9A		15, 314°, 52	3, 292°, 99.9	14, 32°, 59
Composite sandstone facies				
Z-6	40, 269°, 29	16, 328°, 46	6, 349°, 86	
Z-14	18, 209°, 40	18, 221°, 19	8, 62°, 98	
Z-15	25, 25°, 22	9, 75°, 9		
Z-16	12, 11°, 57	22, 320°, 1	8, 46°, 99	
Z-23	2, 195°, 17	7, 210°, 15	14, 345°, 95	
Z-18	26, 279°, 27	37, 339°, 18	12, 300°, 65	
Z-17	12, 166°, 37	11, 340°, 68		
Z-3A	34, 340°, 23	90, 40°, 33	38, 9°, 71	
Z-9B	4, 25°, 99			
Z-9A	5, 355°, 92	33, 356°, 43	15, 344°, 83	
Z-2B		8, 180°, 50	16, 9°, 98	
Z-2A		17, 308°, 26	14, 358°, 93	
Z-10A		21, 306°, 26	12, 327°, 51	
Z-13	12, 226°, 31	7, 197°, 82	8, 33°, 57	
Z-5		8, 290°, 29	32, 350°, 64	
Rippled silty facies				
Z-4		2, 48°, 79		
Z-13		6, 177°, 68		
Z-12		10, 180°, 90		

Z-14	18, 209°, 40	18, 221°, 19	8, 62°, 98
Z-15	25, 125°, 22	9, 75°, 9	
Z-16	12, 110°, 57	22, 320°, 1	8, 46°, 99
Z-23	2, 195°, 17	7, 210°, 15	14, 345°, 95
Z-18	26, 279°, 27	37, 339°, 18	12, 300°, 65
Z-17	12, 166°, 37	11, 340°, 68	
Z-3A	34, 340°, 23	90, 40°, 33	38, 9°, 71
Z-9B	4, 25°, 99		
Z-9A	5, 355°, 92	33, 356°, 43	15, 344°, 83
Z-2B		8, 180°, 50	16, 9°, 98
Z-2A		17, 308°, 26	14, 358°, 93
Z-10A		21, 306°, 26	12, 327°, 51
Z-13	12, 226°, 31	7, 197°, 82	8, 33°, 57
Z-5		8, 290°, 29	32, 350°, 64
Rippled silty facies			
Z-4		2, 48°, 79	
Z-13		6, 177°, 68	
Z-12		10, 180°, 90	
Z-8		19, 156°, 34	2, 320°, 99
Redbed facies			
Z-19		5, 100°, 22	
Z-22	5, 28°, 92	7, 48°, 75	
Summerville Formation			
Reddish-brown silty facies			
Z-6		4, 55°, 79	
Z-14		41, 56°, 76	9, 47°, 94
Z-16		15, 77°, 66	2, 62°, 99
Z-23		2, 60°, 99	
Z-18		2, 349°, 99	
Z-3A		3, 339°, 86	
Z-9A		10, 8°, 57	
Z-8		6, 187°, 47	
Gypsiferous facies			
Z-3A		5, 95°, 54	
Z-2A		14, 124°, 68	
Z-10A		4, 6°, 35	
Z-8		6, 174°, 83	

Table A.1. Continued

Stratigraphic Section	Crossbedding	Ripple Foresets	Parting Lineation	Ripple Crests
Moab Tongue				
Crossbedded sandstone facies				
Z-21	2, 317°, 92			
Z-20	9, 281°, 25			
Z-19	9, 246°, 52			
Z-22	22, 236°, 37			

APPENDIX 2

Petrologic Data

Table A.2

Table A.2. Summary of raw data. Results in percent are from petrographic analysis of sam
Curtis-Moab-Summerville interval

	Quartz		Feldspar			Rock Fragments				
SAMPLES	Monocrystalline	Polycrystalline	Orthoclase	Plagioclase	Microcline	Chert	Carbonate	Sandstone-siltstone-shale	Igneous	
CURTIS FORMATION										
Sandstone-mudstone facies										
Z-3A S-2	75	2	3	1	0.5	5	14	--	--	
Z-3A S-2A, U-3	55	1	1	1	--	12	26	0.3	--	
Z-6 S-1	28	0.3	--	0.3	--	6	59	--	--	
Z-9 S-1	75	4	6	1	--	6	--	--	2	
Z-9 S-2	87	2	4	1	--	2	1	--	--	
Z-9 S-2 Re	55	1	2	2	--	13	14	--	1	1
Z-9B S-2	86	--	6	0.5	--	6	--	--	--	
Z-9B S-3	81	3	8	3	--	5	--	--	--	
Z-9B S-4	82	2	5	6	--	4	--	--	--	
Z-9B S-5	83	2	2	5	--	7	--	--	--	
Z-15 S-4	27	--	0.5	0.5	--	50	21	--	--	
Z-15 S-5	40	1	5	3	--	26	10	1	--	1
Z-16 S-2	46	3	2	1	--	14	30	1	--	
Z-16 S-3	78	2	5	0.7	--	9	--	1	--	
Composite sandstone facies										
Z-3A S-3	77	2	5	--	0.3	--	5	1	--	
Z-3A S-3 Re	79	3	4	1	0.8	3	--	--	--	
Z-3A S-4	57	--	14	14	--	14	--	--	--	
Z-6 S-1A	91	0.3	2	0.3	--	1	0.3	--	--	
Z-6 S-1b	79	0.9	9	2	--	--	--	--	--	
Z-6 S-2	86	3	3	1	--	5	--	--	--	
Z-6 S-2 Re	71	6	9	5	0.3	--	1	--	--	
Z-6 S-4	76	2	10	2	1	5	--	1	--	
Z-6 S-5	81	--	9	2	0.5	2	3	--	--	
Z-6 S-6	82	--	5	2	--	6	--	--	--	
Z-9B S-6	77	3	3	1	--	10	2	--	--	
Z-18 S-3	81	2	5	2	--	--	--	--	--	

nt are from petrographic analysis of samples from facies in the

Feldspar		Rock Fragments									
Plagioclase	Microcline	Chert	Carbonate	Sandstone-siltstone-shale	Igneous	Fossils and other allochemical grains	Glauconite	Heavy minerals	Evaporite	Matrix	Cement
1	0.5	5	14	--	--	--	--	--	--	--	32
1	--	12	26	0.3	--	0.3	1	1.3	--	--	40
0.3	--	6	59	--	--	4	0.3	1	--	1	15
1	--	6	--	--	2	6	--	--	--	--	24
1	--	2	1	--	--	--	3	0.5	--	0.5	27
2	--	13	14	--	1	10	1	1	--	--	41
0.5	--	6	--	--	--	--	--	2	--	--	36
3	--	5	--	--	--	--	--	--	--	--	40
6	--	4	--	--	--	--	--	1	--	--	34
5	--	7	--	--	--	--	--	0.5	--	--	37
0.5	--	50	21	--	--	1	--	--	--	--	22
3	--	26	10	1	--	13	0.5	--	--	--	56
1	--	14	30	1	--	4	0.5	--	--	--	24
0.7	--	9	--	1	--	3	1	0.3	--	--	41
--	0.3	--	5	1	--	3	5	0.3	--	--	19
1	0.8	3	--	--	--	7	2	0.2	--	--	12
14	--	14	--	--	--	--	0.7	0.3	--	--	48
0.3	--	1	0.3	--	--	--	4	1	--	5	11
2	--	--	--	--	--	1	7	--	--	10	6
1	--	5	--	--	--	--	2	--	--	--	38
5	0.3	--	1	--	--	0.3	7	0.3	1	0.5	43
2	1	5	--	1	--	2	1	--	--	--	41
2	0.5	2	3	--	--	--	2	0.5	--	--12	
2	--	6	--	--	--	2	2	1	--	--	45
1	--	10	2	--	--	4	--	--	--	--	24
2	--	--	--	--	--	2	7	--	--	--	25

Table A.2. Continued

SAMPLES	Quartz		Feldspar			Rock Fragments			
	Monocrystalline	Polycrystalline	Orthoclase	Plagioclase	Microcline	Chert	Carbonate	Sandstone-siltstone-shale	Igneous
CURTIS FORMATION									
Rippled silty facies									
Z-3 S-1	87	--	3	2	0.3	5	--	--	--
Z-3 S-2	80	--	4	2	--	10	--	--	--
Z-8 S-1b	80	--	13	1	--	3	--	--	--
Z-12 S-3	71	1	5	2	--	11	--	--	--
Z-13 S-4	71	--	8	2	--	7	--	--	--
Z-14 S-1a	80	1	2	1	--	6	--	5	--
Z-14 S-1	80	--	3	3	--	5	--	--	--
Z-14 S-2	69	2	8	2	--	7	--	--	--
Z-14 S-3	72	--	4	2	--	14	--	--	--
Z-18 S-4	60	--	1	2	--	8	--	--	--
Z-18 S-5	73	2	4	3	--	4	--	--	--
Redbed facies									
Z-7 S-1	92	--	3	3	--	1	--	--	--
Z-7 S-2	94	--	0.3	1	--	3	--	--	--
Z-7 S-4	89	2	2	0.9	--	6	--	--	--
Z-11 S-1	70	--	13	4	--	10	--	--	--
Z-11 S-2	87	4	4	2	--	2	--	--	--
Z-21 S-1	89	2	--	1	0.9	6	--	--	--
Z-21 S-3	94	2	2	--	--	1	--	--	--
Z-21 S-4	94	0.5	2	--	--	1	--	--	--

ldspar		Rock Fragments									
Plagioclase	Microcline	Chert	Carbonate	Sandstone-siltstone-shale	Igneous	Fossils and other allochemical grains	Glauconite	Heavy minerals	Evaporite	Matrix	Cement
	0.3	5	--	--	--	0.3	2	0.3	--	--	34
	--	10	--	--	--	--	2	1	--	--	
	--	3	--	--	--	--	3	--	--	--	58
	--	11	--	--	--	--	9	1	--	--	57
	--	7	--	--	--	--	10	2	--	--	35
	--	6	--	5	--	--	3	2	--	--	57
	--	5	--	--	--	--	8	1	--	--	30
	--	7	--	--	--	--	12	--	--	--	48
	--	14	--	--	--	--	7	1	--	--	38
	--	8	--	--	--	1	16	12	--	--	70
	--	4	--	--	--	0.9	6	2	--	--	60
	--	1	--	--	--	--	0.5	0.5	--	--	75
	--	3	--	--	--	0.3	--	0.3	--	--	88
.9	--	6	--	--	--	--	--	--	--	--	83
	--	10	--	--	--	0.5	0.5	2	--	--	83
	--	2	--	--	--	1	--	1	--	--	32
	0.9	6	--	--	--	--	1	1	--	--	57
--	--	1	--	--	--	--	--	0.9	--	--	41
--	--	1	--	--	--	1	--	0.5	--	--	37

Table A.2. Continued

SAMPLES	Quartz		Feldspar			Rock Fragments			
	Monocrystalline	Polycrystalline	Orthoclase	Plagioclase	Microcline	Chert	Carbonate	Sandstone-siltstone-shale	Igneous
Summerville Formation									
Gypsiferous facies									
Z-2 S-1	--	--	--	--	--	--	--	--	--
Z-3B S-1	91	--	3	1	--	2	--	--	--
Z-10 S-2	90	--	4	--	--	4	--	--	--
Z-10 S-3	84	--	5	5	--	6	--	--	--
Z-8 S-2	76	3	13	4	--	2	--	--	--
Z-8 S-3	85	2	8	1	--	3	--	--	--
Reddish-brown silty facies									
Z-6 S-7	80	--	7	6	--	4	--	--	--
Z-16 S-4	75	1	4	2	--	17	--	--	--
Z-18 S-1	81	2	5	2	--	7	--	--	--
Z-24 S-1	83	1	9	0.5	--	5	--	--	--
Z-24 S-2	86	--	3	2	--	6	--	--	--
Z-24 S-4	81	--	2	3	--	12	--	--	--
Z-24 S-5	86	--	3	1	--	1	--	--	--
Z-24 S-7	87	--	5	3	--	4	--	--	--
Z-24 S-8	86	--	6	1	--	6	--	--	--
Moab Tongue									
Crossbedded sandstone facies									
Z-25 S-3	94	1	2	--	--	3	--	--	--
Z-25 S-4	93	1	2	--	--	3	--	--	--
Wrinkled sandstone facies									
Z-25 S-2	96	2	1	--	--	--	--	--	--
Wavy sandstone facies									
Z-19 S-6	94	0.5	2	0.5	--	3	--	--	--

eldspar		Rock Fragments									
Plagioclase	Microcline	Chert	Carbonate	Sandstone-siltstone-shale	Igneous	Fossils and other allochemical grains	Glauconite	Heavy minerals	Evaporite	Matrix	Cement
--	--	--	--	--	--	--	--	--	100	--	--
1	--	2	--	--	--	3	--	--	--	--	55
--	--	4	--	--	--	--	--	2	--	--	83
5	--	6	--	--	--	--	--	--	--	--	79
4	--	2	--	--	--	--	0.5	0.5	1	--	53
1	--	3	--	--	--	--	0.9	--	--	--	43
6	--	4	--	--	--	0.3	0.3	2.3	--	--	55
2	--	17	--	--	--	--	--	1	--	--	67
2	--	7	--	--	--	--	1	2	--	--	54
0.5	--	5	--	--	--	--	1	0.5	--	--	54
2	--	6	--	--	--	--	2	--	--	--	65
3	--	12	--	--	--	--	2	--	--	--	80
1	--	1	--	--	--	--	0.9	8	--	--	71
3	--	4	--	--	--	--	--	1	--	--	38
1	--	6	--	--	--	--	0.5	0.5	--	--	43
--	--	3	--	--	--	--	--	--	--	--	--
--	--	3	--	--	--	--	0.2	--	--	--	0.5
--	--	--	--	--	--	--	--	--	--	17	19
0.5	--	3	--	--	--	--	--	--	--	17	16

APPENDIX 3

Stratigraphic Sections

(Arranged in numerical order and reproduced on pages which follow and on fold-out pages in rear pocket)

Explanation of symbols and abbreviations used on stratigraphic sections not included in table 1.3 (Chapter 1, Introduction)

Symbol or Abbreviation	Explanation
S-1, 2, 3, etc.	Rock sample and its stratigraphic position
BBSK	Bed at Black Steer Knoll, redbed facies of the Curtis Formation
BAGV	Beds at Goblin Valley, Entrada Sandstone
Grain size column:	
C	Clay
S	Silt
V	Very fine sand
F	Fine sand
M	Medium sand
C	Coarse sand
V	Very coarse sand
G	Granules
P	Pebbles
C	Cobbles
Facies of the Moab Tongue:	
1:	Crossbedded Sandstone
2:	Wrinkled Sandstone
3:	Wavy Sandstone

Z–2B

SAN RAFAEL SWELL EAST

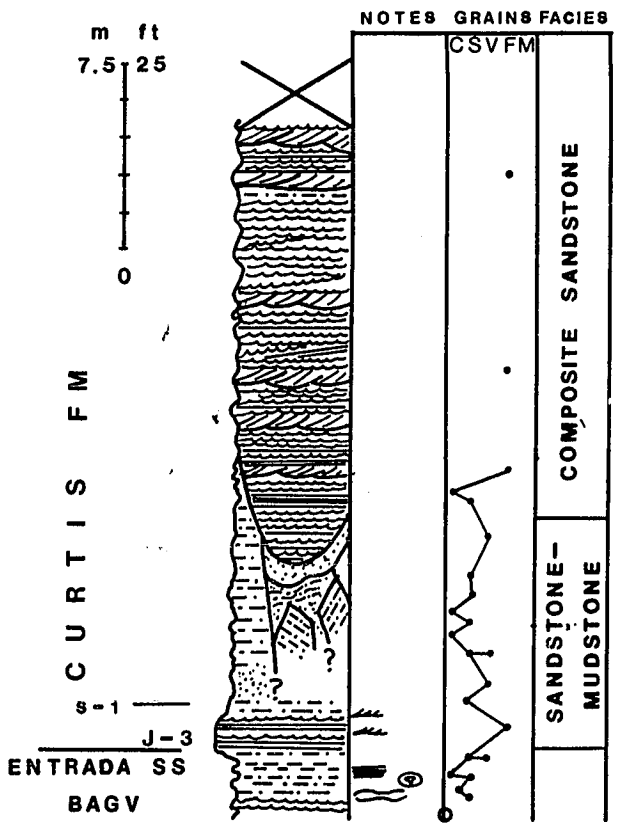

Z – 7

DUMA POINT

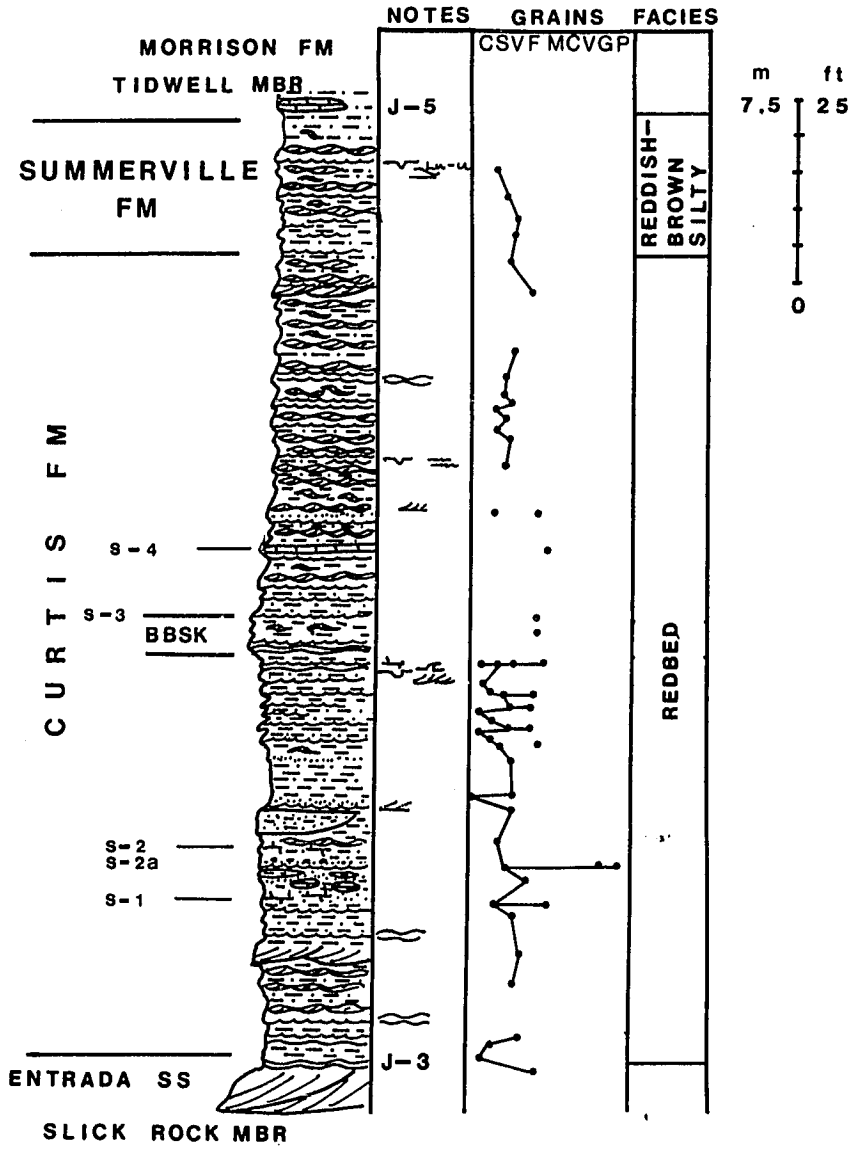

Z-9B

T I D W E L L D R A W N O R T H

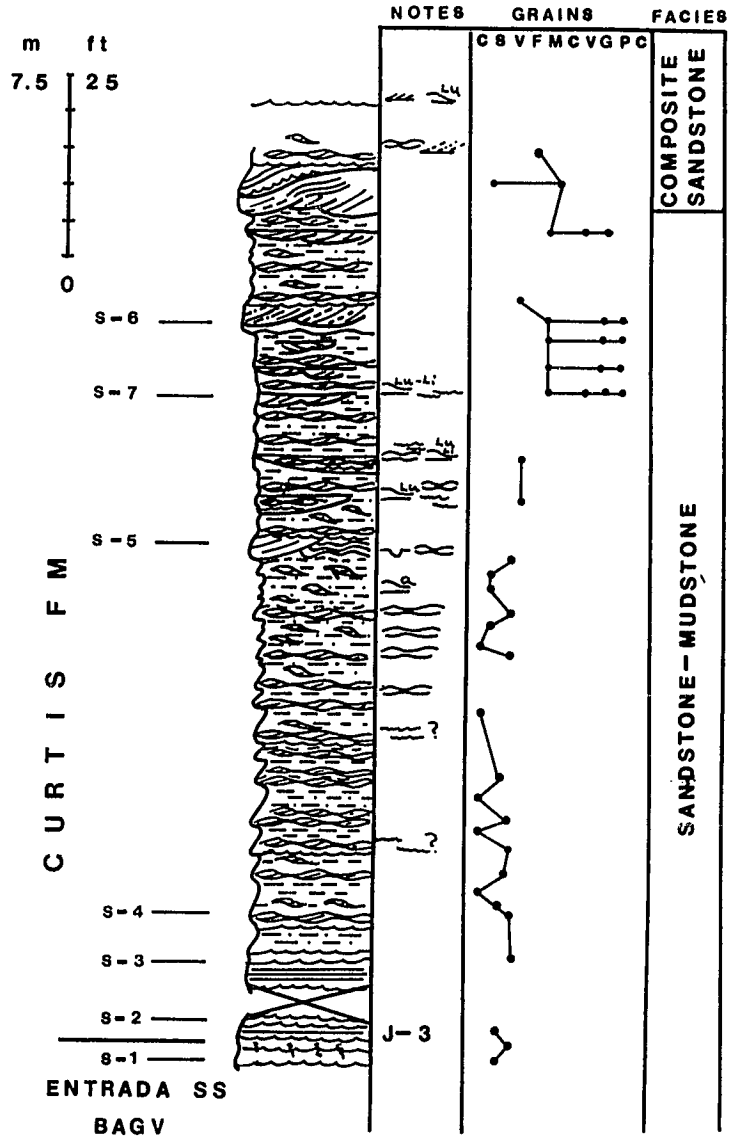

Z – 10 B

HATT RANCH

HUNTING FARM

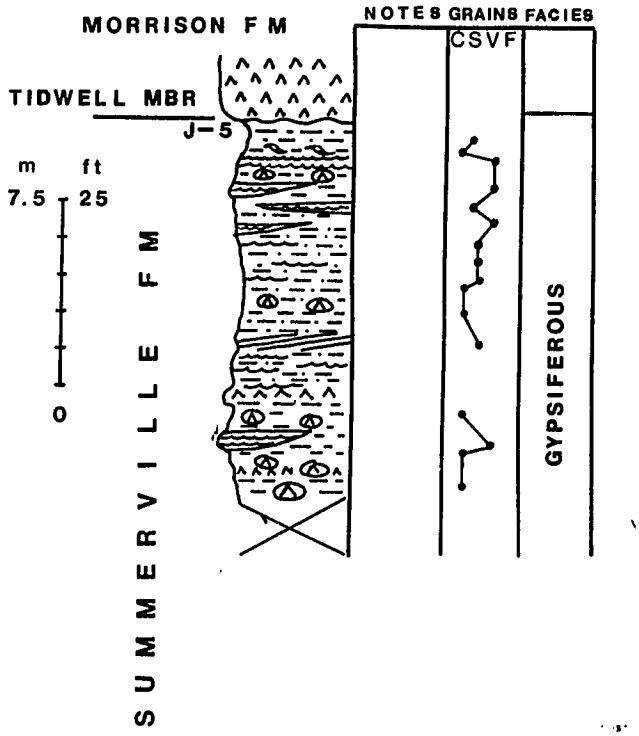

WHITE WASH

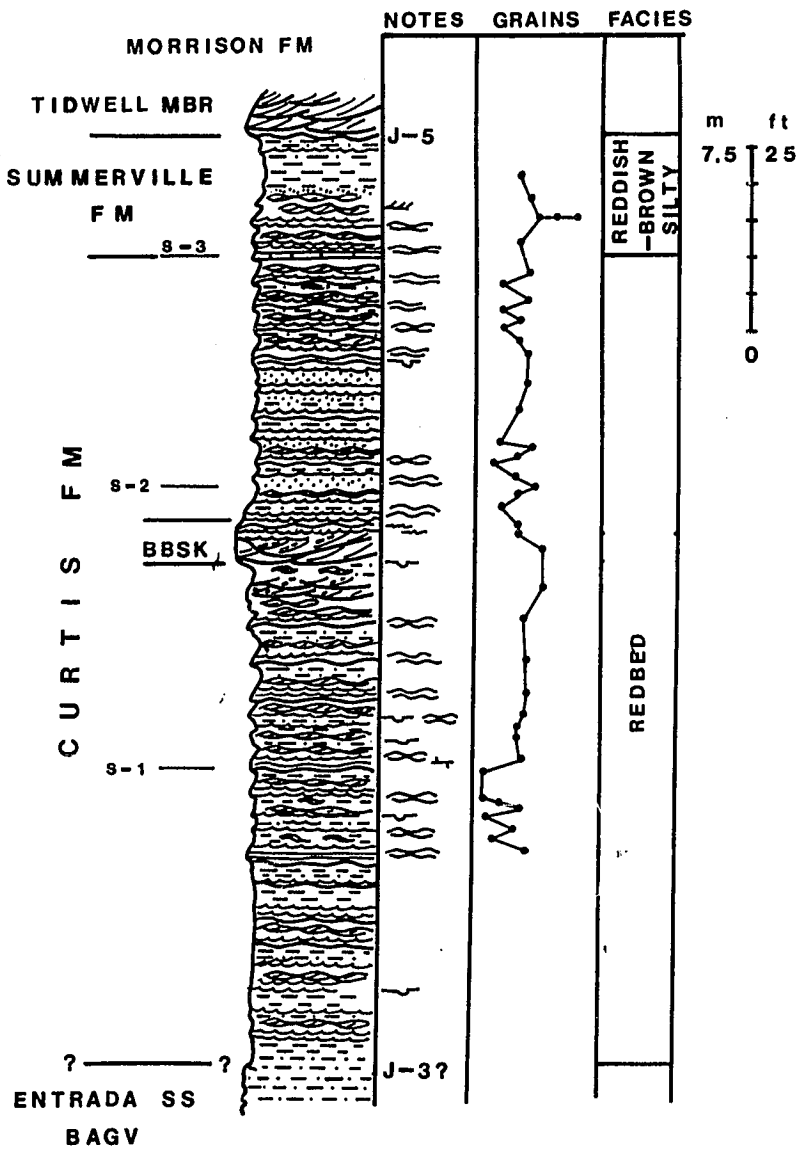

HORSE BENCH

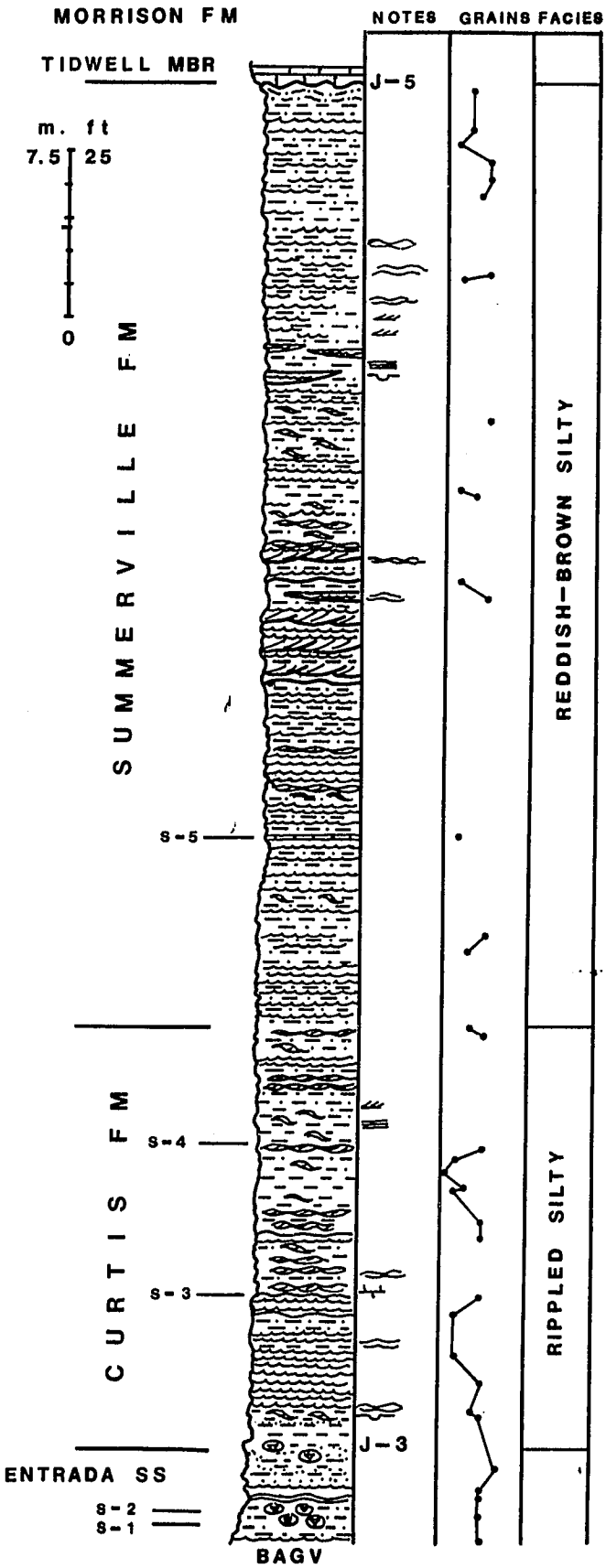

Z–15

S O U T H S A N D B E N C H

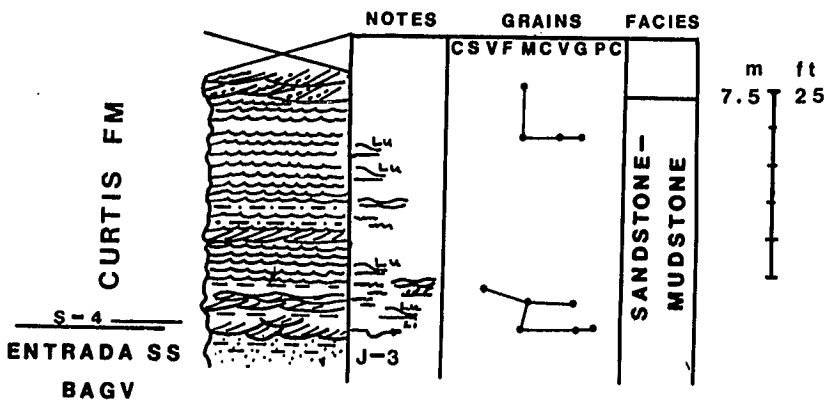

DUBINKY WELL

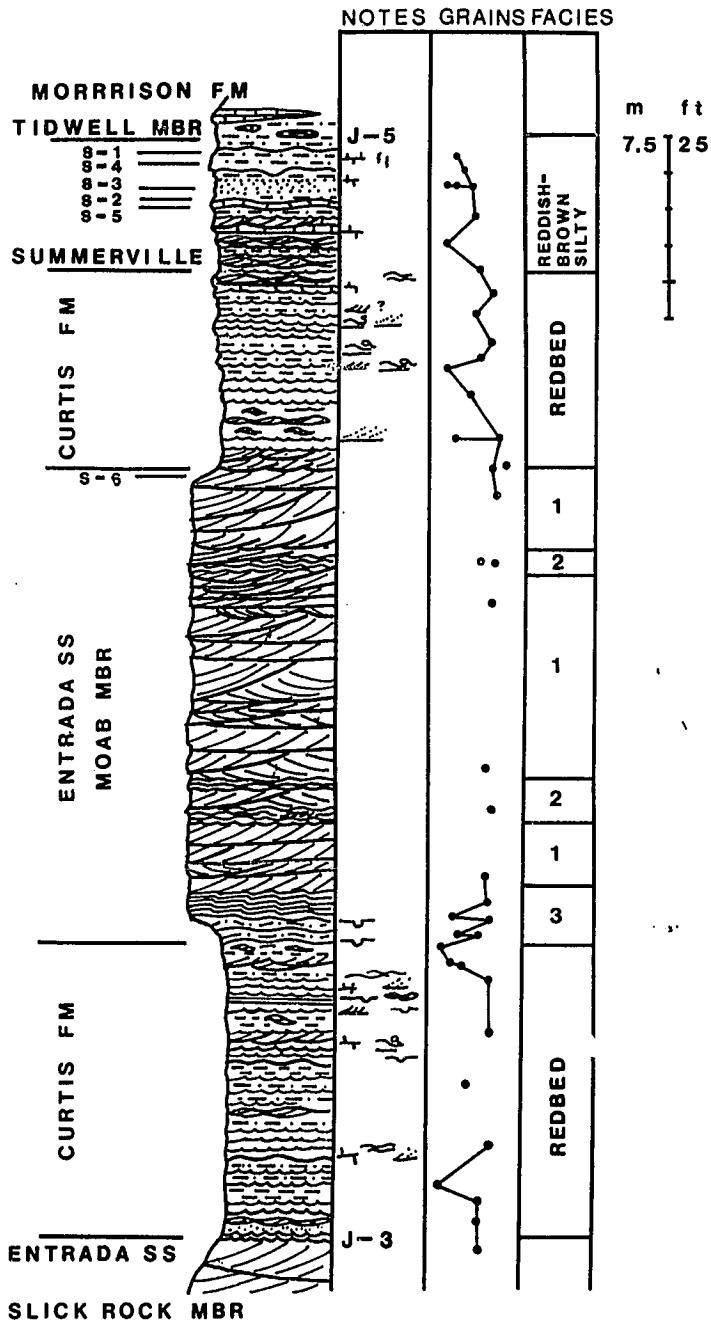

Z-20

TENMILE CANYON NORTH

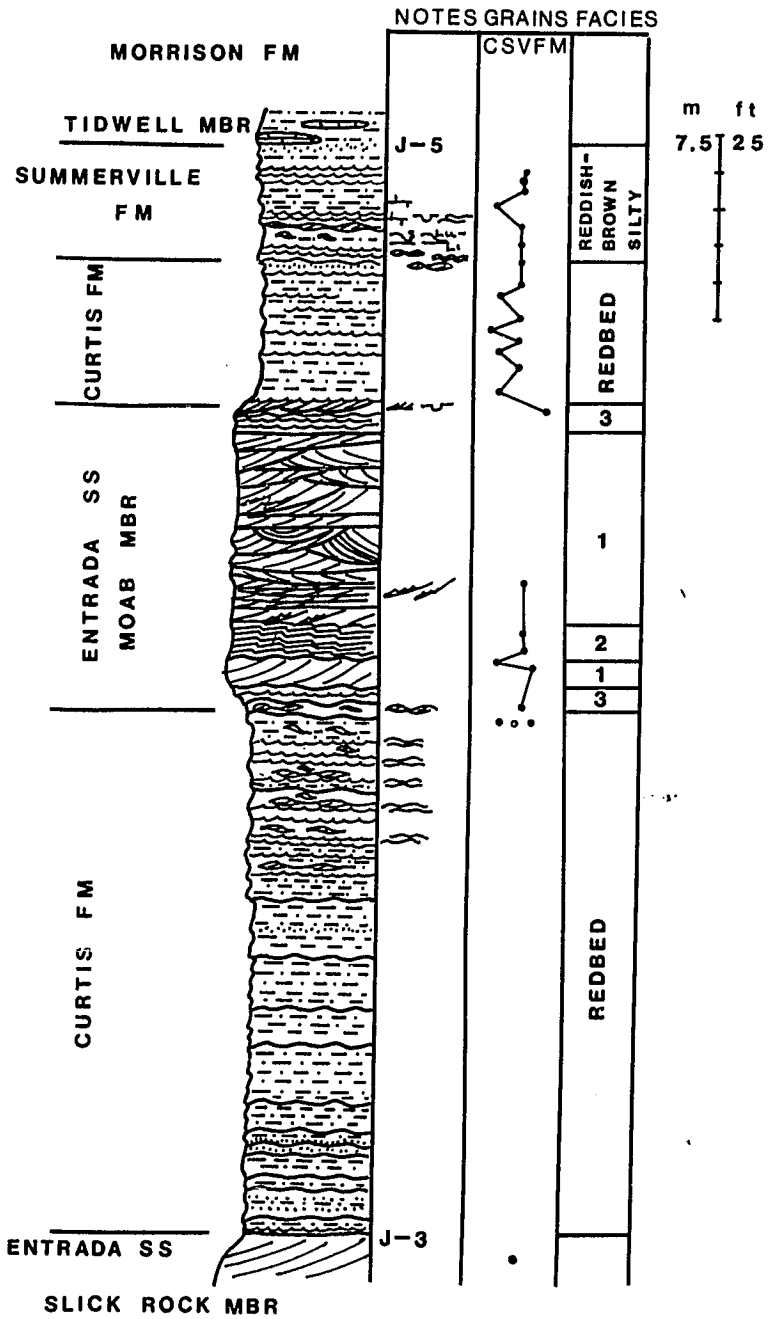

Z – 21

TENMILE CANYON SOUTH

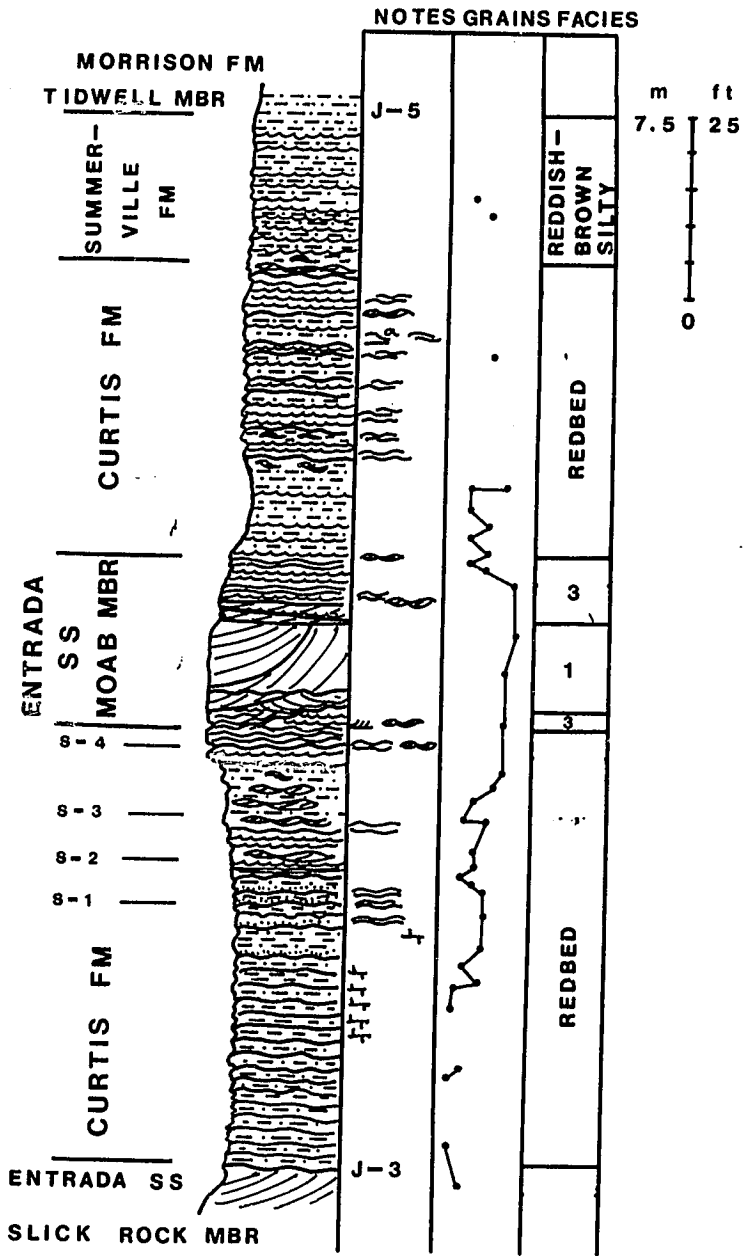

Z – 22

BARTLETT FLAT

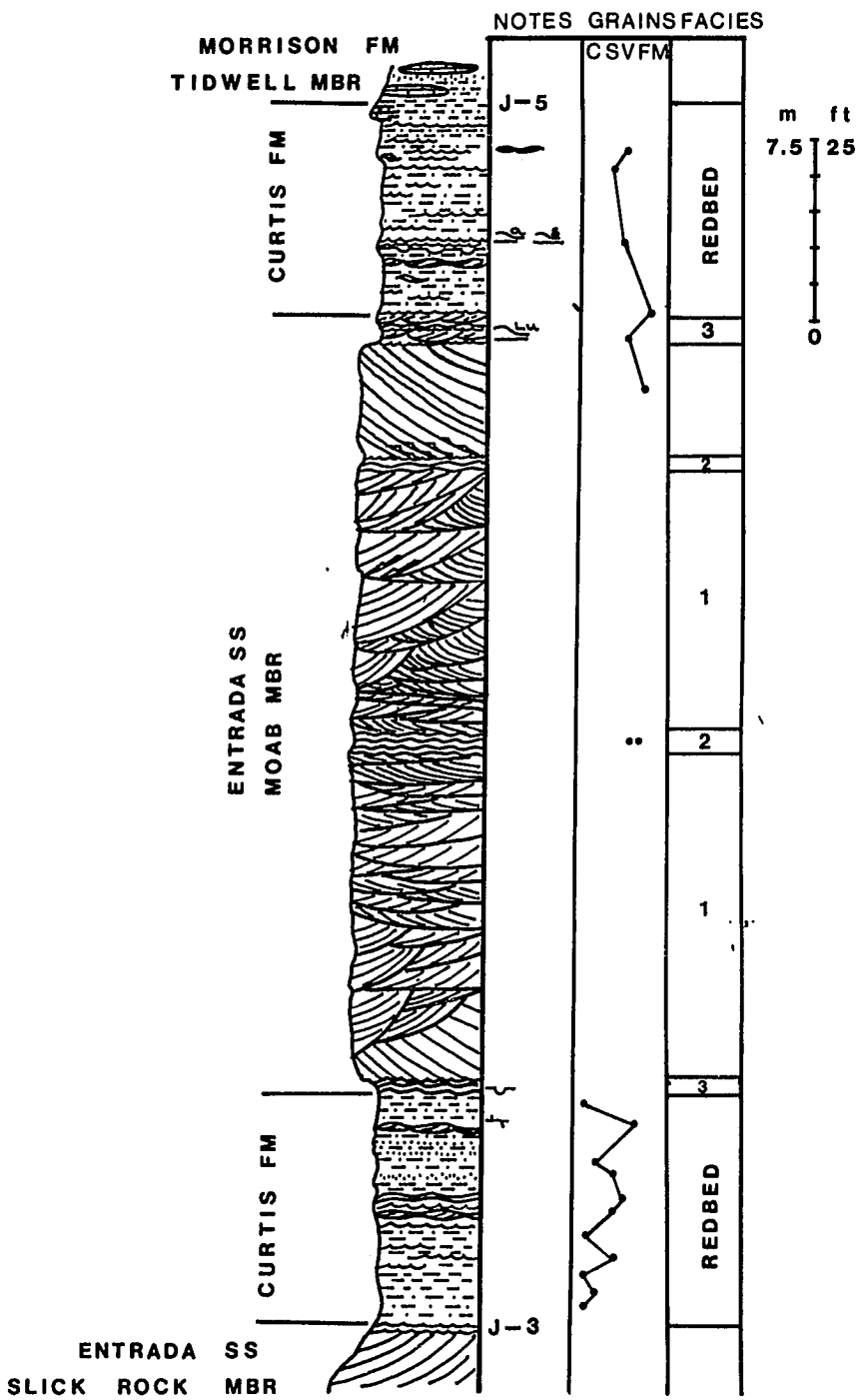

Z – 2A

SAN RAFAEL SWELL EAST

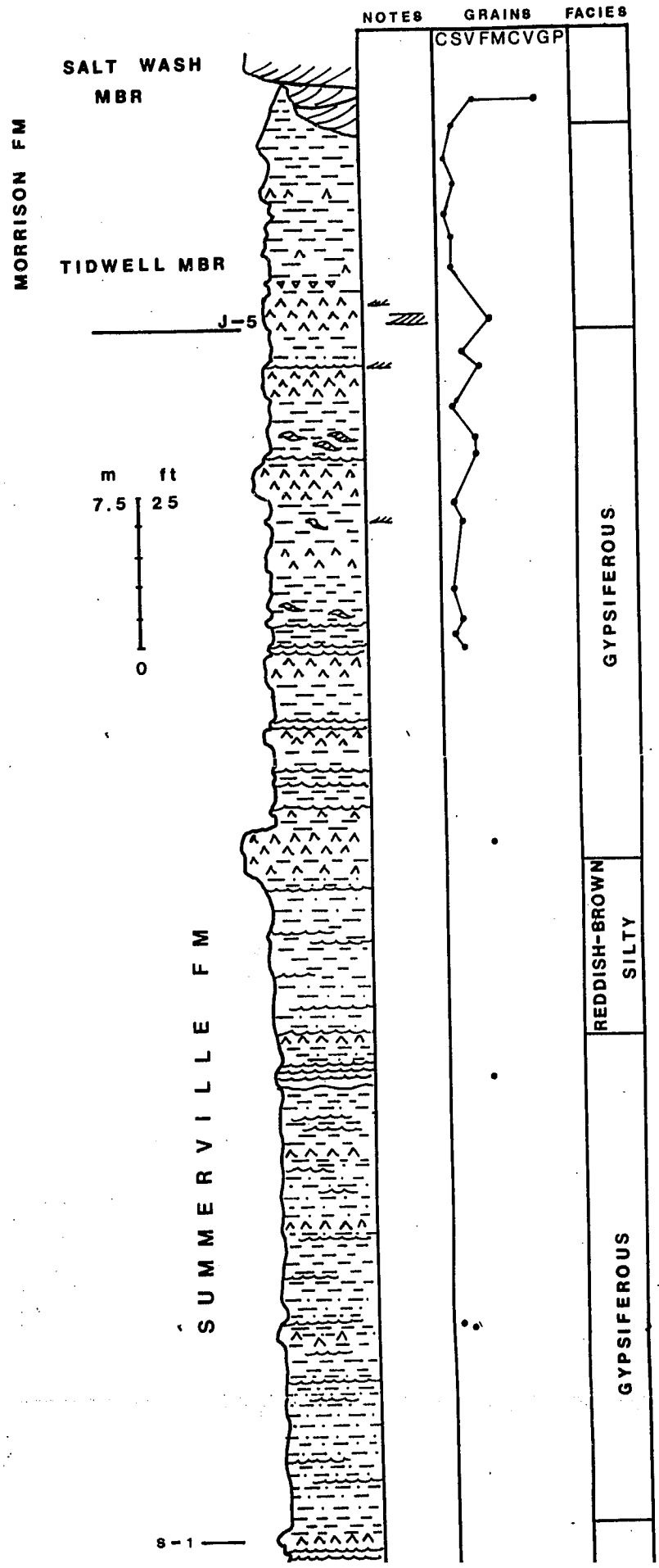

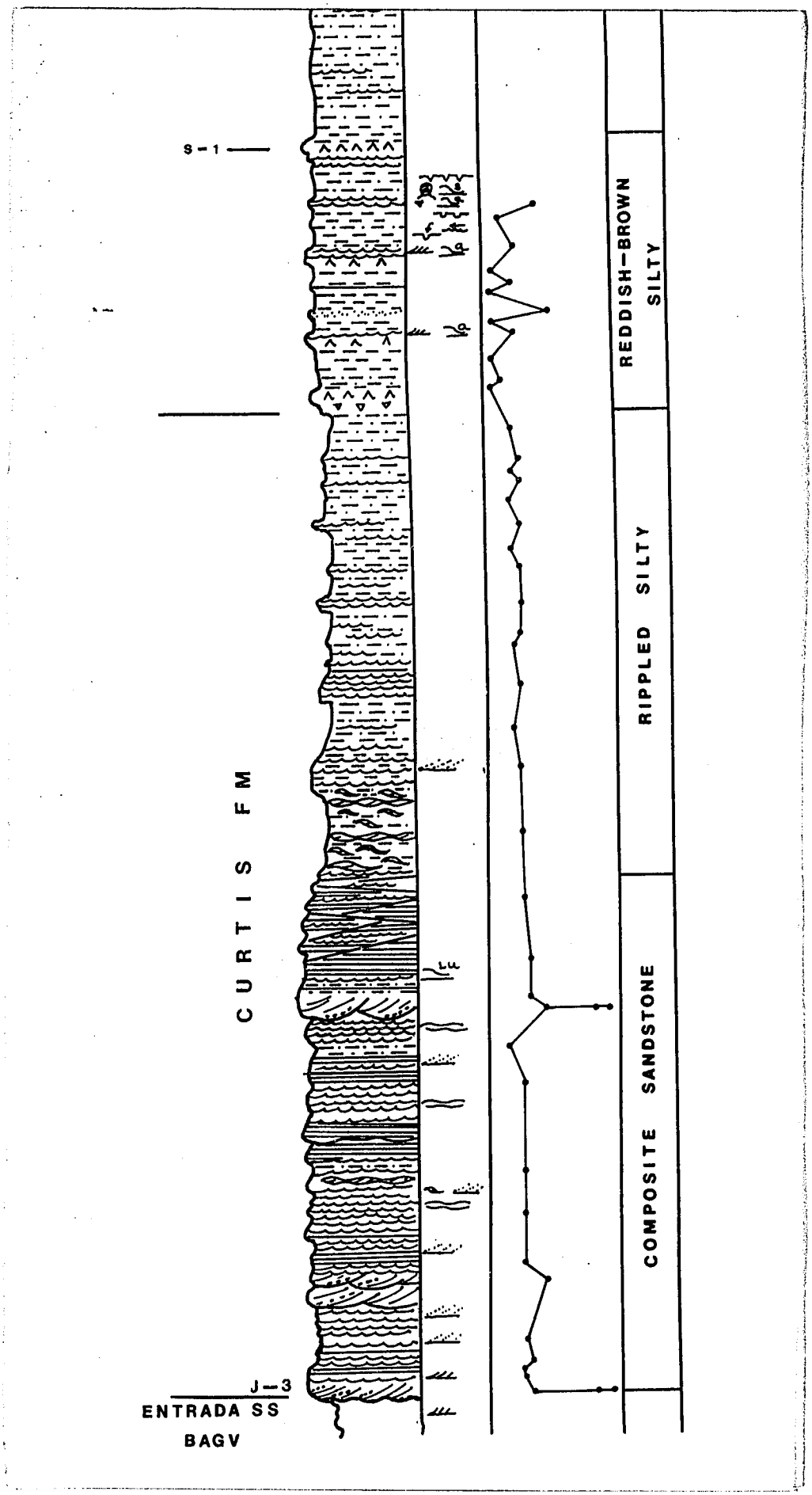

Z – 3

SAN RAFAEL SWELL NORTHEAST

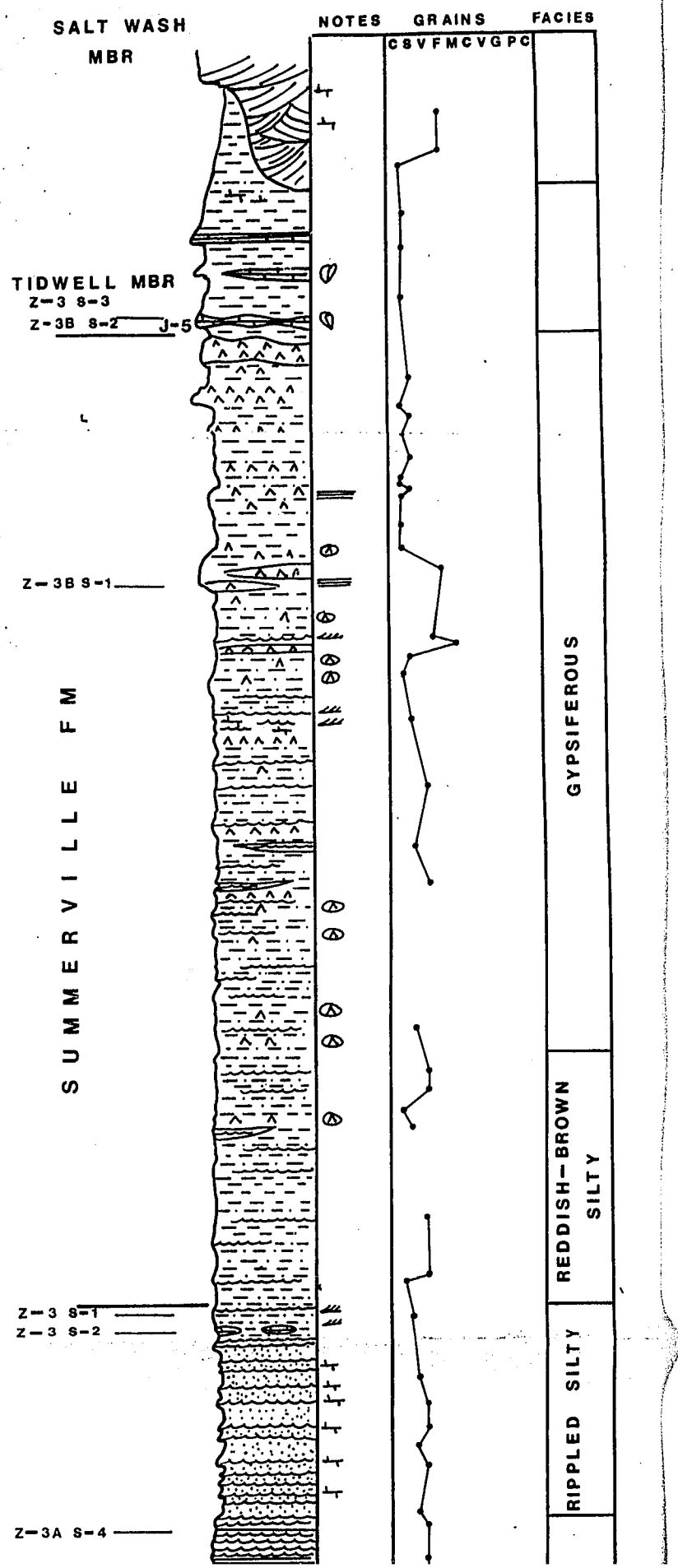

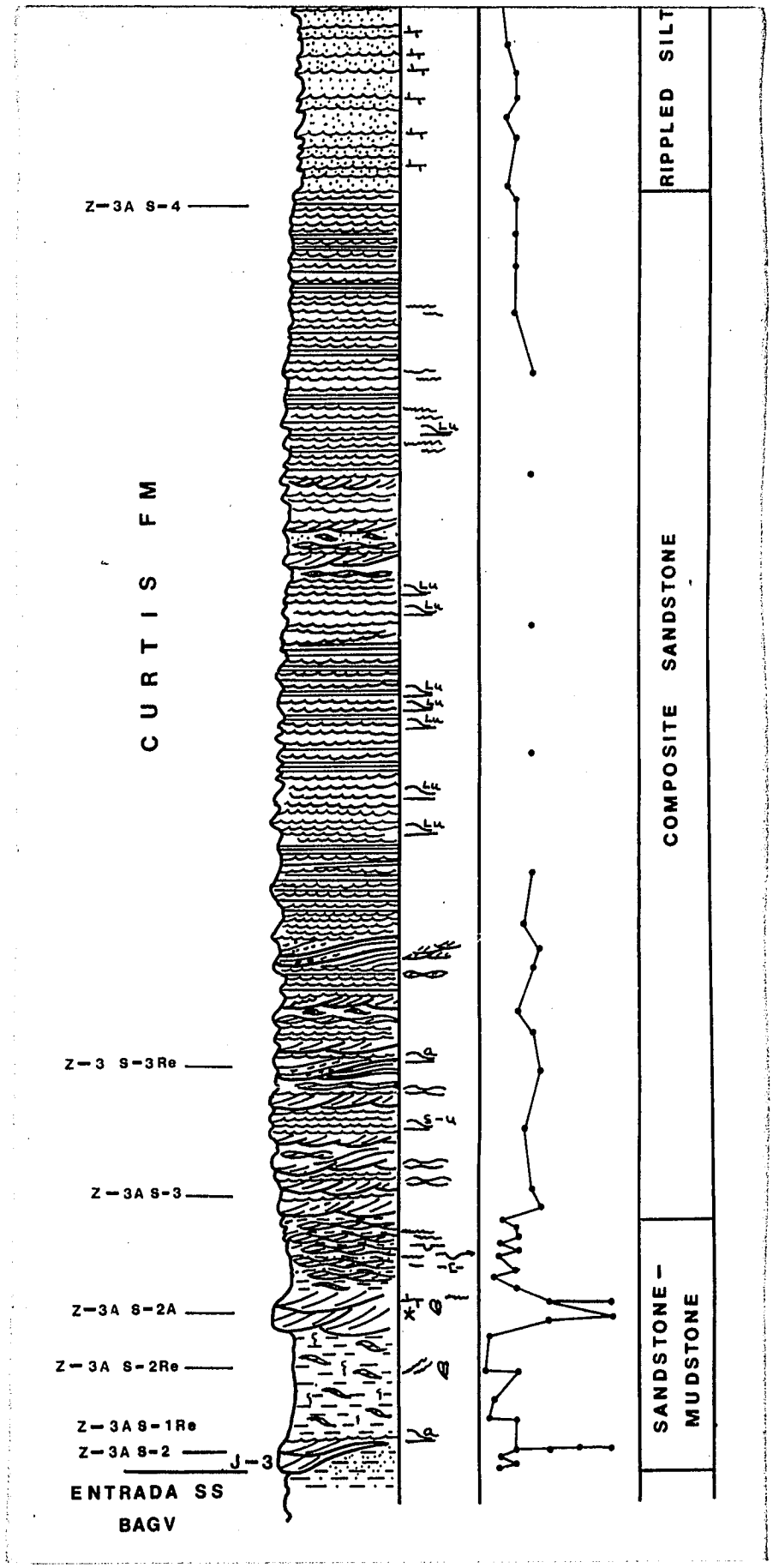

PLEASANT CREEK

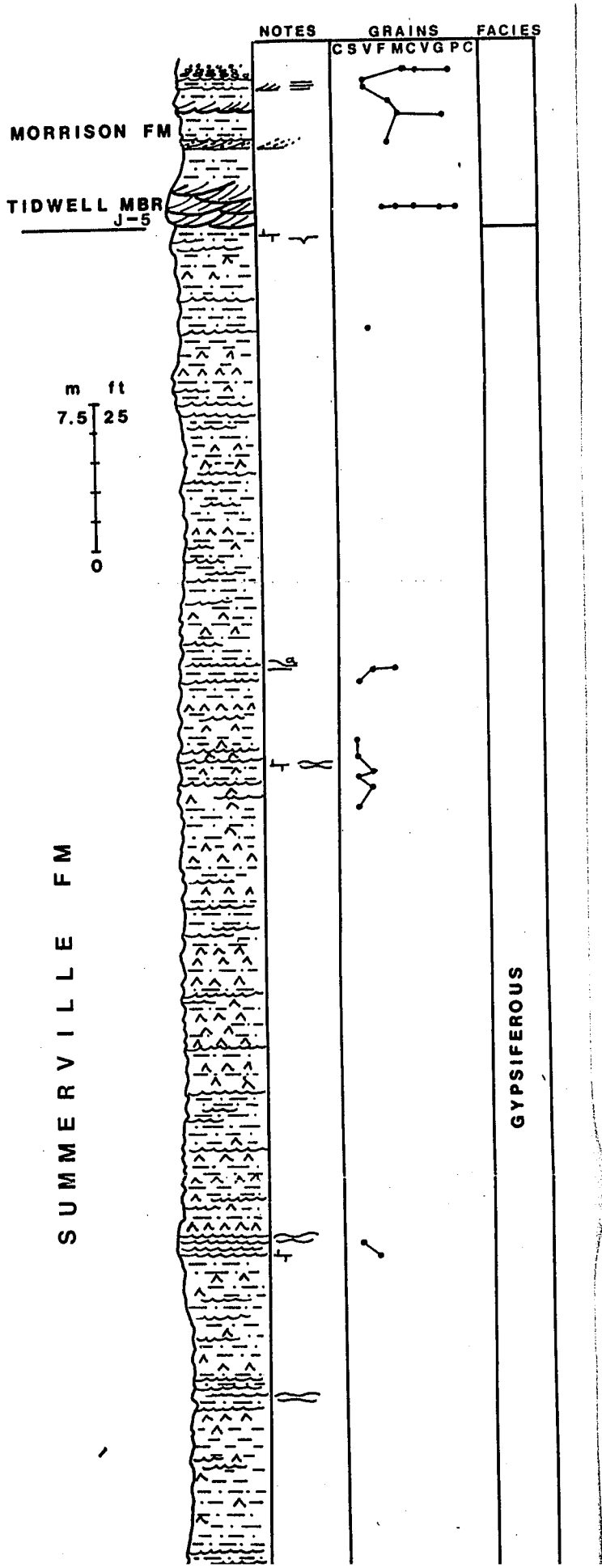

Z-5

HANKSVILLE

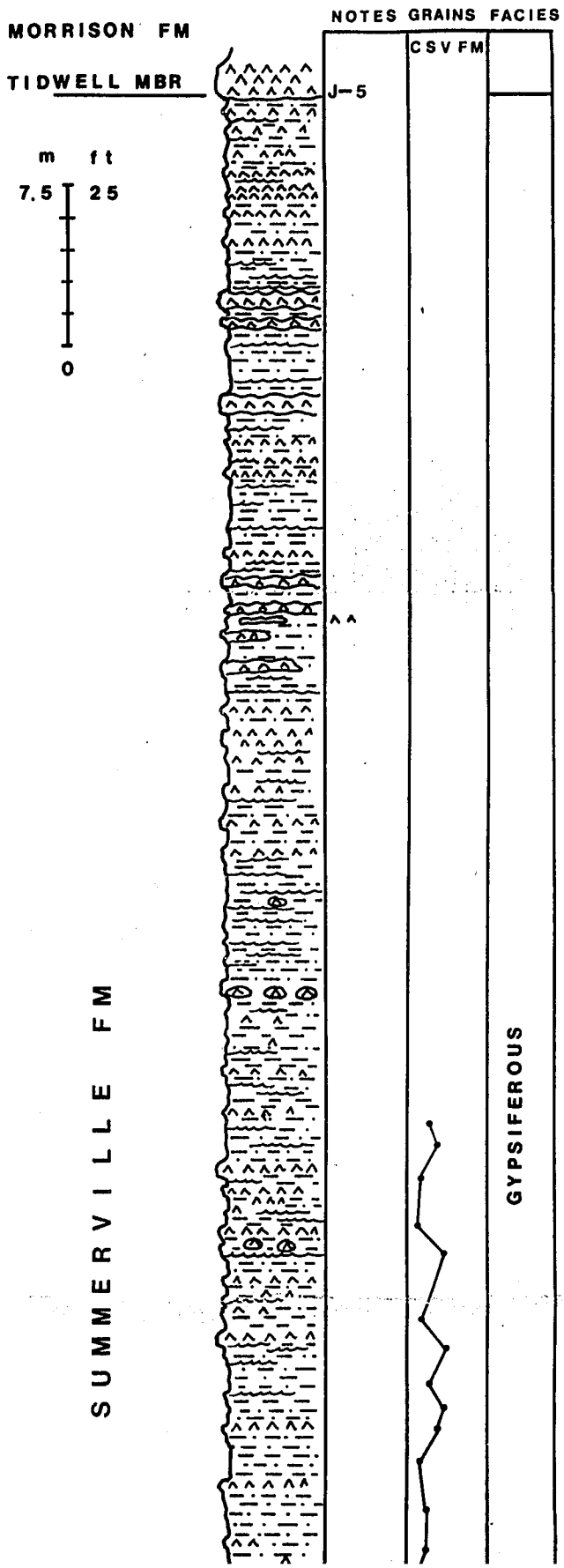

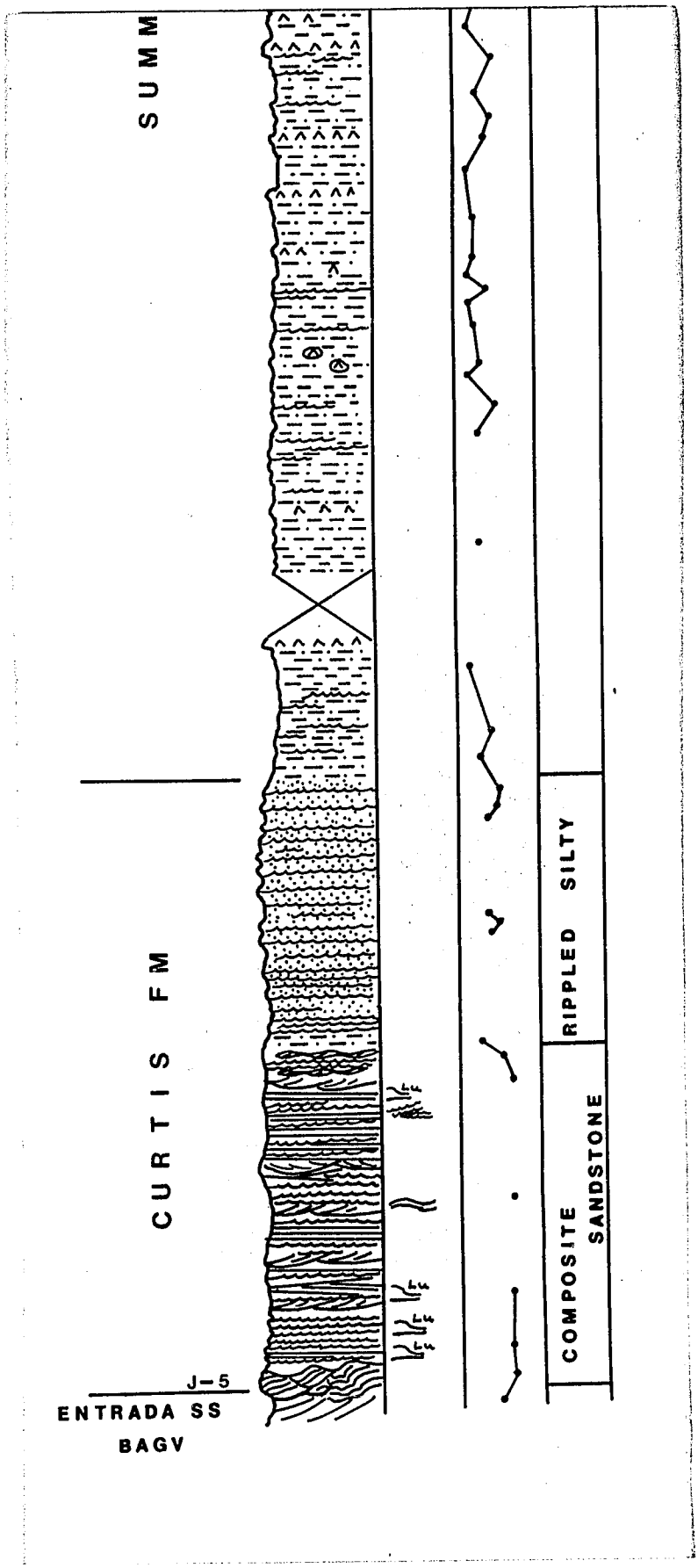

Z – 6

SAN RAFAEL SWELL WEST

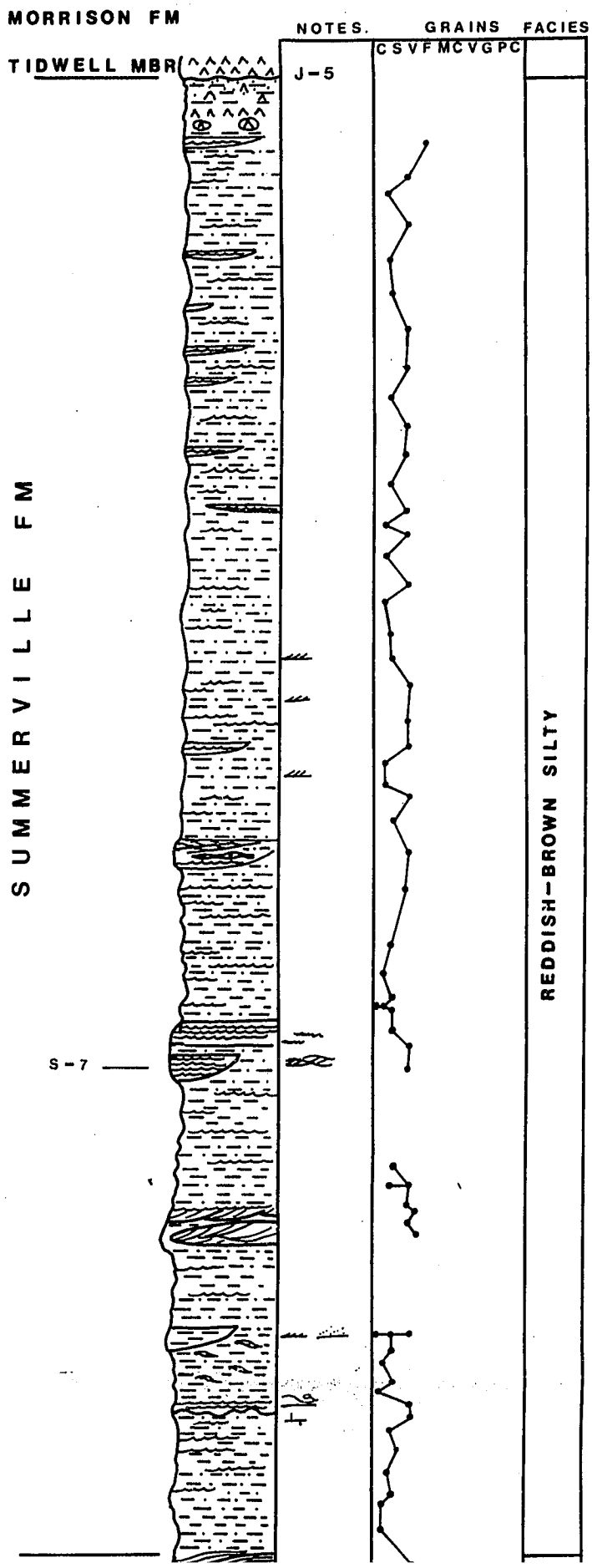

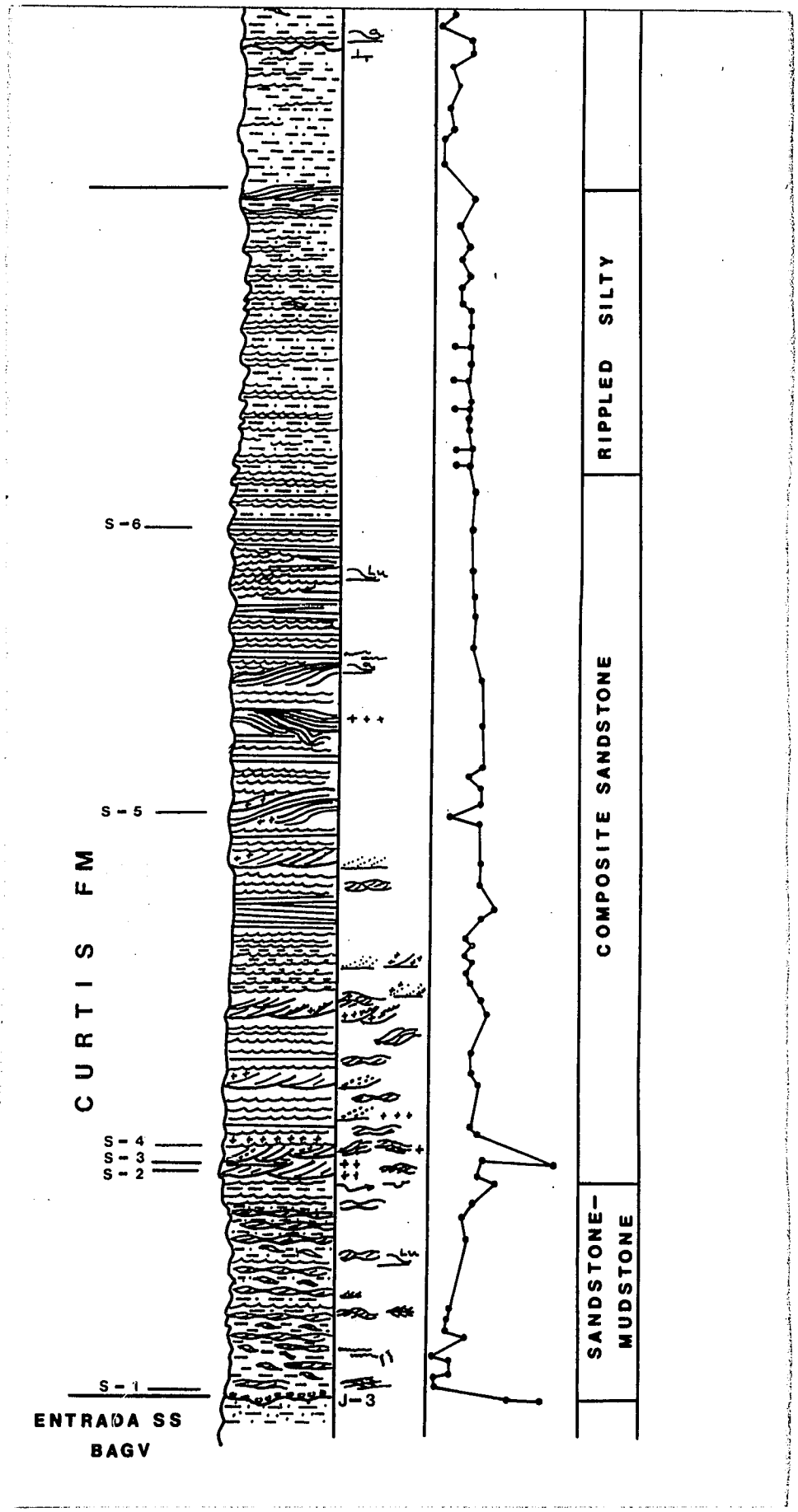

Z-8

DELLENBAUGH BUTTE

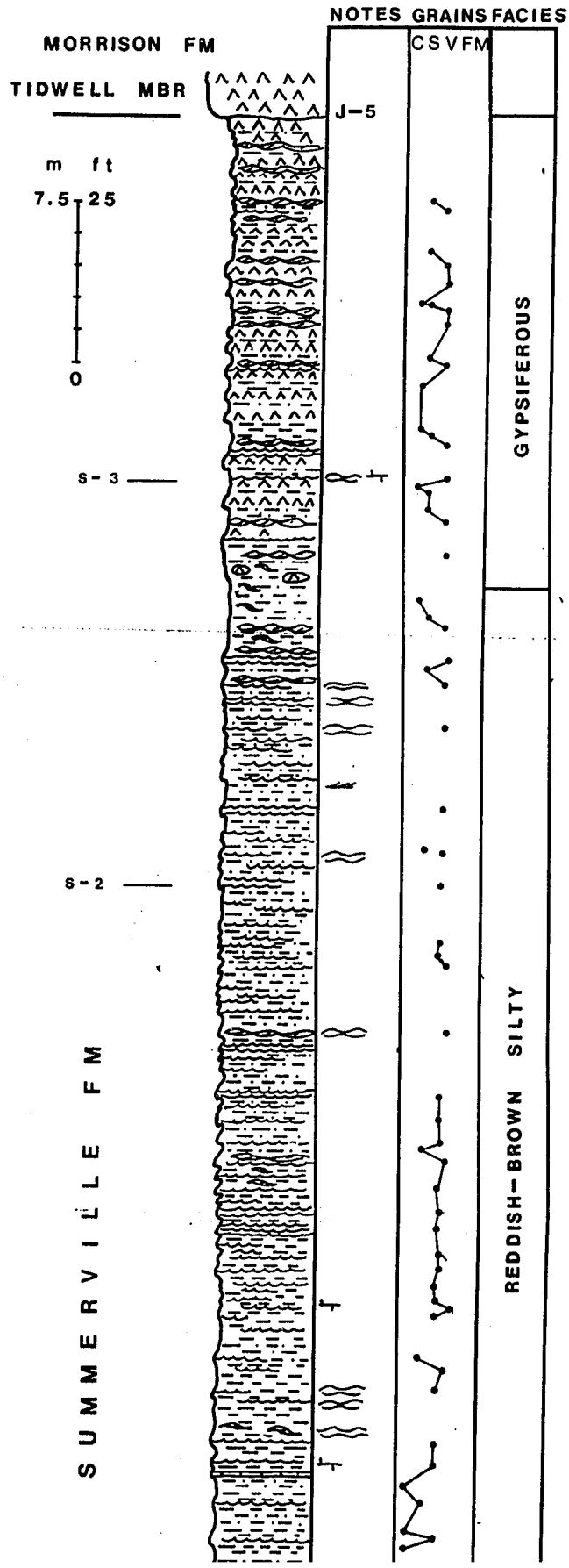

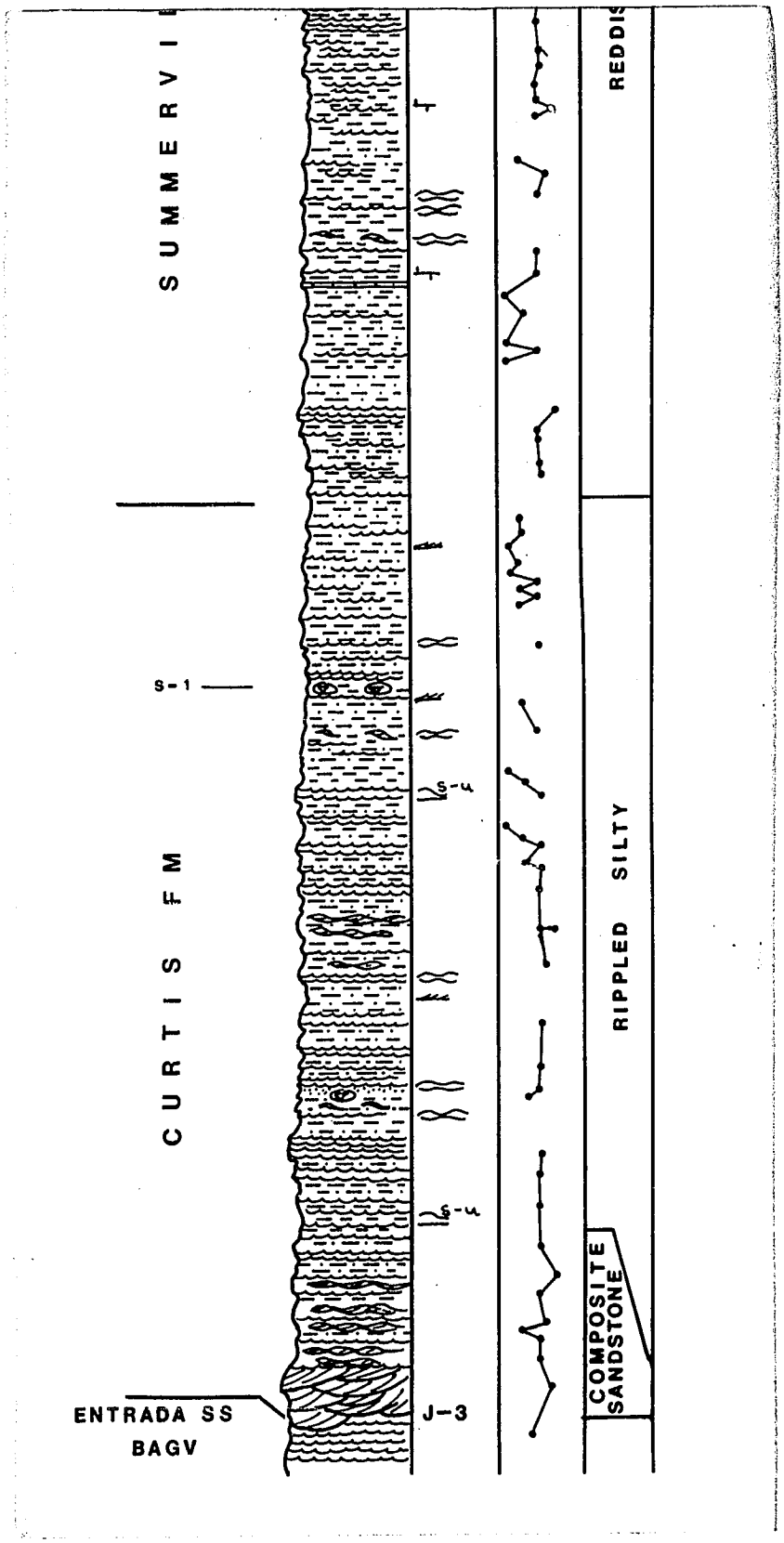

Z-9A

TIDWELL DRAW SOUTH

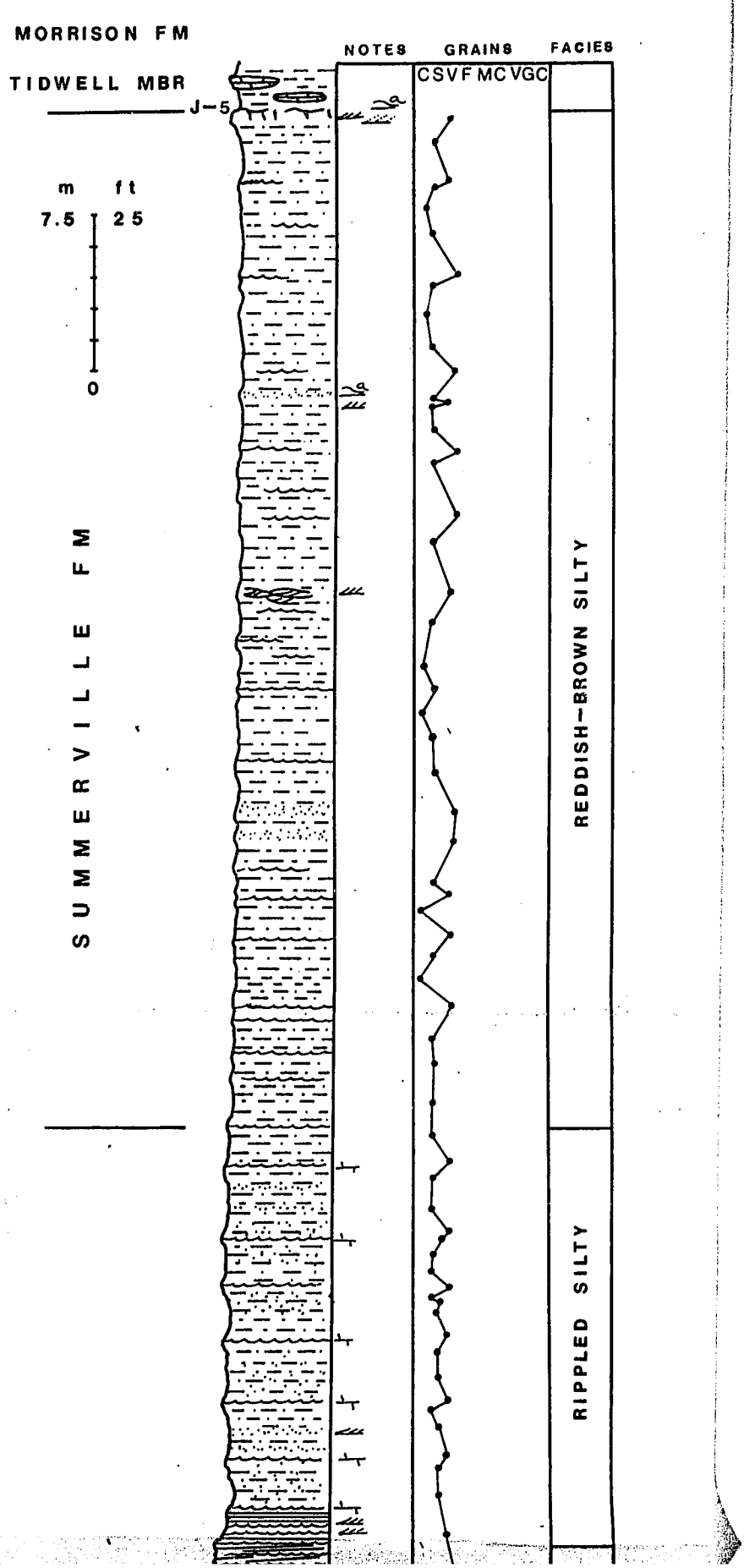

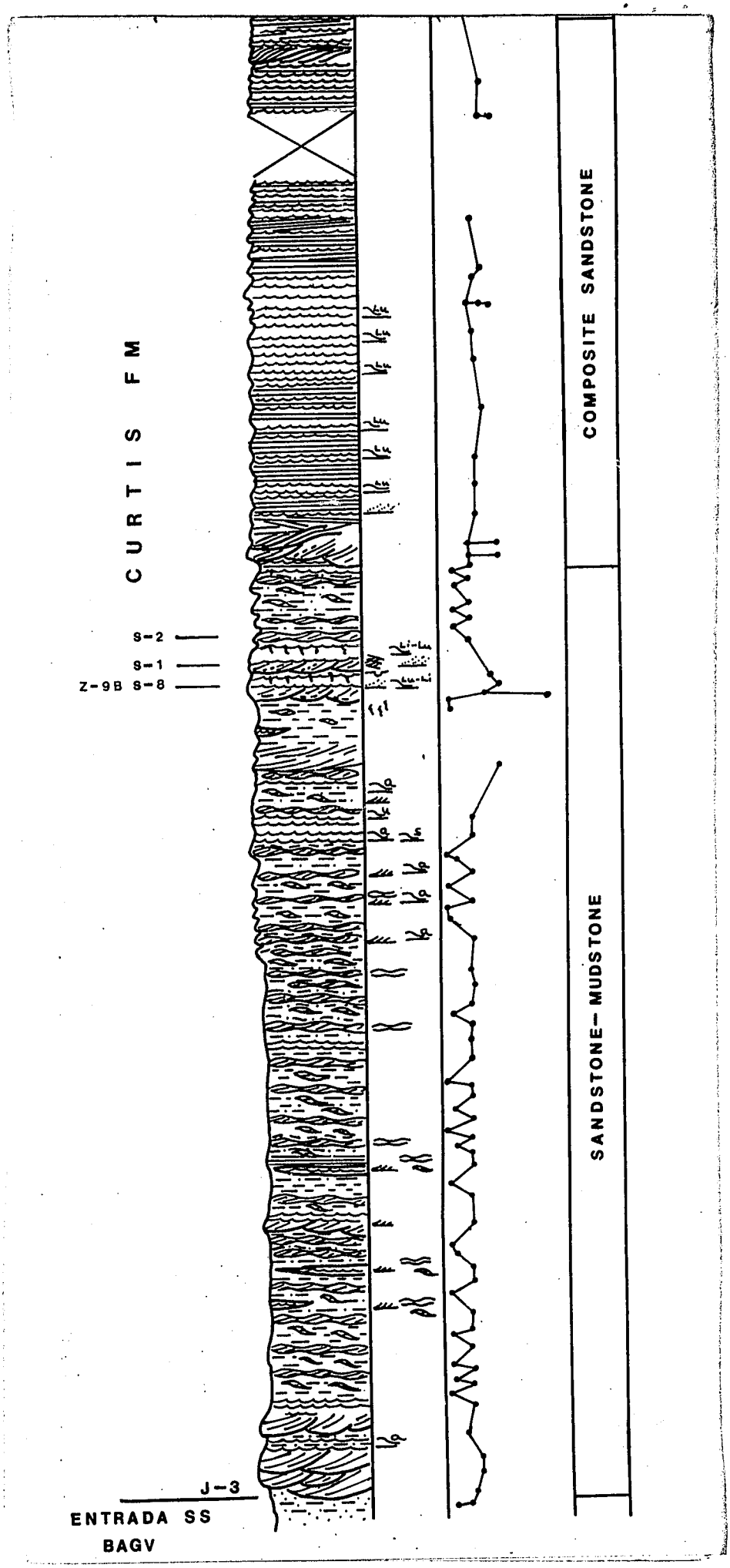

Z-10A

HATT RANCH WEST

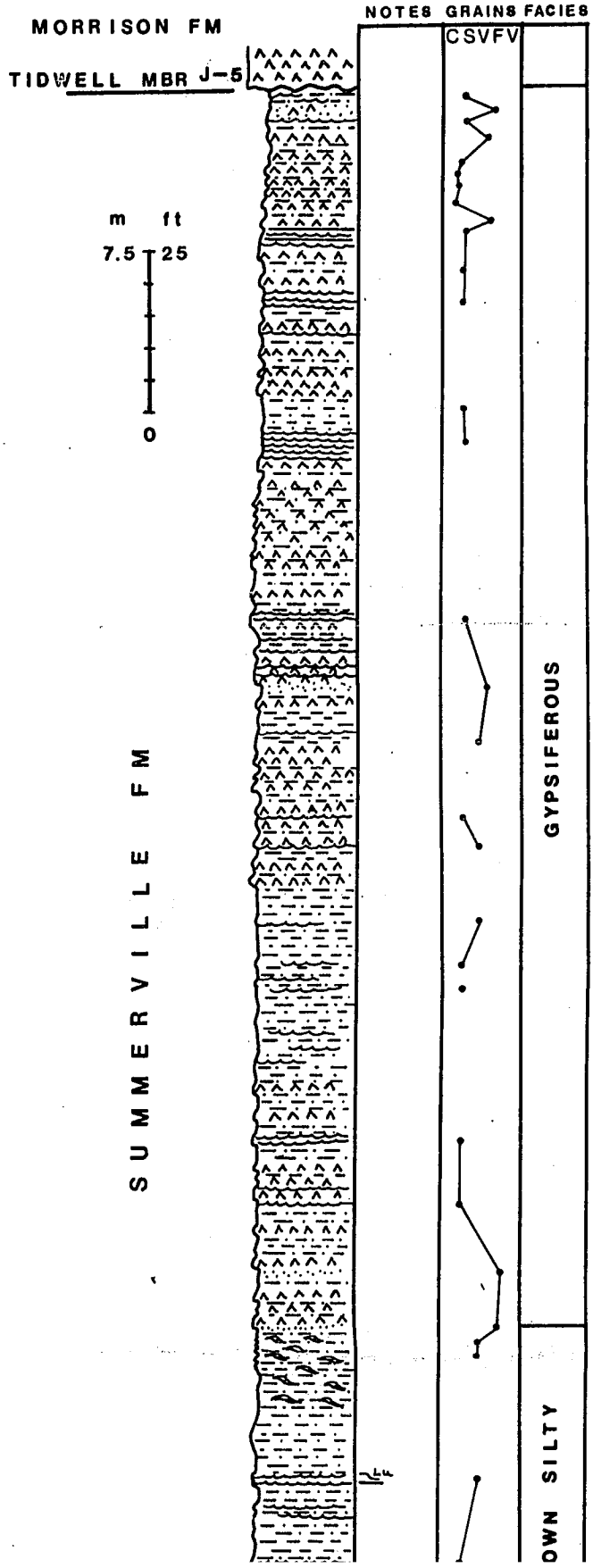

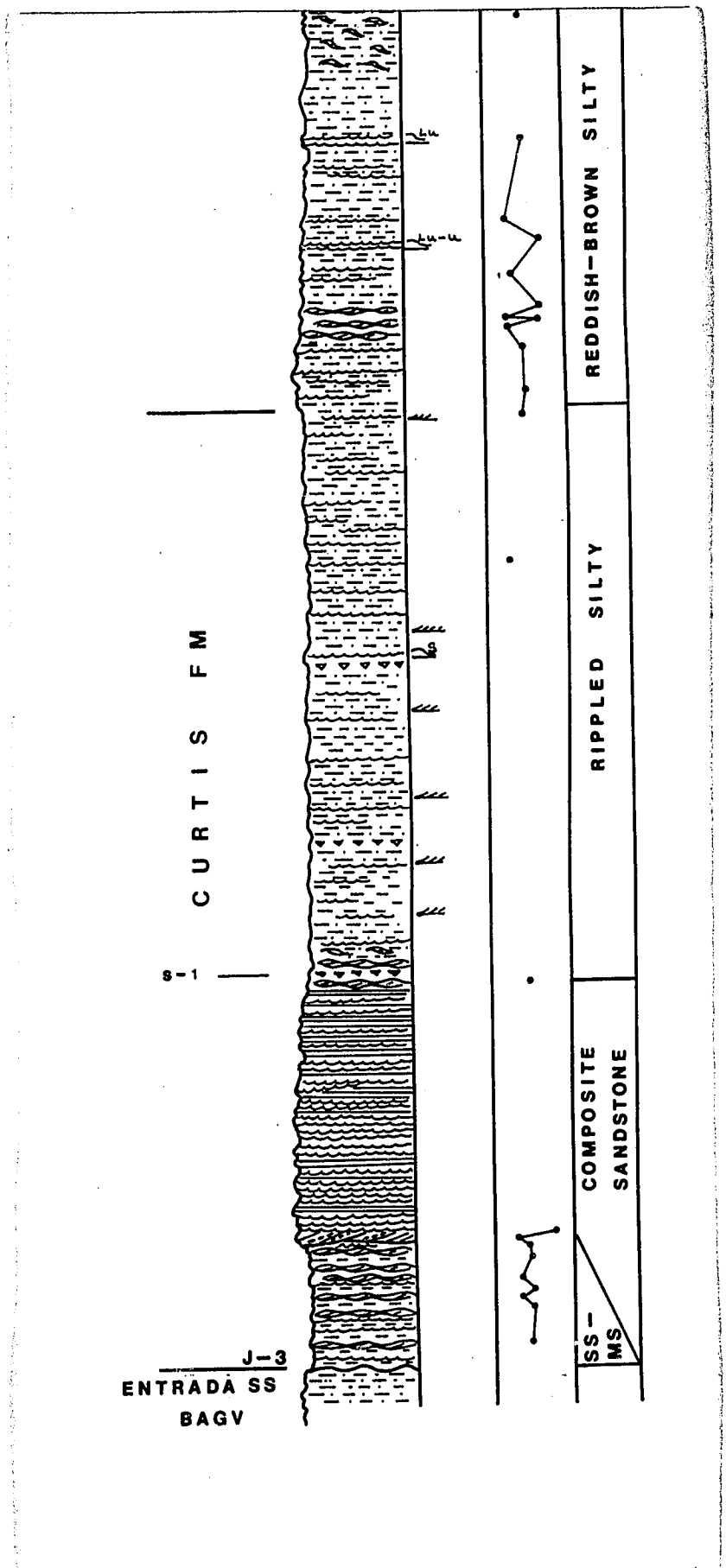

WILD HORSE CREEK

GOBLIN VALLEY

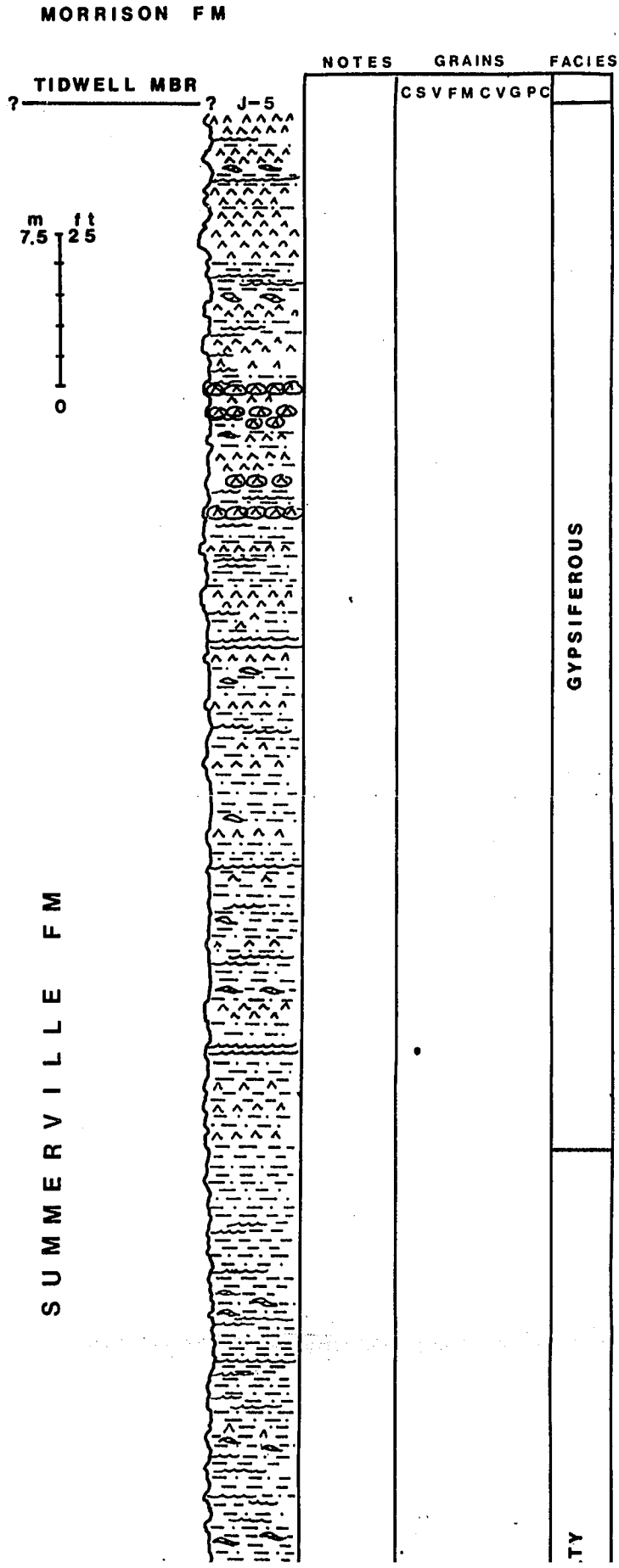

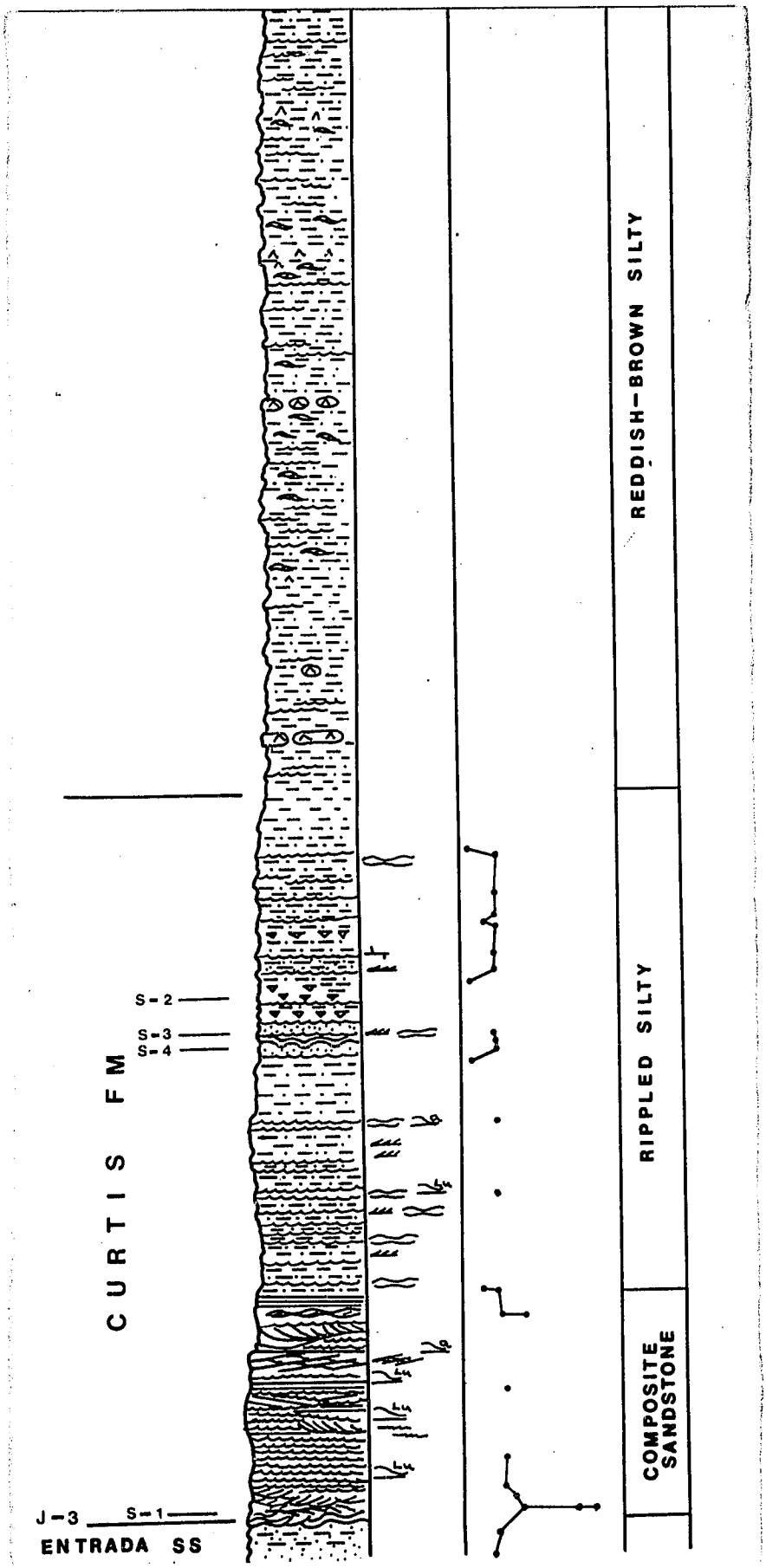

Z-14

LOOKOUT POINT

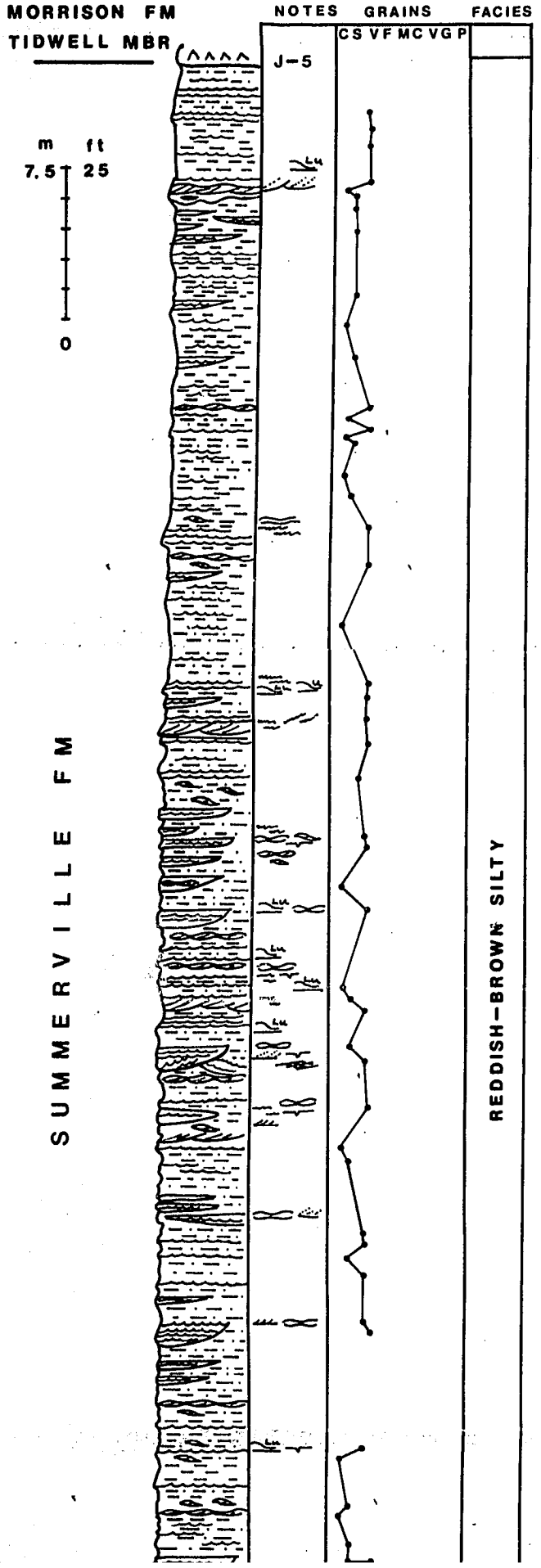

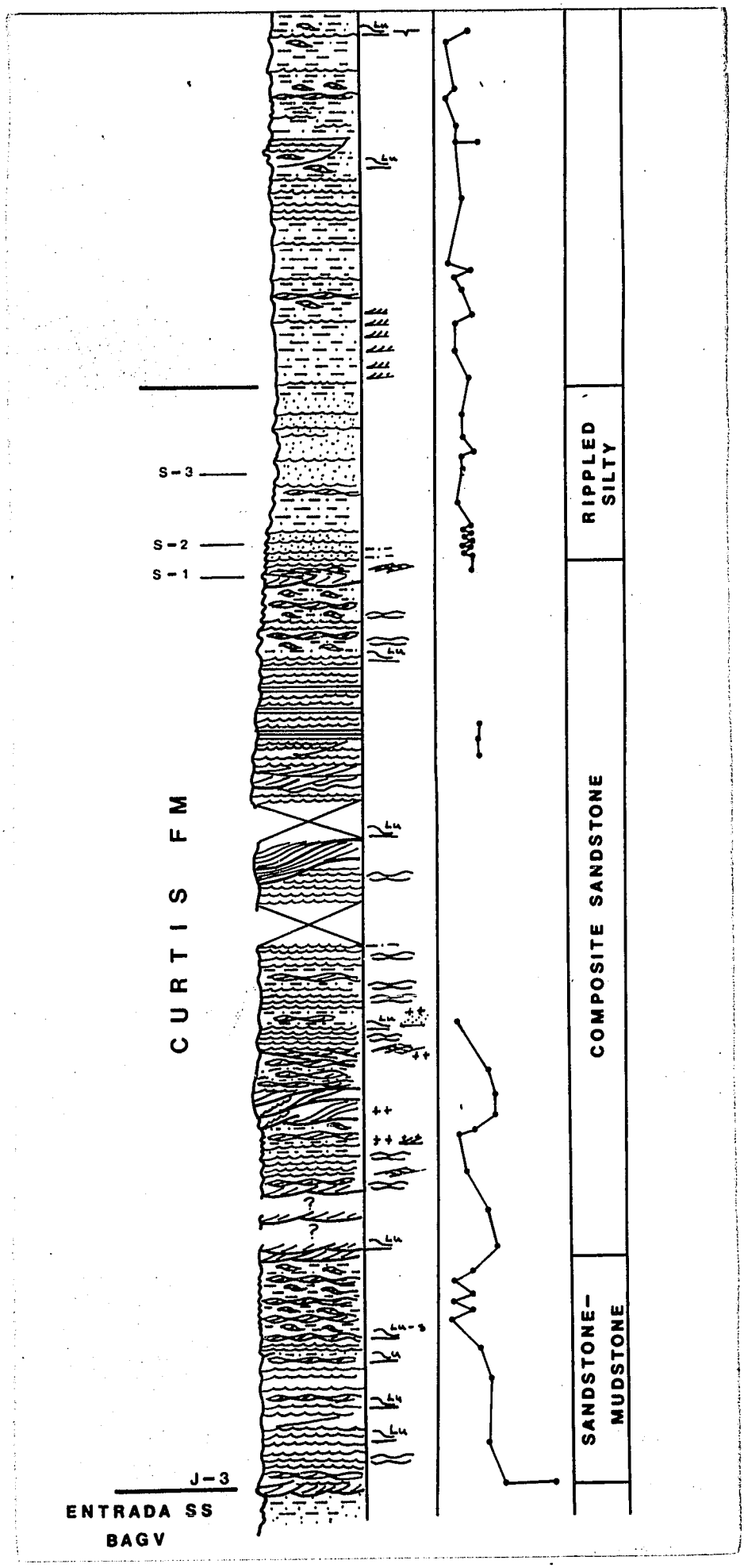

NORTH SALT WASH

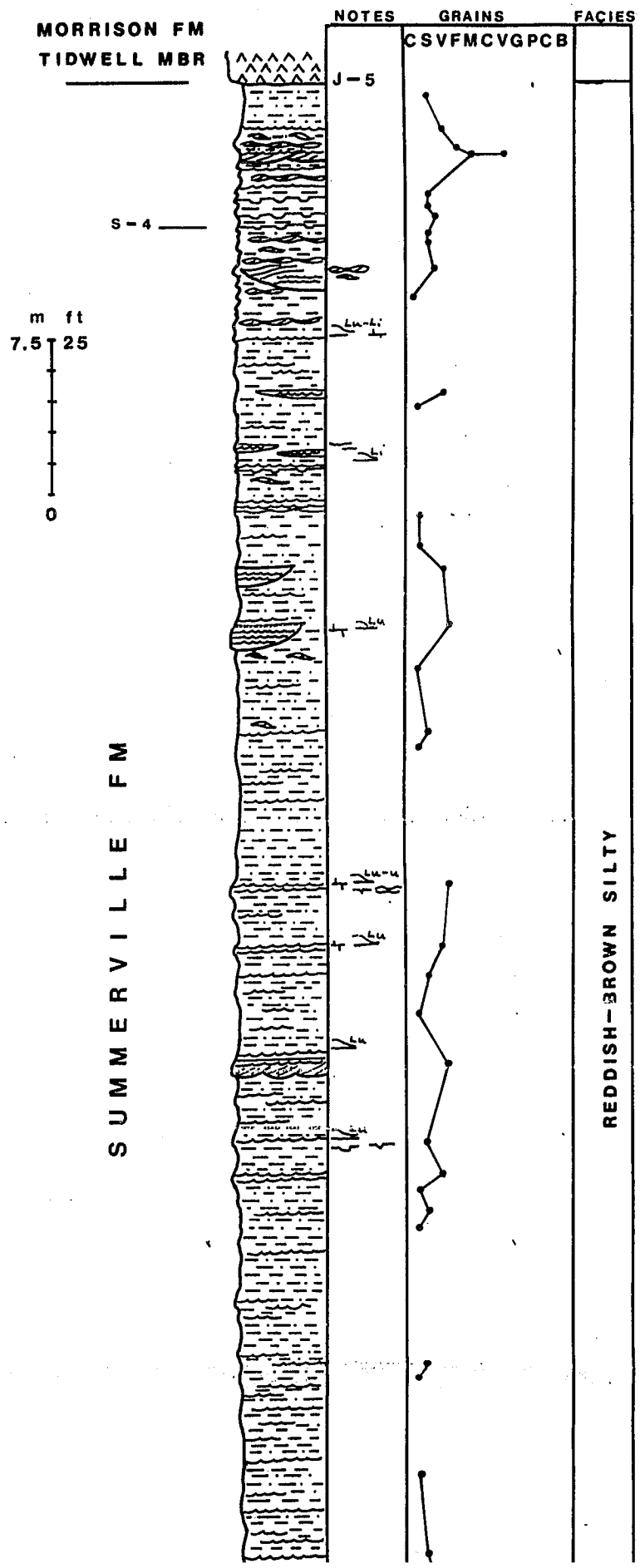

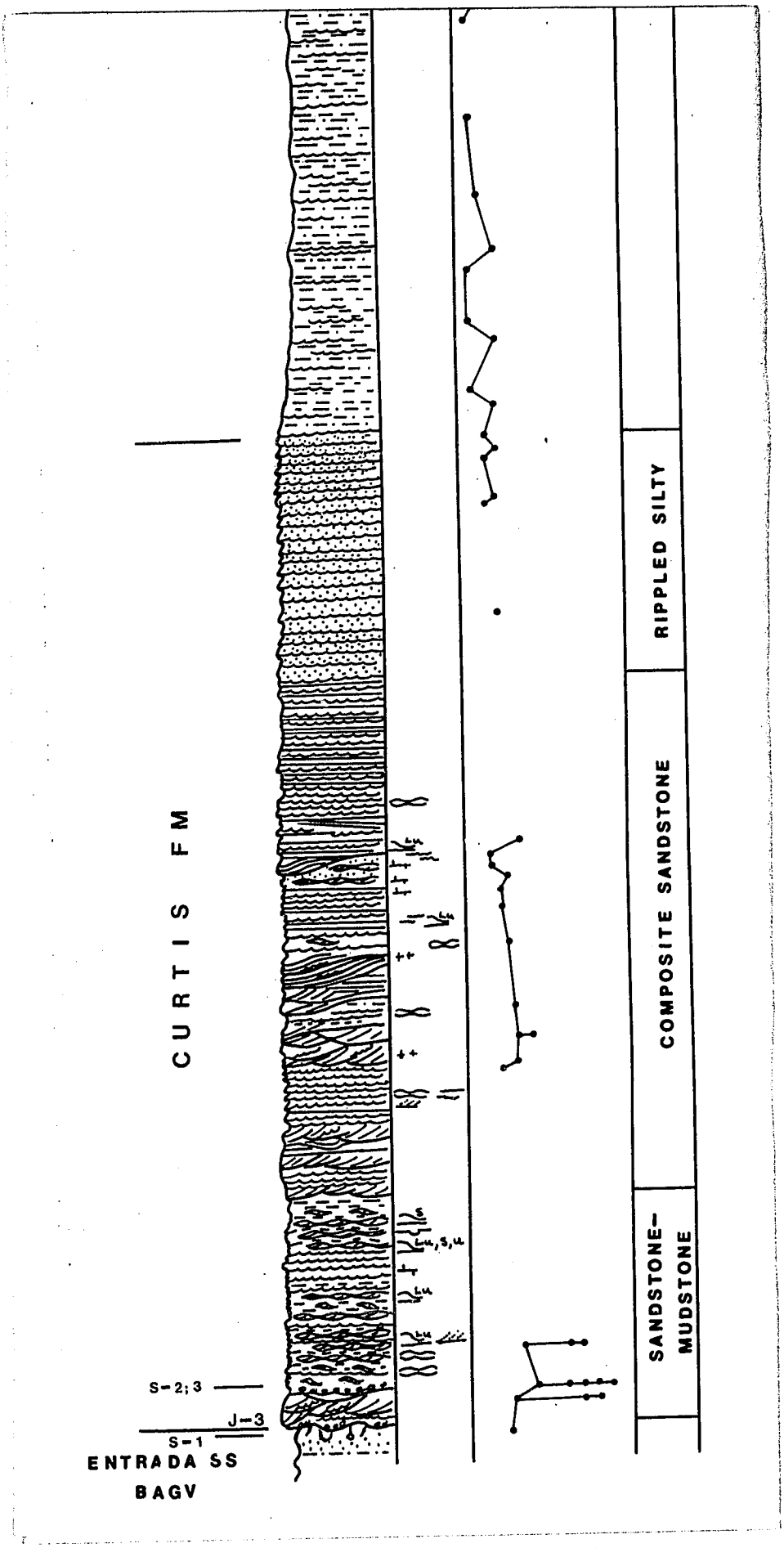

CEDAR MOUNTAIN

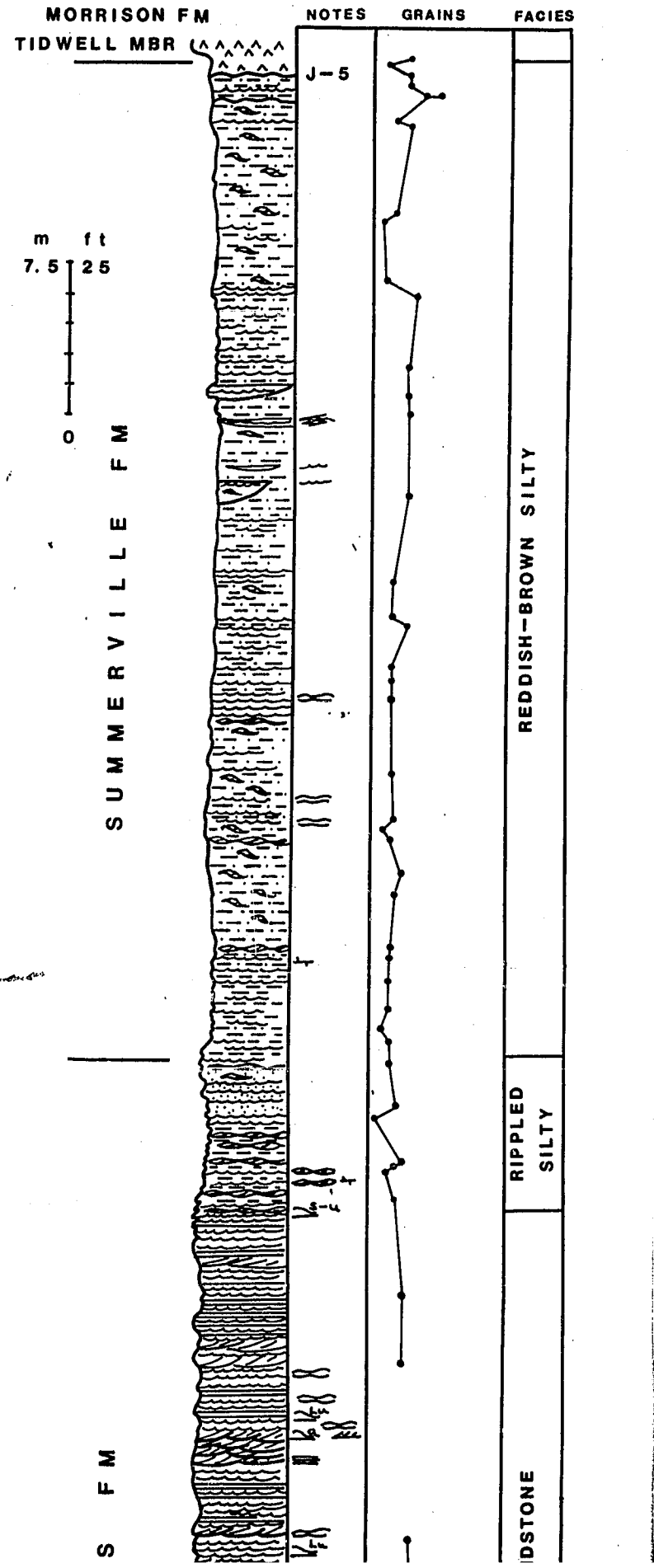

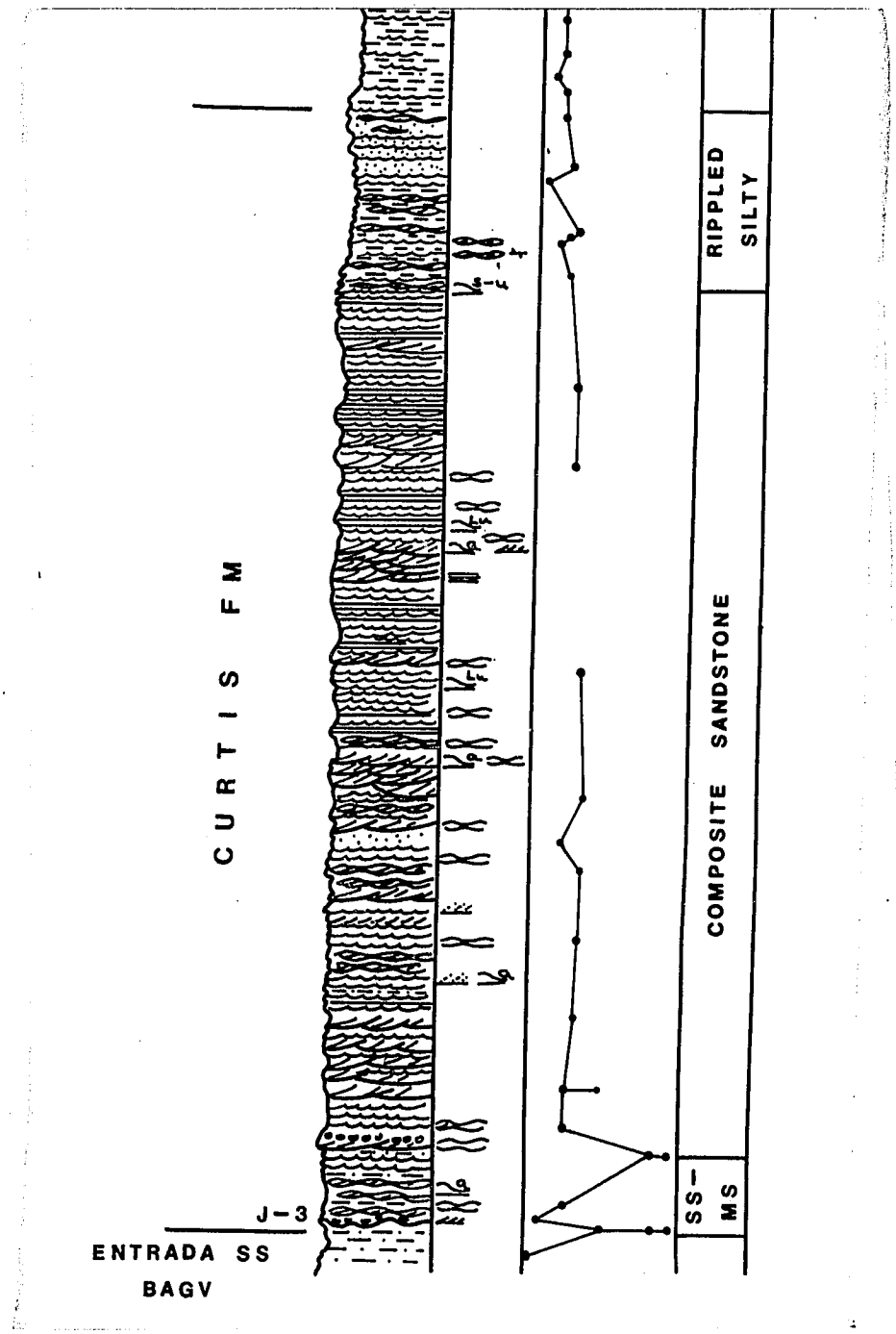

BUCKHORN WASH NORTH

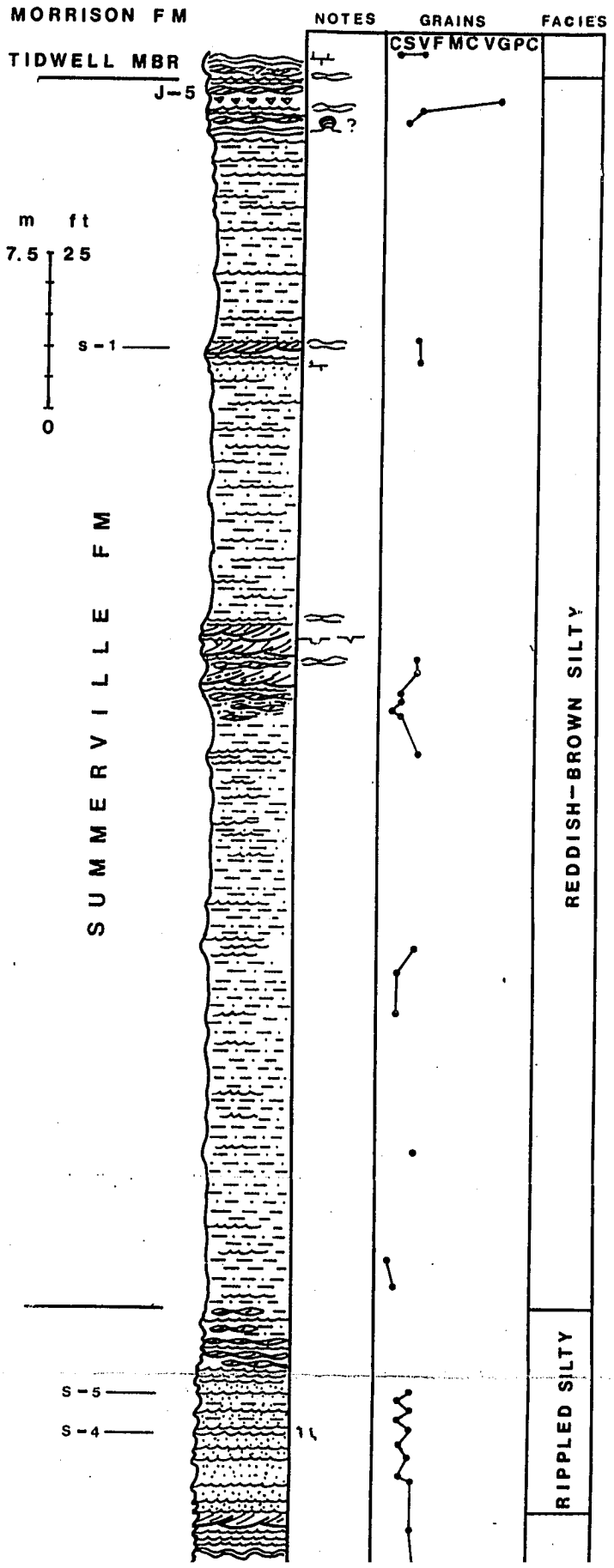

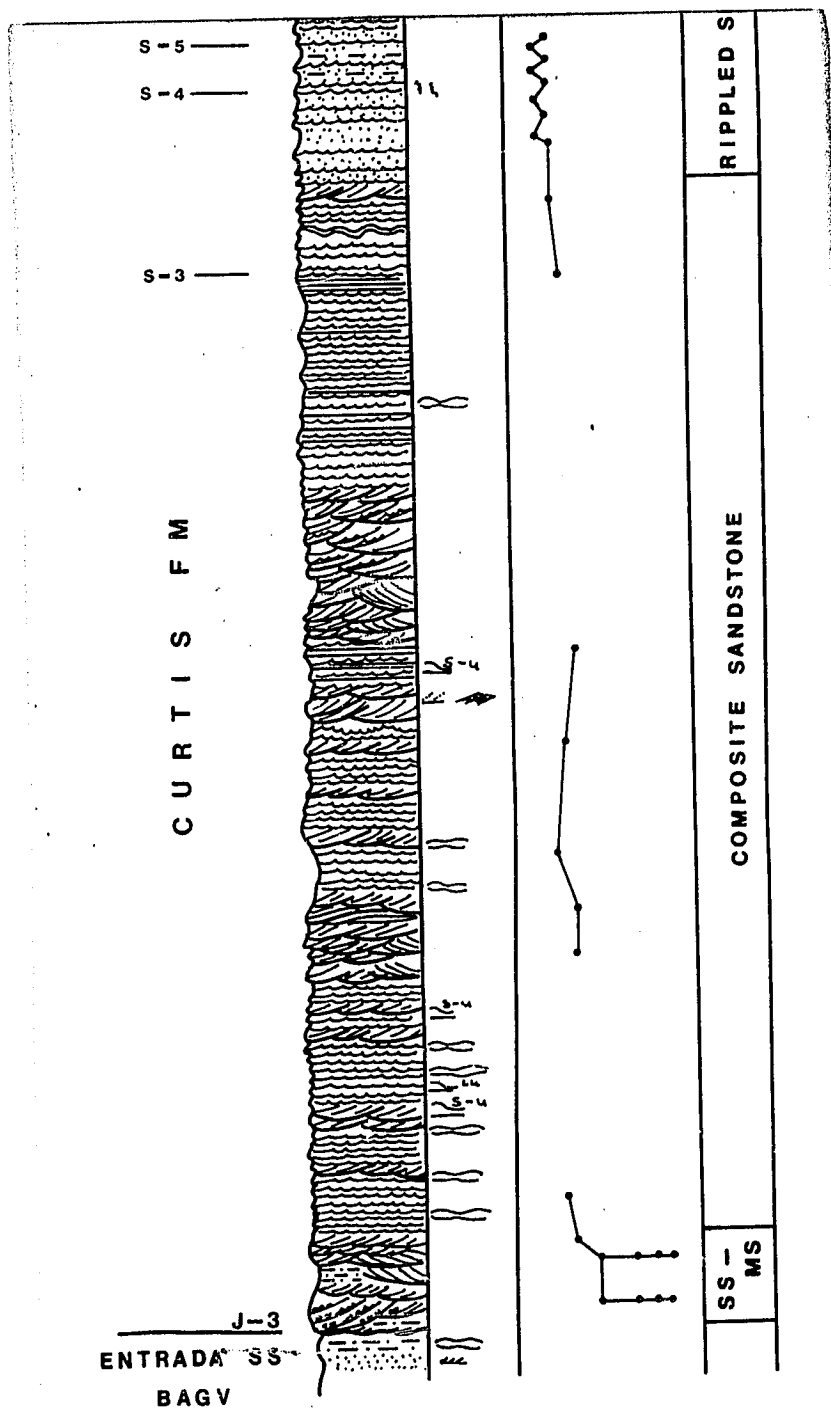

Z-23

BUCKHORN WASH SOUTH